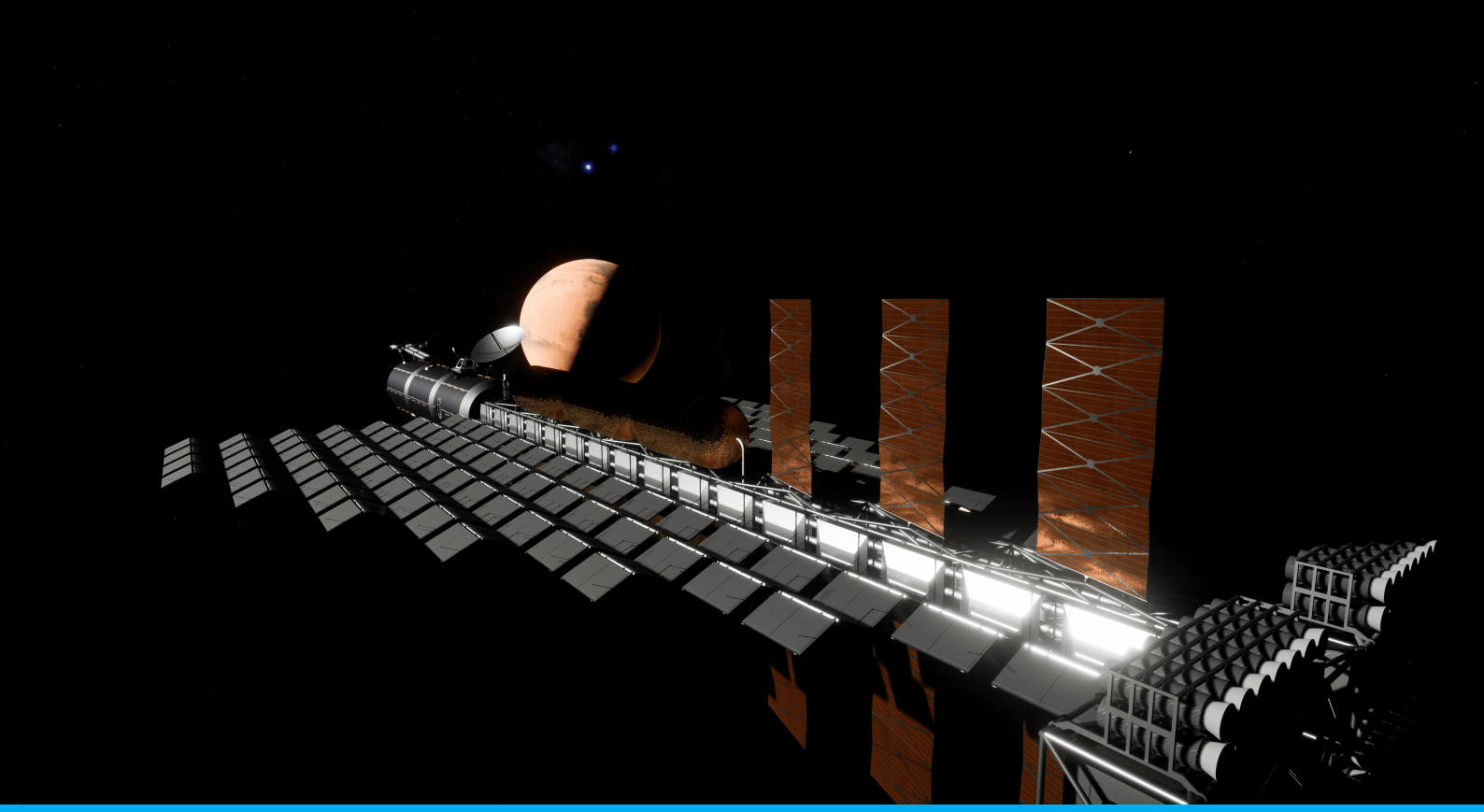

Delft University of Technology

Final Report

DSE: Transfer to Mars and Back in the Next Two Decades

TU Delft

Final Report

DSE: Transfer to Mars and Back in the Next Two Decades

by

P.M.F. Elferink
T. Faschinger
N. van der Hijden
M. Katona
C. Klop
P.L.M. de Kok
T. Kukucka
M. Osowski
P. Papadopoulos
A. Thiam

to obtain the degree of Bachelor of Science
at the Delft University of Technology,
to be presented publicly on Thursday July 4, 2019.

Pepijn Elferink	4444582
Tristan Faschinger	4549155
Nick van der Hijden	4486102
Misha Katona	4537688
Casper Klop	4455339
Pieter de Kok	4599934
Tomáš Kukučka	4542703
Martin Osowski	4546873
Panos Papadopoulos	4498828
Arthur Thiam	4472586

Project duration:	April 23, 2019 – July 2, 2019	
Project committee:	Dr. ir. J.M.J.F. van Campen,	TU Delft, tutor
	Dr. ir. A.C. in 't Veld,	TU Delft, coach
	Ir. V.M. Villalba Corbacho,	TU Delft, coach

This project is confidential and cannot be made public until July 2, 2019.

An electronic version of this report is available at `http://repository.tudelft.nl/`.

TU Delft

Change Log

Issue	*Date Changed*	*Pages Affected*	*Description of the changes made*
1	24th of June 2019	All	New Document
2	1st of July 2019	All	Improved layout and report consistency
		All	General spelling and grammar improvements
		1	Acknowledgements Added
		9	Changed to ”Summary of Previous Design Work”
		11	Mission need statement added to chapter 3
		15	Adjusted budget units
		21	Added figure caption
		22	Added explanation of how mass is calculated
		22	Added pseudocode representation of simulation loop
		25	Improved validation reasoning
		27	Added subsection Results and Implications
		28	Added sensitivity analysis of orbit altitudes
		30	Specified C_2H_2 venting
		33	Specified exercise equipment location
		37	Table changed to text for format consistency
		40	Added symbol explanation
		42	Improved explanation of radial burn
		42	Added the section ”Capture burn”
		43	Specified the amount of propellant for momentum dumping
		43	Based the sensitivity analysis on torque required and added a limits table
		51	AC/DC Converter DC explained
		52	Preliminary PMAD, removed robust
		56 to 58	Changed order of Trade-Off
		64 to 65	Updated Sensitivity Analysis
		80	Sensitivity and V&V format consistency
		81	Radiation code verified
		88	Changed dose of reflector material
		93	C&CDH architecture added bandwidth
		93	C&CDH architecture added flow distinctions
		93	C&CDH architecture added system boundaries
		93	C&CDH effects on entire system added
		99	Payload Section Added
		106 to 111	Operational and Overhead cost estimate revised and detailed
		114	Extended discussion on expandibility
		119	Updated FBS
		121	Additional Explanation in Compliance Matrix
		138	Conclusion updated

Acknowledgements

Several people have helped making this Design Synthesis Exercise a very enjoyable and interesting closure of the Bachelors Degree. First of all, we would like to thank Julien van Campen, Alexander in 't Veld and Victor Villalba Corbacho for their ongoing feedback and the many times they came by to help, as well as Kipras Paliušis for his many useful comments on the System Engineering aspects of the project.

Furthermore, we would like to express our gratitude to those people who have helped us in our research to the many aspects involved in a manned mission to Mars: Alessandra Meniucci for her advise on deep-space radiation, Barry Zandbergen for his recommendations on space vehicle concepts and Sytze Kampen, Henk Cruijssen and Edward Bongers for their help on solar panel design. We would also like to thank Bernard Foing, for his invitation to present on the EuroMoonMars workshop at ESA ESTEC.

Finally, we would like to thank Arend-Jan Krooneman, Luuk Goossen, Jeroen Boots, Roland van Roijen and Arno Freeke for their help in the VR lab, where we could visualise everything we have designed and get a sense of scale of the vehicle that is required for a Mars mission.

Contents

Nomenclature

Abbreviations

ADCS	Attitude Determination and Control System
ALSS	Advanced Life Support System
BOL	Beginning of Life
C&CDH	Communication and command and data handling
CBM	Common Berthing Mechanism
CCMHD	Closed Cycle MHD
CDRA	Carbon dioxide removal assembly
CG	Center of Gravity
CRS	Carbon dioxide removal system
DOD	Depth of Discharge
DSE	Design Synthesis Exercise
EATCS	External Active Thermal Control Subsystem
ECLSS	Environmental Control and Life Support System
EOL	End of Life
EPS	Electronic Power System
ESA	European Space Agency
EVA	Extravehicular Activity
IATCS	Internal Active Thermal Control Subsystem
IDDS	International Docking System Standard
ISPR	International Standard Payload Rack
ISS	International Space Station
LAR	Liquid Argon
LCA	Life Cycle Assessment
LDR	Liquid Droplet Radiator
LOX	Liquid Oxygen
MHD	Magneto-Hydrodynamic converter
MMOI	Mass Moment of Inertia
MTV	Mars Transfer Vehicle
NASA	National Aeronautics and Space Administration
NEP	Nuclear Electric Propulsion
NERVA	Nuclear Engine for Rocket Vehicle Application
NTP	Nuclear Thermal Propulsion
OGA	Oxygen generation assembly
ORU	Orbital replacement unit
PMAD	Power Management and Distribution
PPA	Plasma pyrolysis assembly
R&D	Research and Development
RAMS	Reliability, Availability, Maintainability and Safety
REACH	Registration, Evaluation, Authorisation and Restriction of Chemicals
RMS	Remote Manipulator System
RMSE	Root Mean Squared Error
t	tonnes
TRL	Technology Readiness Level
U^{235}	Uranium-235 isotope
UPA	Urine processor assembly
VASIMR	Variable Specific Impulse Magnetoplasma Rocket
WPA	Water processor assembly

Constants

ϵ	The Stefan Boltzmann Constant $[5.67 * 10^{-8} W m^{-2} K^{-4}]$
g	The Gravitational Acceleration in m/s^2, 9.807 m/s^2

Variables

ϵ_{eff}	effective emissivity coefficient $[-]$
A_{rad}	The radiator surface area $[m^2]$
I_{sp}	Specific Impulse
T_i	The initial equilibrium temperature $[K]$

Executive Overview

This report presents the final design of the Delta Mars Transfer Vehicle designed by DSE Group 14 at the TU Delft Faculty of Aerospace Engineering. The objective of this project, conducted over the course of 10 weeks, has been to design a modular, reusable spacecraft for crewed missions to Mars and back. The Executive Overview provides a standalone summary of the final spacecraft design and the reasoning behind major design decisions. It covers the key requirements placed on the design of the spacecraft, an overview of the complete vehicle and mission architecture, a description of each major subsystem design, as well as technical operations, sustainability, business planning, RAMs, technical risks and project planning.

Key Requirements

The Key requirements identified from the user requirements are:

- The system shall have the capability of transferring at least 4 astronauts to Mars orbit and back.
- The system shall consist of interchangeable modules.
- The system shall have the capability of transferring 12 astronauts to Mars and back using additional modules.
- Each module of the spacecraft shall have a service life of at least 20 years.
- The human occupants of the system shall have a maximum exposure of maximum total of 1500 mSv per mission
- The system shall generate at least 20 % return on investment over a 10 year window after start of operations

From these, system and subsystem requirements have been identified, on which the design of the system has been based.

Mission and System Description

An overview of the spacecraft's characteristics is given in Table 1.

System characteristics		Mission characteristics	
Wet Mass	399.2 t		
Dry Mass	180.7 t	Astronauts (baseline)	4
Payload Mass	15 t	Mission duration	1148 days
Length	65 m	Mars stay	520 days
Width	41 m	First scheduled launch	2041
Height	6 m	Earth orbit altitude	950 km
$MMOI_x$	5 Mkgm^2	Earth orbit decay time	200 year
$MMOI_y/z$	110 Mkgm^2	Earth orbit period	1h 44m
Habitable volume	100 m^3	Mars orbit altitude	400 km
Pressurised volume	260 m^3	Mars orbit decay rate	Undefined
Engine	VASIMR	Mars orbit period	1h 58m
Propellant	Liquid Argon	Launcher	Falcon family
Thrust	278.4 N	No. of initial launches	17
ΔV	35.2 km/s	No. of resupply launches	9
Thermal Power	20 MW_{th}	Expected received radiation	1300 mSv
Electrical Power	11 MW_e		
Backup Power	10 kW_e		
Data rate	5 Mbit/s		
Transmitting power	800 W		
Memory size	500 GB		

Table 1: Overall spacecraft characteristics

The mission architecture of the Mars Transfer Vehicle consists of three distinct phases. The first is the assembly phase, in which the disassembled vehicle is launched into low Earth orbit where it is assembled. The second phase involves the spiral escape from Earth orbit, astronaut boarding, transfer to Mars, stay in low Martian orbit, and return to Earth. The astronauts unboard the spacecraft and use a crew capsule to return to Earth surface before the MTV spirals down to parking orbit. The third phase consists of preparing the vehicle for further transfers to Mars by means of inspection, maintenance, repair, and resupply.

Propulsion

The Mars Transfer Vehicle (MTV) is propelled by 48 Variable Specific Impulse Magneto-Plasma Rocket (VASIMR) engines. These electric engines use argon as their working gas.

The argon is heated up until it reaches a plasma state, and is then magnetically accelerated through a nozzle. The engines use 200 kW of electrical power to generate 5.8N of thrust. For a total of 48 operational engines (4 for redundancy), this propulsion system will require 9.6 MWe of electric power. The full mission will require 156.5 m^3 of liquid argon. Due to launcher payload mass limitations, the fuel will be launched in 6 tanks. These tanks are located on the truss structure supporting the radiators.

Trajectory

The trajectory of the Mars Transfer Vehicle was optimised using a custom-built simulation. The transfer from Earth to Mars orbit will consist of a low-thrust spiral escape from Earth, an interplanetary low-thrust transfer consisting of two burns and a low-thrust spiral capture at Mars. The transfer from Mars to Earth will consist of similar manoeuvres. Interplanetary transfer trajectories were optimised for the required ΔV by an optimising algorithm that made use of the Steepest Gradient Descent method. A compromise was made between the transfer time and required ΔV. Finally, it was established that the propulsion system needs to deliver a total ΔV of 35.2 km/s with a safety margin and an initial acceleration of at least 0.7mm/s^2.

ECLSS

The Mars Transfer Vehicle features resource recovery and cabin regulation by means of an environmental control and life support system (ECLSS). Requirements on the ECLSS derive from the required inputs of the human body in the space environment, and its waste outputs. Additional requirements stem from environmental conditions that must be maintained in the pressurised cabin. CO_2 is removed from the cabin atmosphere using a carbon dioxide removal assembly (CDRA) and then processed into water and methane in the carbon dioxide reduction system (CRS). Urine is processed into non-potable water in the urine processor assembly (UPA). The water processor assembly (WPA) purifies output water from the UPA, CRS, and cabin humidity condensate into potable water which is either stored in the potable water tank, or fed to the oxygen generation assembly (OGA) where oxygen and hydrogen is formed. The ECLSS is able to recover 88 % of waste water, leading to a required water supply mass over the course of a mission of 4,182 kg. Additional supplies taken on board include nitrogen, to mitigate cabin leakage, and food for the duration of the mission. The ECLSS is sized along with spare parts to obtain a reliability of 99.9 % over the course of a mission. The mass the power budgets of the ECLSS are 19,984 kg and 5.4 kW respectively.

ADCS

The ADCS of the spacecraft provides the ability to stabilise, control and sense the orientation of the vehicle relative to reference points. The driving requirement is the avoidance of space debris, since a collision would impose catastrophic failure and there is more than 500,000 pieces of debris orbiting Earth. The main ADCS-requirements resulting from this are the following:

- The spacecraft shall be able to rotate 180 ° in 2 hours.
- The spacecraft shall be able to climb or descent 10 kilometres in 1 hour.

Sizing is performed according to these requirements. This resulted in the use of 4 Control Moment Gyroscopes (CMGs) that each can provide a torque of 28 Nm, 24 hot-gas bi-propellant thrusters with a thrust of 200 N each, 6 sun sensors, 3 star sensors and two Inertial Measurement Units (IMU). The CMG is chosen for its high output torque with low power consumption and the ability to operate without propellant. The thruster are there for momentum dumping and the ability to climb or descent 10 km within 1 hour. Six sun sensors for omnidirectional attitude determination and 3 star sensors for redundancy. The IMU measures the translational and rotational movement.

Electrical Power

The electrical power system uses Magneto-Hydrodynamic Converters (MHDs) and Fission Reactors to generate 11 MW of power and distribute it throughout the spacecraft. It also includes solar arrays and batteries, which act as a second source of energy when the reactors are not active. These Closed Cycle MHDs (CCMHDs) require power to activate. By using the

solar arrays and secondary batteries, one MHD can be activated, which will then activate the other three MHDs. Should there be a necessary shutdown of the reactors after activation, the solar arrays and secondary batteries are designed to sustain all spacecraft systems in a critical power state with exception of the engines and thermal pumps. By taking a solar cell beginning of life efficiency of 32.2 % and batteries that have a specific energy of 160 Wh/kg, the backup power system is estimated to weigh 2,990.19 kg. These values are designed for the worst-case scenario of the mission which is at the aphelion of mars in a Low Martian Orbit of 400 km, after 20 years of radiation degradation. The power management and distribution (PMAD) system incorporates AC buses due to the increased efficiency when compared to DC buses at this high power constraint. The PMAD system also includes an electromagnetic interference filter and a compensation capacitor. The compensation capacitor is to increase the efficiency of the AC circuits over cable lengths. There is also a shunt regulator so that excess power can be dissipated into the external environment. There are 2 main AC buses, one for redundancy, and every module has its own AC bus. As this is an iterative process, the circuitry is bound to change before its final iteration.

Thermal Control

The thermal control subsystem regulates the heat transfer and temperature for the habitat and temperature sensitive components. The subsystem is also designed to get rid of excess heat by use of radiators. Since significant excess heat is generated from the MHD, high performance radiators were necessary to efficiently radiate the heat outwards. After a trade-off, taking into account the single point of failure, radiator usability during manoeuvres, thermodynamic stability, inter-reflective efficiency, and the development schedule and cost, it was decided to use a high temperature aluminium-carbon hybrid radiator panel with carbon-carbon fins and heatpipes with a carbon lining. The panel will be painted black to increase emissivity efficiency and will be positioned under a 25 degree angle to reduce the width of the radiator subsystem. After iteration, 630 m^2 of radiator panels is necessary (including a safety factor of 1.15) to radiate out the excess heat. The radiators are placed in a ”Delta-wing” configuration to optimise the heat transfer coefficient. Two Loops are used to distribute the heat with two types of working fluids; The MS-2 fluid will flow through the radiator and MHDs. A glycol/water combination will be used to control the habitat temperature. Redundant heaters and coolers are installed in phases for mission scenarios where the nominal thermal flow is disturbed. The habitat will be covered in Multi-Layered Insulation to establish an equilibrium temperature range of 20 degrees Celsius. The mass and electric power required for the thermal control system is estimated to be 19,445.5 kg and 246 kW, respectively.

Spacecraft Structures

Two different types of docking interfaces are implemented in the spacecraft structure. Large Common Berthing Mechanism docking interfaces are used to connect the habitat modules together and allow for the transfer of electricity, fluids and oxygen and smaller interfaces conforming with the International Docking Standard are used to dock with external payloads and crew capsules. A Remote Manipulator System similar to the so called Canadarm2 on the ISS will be implemented to aid in the docking of modules and to allow for inspection and repair during the mission. The habited modules are shielded form both micrometeorites and interplanetary radiation, in order to protect from orbital impacts a stuffed Whipple shield is used, this is made up of two aluminium plates with 12 cm of space between with as well as a few layers of Kevlar and thermal insulation. The bulk of the radiation protection comes form the 12 cm thick polyethylene lining that is inside the pressurised module, this provides an acceptable level of protection. The structural shells of the habited modules are design to withstand launch loading and pressurization.

Communication and Command & Data Handling

An elaborated data rate analysis has been performed for three scenarios where astronauts and spacecraft have to communicate by radiowaves to the existing agencies Deep Space Network ground-station, under nominal conditions with an eclipse length of 2024 s, after a 10 day Mars-Sun-Earth conjunction and when power consumption should be limited during

reactor failure. The driving parameters that resulted from this were a maximum data rate after conjunction of 1.7 Mb/s where 61.1 GB of storage is required during conjunction, an uplink data rate of 1.0 Mb/s and 0.066 Mb/s during reactor failure. A deep space proven CDH-bus was selected together with a 0.5 TB flash solid state memory to fulfil the data handling processes. The communication system has a Cassegrain configurated reflector antenna with a main reflector diameter of 3.45 m and a sub-reflector diameter of 0.27 m. These are fed by a dual polarised corrugated horn antenna which makes it possible by using a orthomode transducer to double the data rate that can be sent with the same power and diameter. Downlink frequency of 32.27 GHz and uplink frequency of 34.56 GHz (Ka-band) will be used. An extensive link budget has been developed to analyse the worst case scenario for the attenuation-sensitive Ka-band and by using state-of-the art deep space transponders and amplifiers of 200 W and 40 W for Ka-band, the link budget could be closed with a SNR of 21 (limiting requirement, for audio communication). A gimbal will be used to point the antenna. The whole system will be completely redundant due to previous high critical mission failure rates.

Operations & Logistics

17 Falcon launches are required to bring the various modules to Low-Earth Orbit (LEO), with a maximum mass of 35 t each. The first module will be the truss section closest to the habitat module, which will include the CMGs, the antenna dishes, and the robotic arm. With a rudimentary board computer, this will provide a base platform for the rest of the assembly procedure. Using a ”space tug”, the other modules (trusses, habitat modules, Argon tanks and propulsion modules) are brought to the spacecraft one by one, and berthed using the robotic arm. After assembly, the spacecraft is inspected by astronauts performing EVAs, especially for electrical functioning and feedsystem attachments. The astronauts leave the spacecraft again before it starts spiralling out of LEO, and the crew is docked to the spacecraft in HEO.

Important logistic stations that are identified are manufacturing halls, astronaut training centres, the SpaceX integration halls, and ground stations such as Tracking, Mission Control and Communication stations.

Sustainability

Space missions have a large environmental impact due to their complexity, the required launches, the removal of materials from Earth’s ecosphere and the difficulties connected with the decommissioning of space vehicles. As a first step elements of concern were identified, their impact was quantified and mitigation strategies or alternatives were proposed. The developed debris mitigation plan includes the change of assembly orbit to a higher altitude with a lower space debris density, the application of shielding against impacts for all critical systems, the active tracking and avoidance of all debris objects of concern and the end-of-life disposal of the vehicle. The disposal process consists of the retrieval of resources where possible after which all decommissioned modules will be brought to a graveyard orbit while the reactors will be brought into a heliocentric that poses no risk of a future planetary impact. The probability of an inadvertent atmospheric entry at Earth or Mars of a reactor was evaluated to be small and will be considered for future trajectory planning. Furthermore, all harmful substances implemented in the vehicle were identified and their compliance with EU regulations has been reviewed, alternatives have been analysed and proposed where feasible. Lastly, a life cycle assessment has been applied to evaluate the environmental impact over the full mission duration of 50 years.

Business Model

The team is given a driving requirement of providing a Return on Investment (ROI) for the system of 20 % within 10 years. The total accumulated cost of the mission is estimated to be 98.5 billion Euro in 2050 and 130.5 billion Euro in 2060. This requirement makes an extensive business plan a necessity. The ideas to create income consist of the following:

- Transport of non-human payload
- Making a documentary and vlogs
- Selling broadcast rights
- Find private investors, like private equities
- Space agencies funding and collaboration
- Sell scientific research data
- Selling maintenance contracts of in-orbit satellites
- Remote robot control on Mars surface (for example building bases
- Conclude long- and short-term sponsor contracts

As the external cash flows are limited, a thorough analysis by using an income statement, showed that the 20 % ROI can be given to the private investors in 2050 if they invest 23.1 billion Euro between 2039 and 2040. The agencies will fund 55.0 % of the costs and do not get a 20 % ROI, while from statistical data the investments of these agencies will return 9 dollar as scientific and technology return for every invested dollar over decades [83], hence motivating these agencies to invest in the team's mission. This is the business philosophy from Delta Mars that is defined to still fulfil the requirement on ROI by the limited percentage of costs that can be covered by external cash flows that do not have a share in Delta Mars.

RAMS Analysis

The RAMS analysis showed several benefits and challenges in the overall system. A reliability analysis showed that adding redundancies for each subsystem makes the system very heavy, while for adding partial redundancies an overall reliability of 91 % could be achieved for the full 20 year mission. By ensuring life-critical systems are redundant and by resupplying broken components each mission, a reliable system can be created. The spacecraft is available 78.4 % of the time, due to the fact the spacecraft has to wait in LEO in between missions before the next transfer window opens.

Maintenance remains a large challenge for interplanetary missions, due to radiation levels forbidding EVAs during transfer and the long travel times. By adding ISS-type robotic arms, minor repairs can be performed 90.7 % of the mission duration, while only in between missions, when the spacecraft is orbiting in LEO, major repairs can be performed. Finally, the safety aspects of the system are assessed, and taken into account in the whole design by adding redundancies and performing a technical risk analysis, described in the next section.

Technical Risk Analysis

Risk analysis was performed in two distinct fields. Mission risk analysis considered risks associated with the overall mission, while operational risk included all the risks associated with the spacecraft. For both, mitigation and contingency strategies were developed in order to minimise the total risk exposure. The development of the spacecraft was found to be very risky and special care should be taken during planning in order to develop the system on time.

Project Planning

The framework for the future design and development in the post DSE phase has been laid out. The identified seven big phases of the project are the detail design phase, the development phase, the production and certification phase, the mission preparation phase, the in-orbit assembly phase, the mission execution phase and finally the decommissioning phase. These phases have been worked out in more detail and all identified tasks have been scheduled in a Gantt chart forming the basis for the following steps. The production phase has been further defined and the work flow from raw materials to final assembly has been outlined.

Conclusion and Recommendations

With a first launch of 2041 the dealt mars mission will be the first trip to mars humanity has embarked on in a manned spacecraft. The MTV will have to face many challenges ranging from overcoming the large required ΔV to ensuring that the astronauts radiation exposure is within safe limits. With a number of subsystems used that are still in their development, the spacecraft will have to be developed along side projects such as the VASIMR ion engine, zero boil off cryogenic coolers, and high powered space optimised nuclear reactors. While daunting, these challenges can be overcome through the project's close collaboration with the planets largest space agencies and funding from the private sector.

1

Introduction

This report documents the detailed design of the Delta Mars Transfer Vehicle. As such, it concludes the graduation work that has been carried out over the course of 10 weeks by DSE Group 14 at the TU Delft Faculty of Aerospace Engineering. The project objective of this Design Synthesis Exercise (DSE) has been to design a modular spacecraft for crewed missions to Mars and back by 10 persons within 10 weeks. Key top level requirements placed on the project have been to safely transport a crew of four to Mars orbit and back, limit astronaut radiation exposure to 1500 mSv, have the mission be feasible by 2040 with a service life of 20 years, and to create 20% return on investment following 10 years of operation. The DSE has been carried out in four phases: a project planning phase lasting one week, a baseline conceptual design exploration phase of one week, a midterm phase in which the conceptual design was finalised of three weeks, and a final detail design phase of four weeks. A strong emphasis has been placed on systems engineering and integration throughout the project.

The Mars Transfer Vehicle is a reusable spacecraft using electro-thermal propulsion powered by four low-enriched fission reactors. It carries a crew of four astronauts to Martian orbit and back over a mission duration of approximately 1150 days, including a 520 day stay in Martian orbit. Systems currently supporting human life aboard the ISS are used as a baseline in designing the vehicle. During the course of the project, many elements of the vehicle design have been considered, including propulsion, low thrust trajectory simulation, optimisation and determination, radiation and micro-meteorite shielding, thermal control, in-orbit assembly, and crew considerations such as the layout of the pressurised cabin. As the mission concept is based on the assumption of the feasibility of the VASIMR and CCMHD nuclear reactors, it is decided to make the project a concept study on the mission outline of a Nuclear-Electric Propulsion spacecraft. Because of this, the Power & Propulsion systems are only designed to a preliminary level, and focus is put on the subsystems surrounding it, as well as the impact of the reactors and engines on them. The resulting spacecraft is 70 m long with 250 m^3 of pressurised cabin space, has a wet mass of 360 metric tonnes, carries 15 metric tonnes of payload, and provides a mission ΔV of 35.2 km/s.

The report is structured as follows. Chapter 2 summarises the work done in previous design phases and the resulting key outcomes. Chapter 3 presents the final design of the Mars Transfer Vehicle and describes the Mars mission architecture. Chapter 4 provides an overview of the systems engineering approach taken in the detail design phase. Following this, the detailed design of the spacecraft subsystems is documented in Chapter 5 to Chapter 12. This is followed by a description of the spacecraft operations in Chapter 13. Chapter 14 elaborates the technical approach to sustainability and evaluates the extent to which the project meets sustainability goals. The business case for the project is argued in Chapter 15. Chapter 16 describes how all the subsystems are integrated, provides an analysis of the complete system, and describes how the design iterations have been performed. A technical risk assessment, including strategies for risk mitigation is documented in Chapter 17. Specific technical solutions to mitigate major risks are elaborated in the relevant subsystem design chapters. Finally, Chapter 18 describes the planning of the project past the Design Synthesis Exercise.

2

Summary of Previous Design Work

The Design Synthesis Exercise is structured into four distinct phases: Project Planning, Baseline phase, Midterm phase, and Final phase. In each of these phases, the design of the Mars Transfer Vehicle has been carried out in increasing levels of detail, converging to the final detailed design as presented in this report. This chapter discusses the progress made in the stages before the Final phase.

2.1. Project Planning Phase

During the project planning phase the team focused on structuring the work that would be done up to the conclusion of the midterm phase. Several documents where compiled to this end, including a work flow diagram and corresponding work breakdown structure and a detailed Gantt chart up to the end of the midterm. Organisational and technical roles were assigned to all team members. Organisational roles were divided into a chairman, secretary, quality control officer, business officer, sustainability officer, and risk manager. Technical roles were defined per spacecraft subsystem. Additionally, a systems engineers was appointed. Operational risks associated with the project were identified, assessed, and mitigation strategies were developed. The operational approach to sustainability was developed, defining the responsibilities of the sustainability officer. A strengths, weaknesses, opportunities, and threats (SWOT) analysis to identify challenges and strengths the team would have moving into the following design phases.

2.2. Baseline Phase

Technical design work commenced during the baseline phase. Design requirements were determined, and design option trees were explored in order to finalise a set of concepts which would be further explored and traded in the midterm phase. Based on the user and stakeholder requirements specified in the project assignment, system requirements were defined, which were then broken down further to subsystem requirements. This was followed by the generation of a functional flow diagram and functional breakdown structure. Design option trees were explored, leading to a set of concepts for the Mars transfer vehicle.

Most notable were the three vehicle level concepts which were developed: a single vehicle concept, dual vehicle concept, and Mars cycler vehicle. The single vehicle concept involves a single vehicle executing the entire mission. The dual vehicle concept features an unmanned vehicle which is first sent to Martian orbit with crew supplies and fuel using an efficient but long transfer. A second, crewed vehicle is then sent to Martian orbit on a fast but fuel intensive transfer where it docks with the first vehicle and resupplies. The benefit of this concept is that a large portion of the supply mass is transferred using efficient methods, and that the time spent in deep space by the crew is minimised. The Mars cycler concept involves the establishment of a vehicle in a Mars-Earth cycler orbit. Such a heliocentric orbit is stable and passes by Earth and Mars at predictable intervals. The cycler vehicle would be a permanent station which provides life support and crew quarters and transfer the crew to Mars and back, A smaller vehicle would be used to ferry the crew from Earth and Mars orbit to rendezvous with the cycler. Due to the fact that the cycler would spend a significant amount of time beyond Mars orbit, at least two cycler vehicles would be required to send and retrieve the crew from Martian orbit.

Concepts were also explored for the use of an Earth or Moon orbiting station. Such a station would aid in resupply, repair, and maintenance of the Mars Transfer Vehicle. Positioning the station in Moon orbit provided the benefit of not having to bring the vehicle as deep into Earth's gravity well, reducing the required mission ΔV. Design option trees were explored as well for vehicle subsystems and business models. A preliminary technical risk assessment was performed, and the technical approach to sustainability outlined.

2.3. Midterm Phase

Concepts identified in the baseline phase were analysed and traded off during the midterm phase. Vehicle level trade-off was performed based on the criteria of wet mass over 20 years, technological-readiness-level (TRL), maintainability, transfer duration, and operational risk. Preliminary mission analyses of all vehicle concepts considered showed that with current state of the art chemical engines the wet mass of all three was unfeasible. The single vehicle was the heaviest by a large margin, however the mass of each vehicle was prohibitive, and significant risks were introduced by the Mars cycler. This led to an investigation of several low TRL options which had the potential to significantly reduce the vehicle mass. These were the establishment of a Moon or Mars base from which propellant could be produced, and the use of nuclear-thermal and nuclear-electric propulsion. It was found that nuclear-electric propulsion with VASIMR engines provided the lowest vehicle wet mass with acceptable technological gaps and challenges. Low-enriched uranium fission reactors with closed-cycle magneto hydrodynamic generators (CCMHDs) were chosen to provide electrical power to the engines. The vehicle trade-off was performed once more with nuclear-electric propulsion factored in to the analysis. Based on the trade-off criteria specified, the single vehicle concept was chosen. An Earth orbiting station was selected as well, however has since in the detailed design phase been changed to a ”space tug”, a dockable propulsion module assisting in assembly.

Following the decision on mission architecture and vehicle concept, trade-offs were performed on subsystem level to further define the vehicle. The following decisions were made.

Trade-off	**Decision**
Spacecraft layout	Modular stacked configuration
Transfer trajectory	Low thrust conjunction class trajectory with spiral escape
Electrical power	Low-enriched fission reactors with CCMHGs and solar panels for reactor shutdown scenarios
Revenue model	Payload delivery, space tourism, documentary film
ECLSS and supply	ISS based chemical oxygen generator and water recovery system, overboard waste disposal, 98 % of nutrition from Earth with supplemental vegetables produced on board.
Radiation shielding	Structural Aluminium with Kevlar outer layer and polyethylene backing
Launcher	SpaceX Falcon family

Table 2.1: Results of Midterm Report subsystem trade-offs

The results of these trade-offs are taken as the starting point for the final phase which is documented in this report. A functional flow diagram and breakdown structure were elaborated upon in further detail along with a technical sustainability analysis. A detailed technical risk assessment was conduction on the chosen vehicle concept. Preliminary vehicle budgets were compiled. The midterm phase was concluded with the planning of the final design phase, as well as a reshuffling of operational and technical positions within the team.

3

Vehicle and Mission Description

This chapter presents the mission need statement, key final design elements of the Mars Transfer Vehicle, and provides an overview of the Mars Mission Architecture. The aim is to provide the reader with an understanding on a system level. Further detail into individual subsystems and integration follow in Chapter 5 to Chapter 13 and Chapter 16 respectively. A full functional flow diagram is found in Chapter 16.

3.1. Mission Need Statement

As a first step in a new age of human exploration, we need a modular platform for human missions to Mars that will form the basis for a future cost-effective interplanetary transportation system.

3.2. Mars Transfer Vehicle Overview

The Mars transfer vehicle is a modular and reusable spacecraft designed to transport a crew of four astronauts to Martian orbit and back. The vehicle is capable of performing Earth orbit escape, establishing a transfer trajectory to intercept Mars, capture into Martian orbit, and return to Earth orbit. It provides reliable life support to the crew over a mission duration of approximately 1150 days. The exact mission duration varies with the launch year that is chosen due to the eccentricity of Mars' heliocentric orbit. Such mission requirements entail a large and complex spacecraft. Therefore the design is broken down into subsystems which are integrated to form the complete vehicle. A brief description of each subsystem follows. A summary of the key subsystem characteristics is found in Table 3.1

Subsystem	Description
Propulsion	52 VASIMR electrothermal engines with Argon propellant
Trajectory	Conjunction class low thrust trajectory
Environmental control and life support	Recovery systems for water, oxygen, and carbon dioxide
Attitude determination and control	4 Control moment gyros and 16 monopropellant thrusters
Electrical power	11MW from four fission reactors, solar panels for reactor shutdown scenarios
Thermal control	Active system with high temperature hybrid radiators
Structures	Three pressurised modules with truss connecting engines to spacecraft. Robotic arm for berthing, repairs, and maintenance.
Communication	Cassegrain reflector configuration with a dual polarised corrugated horn
Command and data handling	MIL-STD 1553 bus configuration with a 0.5TB flash solid state memory
Technical operations	20 initial Falcon family launches with assembly in low Earth orbit

Table 3.1: Subsystem design summary of the Mars Transfer Vehicle

Propulsion

The Mars transfer vehicle uses 52 (including 4 redundant) VASIMR electro thermal engines divided in four clusters with argon propellant. This provides a total thrust of 278.4 N at an ISP of 5,000 s. The engines are powered by four fission reactors on board the spacecraft. VASIMR engines are chosen due to their high specific impulse, which drastically reduces the wet mass of the spacecraft.

Trajectory

A conjunction class trajectory is used due to the limited availablilty of Mars launch and return windows. This trajectory class involves a long stay at Mars of approximately 520 days. The alternative: an opposition class mission, involves a stay duration of approximately 30 days, and uses a Venus swing by on return, creating unacceptable risks. A low thrust transfer

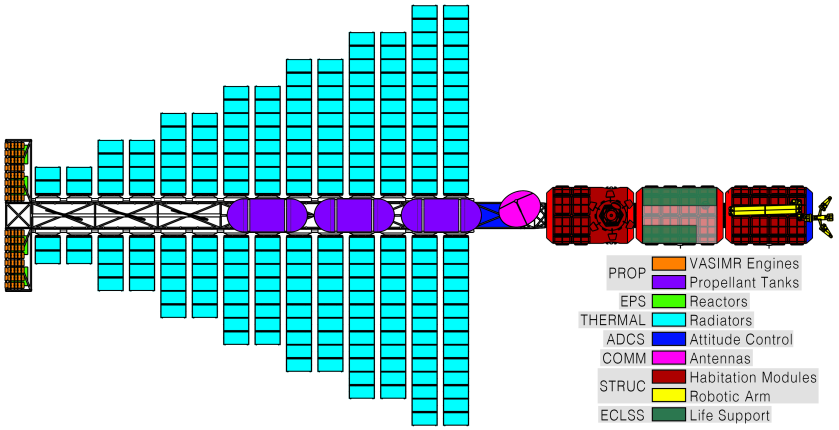

Figure 3.1: Mars Transfer Vehicle layout and subsystem overview

determination tool is built to determine exact transfer profiles. The first astronaut launch window occurs in February 2046.

Environmental Control and Life Support

The environmental control and life support system (ECLSS) is modelled on systems currently on the International Space Station and adapted to the requirements of a Mars mission with a crew of four. The ECLSS provides astronauts with potable water and oxygen, and recycles carbon dioxide and waste water with a water recovery efficiency of 88 %. The ECLSS is sized to 99.9 % reliability.

Attitude Control and Determination

The attitude control and determination system is designed to provide a pointing accuracy of 0.001 deg and a slew rate of 0.0060 deg/s It uses 4 control moment gyros and 16 monopropellant thrusters for control, as well as 6 sun sensors, 3 star sensors for attitude determination. These specifications are driven primarily by requirements on space debris avoidance.

Electrical Power

Four low-enriched uranium fission reactors are capable of providing 11MW of electrical power to the spacecraft. 9.6 MW are delivered to the VASIMR engines. The remaining spacecraft systems use a peak power load of 350 kW. In the event of a reactor shut down, deployable solar panels provide 10 kW to sustain systems in safe mode.

Thermal Control

The thermal control system of the spacecraft uses 620m^2 of high temperature hybrid radiators to dissipate 8 MW of thermal power. A cooling loop using MH-2 fluid regulates the temperature of the radiators to 350 degrees celcius. A glycol/water working fluid with electrical cooling units regulates the temperature of the pressurised cabin.

Structures

The primary structures of the spacecraft consist of three pressurised crew modules, docking ports, and the truss structure which connects the pressurised cabin to the engines and reactors, as well as supports the radiators. The pressurised modules are shielded against both micrometeorites and the deepspace radiation. The micrometeorite shield consists of a thin standoff shield of aluminium from the main aluminium structure, with a thermal, kevlar, nextel layer between the two. A 12 cm polyethylene shell is used for radiation protection. A robotic arm on the exterior of the vehicle is used for assembly, berthing, repair, and maintenance.

Communications, Command, and Data Handling

The communications susbsystem provides 1.7 Mb/s downlink and 1Mb/s uplink during all mission phases in nominal operation using a Cassegrain reflection configuration with a dual polarised corrugated feeder horn. The main reflector and sub-reflector are designed to

diameters of 3.45 m and 0.27 m respectively. Data handling is executed by a MIL-STD 1553 bus configuration with 0.5 TB flash solid state memory to sustain the required command and downlink data handling rates.

Technical Operations

To comply with launcher fairing constraints, the spacecraft is designed for packaging into 17 Falcon family launches. Assembly of the spacecraft occurs at an orbital altitude of 950 km in order to avoid debris dense regions and the Van Allen belts. A ”space tug” concept, consisting of a dockable propulsion module, guides the modules to the correct orbit for assembly.

3.3. Mission Architecture

The mission architecture executed by the Mars Transfer Vehicle consists of the phases of assembly and start up, Mars transfer, and post-mission resupply, repair, and maintenance. The mission begins with 17 Falcon family launches to bring the spacecraft components into orbit at 950 km altitude. The spacecraft launch and assembly steps are staggered such that further modules are launched once partial assembly is completed. Further details on launcher packing can be found in Section 13.4. Following the assembly phase, inspection and testing are performed to prepare the spacecraft for the transfer phase.

The Mars transfer phase begins with the initiation of a 103 day spiral escape orbit during which the spacecraft carries no crew. This is such that astronauts are not exposed to radiation in the Van Allen belts for prolonged periods during the spiral escape. Once the spacecraft has passed the Van Allen belts, the crew is delivered to the Mars transfer vehicle via a chemically propelled crew capsule. This crew capsule is undocked from the Mars transfer vehicle prior to the initiation of the Mars-bound transfer trajectory. Following successful crew transfer and a systems check, the vehicle finalises it’s escape from Earth orbit and begins a heliocentric trajectory towards Mars interception.

Transfer to Mars takes approximately 200 days, depending on the launch window. During this phase the spacecraft’s VASIMR engines follow a thrust profile specified by the chosen launch date and transfer duration. Upon approach of Mars, the spacecraft begins a spiral capture into low Martian orbit, taking 33 days. It takes approximately 520 days until the Earth return window occurs. During this time, the vehicle may carry out several mission profiles. The astronauts may remain in Martian orbit. Additionally, 15,000 kg are allotted to payload carried by the vehicle, allowing for the attachment of a Mars lander. The spacecraft may additionally be used to control robotic systems on the Martian surface by orbiting crew.

Following the Martian stay, the vehicle begins transfer back to Earth. The spiral Mars escape takes 31 days, and the transfer to Earth 195 days. Upon capture into high Earth orbit, the Mars Transfer Vehicle performs rendezvous with the crew capsule. The crew unloads into the capsule and begins the process of lowering orbital height and Earth reentry. The vehicle spirals down to an orbital altitude of 950 km, passing through the Van Allen belts once again without crew on board. This final spiral takes 52 days. Total mission duration, including astronaut boarding and unboarding is approximately 1,150 days. The crew spends a total of approximately 990 days in space. This however varies with launch year.

Once the Mars Transfer Vehicle has established orbit at 950 km, a period of 1.1 years exists until the next available launch window. During this period, inspection, maintenance, repair, and resupply are performed to prepare the vehicle for its next mission to Mars. At least 8 launches are required in this phase. Waste aboard the space is removed and deorbited. Argon and ADCS propellant tanks are removed and replaced. Along with supplies and new payloads. Following the completion of this phase, a new Mars Transfer Phase is initiated.

4

Systems Engineering Overview

This chapter provides an overview of the systems engineering approach used to aid the detail design phase. Included are the system requirements, as well as the N2 chart to identify interdependencies and the finalised technical budgets.

4.1. System Requirements

The User Requirements [125] have been analysed and discussed with the relevant stakeholders. After this, they have been translated to System Requirements, which were agreed upon with all stakeholders:

- **SYS-01 The system shall have the capability of transferring at least 4 astronauts to Mars orbit and back.**
- **SYS-02 The system shall put humans in Mars orbit before 2040**
- **SYS-03** The system shall have the capability to stay in Mars orbits for at least 2 Earth weeks.
- **SYS-04 The system shall consist of interchangeable modules.**
- **SYS-05** The system shall be expandable with further modules.
- **SYS-06** Each module of the system shall be able to autonomously rendezvous and dock in orbit.
- **SYS-07 The system shall have the capability of transferring 12 astronauts to Mars and back using additional modules.**
- **SYS-08 Each module of the spacecraft shall have a service life of at least 20 years**
- **SYS-09** The system shall be launched using one existing launcher family.
- **SYS-10** The system shall have the capability of being resupplied for a new mission to Mars
- **SYS-11** The system shall maintain environmental conditions to within the same bounds as the International Space Station.
- **SYS-12** The system shall have a window with a transparent surface area of 1.0 m^2.
- **SYS-15 The human occupants of the system shall have a maximum exposure of maximum total of 1500 mSv per mission**
- **SYS-16** At least half of the system volume shall be reserved for payload.
- **SYS-17 The system shall generate at least 20 % return on investment over a 10 year window after start of operations**
- **SYS-18** The cost to launch payload to Mars orbit using the system shall be less than 2 M€/kg
- **SYS-19** Each subsystem shall be dual modular redundant.
- **SYS-20** All materials onboard of the systems shall comply with REACH regulations.
- **SYS-21** All electronic components shall comply with RoHS regulations
- **SYS-22** The system shall create no orbital debris at nominal end-of-mission
- **SYS-23** The system design process shall be documented for continuation missions

Here, the bold requirements have been identified as *Key requirements*. The compliance of the designed system with these requirements will be analysed in Section 16.8.

4.2. Design N2-chart

In order to determine the dependencies of the departments and to identify the most important iteration loops, an N2-chart was set up showing the interfaces between the design processes, shown in Figure 4.1. The design processes on the diagonal have been placed in such a way as to minimise the iterative interfaces (shown below the diagonal), and critical interfaces have been marked bold. From this an important iterative loop between the dry mass and the propulsion system size can be identified, well known in aerospace design. Other important iterative designs identified from this are the sizing of the ADCS as the Mass Moment of Inertia (MMOI) of the whole spacecraft is required, and the logistics of the in-orbit assembly of the spacecraft. The latter iteration was tackled by designing each module to fit inside the Falcon fairing (chosen during the preliminary design phase) from the start, and to plan the assembly logistics only once an initial layout and mass estimate is determined. The constraints and requirements coming from these logistics were then taken into account during the next design iteration.

Inputs:	Mission requirements	Selected launcher	Initial sizing	Data rate required														Outputs:
TRAJECT	Determine trajectory		**Thrust and Delta-V required**	Orbital altitude			Mission duration					Sun distance			Pointing accuracy requirements		→	Mission trajectory
GROUND		Design packing method	Packing constraints			Packing constraints		Packing constraints						Packing constraints			→	
PROP	Thrust and Delta-V available		Size propulsion system							Engine power consumption		Heat generation?	Engine packing	**# of engines size of tanks**			→	
COMMS				Size Antenna						Communication power consumption	Communication power consumption			Antenna size	Pointing accuracy requirements		→	
CD&H					Size computer systems						Computer power consumption			Computer size			→	
LS						Size ECLSS systems	Recycling efficiency	Atmospheric requirements			**ECLSS power consumption**	Atmospheric requirements	Habitat layout requirements	ECLSS size			→	
LS							Determine supplies						Supply volume	**Supply mass**			→	
STRUC								Design docking method	Docking port size	Docking power consumption	Docking power consumption		Docking port layout	**Arm sizing**	Slew rate and stability requirements		→	
PAY									Size payload		Payload power consumption			Internal and external payload size			→	Payload capabilities
EPS										Size primary energy source		Reactor heat generation		Reactor + MHD sizing			→	
EPS											Size backup power source		Backup power type	**Backup power sizing**			→	
THERMAL											Power required?	Design thermal control	Conduction path Cooling method	**Radiator sizing**	Pointing requirement?		→	
STRUC						# of habitat modules							Determine layout		MMOI	# of modules to orbit	→	Spacecraft layout
STRUC			**Dry mass**					Module mass Maximum length				Spacecraft area		Overall sizing	Mass	Mass to orbit	→	Spacecraft size
ADCS											ADCS power consumption			ADCS size	Design ADCS		→	
OPS								Docking operations					Module launch order	Size constraints		Write in-orbit assembly plan	→	Operational procedures

Figure 4.1: The design process N2-chart

4.3. Overall sizing

Sizing of the spacecraft is done by following the following steps:

- Sum the dry mass of all subsystems except propulsion and add a contingency factor
- Determine the required ΔV and initial Thrust-to-Weight ratio from the simulations. The approach for this is discussed in Chapter 6.
- Using a simple Python script, determine the required propellant, the required amount of engines and the amount of reactors required to power these engines. The power density of the reactors is explained in Chapter 9.
- From the required thermal excess power, determine the radiator mass (Chapter 10)
- Iterate this process with the new radiator masses until the values converge

In the final design phase of this project, two main iterations have been performed, in which the technical budgets (discussed below) have been updated and each subsystem has been resized accordingly. The iterations are discussed in more detail in Section 16.1.

4.4. Final Technical budgets

During the design iterations of the spacecraft, various technical budgets are used and regularly updated, in order to keep track of the technical specifications of the system and to set design targets for the subsystems. The technical performance measures used are mass,

(backup) power, Signal-to-Noise Power, ΔV and received radiation. The budgets of the final iterations are displayed below; for a discussion on the development of these budgets during the design iterations so far, the reader is referred to Chapter 16.

4.4.1. Mass budget

A top-level mass budget is shown in Figure 4.2, showing the distribution of payload, dry mass and propellant. The dry-mass is further broken down in Figure 4.3, where the various subsystems get assigned a mass. A contingency of 10 % on the dry mass has been used to size the system compared to the mass estimates in the following subsystem chapters.

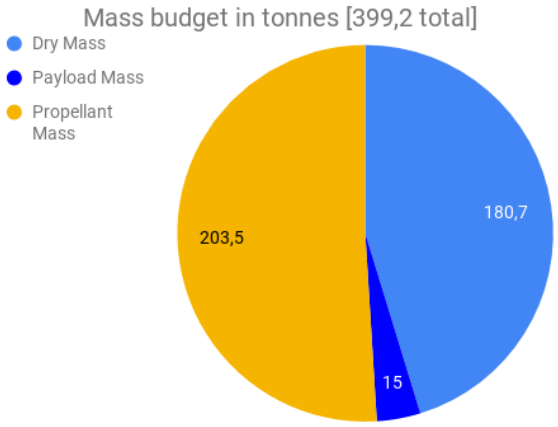

Figure 4.2: The top-level mass budget for the Mars mission

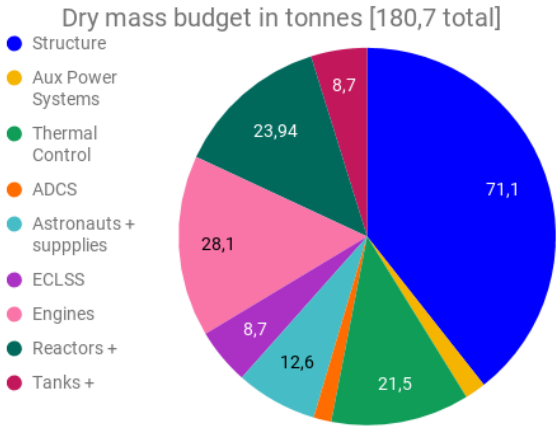

Figure 4.3: The dry mass budget for the Mars mission

4.4.2. Power budget

To assign a maximum power usage to each subsystem and determine the total required power on board of the spacecraft, a power budget is set up, shown in Figure 4.4. This budget excludes the power required for the electric propulsion system, as this is orders of magnitude larger, but it should be noted the power comes from the same source, the fission reactors. As can be seen in the figure, the largest part of the energy is used to cool the reactors. Next to this, 30 kW has been reserved for payloads as a baseline. In the current configuration of 4 reactors, more power is however available if required.

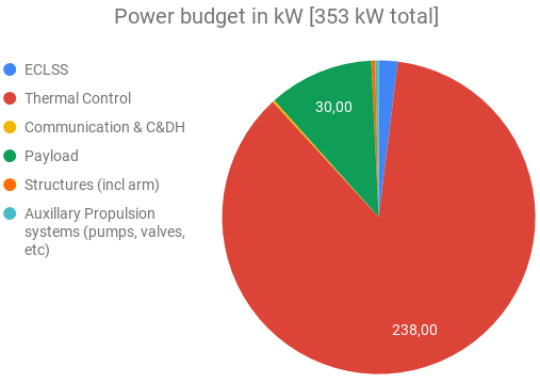

Figure 4.4: The power budget for the Mars mission

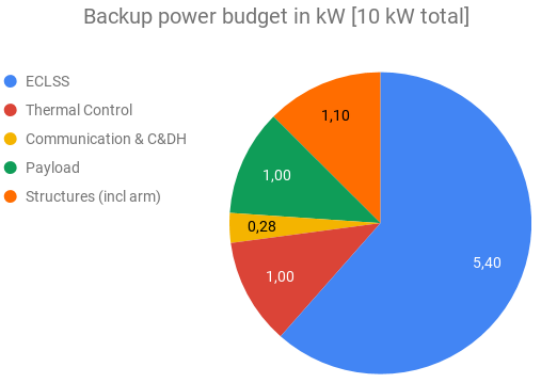

Figure 4.5: The backup Power budget for the Mars Mission

In case of emergency, the reactors could be shut down, and the system can operate on its backup solar power. As the power delivered by the solar panels is very limited, a backup power budget was made, shown in Figure 4.5. As can be seen, only the life-critical systems are operational: the ECLSS, the communication system, a backup electrical heater and the robotic arm. A small amount of power is reserved for payloads which might need to keep

running. As will be explained in Chapter 9, the solar panels are sized for a 10 % safety factor on the budget shown in the figure, so for 10 kW.

4.4.3. Link budget

The link budget will be described in Section 12.3.2, as it is relatively independent of the rest of the mission. Its main interface with the rest of the system, the power consumption of the communication systems, has been incorporated into the power budget.

4.4.4. ΔV budget

Figure 4.6 gives an overview of the ΔV required for the mission. As the required ΔV can change per mission depending on the relative position of Earth and Mars, the worst case has been assumed. The numbers come from simulated trajectories which are discussed in Chapter 6.

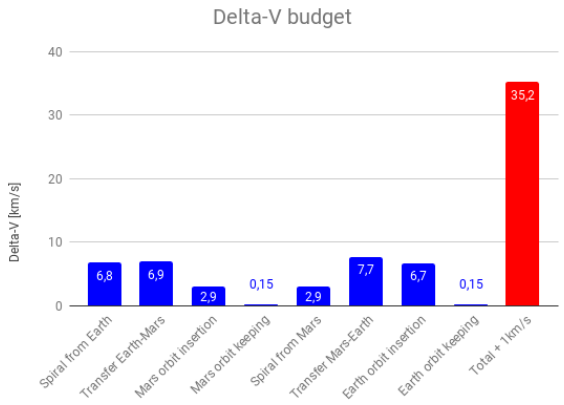

Figure 4.6: The ΔV budget for the Mars mission

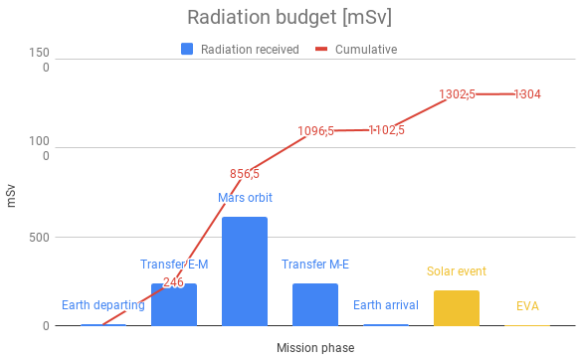

Figure 4.7: The radiation budget for the Mars mission

4.4.5. Radiation budget

The amount of radiation received per mission phase is shown in Figure 4.7, as well as the cumulatively received radiation. This overview can be used to check the total amount of radiation received stays below 1500 mSv, as specified by the requirements.

The first five columns are the standard mission outline, and the last two are additional events which add significantly to the radiation received, even though they only occur infrequently.

4.5. V&V and Sensitivity

Verification and Validation and the sensitivity of the design to assumptions and requirements has been approached by analysing them for each subsystem, and integrating the most important conclusions on a system level. The end of the coming chapters will describe V&V and Sensitivity of each specific subsystem, and Chapter 16 will discuss the most important findings and their impact on the overall design. The only exception is that Chapter 6 discusses Verification and Validation during the calculation process to justify the programmed code.

5
Propulsion

This chapter begins the discussion of the Mars Transfer Vehicle subsystem detailed design. The results of the propulsion trade-off performed during the baseline phase are briefly presented, followed by a description of the final design.

5.1. Key requirements and constraints

An important design factor for the Propulsion system was the high ΔV requirement to get to Mars orbit, and especially to return to Earth orbit, which is unlike many other missions which burn up in Earth atmosphere[11]. This resulted in the choice between bringing large amounts of propellant, and using very efficient (and thus low-thrust) propulsion systems.

5.2. Midterm Trade-off Results

Several propulsion systems were considered during the midterm: Chemical, Nuclear Thermal and Nuclear Electric Propulsion (NEP, NTP) were considered for different mission profiles. NEP was chosen based on the significant reduction in wet mass and spacecraft volume. Chemical propulsion required a large total mass to be launched, whereas NTP uses low-density hydrogen as fuel: both would significantly increase the number of launches. The VASIMR was specifically chosen due to its relatively high TRL and large amount of documentation available. Next to this, it was chosen over NASA's Xenon-fuelled X3 Ion thruster, as Xenon is too rare on Earth to use for such a large mission, while the VASIMR uses the widely available Argon. As mentioned in the introduction, this concept design is largely based on the assumption that nuclear electric propulsion will be readily implementable by 2040. As this is a system with a low TRL in comparison to other subsystems in this concept design, it was developed to a lower level of detail. Focus was put on performing initial sizing, and determining the impact of the propulsion system on the other subsystems.

5.3. VASIMR

The Variable Specific Impulse Magneto-plasma rocket (VASIMR) engine uses electric power to heat up the liquid argon to a plasma. A set of magnetic fields then further accelerate this plasma through a nozzle to provide thrust. Figure 5.1 shows the general functioning of the engine, and the engine specifications are resumed in Table 5.1.

To achieve an acceleration of 0.7 mm/s^2, a total of 48 engines are required. 52 engines will be used to provide redundancy. This results in an engine mass of 28,080 kg and a total argon mass flow of 9 g/s. Engines were clustered in 4 racks that could be individually launched. Each rack also contains a reactor-MHD assembly to provide power, as will be discussed in Chapter 9.

5.4. Tank sizing

As the rest of the Propulsion system, the tanks have only been sized to a preliminary amount of detail. The main focus is put on identifying the required subsystems and obtaining a first order mass and size estimate.

5.4.1. Propellant sizing

As discussed in Section 5.2, Argon will be used as propellant for the VASIMR engines, which is a cryogenic fluid. In order to store the propellant, it needs to be cooled to temperatures below 150 K, and kept at this temperature during the entire mission. As can be seen in Figure 5.2, the lower the temperature of the liquid Argon (LAR), the lower the pressure at which it can be stored. This means a trade-off needs to be made between using stronger cooling systems and stronger tanks.

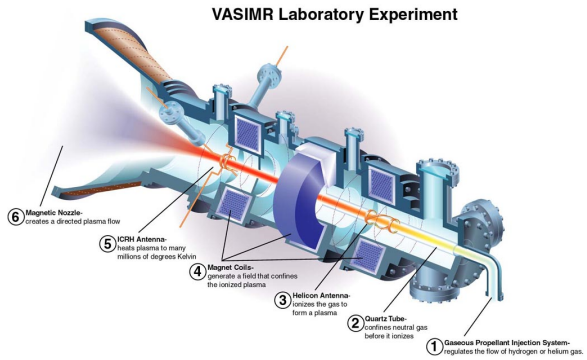

Figure 5.1: VASIMR Engine cycle

Specification	
Required Power [kW]	200
Specific Impulse [s]	5,000
Thrust [N]	5.8
Weight [kg]	540
Argon massflow [g/s]	0.118

Table 5.1: VASIMR Specifications

For now, it was assumed that low-pressure tanks were more favourable, especially considering the large required tank size and the relatively high storage temperature of Argon compared to Hydrogen and Oxygen. As baseline, it is chosen to store Argon at a temperature of -170 ^oC and pressure of 7 bar, giving it a density of 1,300 kg/m^3 according to Figure 5.3.

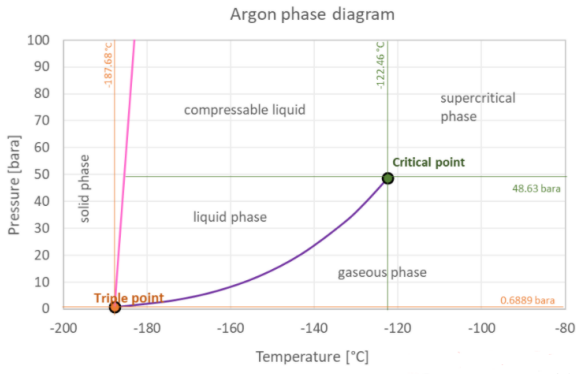

Figure 5.2: The phase diagram of Argon [1]

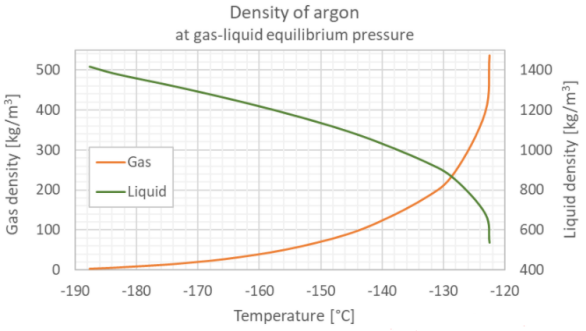

Figure 5.3: The relation between temperature and density of Argon

5.4.2. Tank geometry

Based on the most recent sizing and budgets from the previous chapter, 203.5 t of LAR is required for the full mission. As will be explained in Chapter 13, the Falcon Heavy has a capability to LEO of 35 t, meaning the propellant will have to be brought to orbit in six launches. To prevent having to siphon the launched Argon into another tank, it is decided to use six separate tanks on board of the spacecraft as well. Using the before mentioned density and an ullage of 2 %, this results in a required volume of 24.1 m^3 per tank. The standard shape of a cylinder with spherical endcaps[130] is used. As initial sizing showed that the tanks will be located in between the radiators on top of the central truss, the radius is chosen to be 1.2 m, in order to limit the heat influx on the cryogenic tanks from the radiators. This results in the dimensions described in Table 5.2.

As tank material, the same Whipple shield configuration as described in Section 11.4.1 is used, to protect the tanks from micro-meteorites. Extra Multi-Layer-Insulation is used to reduce heat-flow through the tank liner. Using Equation 5.1, it is calculated that for a pressure of 7 bar, the inner aluminium liner provides enough strength with a safety factor of 2.

$$\sigma_{hoop} = \frac{p_{tank} \cdot r}{t_{wall}} \tag{5.1}$$

5.4.3. Other required subsystems

The main auxiliary systems required are the cooler systems, pressurant tanks and the feed system. Regarding the cryocooler, NASA has been actively researching Reduced- [27] and

[1] Retrieved from `https://www.engineeringtoolbox.com/argon-d_1414.html`

Zero-Boiloff [66] storage of cryogenics, including specific systems to use for Mars exploration [67]. Due to the long duration of Mars mission, the amount of propellant that would boil off when using current crycoolers would become prohibitive, as also identified in the Mars Reference Design Mission [11]. It is assumed Zero-Boiloff storage of cryogenics is possible by 2040, and further sizing of the system has not been performed.

The feed system required for the propulsion system consists of pumps, pipes and valves to transport the Argon from the tanks to the VASIMR engines. The system has not been sized, but is assumed to be relatively small due to the low total mass flow of 9 g/s required. Next to this, pressurant is required to keep the tanks at 7 bar while they are being emptied, which for this volume will be a significant amount.

Argon Input	
LAR mass	203.5 t
Storage temperature	-170 ^oC
Tank Pressure	7 bar
LAR Density	1,300 kg/m^3
LAR Volume per tank	26.1 m^3
Ullage	2 %
Tank Volume	26.6 m^3

Tank dimensions	
Inner radius	1.2 m
Inner Al liner thickness	4.8 mm
Insulation space (Kevlar, MLI)	107 mm
Outer Al liner thickness	2 mm
Cylindrical length	4.3 m
Total length	6.7 m
Mass per tank	1,040 kg
Total mass for six tanks	6,240 kg

Table 5.2: Tank sizing results

5.5. Further research

As mentioned, the propulsion system has only been designed to a very preliminary level. Several aspects are identified that require more research to come to a conceptual design level:

- Research and test burn times for the VASIMR engine of up to 4 months, as only tests of 100 hours have been performed so far.
- Size the feedsystem, cryocoolers and pressurant tanks by identifying the required components and their size.
- Find the optimal storage temperature of Argon: lower temperature means higher density and thus smaller tanks, but requires stronger cryocoolers and more insulation.
- Design the system in such a way that the amount of interfaces during docking operations are kept to a minimum to avoid leaks. Similarly, research reliable methods for hydraulic connections during autonomous docking.

5.6. Sensitivity Analysis

The current tank design is based on the assumption that Zero-Boil Off cryocoolers are feasible in the future. If not, the amount of Argon rapidly increases, especially for such a long mission. With a representative boil-off rate of 0.1 % per day [66], 70 % of the propellant is lost during the mission, meaning more than triple the initial amount of propellant needs to be taken. Without a ZBO cryocooler, the mass of the spacecraft will increase so rapidly that the design becomes in-feasible, and thus the development of it will be a critical aspect of the mission. The sensitivity to changes in engines will be discussed on a system level in Chapter 16.

5.7. Verification & Validation

VASIMR tests are required to verify the specifications on which the system has been sized, especially when used for such a long duration. Furthermore, validation tests are required when the 48 VASIMR engines are integrated into the rest of the feedsystem.

Various tests are required for the tank. First of all, it will need to be pressure tested, first at above-zero and after at cryogenic temperatures. Then, a long-duration cooling test is required, to verify no leaks, boil-off or warming takes place over time. For validation, full propulsion system tests will have to be done, to ensure the tanks work together with the feedsystem, pumps and engines.

6

Trajectory Design

The design of low-thrust interplanetary trajectories is an interesting mathematical problem that has been discussed in many research papers. Unlike Hohmann transfers, low-thrust interplanetary trajectories cannot be approximated by mathematical functions and therefore numerical simulation is required. Many variables govern a low-thrust trajectory and all of them have to be optimised with respect to the parameters of interest such as the required thrust, fuel mass and transfer-time. This chapter will describe the methods that were used for simulating and optimising the trajectory for a range of possible missions in order to determine the thrust and total ΔV that needs to be delivered by the spacecraft.

6.1. Problem Statement

While electric propulsion has the advantage of delivering a high I_{sp} compared to chemical propulsion, and therefore consuming less fuel for a given ΔV, it can only deliver low levels of thrust. Long burn times, in the order of 100 days are therefore required for a transfer from Earth to Mars. A typical transfer from Earth to Mars orbit will consist of the following manoeuvres:

- **Escape burn**: A continuous burn in the direction of velocity (with respect to Earth) until escape velocity is reached. The spacecraft travels along a spiral trajectory and is taken from an orbit around Earth into an orbit around the Sun, similar to Earth's orbit around the Sun.
- **Burn 1**: Departure burn that puts the spacecraft on an interplanetary transfer orbit (an elliptic orbit around the Sun). This burn takes place shortly after the Escape burn.
- **Burn 2**: Arrival burn that takes the spacecraft from an interplanetary transfer orbit into an orbit around the Sun, similar to Mars' orbit around the Sun.
- **Capture burn**: A continuous burn opposite to the direction of velocity (with respect to Mars). The spacecraft travels along a spiral trajectory until an orbit of the desired altitude around Mars is established.

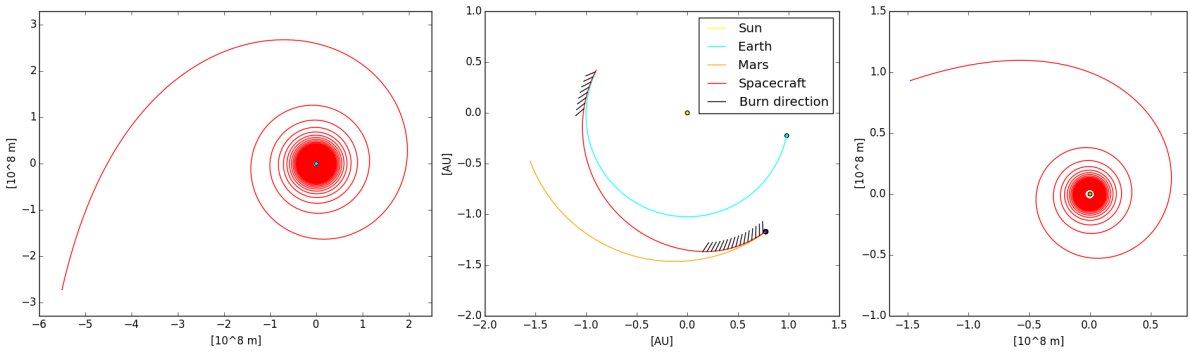

Figure 6.1: A typical low-thrust trajectory transfer from Earth to Mars. The spiral Earth-escape trajectory is shown on the left, the interplanetary transfer is shown in the centre and the spiral Mars-capture is shown on the right.

The escape and capture burns are most efficient when the thrust vector is pointing in (for escape) or opposite (for capture) to the direction of velocity with respect to the orbited body. Therefore little optimisation is required and the ΔV needed for such a manoeuvre can be easily computed using numerical simulation. Optimisation of Burn 1 and 2 however, requires much more attention. For a given launch date there is an infinite amount of possible transfer trajectories with varying amounts of ΔV and transfer-time. Typically, shorter transfer-times require a higher ΔV and therefore a compromise solution has to be found, also taking into account the launch date. Transfers from Mars to Earth consist of similar manoeuvres.

6.2. Simulation and Optimising Algorithm Development

This section will firstly describe the steps taken to develop a numerical simulation capable of simulating trajectories with continuous low thrust burns. The simulation will be mostly discussed with respect to simulating the interplanetary transfer, however it will also be capable of simulating continuous burns for spiral escape or capture orbits. Secondly the development of an optimising algorithm used to find the optimum interplanetary transfer trajectory between the point of Earth escape and Mars capture (or vice versa) will be discussed.

6.2.1. Trajectory Simulation

Based on a set of given input variables such as launch date, initial mass, I_{sp} of the propulsion system, thrust vector as a function of time, desired transfer-time, etc. the simulation shall output the trajectory of the spacecraft (position as a function of time). The following assumptions were made with the aim of making a simulation with reasonable accuracy and reducing computing time:

- The simulation is limited to taking into account the gravitational effects due to the Sun, Earth, Mars and the spacecraft only. It was calculated that the gravitational force from Jupiter, which is the next largest force acting on the bodies in the system is 5 orders of magnitude smaller than that of the Sun.
- All objects are assumed to be point masses.
- The position of the bodies is restricted to two dimensions; the inclination of the planetary orbits is neglected.
- Gravitational attraction is the only force acting on the bodies with the exception of the spacecraft which is also subject to thrust from rocket engines.
- Thrust and I_{sp} of the propulsion system is assumed to be constant. Ad Astra Rocket Company, the developer of the VASIMR thruster claims that by varying the I_{sp}, a 15 % propelant saving can be achieved [35], however the thruster has only been proven to work at a maximum I_{sp} of 5,000 s as opposed to the assumed 30,000 s [37].
- The thrust vector angle α is approximated as two third degree polynomials; one for Burn 1 and one for Burn 2. Burn 1 takes place from start of simulation until t_1 and Burn 2 takes place from t_2 until the desired transfer-time is reached. This means that 10 variables are used to define the thrust vector in time. From now on, the set of variables will be referred to as $\vec{x}$. Below is the mathematical formulation of the thrust vector angle as a function of time as well as an example shown in the plot.

$$\alpha(t) = \begin{cases} C_1 + C_2 t + C_3 t^2 + C_4 t^3 & 0 \le t \le t_1 \\ C_5 + C_6 t + C_7 t^2 + C_8 t^3 & t_2 \le t \le t_t \end{cases} \quad (6.1)$$

$$\vec{x} = [C_1,\ C_2,\ C_3,\ C_4,\ C_5,\ C_6,\ C_7,\ C_8,\ t_1,\ t_2] \quad (6.2)$$

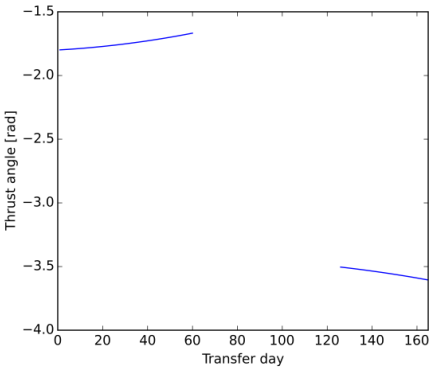

Figure 6.2: Example of calculated thrust angle as function of time for a given $\vec{x}$ using Equation 6.1.

Python was chosen as the programming language of choice. Bellow is an overview of the important functions and their integration which creates the trajectory simulation.

- A class definition *body* was created. When called, *body* creates an object with all relevant parameters; such as mass, position and velocity. Additionally, *body* also has an *update* function where a list of all the other bodies in the system is passed as well as a time interval. When called, *update* first calculates the resultant acceleration vector due to

the gravitational force of the bodies in the system using Newton's law of gravitation and thrust if applicable. The acceleration vector is then used to update the velocity of the object after the specified time interval. The updated velocity vector is used to update the position of the spacecraft after the time interval. If applicable the mass of the object is also updated by subtracting the mass of expelled rocket fuel based on the mass flow. The mass flow is assumed to be equal to the thrust divided by the exhaust velocity.

- The class definition *var* was created. When called, *var* creates an object which stores all the input and output variables of a trajectory simulation. This made accessing and tracking information of various runs of the simulation possible. Input variables include launch date, transfer-time, positions of planets at launch date, time step dt after which bodies shall be updated and the set of coefficients $\vec{x}$ defining the thrust angle in time.
- The simulation loop *sim* was defined and was a function of a *var* instance. When called, the simulation is initialised by unpacking the input variables and creating appropriate bodies using *body*. Then the simulation loop is ran until the specified transfer-time is reached. Each run of the loop consists of updating all bodies and increasing time by dt.

Using the above functions a trajectory simulation can be performed by creating a *var* instance with the desired input variables, executing *sim* using the *var* instance and then unpacking the desired outputs from it.

```
unpack passed variables
create the Sun, Earth, Mars and the spacecraft with appropriate position, velocity and mass
set time to zero
set ΔV to zero
while time is less than desired transfer time do
    increase time by dt
    for all bodies in the system do
        calculate gravitational acceleration due to all other bodies
        if body is spacecraft then
            calculate thrust vector angle using Equation 6.1
            calculate acceleration from thrust
            add acceleration from thrust times dt to ΔV
            subtract used fuel from mass
        end
        adjust velocity based on calculated accelerations
        adjust position based on velocity
    end
end
return position as a function of time and used ΔV
```

Algorithm 1: Simplified representation of the simulation loop.

6.2.2. Boundary Conditions

In order to produce any valid transfer trajectory between Earth and Mars, certain boundary conditions have to be met. The spacecraft has to arrive to a desired location with respect to Mars and has to have zero excess velocity. In order to find such trajectories the *pos_opt* boundary condition optimising algorithm was developed. Using desired input variables and a guessed $\vec{x}$ that produces a trajectory that does not meet the boundary conditions (ie. does not arrive to Mars), the *pos_opt* algorithm tries to find a solution that meets the boundary conditions by adjusting $\vec{x}$. The *pos_opt* algorithm makes use of the steepest gradient descent minimum finding method. First the simulation is ran with the guessed $\vec{x}$ and a scoring function evaluates how far the trajectory is from meeting the boundary conditions. Then, derivatives of the score s are taken with respect to $\vec{x}$ by adjusting all coefficients within $\vec{x}$ (one at a time) by a small amount dC, running the simulation with the adjusted $\vec{x}$ and calculating the difference in score over the difference in coefficient, ds/dC. Once $ds/d\vec{x}$ (the set of derivatives ds/dC) is known, $\vec{x}$ is adjusted by an amount γ times the gradient in the direction of $ds/d\vec{x}$, ie. the direction of the steepest descent of the score:

$$\vec{x}_{new} = \vec{x}_{old} - \frac{ds}{d\vec{x}} * \gamma \tag{6.3}$$

The value of γ can be adjusted for the desired result; a larger γ yields a faster convergence but will stop converging at a lower accuracy. The algorithm can be ran multiple times with gradually decreasing γ.

while *boundary conditions not met* **do**
  run simulation with current $\vec{x}$
  use scoring function to evaluate trajectory
  for *coefficient in* $\vec{x}$ **do**
    adjust coefficient by dC
    run simulation with adjusted $\vec{x}$
    use scoring function to evaluate trajectory
    calculate ds/dC and place it into $ds/d\vec{x}$
  end
  adjust $\vec{x}$ by γ in the direction of $ds/d\vec{x}$
end

Algorithm 2: Simplified representation of the position optimising algorithm.

6.2.3. Fuel Optimising Algorithm

Using the *pos_opt* algorithm described in the previous subsection, a transfer trajectory from Earth to Mars for a given launch date and transfer-time can be found. This algorithm will however yield different solutions when different initial guesses are used. This means that the solution found is not unique and further optimisation is required in order to find the specific solution that requires least amount of fuel. For this, the fuel optimising *fuel_opt* algorithm was developed. The *fuel_opt* algorithm uses the solution found by *pos_opt* as input. Because the thrust and I_{sp} are assumed to be constant, the solution that requires the shortest burn time will also require the least amount of fuel. Two nested loops are therefore used to find the solution with the shortest burn time. The outer loop decreases the burn time by decreasing t_1 and increasing t_2 by a small amount. It then runs the inner loop which is very similar to the *pos_opt* loop, it tries to meet the boundary conditions by changing all variables within $\vec{x}$ except for t_2; which is always adjusted such that the total burn time is kept constant. The cycle is repeated until the boundary conditions cannot be satisfied with the allocated burn time. The last solution which could satisfy the boundary conditions was deemed as the trajectory that requires the least amount of fuel given the launch date and transfer-time.

while *convergence in inner loop still possible* **do**
  lower total burn time by small amount
  while *boundary conditions not met* **do**
    run simulation with current $\vec{x}$
    use scoring function to evaluate trajectory
    for *coefficient in* $\vec{x}$ *except* t_2 **do**
      set t_2 such that burn time is satisfied
      adjust coefficient by dC
      run simulation with adjusted $\vec{x}$
      use scoring function to evaluate trajectory
      calculate ds/dC and place in into $ds/d\vec{x}$
    end
    adjust $\vec{x}$ by γ in the direction of $ds/d\vec{x}$
  end
end

Algorithm 3: Simplified representation of the fuel optimising algorithm.

Performing boundary condition and fuel optimisation in a single loop was was also developed, however it was only partially successful and did not reliably converge for a range of possible transfers. Accuracy that could be reached was also lower.

6.3. Simulation Verification

The simulation loop utilises simple Newtonian mechanics to model the motion of objects subjected to gravitational forces. The correct implementation of the physical laws can be verified by simulating a simple case for which an analytic solution exists. For this analysis an object of negligible mass (1 kg) was introduced into a circular orbit abound the sun at one astronomical unit. The orbital period of the object was calculated using Kepler's third law and the simulation was ran for the specified time. As predicted, the object returned close to its original position suggesting that the physical laws of motion were implemented correctly. This was also a good opportunity to analyse the effect of the size of the time-step. The simulation was ran multiple times with gradually decreasing time-steps. The results are summarised in Figure 6.3. As can be seen, the distance to the point of departure decreased with decreasing time-step, indicating an increase in simulation accuracy. Note that the dips in the graph represent solutions which by chance achieved a higher accuracy. The important parameter is the minimum accuracy that will be achieved with a given time-step. This can be determined by interpolating the peaks of the graph. As can be seen, this will form a straight line on the log-log plot and an order of magnitude decrease in time-step leads to an approximately order of magnitude increase in accuracy. Note that in this case, 10^7 m represents 0.001 % of the total distance travelled.

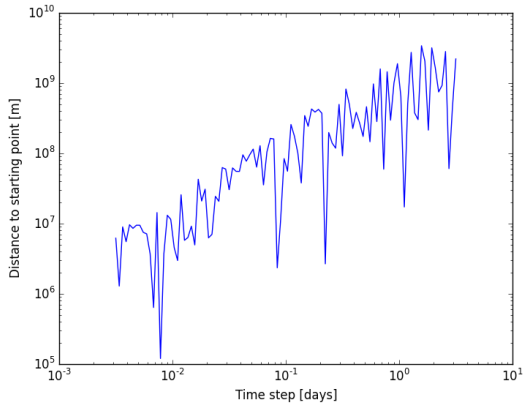

Figure 6.3: Results of the verification of the implementation of the physical laws of gravity and motion.

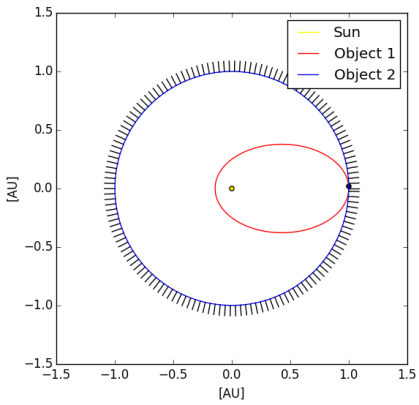

Figure 6.4: Results of the verification of thrust implementation. Black lines represent the direction of thrust.

In order to verify that the application of thrust was modelled correctly, once again a simple situation with an analytic solution is considered and computed both numerically and analytically. The following situation was chosen: Two objects of 1 kg are placed at a distance of 1 AU from the sun and both are given exactly half the velocity required for a circular orbit. The first object is only subjected to gravitational forces and should enter an elliptic orbit with its aphelion at 1 AU. For the second object, the thrust perpendicular to its velocity required to keep it in a circular orbit is calculated. If the thrust is applied correctly, the second object should enter a circular orbit around the sun at 1 AU and have an orbital period of exactly two years (since it is travelling at half the velocity of Earth). In order for an object to have circular motion, a constant resultant force F_c given by Equation 6.4[1] is required in the direction perpendicular to its velocity. This will not be equal to the gravitational force given by Equation 6.5[2]. The magnitude of the thrust perpendicular to the velocity is therefore calculated such that the sum of the gravitational force and the thrust is equal to the required centripetal force. For this particular test, the function that updates the mass of the

[1] where m is the mass of the object, v is the velocity of the object and r is the radius of the orbit.
[2] where G is the universal gravitational constant and M is the mass of the orbited body (Sun).

spacecraft is disabled in order to keep the acceleration due to the thrust constant.

$$F_c = \frac{mv^2}{r} \qquad (6.4) \qquad\qquad F_g = \frac{GMm}{r^2} \qquad (6.5)$$

As can be seen from Figure 6.4, and was also confirmed by analysing the output of the simulation, Object 2 has entered a circular orbit around the Sun at 1 AU with a period of two years. This suggests that the thrust was implemented correctly and is working as expected.

The last part of the simulation that needs to be validated is the implementation of the mass flow leading to the change of the mass of the spacecraft over time. This was easily verified by simulating a single transfer to Mars. The required ΔV and change in mass was verified to correspond to theory using Tsiolkovsky's equation.

6.4. Validation of Optimised Trajectories

Validation of the trajectories produced by the simulation was done by comparing our results to results produced by more sophisticated simulations. This method was chosen due to the lack of available trajectory data of actual spacecraft. Simulation developed by Aaron M. Schinder was chosen due to the available results presented in his research paper [110]. The research paper contains a plot showing the required ΔV for optimised Earth-Mars transfers departing on the 1st of August 2020 for a range of transfer-times. The data was carefully extracted and plotted along with data produced by our own simulation. The results are presented in Figure 6.5. As can be seen, the general shape of our simulated data matches the shape of the validated data. It is however evident, that our simulated data contains a lot more noise and sometimes converges to lower ΔV solutions. The extra noise was likely introduced by the fact that our simulation used less strict requirements on meeting boundary conditions in order to reduce computational time. Our simulation was stopped when a score of less than 0.5 was achieved. This is equivalent to reaching the destination within a distance of 0.015 AU and an excess velocity of less than 707 m/s. This can also be the cause for the simulation to converge to lower ΔV solutions, however different departure and arrival states may also be the cause. It is not clear from from the paper what departure and arrival states were assumed. Our simulation started at position when the spacecraft reached escape velocity after spiralling out and finished at the start of the spiral Mars capture; these points were calculated by simulation beforehand. Both of the simulations that are being compared used a time step of approximately one day.

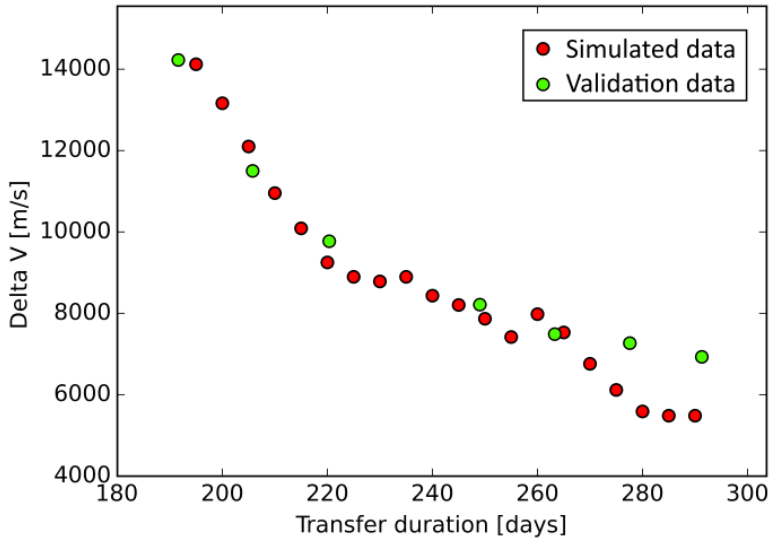

Figure 6.5: Earth-Mars transfer trajectories departing on the 1st of August 2020 optimised for minimum ΔV.

6.5. Results and Trajectory Planning

6.5.1. Trajectory Analysis

Using the functions described in the previous sections, it was now possible to calculate the required ΔV for a given launch date within a launch window and a given transfer-time. The launch window for an Earth-Mars transfer occurs every synodic period which is approximately 2.1 years. The launch window in early 2046 was chosen as a case study. A thrust of 348 N, an initial acceleration of 1 mm/s^2 and a I_{sp} of 5000 s was assumed. The required ΔV was computed for a variety of launch dates and transfer-times. In order to decrease computation time, the thrust vector function of both burns was assumed to be constant in time (coefficients C_2, C_3, C_4, C_6, C_7, and C_8 were neglected). The results are presented in Figure 6.6.

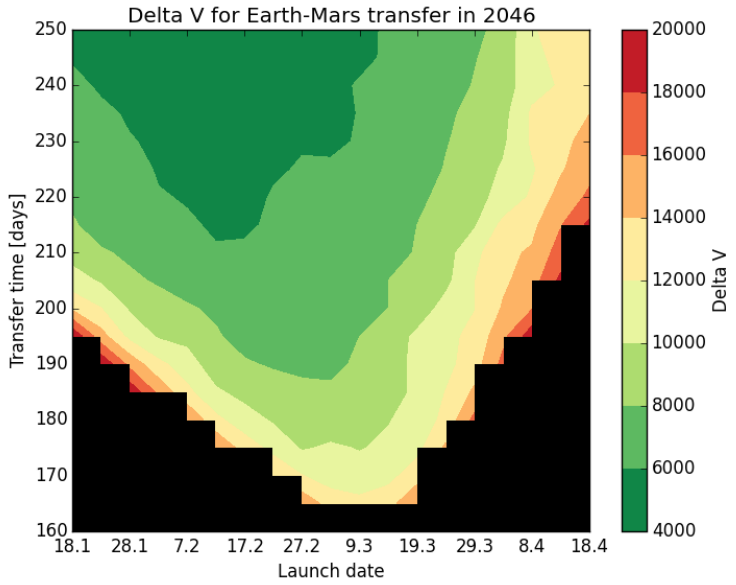

Figure 6.6: ΔV required for a range of possible launch dates and transfer-times within the 2046 launch window. The separation between individual data points is 5 days on both axes. Note that launch date is assumed to be the start date of the Earth-Mars transfer and not the actual launch from Earth surface.

As can be seen, longer transfer-time trajectories require a smaller ΔV and the ΔV increases as you move away from the ideal launch date. The ideal launch date also changes slightly for different transfer-times; as the transfer-time decreases, the ideal launch date moves forward. Transfers within the black region are not possible, a higher thrust would be required. The trajectories on the boundary are ones where Burn 2 takes place immediately after Burn 1 (continuous thrusting) and all trajectories above the boundary are characterised by two distinct burns.

Figure 6.6 is a powerful tool for trajectory planning and sensitivity analysis. When planning the trajectory for the Delta Mars mission, it is important to choose a fast trajectory in order to minimise the consequences of time spent in deep space, such as exposure to radiation and psychological effects. As can be seen, a 200 day transfer is about as short as it can get before the ΔV starts to increase rapidly. The ΔV for such a transfer was also found to be similar to the previously assumed ΔV. Further optimising was done using the full ten coefficient thrust vector representation. Analysis on the required acceleration was also performed and it was found that the initial thrust can be lowered to about 0.7 mm/s^2 without significantly changing the required ΔV and the transfer time. In order to accurately predict the required ΔV for the complete mission, a similar ΔV plot should be produced for the transfer back as well. For now, limited analysis was done on the transfer back and a semi-optimised trajectory was assumed in order to get an estimate for the required ΔV.

6.5.2. Results and Implications

The proposed trajectory is presented in Figure 6.7 and Figure 6.8.

	Earth spiral-out	Earth-Mars transfer	Mars spiral-in	Mars spiral-out	Mars-Earth transfer	Earth spiral-in
Initial acceleration [mm/s^2]	0.709	0.814	0.988	1.049	1.113	1.379
Manoeuvre duration [days]	103	200	33	31	195	52
Initial orbit altitude [km]	950 (Earth)	610000 (Earth)	170000 (Mars)	500 (Mars)	610000 (Earth)	950 (Earth)
Delta V [m/s]	6768	6926	2938	2932	7679	6657
Fuel fraction used [-]	0.129	0.115	0.044	0.041	0.097	0.073

Figure 6.7: Trajectory plan for a mission in 2046. The Earth-Mars and Mars-Earth transfers start on 4.3.2046 and 26.4.2048 respectively.

Using information from Figure 6.7, a full mission including all the manoeuvres was planned. A period of 7 days was estimated for loading and unloading crew in high Earth orbit. The results are presented in Figure 6.8 and Figure 6.9. It was further estimated that the spacecraft will spend 412 days in LEO in between missions. All refuelling, resupplying and maintenance activities must be performed within this window.

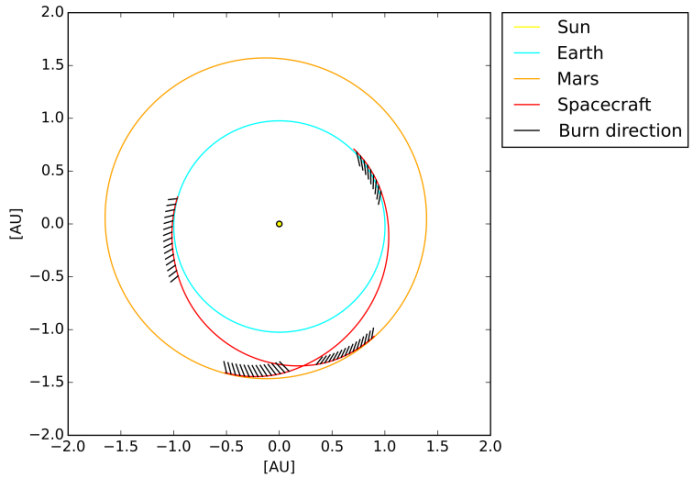

Figure 6.8: Depiction of chosen trajectories.

Event	Start Date	Duration [days]
Spiral out:	14.11.2045	103
Astronaut loading:	25.02.2046	7
Transfer:	04.03.2046	200
Spiral in:	20.09.2046	33
Stable Mars orbit:	23.10.2046	520
Spiral out:	26.03.2048	31
Transfer:	26.04.2048	195
Astronaut unloading:	07.11.2048	7
Spiral in:	14.11.2048	52
Arrival	05.01.2049	-

Figure 6.9: Mission plan for the 2046 launch window. Mission duration from LEO to LEO is **1,148 days** and the approximated astronaut time spent in space is **993 days**.

Implications for spacecraft subsystems that flow from the trajectory analysis are as follows:

- The propulsion system shall provide an initial acceleration of at least 0.7 mm/s^2.
- The propulsion system shall deliver a Delta V of at least 35,200 m/s. This includes a safety margin of 4 %.
- The spacecraft shall be able to support astronauts for at least 993 days.
- All refuelling, resupplying and maintenance activities must be performed within 412 days.
- Requirements flowing from nominal trajectory are not considered to be driving for the ADCS as the manoeuvres do not require rapid change in pointing. The time between Burn 2 and spiral deceleration (during which the spacecraft needs to flip) can take in the order of one day with negligible consequences.

6.6. Sensitivity Analysis and Recommendations

One of the highly sensitive parameters of the trajectory is the departure date. To help visualise this, the ΔV was plotted for a set transfer duration and a range of launch dates. The results are presented in Figure 6.10. As can be seen, the required ΔV increases rapidly as soon as the launch date is missed by more than two days. Careful planning is therefore critical for the success of the mission and time reserve before departure is probably a better strategy to deal with possible delays rather than taking extra fuel to account for a possible less favourable trajectory. Since moving the launch date was shown to be very sensitive, it

is suspected that the trajectory will be also sensitive to power outages (ie. any malfunctions leading to temporary shut down of the propulsion system). For now a similar sensitivity can be assumed and more analysis should be performed in this area. The required ΔV for missions departing in different launch windows is expected to vary by less than 10 %, neglecting particularly bad launch windows which occur around every 15 years [79]. A ΔV plot should therefore be produced for every potential launch window in order to confirm that a mission can take place.

Sensitivity analysis of the target altitude at mars was also performed. The results are shown in Figure 6.11. As can be seen, the required ΔV for an escape from a 500 km orbit does not significantly change with altitude. Increasing the altitude by 100 km decreases the required ΔV by roughly 0.036 m/s. The other spiral manoeuvres were shown to have similar sensitivity.

It was also shown that the required thrust is less sensitive and can possibly be lowered. Lower thrust requires longer burn times, however the overall ΔV does not significantly change. Further optimising should therefore be investigated by generating solutions for range of possible thrusts. Further, more time should be invested into validation and a sample trajectory of an actual spacecraft should be reproduced. Finally, the simulation and optimising algorithms should be adjusted to incorporate deviations caused by debris-avoidance manoeuvres or delays and extensive analysis should be done in order to determine the required reserve fuel.

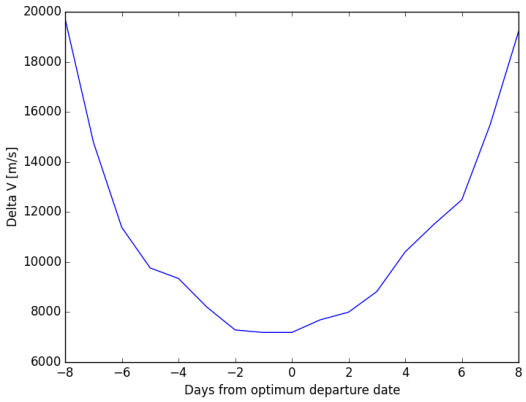

Figure 6.10: Sensitivity analysis of departure date on the required ΔV for a one way transfer.

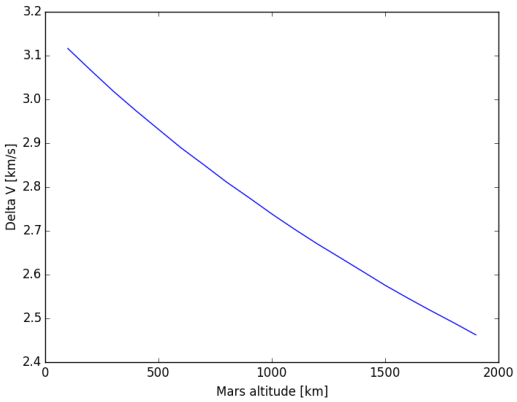

Figure 6.11: Sensitivity analysis of Mars orbit altitude on the required ΔV for spiral escape.

7

Environmental Control and Life Support

This chapter details the design of the Environmental Control and Life Support Subsystem (ECLSS) on board the spacecraft. The ECLSS design is based off of equipment currently in use on the International Space Station, adapted to the requirements of a Mars mission. The chapter begins with a discussion of the human design requirements on the ECLSS in Section 7.1. Section 7.2 provides an overviews of the process flow through the spacecraft and describes the ECLSS assemblies chosen to fulfil all necessary processes. Sizing of the ECLSS, including determining the required spare parts to ensure a reliability of 99.9 % is performed in Section 7.3. Section 7.4 discusses the considerations made in the design of the crew cabin. Section 7.5 provides a brief discussion of further ECLSS design that must be carried out, however is beyond the scope of this design phase. A sensitivity analysis of the ECLSS under changing reliability and mission duration requirements is conducted in Section 7.6. Methods to verify and validate the ECLSS are discussed in Section 7.7.

7.1. Design Requirements

Design requirements on the ECLSS stem from the biological needs of the astronauts in order to survive the mission to Mars. These can be modelled as a set of inputs which need to be provided to the astronauts, as well as a set of astronaut outputs that need to be removed and processed. Additional requirements stem from the environmental conditions needed in the pressurised cabin. Flowing down from these are requirements on the reliability of the system and functions which the system needs to fulfil in the case of a failure in order to keep the astronauts alive.

Human inputs and outputs are taken as the starting point for specifying the ECLSS requirements. A crew load of four astronauts is used to determine the total input and output amounts. The inputs required consist of potable water for drinking and food preparation, washing, toilet flushing, oxygen for respiration, and food for consumption. Astronaut outputs consist of urine combined with flush water, humidity condensate from respiration and perspiration, used wash water, carbon dioxide, and fecal waste. These are summarised in Table 7.1 and Table 7.2.

Human input	Amount [kg/crew-day]	Amount per Day [kg/day]	Mission Amount [kg]
Drinking and food preparation water	2.38	9.52	10282
Wash Water	1.29	5.16	5573
+ Urine flush water	0.50	2.00	2160
Oxygen	0.84	3.36	3629
Food	1.50	6.00	6480

Table 7.1: Required daily human inputs in the space environment [61] [68]

Human Output	Amount [kg/crew-day]	Amount per Day [kg/day]	Mission Amount [kg]
Urine plus flush water	2.00	8.00	8640
Used wash Water	1.29	5.16	5573
Water condensate	0.50	2.00	9850
Carbon dioxide	1.00	4.00	4320
Solid waste	1.50	6.00	6480

Table 7.2: Daily human outputs in the space environment [61] [68]

Additional requirements derive from environmental conditions which must be sustained in the pressurised cabin. A cabin pressure range of 96.5 - 102.7 kPa and temperature range

of 15 - 25 degrees Celsius are taken as requirements based off of the International Space Station. Oxygen partial pressure is maintained at 19.4 - 23.7 kPa. The remainder of the atmosphere is composed of nitrogen as well as carbon dioxide exhaled by the crew [98]. Active air circulation systems are required to prevent carbon dioxide build-up in any region of the cabin as convection does not naturally circulate air due to the lack of gravity. The ECLSS is designed to a reliability of 99.9 % for one mission. The following sections detail the design employed to meet these requirements.

7.2. ECLSS Process Overview

Human inputs and outputs must be provided and respectively removed by the ECLSS. This may be accomplished by taking all supplied required for the entire mission, or by recycling resources over the duration of the mission. Systems for recycling resources add significant mass and power requirements to the spacecraft; however, the overall mass of the spacecraft is reduced by recycling resources as opposed to carrying all resources for a mission of this duration [61]. Systems are therefore employed for the recycling of waste water and urine to potable water as well as the generation of oxygen and removal of carbon dioxide. These are based on the ISS ECLSS consisting of a urine processor assembly (UPA), water processor assembly (WPA), oxygen generation assembly (OGA), carbon dioxide removal assembly (CDRA), and carbon dioxide removal system (CRS). These systems process the outputs generated by humans and provide the conditions and materials necessary to sustain life. Collection points, namely the spacecraft toilet and urinal, as well as vents from the pressurised cabin moving air to the respective ECLSS components. A trace contaminants control assembly is used to monitor the cabin atmosphere for contaminants and absorb unwanted substances. A schematic of the ECLSS process flow can be seen in Figure 7.1. These systems are capable of handling a 6 person crew load based on the requirements laid out in Table 7.1 and Table 7.2 [97] [31]. The ECLSS is a closed system with the exception of food and nitrogen inputs, as well as solid waste and acetylene overboard venting. An initial water supply is taken to account for the non-complete recycling performed by the ECLSS. Nitrogen is required to maintain cabin pressure and to account for leakage of the pressurised cabin.

7.2.1. Carbon Dioxide Removal Assembly

The purpose of the CDRA is to scrub CO_2 from the air in the pressurised cabin. The CO_2 is separated from the air and sent to the CRS, where it undergoes a Sabatier reaction and is converted to H_20 and CH_4. Removal of CO_2 is done through a set of 4 desiccant/sorbent beds, each contained in an orbital replacement unit (ORU). Cabin air is first purified in a desiccant bed, following which CO_2 is removed in a sorbent bed. The air then passes through a further desiccant bed where it is rehumidified before entering the cabin. The ISS CDRA has proven highly effective and removes 100 % of metabolic CO_2 generated by the crew [22] [31].

7.2.2. Carbon Dioxide Reduction System

CO_2 scrubbed by the CDRA is routed to the CRS, where it undergoes a Sabatier reaction with H_2, forming H_2O and CH_4 as shown in Equation 7.1. H_2 is supplied from the products of the OGA. The output H_2O is routed to the WPA for further treatment. In the current ISS configuration, CH_4 is vented overboard. This results in a significant loss of potentially usable hydrogen. For this reason, NASA is currently developing a plasma pyrolysis assembly (PPA) as a post-processor of the CH_4 produced during the Sabatier reaction. The PPA uses a pyrolytic process to convert CH_4 to H_2 and C_2H_2 as per Equation 7.2. The produced H_2 is recirculated into the Sabatier reactor of the CRS [132]. C_2H_2 is vented overboard.

$$CO_2 + 4H_2 \rightarrow 2H_2O + CH_4 \tag{7.1}$$

$$2CH_4 \rightarrow 3H_2 + C_2H_2 \tag{7.2}$$

7.2.3. Urine Processor Assembly

The UPA takes as input astronaut urine and flush water, and processes these to water for further processing as well as urine brine. The distillation assembly of the UPA contains a rotating centrifuge which separate evaporated water from the urine brine/water mixture at

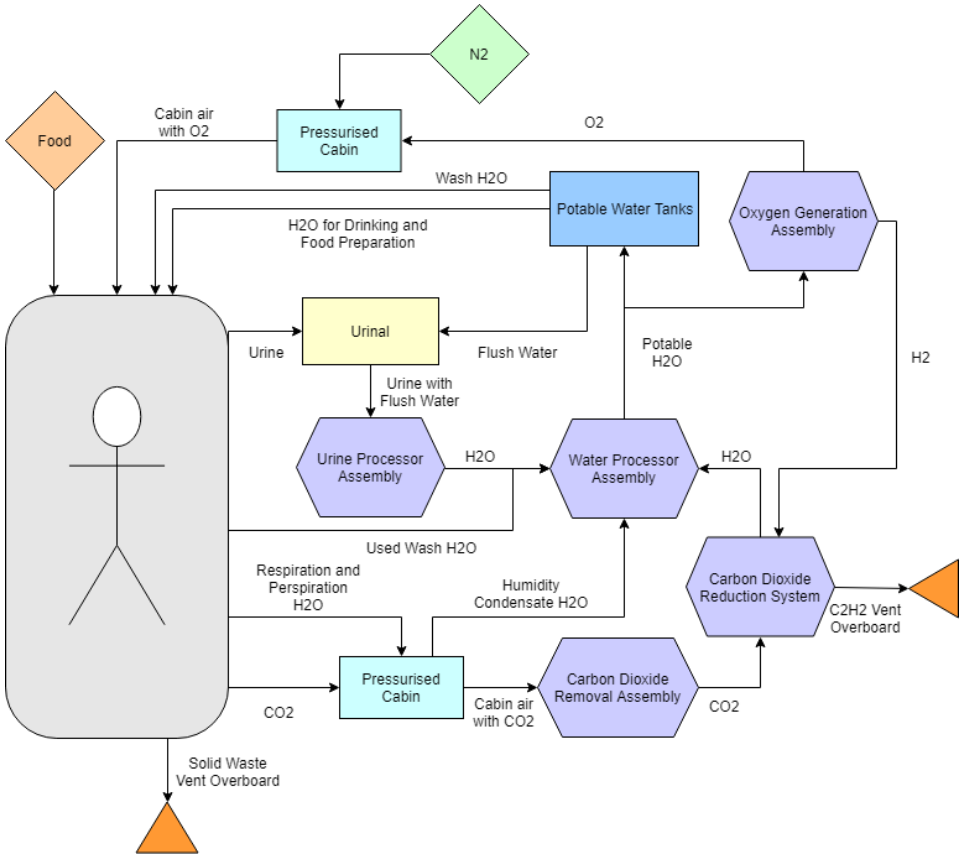

Figure 7.1: Simplified schematic of the ECLSS process flow

low pressure. Further details on the functioning of the UPA can be found in [97]. The UPA has a water recovery efficiency of 80 % [61]. Waste water tanks are used to buffer water from the urinal prior to UPA processing as well as processed water before it enters the WPA.

7.2.4. Water Processor Assembly

The WPA is the final step in the water processing loop. It take pretreated water and processes it to potable conditions. Input sources of the WPA are the products of the UPA, CRS, and humidity condensate removed from the cabin air. The WPA consists of particulate filters, multifiltration beds for dissolved contaminants, and gas-liquid separators [97]. The potable water produced by the WPA is routed to a potable water for astronaut use, as well as the OGA.

7.2.5. Oxygen Generation Assembly

The OGA converts potable water to O_2 and H_2 via electrolytic cells as per Equation 7.3. The products of electrolysis are separated via a rotary separator. The produced oxygen is fed back in to the pressurised cabin. H_2 is circulated to the CRS where it fuels the Sabatier reaction. Hydrogen sensors are used at the outlet to the pressurised cabin to ensure hydrogen containment [97].

$$2H_2O \rightarrow 2H_2 + O_2 \tag{7.3}$$

7.3. System Sizing

7.3.1. Sizing Spares for Reliability

As the proper functioning of the ECLSS is critical to astronaut survival during the Mars mission, a reliability of 99.9 % over the course of a mission is designed for. Data from the ISS ECLSS shows frequent failures and wear-out of various ECLSS components. When failure occurs, spare parts are required to maintain the proper functioning of the ECLSS. Additionally,

the ECLSS must be designed such that components are easily removable and replaceable when such action is necessary. This is accomplished by the use of orbital replacement units (ORUs). Sizing the amount of spares required to ensure a certain reliability requires the use of a statistical approach making use of Poission probability mass functions. The Poisson distribution, shown in Equation 7.4, models the probability of x failures of an ECLSS component over a given course of time given that the probability of each component failing is independent of time at which the last component failed. k is the amount of components, and λ is the mean amount of failures of a component during one mission duration.

$$P(X = k) = e^{\lambda}\frac{\lambda^k}{k!} \tag{7.4}$$

Setting $P = 0.001$, k is solved for using simple iteration. This approach is used in [61] and uses data of the mean time before failure of each ECLSS ORU aboard the ISS. Data for the mass of each ECLSS component is also available in [61], as well as the rack mass of each ECLSS assembly. Based on this data and a mission duration of 1,080 days, the total mass of the ECLSS including spares can be determined. A mass breakdown of the ECLSS per assembly, as well as respective probabilities of failure during one mission, is shown in Table 7.3. These results are compiled from a component level breakdown of each assembly. This can be found in Appendix A

Assembly	Mass [kg]	Probability of all spares failing
Oxygen generation assembly	1874.5	0.000664
Urine processor assembly	1,657.9	0.000694
Water processor assembly	2,403.7	0.000842
Carbon dioxide removal assembly	513.3	0.000827
Carbon dioxide reduction system	1,426.5	No data
Total	**7875.9**	**0.000842**

Table 7.3: Mass budget of ECLSS assemblies including spares required for 99.9 % reliability

7.3.2. Supply Sizing

Sizing of the initial supplies that need to be taken aboard the spacecraft was determined by the recovery efficiency of the ECLSS assemblies and the duration of the mission. Current ECLSS systems aboard the ISS obtain a water recovery rate of 88 % [97]. Stoichiometrically, the OGA is capable of producing 0.89 kg of oxygen from one kg of water. This leads to a mission potable water requirement to the OGA of 4,900 kg, including a 1.2 safety factor to account for potential disparities between predicted and actual oxygen demand. The remainder of the potable water required for all other activities sums to 21,620 kg over one mission with the 1.2 safety factor, leading to a total water requirement of 26,520 kg. With 88 % recovery this leads to an initial water supply of 3,180 kg. Matching ISS requirements of maintaining 1,000 kg of reserve water for emergencies at all times, the total water supply needed amounts to 4,180 kg.

Nitrogen supply is required to account for air leakage of the pressurised cabin. A leakage rate of 0.062 kg/day is assumed, based on the 0.227 kg/day leakage rate on the ISS [107] and the pressurised volume ratio of the spacecraft to that of the ISS of 250/916. This leads to a nitrogen supply requirement of 100 kg over the mission duration using a 1.5 safety factor. A tank plus feed system mass of 70 kg is assumed based on similar systems [70]. Food supply mass is taken from Table 7.1, with a 1.2 safety factor, leading to a food supply mass of 7,780 kg. This leads to a total ECLSS and supply mass of 19,985 kg. The electrical power usage of the ECLSS is estimated at 5.4 kW based on data from [102].

7.3.3. Volumetric Sizing

ECLSS assemblies are fitted into racks which are attached to the interior walls of the pressurised cabin. These racks are modelled after international standard payload racks (ISPR) used on board the ISS, which provide 1.6 m^3 of internal volume each [78]. The OGA, WPA, and UPA require one ISPR each [65]. It is assumed that the combination of the CDRA and

CRS occupy one further rack. Volume required to store spare components is estimated under the assumption that component volume is directly proportional to their mass. Based on component masses shown in Appendix A, the percentage of each assembly mass composed of replaceable parts is calculated and multiplied by the 1.6 m^3 volume of each ISPR. The mass of spare components in each assembly is summed and multiplied by the volume of replaceable parts. This results in a spare components volume of 11.7 m^3.

The volume of the potable water tank is obtained directly from the water supply requirement of 4,180 kg, necessitating 4.2 m^3 of tank space, accounting for the tank itself. 7,780 kg of food supply is stored assuming a density of 306 kg/m^3 [93], resulting in 25.4 m^3 of volume required. 100 kg of nitrogen is stored in tanks with a volume of 0.48 m^3 [70] [26]. A breakdown of the ECLSS volume budget is shown in Table 7.4

Element	Volume [m^3]
WPA	1.6
UPA	1.6
OGA	1.6
CDRA + CRS	1.6
Spare components	11.7
Potable water tank	4.2
Food	25.4
Nitrogen tank	0.48

Table 7.4: Volumetric sizing of the ECLSS

7.4. Crew Considerations in the Pressurised Cabin

Several considerations are made to accommodate the crew in the pressurised cabin over the course of the mission. This is of significance due to the long duration which will be spent in the spacecraft. A minimum requirement of 25 m^3 of liveable space per astronaut is set. Three pressurised modules make up the crew cabin. Each module has a unique purpose in the spacial layout of the spacecraft. The outermost module is dedicated to private quarters for the crew and shared living space. The middle module serves as working space and houses systems such as the ECLSS assembly racks, scientific payloads, and potable water tanks. The third module is dedicated to storage of items such as food and ECLSS spares, and additionally provides supplemental living space and access to the cupola. The internal layout of the crew cabin can be seen in Figure 7.2 Each crew member has their own private sleeping quarters, which are positioned as far as possible from the reactor-engine assembly. A lavatory is located in the living module, along with equipment for exercise. Artificial lighting shall be used inside the cabin to simulate a 24 hour day-night cycle.

Following walk-through of the pressurised cabin in virtual reality, several observations were made as to potential issues that may arise while living in the space for a prolonged period. Although the internal volume of the cabin is considerable, unlike the ISS, astronauts are only able to move in one dimension as the modules are stacked linearly. Experiences in virtual reality showed that this made the cabin feel more constrained, as there is a continuous line of sight through the whole spacecraft. The ability to see all locations where one can go made the interior seem smaller. For this reason, collapse-able translucent screens are placed in the joints between modules to disrupt line of sight, creating distinct spaces within the cabin.

7.5. Further Work

Due to the scope of this design phase, focus has been placed on designing the ECLSS to handle the process flow through the crew cabin. Design for physical and psychological astronaut health in deep space have been largely overlooked, however must be designed for prior to the mission. An extensive list of potential health effects has been compiled based on data from [94]. Key findings are summarised in Table 7.5 and Table 7.6. Additional considerations

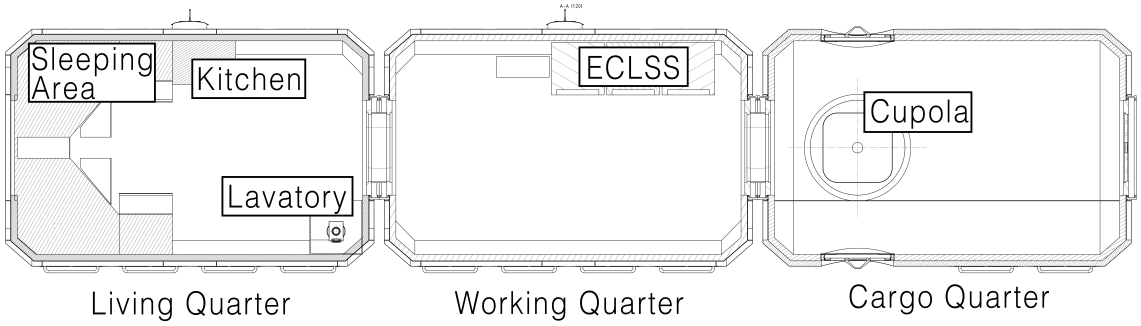

Figure 7.2: Internal layout of the crew cabin

to be made are ECLSS contingency planning in the event of an assembly failure, cabin failure, or atmospheric contamination. Items such as chemical oxygen generators should be considered. Additionally, systems for fire detection and suppression must be designed.

Health issue cause	**Symptoms**
Change in bodily fluid distribution due to microgravity	Tachycardia, hypotension, arrhrytmias , decreased vital lung volume, decrease in body water, hormonal disruption
Microgravity in sensory system	Reduction of vision, taste changes, dizziness
Microgravity on musculoskeletal system	Decrease in mass, change in limb volume, reflex duration change, muscle and bone atrophy, foot disorders
Accumulated radiation (0.5 - 1.0 Sv)	Cataracts,changes in blood cell structure
Accumulated radiation (1.0 - 1.5 Sv)	Neoplasms, Atherosclerosis
Accumulated radiation (1.0 - 2.0 Sv)	Decreases in short term memory, recognition, and search speed, Alzheimers, Parkinsons

Table 7.5: Physiological health concerns in deep space

Health issue cause	**Symptoms**
Distance to Earth	Homesickness leading to stress, decreases in motivation
Radiation and microgravity environment	Change in condition
Limited amount of equipment and activities	Monotony, boredom
1,000 days with three other astronauts	Misunderstandings, impaired communication, interpersonal conflicts, loss of privacy, stress
High work load	Stress, fatigue, decrease in performance
Small living space	Claustrophobia

Table 7.6: Psychological health concerns in deep space

7.6. Sensitivity Analysis

Sensitivity analysis of the ECLSS is conducted with respect to two changeable parameters: the mission duration, and the required ECLSS reliability. These parameters are considered the two most likely to change and to have direct influence on the sizing of the system, primarily through changing the amount of required spare components. Crew mission durations are varied from 850 to 1,150 days, and the acceptable probability of failure from 0.1 to 0.0001. The resulting analysis shows that mission duration does not have a significant effect on system mass, causing variation from 7,620 kg to 8,100 kg in ECLSS assembly and spares mass. Supply water and food mass reduce to 3,500 kg and 6,120 kg from 4,900 kg and 7,780 kg respectively. Food volume reduces to 20 m^3 from 25 m^3. Increasing the mission duration to 1,150 days increases assembly and spares mass to 8,100 kg, water and food mass to 4,390 kg and 8,280 kg, and food volume to 27 m^3.

Changes in the required ECLSS reliability have significant effect on the mass of the system. This is due to the fact that a significant portion of the ECLSS mass consists of spare components. With an acceptable probability of failure of 0.1, ECLSS assembly and spare mass reduces to 5,000 kg from 7,880 kg at baseline 0.001. With a failure probability requirement of 0.0001, the mass increases to 8,950 kg. This results in potential ECLSS system level mass decreases of 14 % and increases of 5 %. Current state of the art ECLSS systems require large amounts of spare parts due to poor component life times and reliabilities. A secondary result of this sensitivity analysis is that ECLSS mass can be significantly reduced with the development and qualification of more reliable ECLSS assemblies.

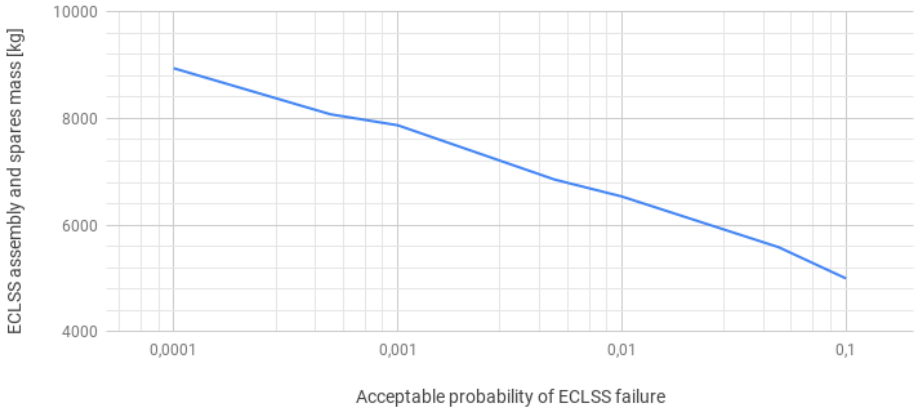

Figure 7.3: Variation of ECLSS assembly and spares mass with reliability requirement

7.7. Verification & Validation

Although the ECLSS of the Mars Transfer Vehicle is based on current ECLSS systems on the ISS, several considerable differences exist between the vehicles and missions which require changes in the ECLSS design and qualification. The deep space radiation environment to which the Mars Transfer Vehicle is exposed requires design for radiation resistance. Additionally, the inability for quick astronaut return to Earth in the event of system failure necessitates high reliability of the system. Due to the fact that current systems are not designed from this environment, systems developed for the Mars Transfer Vehicle will require extensive testing to ensure proper functioning and achieve flight qualification.

Testing of the ECLSS systems shall take place in two distinct phases, first on ground testing in a simulated environment, and secondly following launch and assembly prior to astronaut boarding. Ground based testing shall be conducted during development first of ECLSS assembly components to ensure proper functioning, radiation resilience, and lifespan. This is followed by assembly level testing in which the CDRA, CRS, UPA, WPA, and OGA shall all undergo testing. Upon completion of this testing phase, system level testing shall occur in

which the complete ECLSS is tested in a simulated environment. Low and high load cases shall be tested, as well as the system's ability to respond quickly to changes in process load. Off-nominal cases such as leaks and clogs shall also be tested to ensure that the ECLSS can return to nominal functioning following automated or crew repair. Components that are subject to wear or failure shall undergo further testing to simulate a full mission in order to ensure that design lifetimes are met. This testing phase shall be conducted at radiation testing facilities such as the ESTEC Co-60 facility[1]. Following ground based testing, the ECLSS will undergo a final testing phase following launch and spacecraft assembly. The ECLSS shall be initiated and will do a test run with simulated process flows while in orbit. This stage will qualify the ECLSS and ensure that all systems are functioning before astronauts board the spacecraft.

Verification that ECLSS requirements are met shall be performed using either testing, demonstration, analysis, or inspection. Demonstration will be used to verify the characterisation of the cabin environment, the overboard venting systems, the log masses of input/output water, the UPA converts urine to water, and the temperature measurements during operation. Analysis is used to verify the human needs and mission duration. Inspection to verify the usable volume of the pressurised cabin. Testing to verify the functioning of systems by use of a simulated radiation environment. Finally, demonstration is again used to verify the process flow rate adequacy and output sufficiency based on input resources.

[1] https://escies.org/webdocument/showArticle?id=230&groupid=6

8

Attitude Determination and Control

The importance of the Attitude Determination and Control System (ADCS), comes from the ability for the spacecraft to stabilize, orient in the desired direction, and sense the orientation of the vehicle relative to reference points. This stabilizing, orienting and sensing is performed by a system of sensors and actuators that react to disturbance torques which can be either internal or external and required slewing manoeuvres. [116] [75] [131]

8.1. Key Requirements and Constraints

The key requirement comes from the avoidance of space debris, which is further explained in Section 8.7. The requirement that follows from this is that the spacecraft shall be able to turn 180° in 2 hours and that the spacecraft shall be able to climb an altitude of 10 km in one hour. The constraint regarding these requirements is that the Mass Moment of Inertia (MMOI) and mass itself can not be immensely large since otherwise the CMGs and thrusters become too large and heavy.

8.2. Disturbance Torques

The ADCS must be designed to tolerate the disturbance torques, the applicable worst-case external disturbance torques are listed below.

- **Gravity gradient effects:** This gives a constant torque for Earth-oriented vehicle. The MTV is orbiting Earth for several months while undergoing resupply and maintenance, for this reason it is important to consider the effects of the gravity gradient and design for it. However, after performing the calculations according to [130], the disturbance torque turned out to be so low that it doesn't generate a driving requirement regarding the ADCS.
- **Magnetic field torques:** The torque is induced by Earth's magnetosphere and therefore only applies in this region of space, this is caused by the interaction between the geomagnetic field and the satellite's residual magnetic fields. However, when calculating the generated torque, it is in the order of $*10^{-3}$ Nm [130], which is well within the capabilities of the ADCS.
- **Solar radiation:** Solar radiation disturbance torque imposes the largest external torque when large solar panels are used since these absorb the radiation. However, the MTV only uses solar panels in case of engine shut down. The rest of the spacecraft is mostly reflecting and for this reason is not affected significantly by the solar radiation. On the other hand, the spacecraft is not in the magnetosphere of Earth for most of the mission duration, so the spacecraft is more affected by the radiation. Despite this, SMAD calculations confirm that these torques are significantly smaller than other driving requirements for the ADCS [130].
- **Aerodynamic torques:** The aerodynamic disturbance torque does not impose a huge effect on the spacecraft. This is due to the fact that for the longest duration of the mission, the spacecraft is in a stable orbit around Mars, in which the atmospheric density is extremely small due to Mars' weak atmosphere. Hence, the torque generated by aerodynamics is negligible. [130].

8.3. Sensors

Sensors are important for the ADCS to determine the attitude and the orientation of the spacecraft with respect to a reference frame. This requires measurement of vector quantities in this frame. The following sensors are considered:

- **Sun sensors:** Sun sensors detect visible light and measures the incidence angle between the light and the mounting base, they are widely used, accurate, and reliable [130].
- **Star sensor:** Star sensors map the stars that pass in their field of view, every movement of the spacecraft will result in an apparent shift of the stars. Using this method the spacecraft can maintain and determine its attitude with respect to the stars.

- **Horizon sensor:** Horizon sensors measure the temperature difference between the cold deep space and Earth's warm horizon by means of an infrared device, providing Earth-relative information regarding attitude determination for Earth-pointing spacecraft [130].
- **Inertial measurement unit:** Inertial measurement units use gyros and accelerometers to measure rotational and translational movement. They are used for measuring velocity in navigating and guiding manoeuvres.
- **Magnetometer:** Magnetometers are lightweight, simple, and reliable sensors that measure the attitude with respect to the Earth using the direction and magnitude of Earth's magnetosphere [130].

For the MTV, each module needs its own set of sensors to be able to determine its location since each module docks in LEO at an altitude of 950 km. The launch will be performed by a Falcon family rocket, which has an altitude accuracy of around 10 km. Therefore, the modules can be significantly separated from each other when arriving at the desired altitude. Each module would need to be capable of determining their orientation and location so that the space tug can locate and assemble the modules, the space tug is elaborated on in section Section 11.7. The orientation is then needed to dock the modules so that they both have the correct attitude for a successful dock. The configuration of the ADCS sensors for the MTV is six sun sensors, three star sensors, and an inertial measurement unit. The horizon sensors and magnetometers are not chosen since they provide attitude determination with respect to the Earth. When the MTV is on mission, Mars has a weak magnetosphere so the effectiveness of these instruments is severely decreased. Horizon measurements are not feasible either [130]. Redundancy is of great importance to increase reliability, especially with lives at stake. For this reason, six sun sensors are chosen to provide attitude determination in all directions. Two sun sensors already provide three axis attitude determination, but one sun sensor is added to achieve redundancy. Ensuring that if either one of the sensor systems fails there is still a fully operational sensor system available. The inertial measurement unit is used to process the navigation and guidance manoeuvres.

8.4. Actuators

Actuators bring the spacecraft to a desired orientation and exert a force or torque to either maintain the orientation or change it by use of a slewing manoeuvre. This actuation is performed by actuators, of which the following actuators are considered:

- **Thrusters:** Thrusters are mass expelling torque producers that work on either cold or hot gas with the capability of applying large torques compared to other actuators. They are primarily used to perform a fast attitude manoeuvre, momentum dumping, and avoidance manoeuvres for space debris. The thrusters can be placed in clusters and on all axes to provide omnidirectional manoeuvrability and provide torques large enough to counter disturbance torques or rotate the spacecraft in a desired direction.[75]
- **Reaction wheels:** Reaction wheels are torque motors with a rotor that has a high moment of inertia. This way, when the wheel is spun up the the wheel starts to generate torque in a predetermined axis. The wheel can be spun in either direction but is fixed to a certain axis, for this reason at least three reaction wheels are necessary to provide three axis control. A fourth wheel would be added for redundancy.
- **Control Moment Gyroscopes:** Control Moment Gyroscopes are similar to reaction wheels, the difference is mainly that the rotor inside the CMG is already spinning at a certain rpm to provide angular momentum. The rotor is then tilted at a certain gimbal rate, and due to this tilting of the generated angular momentum a torque is generated. This torque is much higher than with the reaction wheels, but also more complex. The CMG can be considered a torque amplification device because a small gimbal torque input can produce a large control output on the spacecraft. There is the choice between single gimbal CMGs and double gimbal CMGs. The benefit of double gimbal CMG is that it stores large amounts of momentum in a mass-efficient manner, and the single gimbal CMG is able to generate high output-torque in a power efficient way.
- **Magnetic torquers:**
  Magnetic torquers use electromagnetic coils in order to stabilise and orient. It uses

the Earth's magnetic field in order to create torque in a very efficiently, for this reason though it is not applicable in deep space [130].

8.4.1. Singularities

CMGs have some disadvantages, the most important one besides cost and complexity is the condition which is referred to as singularities. CMGs can have gimbal configurations for which there is no torque production, this singular state exists when all individual torques from the CMGs are perpendicular to this direction and must be avoided to perform manoeuvres without errors. Singularities propose a technical difficulty for CMGs, which increases complexity and has to be dealt with.

The double gimbal CMGs are able to create torque in two axes, however the extra actuation capabilities comes with a cost. The set of control torques of these CMGs can oppose each other, resulting in more power usage and less efficient torquing.

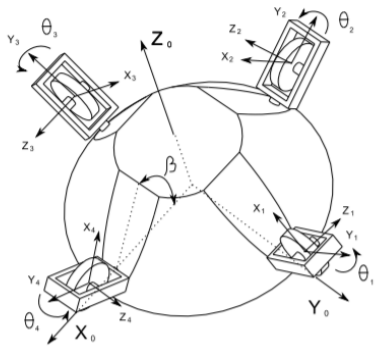

Figure 8.1: Pyramidal configuration of CMGs

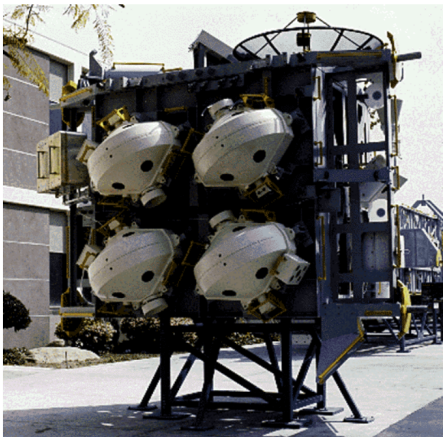

Figure 8.2: CMG configuration of ISS

To be power efficient and avoid singularities, a pyramidal configuration of at least three CMGs is developed [106], displayed in Figure 8.1. Another example is the International Space Station's, in which four CMGs are placed in a cluster next to each other. Two of them for three-axis control and two for redundancy, which is well designed since within the operating life of the ISS two have already failed [116] as can be seen in Figure 8.2.

8.5. Actuators Trade-off Results

Regarding the actuating system, thrusters, CMGs, reaction wheels, and magnetic torquers are considered. Their specifications are displayed in Figure 8.3.

Criterion	Torque capacity	Weight (kg)	Accuracy	Power	Pointing options	Propellant
Thrusters	1-18,000 Nm	4 + 0.03T	0.1-5 deg	1-5 W/(Nm)	No constraints	Requires
Control moment gyros	25-500 Nm	35 + 0.05H (100<H<2500)	0.001-1 deg	15-30 W (standby) 0.02 - 0.2 W/(Nm)	No constraints	-
Reaction wheels	0.01-1 Nm	5+0.1H (10<H<100)	0.001-1 deg	10-20 W at constant speed 500-1000 W/(Nm) when torqing	No constraints	-
Magnetic torque	4.7x10^-4 - 0.18	0.4-50	5 deg	0.6-16	North/South Earth only	-

Figure 8.3: Actuator trade-off table

From this table a combination of CMGs and thrusters are chosen. The CMGs have the advantages of being capable of generating large torques, large enough for the driving slewing

requirement of rotating 180° in 2 hours. CMGs are also power efficient, relatively lightweight, and do not require any propellant, as further explained in Section 8.6. A combination of CMGs and thrusters is chosen since thrusters are needed for momentum dumping when the CMGs are saturated and this combination can perform a manoeuvre of a 10 km climb or descent within one hour.

8.6. Zero-Propellant Manoeuvre

According to NASA [84], no more million-dollar manoeuvres are required anymore when using the CMGs. In the past spacecraft would perform a rotation with thrusters that required nearly $\$10,000$ per pound, costing millions of dollars [84]. Since the CMGs operate on power, and there is an estimated excess power of approximately 1 MW, it is only logical to avoid using thrusters. The power consumption of the CMGs in standby is approximately 25 W, and in the driving slewing manoeuvre is approximately 37 W [130].

8.7. Driving requirement

The driving requirement comes from the avoidance of space debris, since this requires a relatively fast rotation of the spacecraft compared to other slewing manoeuvres such as shield pointing and thrust alignment. The spacecraft will orbit Earth for over a year at an altitude of 900 km. Currently there is more than 500,000 pieces of debris that orbit the Earth, and since they travel with velocities up to 17,500 mph, small pieces can severely damage the spacecraft [80]. Since collision would impose catastrophic failure, measures have to be taken. Earth already possesses a station that tracks all the debris bigger than a fist. For debris smaller than a fist the spacecraft is protected with a strong structure that shall withstand impacts with a risk of penetration of 0.6 %, according to Section 11.4.1. Space debris bigger than a fist is tracked by the ground station and the information is sent to the designated spacecraft. In a worst case scenario, the spacecraft has to be able to rotate 180° in 2 hours and then climb or descent 10 km in one hour.

8.8. Sizing

8.8.1. Sizing CMG

The actual sizing of the CMGs is done with the following equations:

$$\theta = 0.5 * \alpha * t^2 \tag{8.1}$$

$$T = I_{SC} * \alpha \tag{8.2}$$

$$T = I_{CMG} * \omega * c \tag{8.3}$$

$$I_{CMG} = 0.5 * m * r^2 \tag{8.4}$$

$$I_{CMG} = 0.5 * \rho * V * r^2 \tag{8.5}$$

$$I_{CMG} = 0.5 * \rho * h * \pi * r^4 \tag{8.6}$$

In the equations stated above, the θ is the angle which the whole spacecraft has to rotate, α is the angular acceleration at which the spacecraft is rotating, ω is the angular velocity of the spacecraft, T is torque, I_{SC} and I_{CMG} are the MMOI's of the spacecraft and the CMGs, respectively.

According to Equation 8.1, a certain required acceleration is determined. From Equation 8.2, the required torque is calculated, the MMOI of the spacecraft is computed in Chapter 11. From the torque required, the MMOI of the CMG is generated from Equation 8.3 which gives a preliminary sizing in which the CMG is assumed to be of cylindrical shape. The outcome of this is a MMOI of 0.746 kgm^2 and a size of the CMG's rotor of $0.38 \times 0.38 \times 0.1$ m. The size of the whole CMG will be approximately 2.2 times the rotor size according to [117], resulting in CMG's of $0.84 \times 0.84 \times 0.22$ m clustered in a group of 4. With a weight of approximately 100 kg each ,based on calculations of the weight of the stainless steel rotor and the accompanying CMG structure [117].

8.8.2. Sizing Thrusters

$$T = \pi * \sqrt{\frac{(h_a + h_p + R_e)^3}{GM}} \tag{8.7}$$

$$dV = I_{sp} * g * ln\frac{m_d}{m_d + m_p} \tag{8.8}$$

$$T = \dot{m} * Isp * g \tag{8.9}$$

Regarding the variables in Equation 8.7, T is transfer time with h_a and h_p being the height of the apocenter and pericenter, respectively. G is the gravitational constant and M the mass of Earth. For Equation 8.8 dV is the amount of velocity difference needed for the transfer, I_{sp} is the specific impulse of the engine, m_d and m_p are the drymass and propellant mass. For Equation 8.9, T is thrust, $\dot{m}$ is the massflow and g is the gravitational acceleration constant. The driving requirement regarding the sizing of the thrusters is that the spacecraft should be able to avoid the incoming space debris with an altitude change of 10 km. This requires a delta V of 5.082 m/s, according to the Hohmann transfer calculations, and this manoeuvre shall be performed in one hour. This is because the worst-case scenario involves an impact warning three hours prior, with certainty increasing over time, allowing the option to not react at all when determined not necessary to save propellant. This requirement results in an amount of thrust and propellant mass of 807.1 kg, calculated from the rocket equation Equation 8.8. From these numbers, the thrusters and their tanks are sized. The 200 N bipropellant thrusters, manufactured by the ArianeGroup, are selected for propulsion with an Isp of 270 s [115]. This engine is illustrated in Figure 8.4. From Equation 8.9 the mass

Figure 8.4: 200N bipropellant thruster

flow is determined, which is 78 g/s. A total mass of 807.1 kg has to be burned to be able to reach the required delta V for the Hohmann transfer, which assumes a impulsive thrusting. As an assumption the team took 10 minutes as a maximum amount of time to consider the thrusting an impulse. The thrusters should thus be able to burn 807.1 kg in 10 minutes. To meet this, 18 of these engines are required. For redundancy, in case of failure, six extra thrusters are used to provide thrust for each direction. The total amount of engines becomes 24. The amount of propellant is 807 kg per manoeuvre. Assume a maximum of three avoidance manoeuvres per mission, a propellant mass of 2,421 kg is calculated. Monomethyl hydrazine fuel and nitrogen tetroxide oxidiser has a density of 0.875 kg/l [60], resulting in a tank volume of 2.767 m^3.

8.8.3. Placing thrusters

Three clusters of eight thrusters are placed on the spacecrafts truss, evenly spread in terms of distance to be able to provide thrust through the center of mass and not impose misalignments of thrust. These are then used mainly to either let the spacecraft climb/descend the ten km or momentum dump the CMGs. There are three sections of thrusters, with four blocks per section and two thrusters per block, with 24 thrusters in total. When performing the climb of 10 km these thrusters do not have to perform at their full potential of 200 N due to redundancy. In case of one thruster failing, another thruster can be shut down to still

be able to provide thrust through the center of mass without misalignment. The thrusters would be placed on the sides of the truss structure, gimballed thrusters would be used so that torque and thrust can be provided in every direction for momentum dumping and all engines can be pointed in the same direction to provide the necessary thrust for the manoeuvre [45]. The direction of thrusting for this is manoeuvre in the direction of travel, in order to perform the Hohmann transfer.

8.9. Radial Burn

For the team's mission, a Hohmann transfer is used to avoid space debris since this is the primary method learned by the team members to manoeuvre from one altitude to a higher or lower altitude. However, a radial burn that might be more efficient was researched [59]. Unfortunately, this requires simulation models and time which is not on hand. According to this source, radial burn is the most fuel-efficient manner to avoid space debris and can be performed within half an orbit prior. Hence, creating the opportunity to have the most accurate prediction of the incoming space debris. Which then at the last moment might indicate that no manoeuvre is necessary, saving large quantities of propellant [101].
Radial burns would be the best option, however does not in the scope of this project unfortunately. A radial burn is a burn of the thrusters in the direction orthogonal to travel, which then makes the spacecraft climb or descent in the most fuel-efficient and fast manner [59]. The spacecraft can return to its initial orbit by either rotating the spacecraft and then applying low thrust by the main engien or perform the manoeuvre using the ADCS thrusters, depending on which is more efficient.

8.10. Capture burn

To be able to be captured by the Mars' or Earth's gravity field and achieve a circular orbit around these planets a capture burn is performed. The transfer from Earth to Mars is a low thrust transfer and two burns are performed, the first one to leave Earth's orbit and the second one to be captured by Mars. Regarding the second burn, a burn is performed in the opposite direction of travel to decelerate and get in to the orbit of Mars. This capture burn is another low thrust manoeuvre and for this reason the time is not really constraining the manoeuvre since this is performed in approximately 30 days to spiralize in to Mars circular orbit. For ADCS this doesn't impose a driving requirement, since the manoeuvre can be scheduled in such a time frame that the 'flip' of the spacecraft to thrust, in the opposite direction of travel, can be performed over the time of a day. Hence not imposing a driving requirement since this slewing manoeuvre is considered slow. This manoeuvre is explained and demonstrated further in Chapter 6.

8.11. Momentum dumping

The CMGs of the spacecraft can become saturated when they are holding their maximum amount of angular momentum and can not hold more. The solution for this loss of control is to desaturate the CMGs by removing the excess angular momentum from the spacecraft. This is done by using thrusters to create an anticlockwise torque about that axis, slowing the gimbal rate down and desaturating the CMG [117]. The contingencies that were used in sizing the tanks for the thrusters provide sufficient propellant for momentum dumping since this only requires 6kg of propellant per saturated wheel [117], and they only have to be desaturated once in 3-4 months [1]https://ntrs.nasa.gov/archive/nasa/casi.ntrs.nasa.gov/20100024204.pdf.

8.12. Sensitivity Analysis

The ADCS system consists out of sensors and actuators. If there is a sudden change in pointing accuracy, turn rate, or mass moment of inertia, the configurations will change. These changes are explained here.

- **Pointing accuracy** The pointing accuracy is limited by the CMGs, the current maximum accuracy is 0.001°, according to [130]. Since SMAD is a relatively old book, this accuracy has improved but is still the limiting factor. If the required accuracy exceeds this number, then a new type of ADCS is required which doesn't exist yet. A pointing

[1] \unskip\penalty\@M\vrulewidth\z@height\z@depth\dp□

accuracy smaller than 0.001° would prove unfeasible at the current state of technology, there might be new developments of ADCS with a higher accuracy, however these TRLs are too low at this moment.

- **Turn rate** If the turn rate would have to be twice as fast, this would increase the amount of torque required according to Equation 8.2 since the angular acceleration, α, would increase. If the turn rate would be twice as fast, the time for the turn would be half. The relation between angular acceleration and time is quadratic and inverse, so a halved time results in an increase of 2^2 of the required torque. This would increase the mass and power of the CMGs according to [130] with the relations depicted in the trade-off table.
- **Mass Moment Of Inertia** The doubling of the MMOI would double the required torque in accordance with Equation 8.2. This would once again increase mass and power of the CMGs, but not up to an unfeasible extent.

8.13. Feasible limits

According to [130] the maximum accuracy is 0.001° , this is thus the limiting characteristic regarding accuracy. For the turn rate and MMOI of the spacecraft this is determined with respect to the required torque, since the maximum torque of a CMG is 500 Nm according to [130]. For the turn rate this imposes a maximum of a turn in 850 s, since this time constraint would exceed the torque maximum of 500 Nm. Regarding the MMOI of the spacecraft this has a maximum of 2×10^9 kgm^2, when still fulfilling the requirement of performing the turn within 2 hours. The results are displayed in Table 8.1.

Table 8.1: Feasibility limits.

	Accuracy	Turn Rate	Mass Moment of Inertia
Feasability constraints	<0.001°	850 s	2×10^9 kgm^2

8.14. Verification & Validation

The ACDS of the spacecraft consist out of CMGs, thrusters, star sensors, sun sensors, and inertial measurement units. All of these have to be verified and validated in order to perform safe, reliable, and accurate attitude determination and control.

- **CMGs** The CMG needs to be able to perform the required torque, gimbal rate, pointing accuracy, angular momentum, rpm, and MMOI, which are displayed in the results section Section 8.15. In order to verify and validate this, ground tests have to be performed to prove the ability of performing these required specifications.
- **Thrusters** The thrusters of the spacecraft need to be able to generate enough thrust, the tanks need to be big enough to store the required amount of propellant and the total amount of thrusters should be clustered in pairs of 4 as stated in the results sections Section 8.15. Ground tests are to be performed to verify and validate that these requirements are met and that the system does not fail while thrusting.
- **Sensors** The ADCS consists out of six sun sensors, three star sensors, and two inertial measurement unit. These units shall be able to determine the attitude of the spacecraft with sufficient accuracy and sense the rotational and translational movement of the spacecraft. This should first be tested in space simulators or at the International Space Station to verify and validate these specifications.

8.15. Results

	Amount	Torque	Rpm	Gimbal Rate	MMOI	Size
CMG	4	27.88 Nm	6600	3.1 °/s	0.746 kgm^2	$0.8 \times 0.8 \times 0.2$ m
	Amount	Thrust	Tank Volume	Weight	Nozzle size	
Thruster	24	200 N	2.767 m^2	1.9 kg	95 mm	
	Sun	Star	IMU			
Sensors	6x	3x	2x			

9

Electrical Power

The Electrical Power System section elaborates on the design process for the power system, the main power source decided upon, the backup power source, the power management and distribution system, the sensitivity analysis, and the verification & validation procedures.

9.1. Key requirements and constraints

The primary driving requirements for the EPS system include requirements EPS-01, EPS-02, EPS-04, EPS-07, EPS-DIST-03, EPS-GEN-03, EPS-REL-02, and EPS-REL-03. These mainly constrain the peak power driving requirements, mass requirements, backup system requirements, lifetime, and radiation tolerance.

9.2. Midterm Trade-off results

Originally, energy harvesting, chemical, solar, radio-isotope, and fission power systems were considered. Chemical and energy harvesting power systems were found to have unacceptable specific power, while the radio-isotope power system had a specific power that would prove very challenging to use. Fission and solar power systems scored very similarly, however ultimately the fission power system was chosen as the primary power source due to its independence from the solar energy constraints. Photovoltaics will be used as a secondary power source, with secondary batteries for the eclipse duration, in case of emergencies. The solar power system was designed around a critical power mode where mostly necessities are powered until the fission power sources can be operational again.

9.3. Main Power Source Architecture

Nuclear power was chosen as a main power source for the spacecraft. There are two main elements to this power generation system: heat generation and power conversion. The nuclear fission reactors function as a heat source. The fissile isotope of uranium, ^{235}U, is kept in a critical state where it undergoes fission at a stable rate. This generates heat and is then converted to electrical power using a closed-cycle magneto-hydrodynamic generator, or CCMHD. The CCMHD has a conversion efficiency of 55 %. Based on research [104], it was chosen to use 5 MW_t fission reactors. A total of 4 reactor-CCMHD assemblies will thus be needed, with the ability to provide 11 MW_e. Of this, 9.6 MW_e will be used by the 48 engines on board, while the rest will be available for on board systems.

9.4. Multi-MW Fission Reactor

9.4.1. Fission Reactor Fuel Concentration

The main function of the reactor(s) will be to provide the thermal power necessary to run the engines, which require a total of 10.4 MW_e. A number of reactor properties need to be considered for preliminary sizing. From a safety and cost point of view, it is desirable to minimise the mass % of ^{235}U in the reactor core. ^{235}U is the fissile isotope that allows the reactor to generate heat. Natural uranium contains 0.7 % of this isotope, and is enriched to increase the % content of ^{235}U. Low enrichment levels (<20 %) are safer as they naturally reduce reactivity in the core when the temperature rises. This is a passive safety system and prevents inadvertent criticality events[1]. However, it is more difficult to keep the core at the desired critical state during operation, and a higher mass of fuel is required to achieve the same mass of ^{235}U. High enriched uranium (up to 97 %) reduces the amount of mass needed, increases reactivity, but does not benefit from the same passive safety system. Active safety systems can be used to ensure the core can always be brought back to a sub-critical state. These are comprised of control drums and safety rods. The control drums are coated in Beryllium (neutron absorbing) on one side and Bohr (neutron reflecting) on the other. The reaction rate can then be controlled by rotating the rods, and choosing to reflect/absorb

[1] https://www.nuclear-power.net/nuclear-power/reactor-physics/nuclear-fission-chain-reaction/reactivity-coefficients-reactivity-feedbacks/fuel-temperature-coefficient-doppler-coefficient/

more or less neutrons. The safety rods are fully coated in absorbing material, and can be inserted into the core from above in case an emergency shutdown is required. It is unlikely that HEU can be used, as the danger of HEU proliferation restricts its use to government controlled applications. Taking this and the passive safety characteristics into account, LEU was selected for the mission. Figure 9.1 Shows a cross section of a reactor core for space applications. This specific example utilises HEU, but the general layout is identical.

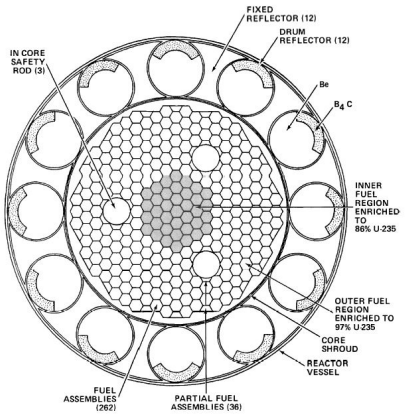

Fig. 3 Midcore cross-sectional view of reactor subsystem, location of safety rods, control drums, and fixed radial reflector segments.

Figure 9.1: Reactor Core Cross Section

9.4.2. Fuel consumption and Sizing

The nuclear reactor on board will have to provide a total power of 10 MW_e (where 9.6 MW_e is for the engines). The CCMHD study performed by NASA [104] states that a 5 MW_t to 2.76 MW_e converter (efficiency of 55 %) is readily scale able to space applications. It will therefore be assumed the reactors are designed to produce 5 MW_t each for 10 years. This means a total of 4 reactors will be needed to provide all the necessary power (resulting in an excess power of 1 MW_e). Since the average recoverable energy per fission is known (200.1 MeV), this thermal power can be used to calculate a required reaction rate per reactor ($1.56 \cdot 10^{17}$ fissions/sec). This results in a daily ^{235}U consumption of 0.005 kg/day[2]. Assuming the engines will run continuously during 10 years (2 years per mission, 5 missions), a total quantity of 19.2 kg of ^{235}U will be consumed by each reactor.

Finally it is important to ensure the reactors can sustain criticality, and thus generate power, for the full mission duration. The critical mass is the mass of ^{235}U needed in a core to sustain fission (where each fission on average causes 1 other fission). This critical mass is dependant on core geometry, core temperature, reflector state and enrichment percentage. For preliminary calculations, it is assumed the critical mass will be similar to that of the core designed in [95], a NERVA derived Low-Enriched uranium core. It can be deduced that the LEU-NTP reactor core has a critical mass of 6.26 kg (it operates for 47h at 450 MW_t). Using Low-Enriched uranium, the reactors would then require 127 kg of uranium. A total of 635 kg of 20 % ^{235}U uranium will thus be launched during spacecraft assembly, and will not require refuelling for a duration of 20 years.

With a density of 19.1 g/cm^3, each reactor will contain a total volume of 6,500 cm^3 of Uranium. Based on the LEU-NTP reactor core [91], it will be assumed the reactor core uses uranium-carbide composite, with 35 % volume Carbide moderator loading. This results in a total fuel height of 35.58 cm, with a hexagonal rib length of 11.86 cm.

[2] https://www.nuclear-power.net/nuclear-power-plant/nuclear-fuel/fuel-consumption-of-conventional-reactor/

9.4.3. Reactor Safety

Nuclear fission reactors are a very reliable source of power, but the operational safety must carefully be analysed to avoid any accidents or negative impacts on the health of astronauts. The main focus of safe design of a reactor is the prevention of inadvertent criticality (i.e. The reactor core enters a (super-)critical state when it was not meant to). The risk prevention guide of the IRSN [16] provides guidelines for the safe design of ground based reactors. These safety design philosophies can be adopted for space reactors. In addition to the use of LEU and control/safety rods, the reactor will be designed such that no single anomaly can generate a criticality event. Secondly, two anomalies that cause a criticality accident will always be independent of eachother. Finally, monitoring systems will be installed to identify anomalies within acceptable time-frames. Also, reactors will also emit a certain level of radiation. With built in shielding, fuel tanks and spacecraft shielding, NASA predicts a nuclear powered trip to Mars will expose the astronauts to 11 mSv. The reactor will thus be designed to limit reactor radiation exposure to this level.

Finally, the safety of the reactor during a potential launch failure has to be investigated. The reactor core will be designed to withstand the worst case temperatures and pressures experienced during a Falcon 9 launch failure. In addition, the reactor housing will need a re-entry shield to prevent inadvertent criticality during unplanned re-entry.

9.5. Closed-Cycle Magneto-Hydrodynamic Generator (CCMHD)

An MHD generator is a device that converts the energy of a working fluid or gas into electrical energy. An electrically conducting fluid is passed through an electro-magnetic field and a set of electrodes. By Faraday's law, a current is then generated[3]. The spacecraft will be using a closed cycle MHD using noble gases as working fluids is considered [104]. This CCMHD uses Helium and Argon as working fluids and uses a Brayton cycle to further compress the fluid. In addition, the working fluid is re-generatively heated using a heat exchanger (re-generator in figure). This cycle therefore achieves a conversion efficiency of 55 %. All stages of the cycle are shown in Figure 9.2

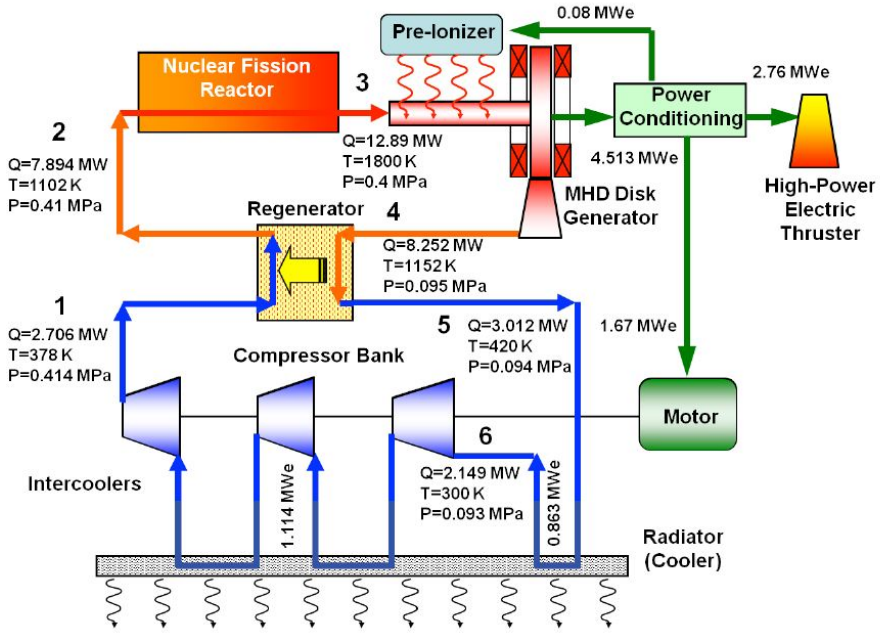

Figure 9.2: MHD cycle

The CCMHD was chosen as it offers a higher thermal power conversion efficiency than any

[3] https://electricalvoice.com/magneto-hydrodynamic-mhd-power-generation/

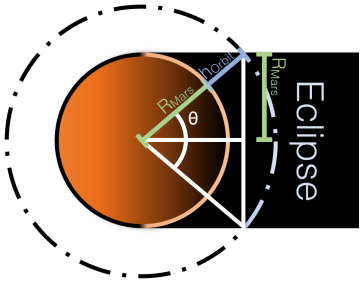

Figure 9.3: Approximation used to get the Eclipse Duration.

other known system. Closed-Cycle MHD's are more complex than open-cycle MHD's, and are at an earlier stage in their development. In addition, the specific mass that can be achieved with such a system only becomes beneficial when a large amount of power needs to be generated (over 1 MW). As of yet, there have been no space missions with such high power requirements. These are the two main reasons that Brayton Cycle CCMHD's have not yet been implemented on space missions. It is worth noting that open-cycle MHD's have been used in coal power plants in the past, but were not widespread as the increase in efficiency is not worth the increased cost for ground based power plants.

To conclude the preliminary sizing of the primary power generation system, the 5 MW_t fission reactors are again considered. Each MHD will convert 5 MW_t to 2.76 MW_e, so one MHD will be necessary for each reactor. This means a total of 8 MW_t of excess thermal power will need to be dissipated with radiators at full power operation. Note that at this operating level, 1 MW_e of excess electrical power is also being generated. The excess heat and electrical power can both be reduced by adapting the reactor power level. For systems generating more than 2 MW_e of power, a specific mass (including radiators) of 3 kg/kW_e [104] or lower can be achieved. This translates to a specific mass of 2.13 kg/kW_e excluding radiators. The radiator mass was calculated for this specific design, and is discussed in Chapter 10.

9.6. Backup Power

One of the implications of using power from nuclear reactors is that there must be an alternative power source to power the ECLSS such that the safety of the crew is ensured in emergency scenarios. After considering both solar panels and stored power, solar panels were chosen for the underlying fact that they can persist for times much longer than batteries or fuel cells alone can. Obviously, using solar panels still needs secondary batteries for power during the duration in eclipse.

Worst Case Scenario

The solar panels were sized by considering the worst case scenario for the mission. This would be located at the aphelion of Mars (249.23 10^6 km [129]), where Mars is at the furthest point from the Sun in its solar orbit. The largest eclipse time would be at Low Martian Orbit (LMO) because of the increased orbit velocity needed to maintain such a close orbit. Specifically an altitude of 400 km was taken. It is worth noting that these calculations were also made for Low Earth Orbit, but were found less stringent than the Low Martian Orbit scenario. The velocity was calculated using Equation 9.1. Using the Mars Fact Sheet [129], the gravitational constant of Mars (GM or μ) was found to be 4.2828 10^4 km^3/s^2. The $r_{SemimajorAxis}$ was taken to be 400 km LMO orbit, assuming a circular orbit, as stated before.

$$V_{Orbit} = \sqrt{\frac{\mu}{r_{SemimajorAxis}}} \tag{9.1}$$

The duration of eclipse time at Low Martian Orbit was found by an approximation. Figure 9.3 shows a graphical representation of the steps taken.
Assuming that the distance of the Sun to Mars is significantly far enough to make Mars' shadow edges parallel, the angle of the semicircle in eclipse was found. This angle was

divided by 360° (or 2π for radians) to get a percentage of the orbit that the spacecraft is in eclipse. With this percentage and the time of an orbit, the duration of eclipse was calculated. Equation 9.2 summarises the mathematics used.

$$t_{eclipse} = \frac{2\theta}{2\pi} t_{orbit} = \frac{2\sin^{-1}\left(\frac{R_{Mars}}{R_{Mars}+h_{Orbit}}\right)}{2\pi}\left(\frac{2\pi(R_{Mars}+h_{Orbit})}{V_{Orbit}}\right)[\text{s}] \tag{9.2}$$

Power Requirements

Equation 9.3 [130] was used to calculate the total power required to sustain the spacecraft with only solar panels. The P_{ECL} and P_{Day} are the powers needed during eclipse and during sun respectively. From the backup power budget in Figure 4.5, the required power during sunlight and eclipse was approximated to 10 kW including a 1.10 safety factor. The t_{Ecl} is the time in eclipse from Equation 9.2, while the t_{Day} was found by subtracting the t_{Ecl} from the t_{Orbit}. The efficiency's listed, η_{Day} and η_{Ecl}, are for how efficient the respective systems are at transferring power to the subsystems. A Direct Energy Transfer (DET or dissipative) power control system was taken due to its higher efficiency and lesser mass as opposed to other control systems [130]. For a DET system the η_{Ecl} and η_{Day} have values around 0.65 and 0.85 respectively.

$$P_{Required} = \frac{\frac{P_{Ecl}t_{Ecl}}{\eta_{Ecl}} + \frac{P_{Day}t_{Day}}{\eta_{Day}}}{t_{InSun}}[\text{W}] \tag{9.3}$$

Under these circumstances, the total power ($P_{Required}$) needed for the solar panels to collect during sunlight operation is about 20.142 kW.

Solar Array Sizing

The next step in sizing the solar panels was analysing the solar cells. After much deliberation between various solar cells, a conservative triple-Junction solar cell called the XTE LILT designed by Spectrolab [114] was taken. The XTE LILT version was designed for the radiation encountered on deep space missions, however the data provided only outlines the XTE-SF (Standard Fluence) designed for LEO or GEO missions. At its Beginning-of-Life (BOL), the solar cell has an efficiency of 32.2 % [114]. To calculate the solar cell's efficiency after a 20 year mission, the yearly radiation degradation was extrapolated using the XTE-SF data provided for a 15 year GEO mission. By taking the life degradation (L_d) as 0.84 [114] for a 15 year mission and using Equation 9.4 to solve, the degradation per year was calculated to be about 1.16 % per year. Then Equation 9.4 was used again to calculate the life degradation for the 20 year mission, found to be about 79.187 %. It is worth noting that the actual spacecraft design will include a shield to defend against a lot of the radiation that degrades the solar cells, however it was not taken into account for calculations on sizing the array because the degradation per year reduction could not be definitively quantified.

$$L_d = \left(1 - \left(\frac{degradation}{year}\right)\right)^{(YearsOperating)} \tag{9.4}$$

The solar irradiance at the Aphelion of Mars was calculated using 1358 W/m^2 as the solar irradiance at 1 Astronomical Unit (AU) from the sun and then taking a linear decrease as a function of the distance to the sun squared. This can be shown being done in Equation 9.5, along with taking the efficiency of the solar cells into account.

$$P_0 = \eta_{SolarCell} 1358\left[\frac{W}{m^2}\right]\frac{(1[AU])^2}{(aphelion_{Mars}[AU])^2} \tag{9.5}$$

The power at the BOL (P_{BOL}) was calculated as shown in Equation 9.6 from SMAD [130]. This includes the Inherent Degradation (I_d) taken to be nominal at 0.77 [130] and the cosine loss, which was assumed have at worst-case a Sun Incidence Angle (θ) of approximately 10°.

$$P_{BOL} = P_0 I_d \cos(\theta) \tag{9.6}$$

With the life degradation from before, the power at the EOL (P_{EOL}) was solved for using Equation 9.7 and found to be about 94.6 W/m^2.

$$P_{EOL} = L_d P_{BOL} \tag{9.7}$$

The area needed was finally solved for by dividing the total power required (22.325 kW) from before by the power at the EOL. Resulting in about 213 m^2 of solar cells being needed. Assuming a standard solar cell packing density of 85 % (that is 85 % of the solar array covered in solar cells), the total solar array area needed is approximately 250.5 m^2.

Battery Sizing

Firstly, the radiation effects for the battery types was analysed. After some research it was found that Lithium-Ion Cells were proven to be tolerant of radiation levels up to 18 Mrads (180 kGray) and exhibit a loss of less than 5% upon such high radiation levels [57]. It also mentions Nickel-Cadmium cells showing absolutely no effects from radiation after intense testing, however Ni-Cd batteries have less performance capabilities than Li-Ion batteries. The radiation sizing for the electronics and batteries will be discussed in Section 9.7. Using procedures outlined by SMAD [130], Equation 9.8 was primarily used for obtaining the capacity of the battery (C_r) needed. The variables from the equation are as follows, P_{ecl} is the power at eclipse, T_{ecl} is the max duration in eclipse in hours, DOD is the depth of discharge for the battery, N is the number of non-redundant batteries, and n is the efficiency of the battery at transferring power to the load (taken to be a nominal 0.9 [130].) At baseline, N was taken to be 3 primarily since there could be one for each module and they would be safely protected from radiation behind each module's shielding.

$$C_r = \frac{(D)P_{ecl}(T_{ecl}[hr])}{(DOD)Nn}[\text{W hrs}] \tag{9.8}$$

After researching several batteries, The LP33037 - 60Ah Space Cell by Eaglepicher[4] was used due to its relatively high specific energy of 160 Whrs/kg. The batteries were derated by 10 % to avoid using the batteries at their nameplate rating[130]. The depth of discharge being 40 % was deemed acceptable since these batteries are still capable of withstanding over 40,000 cycles in LEO for 10 years of operation. Because these batteries are important for the ensured success of the mission and the contingency of having extra batteries would not impose a significant cost on the system, an extra battery for each non-redundant battery will be stored (3 total at baseline.)

Backup Mass Estimate

The following preliminary mass estimates were made using a method designed for satellites [43]. The mass for multi-junction cells can be approximated as about 3.8 times the area of the solar array (A_{SA}.) The mass of the honeycomb substrates can be approximated to about 2.0 times the area of the solar array for composite panels, which are typically used for multi-junction cells. The sum of these two add to the Mass of the solar panels (M_{panels}) as seen in Equation 9.9. The mass of the solar array drives and electronics (M_{SAD}) were taken to be about $0.33M_{panels}$ and the mass of the Solar Array retention and deployment mechanisms ($M_{SAdeploy}$) were taken to be about $0.27M_{panels}$. The Mass of the power systems electronics during backup was estimated as ($0.04P_{oa}$) with P_{oa} being the required orbital average power of 10 kW from before. The mass of the six batteries, calculated using the 160 Whrs/kg from before along with the 10 % derating, is about 265.64 kg. That is about 44.27 kg per battery. These relations are summed in Equation 9.9 and total to approximately $2,990.19$ kg.

$$M_{panels} = M_{elec} + M_{substrates} = 3.8A_{SA} + 2.0A_{SA} = 1452.9 \tag{9.9}$$

$$M_{Backup} = M_{panels} + M_{SAD} + M_{SAdeploy} + M_{battery} + M_{PSE} \tag{9.10}$$

$$M_{Backup} = M_{panels} + 0.33M_{panels} + 0.27M_{panels} + M_{battery} + 0.04P_{oa} \tag{9.11}$$

[4] https://www.eaglepicher.com/sites/default/files/LP%2033037%2060Ah%20Space%20Cell%20%20040319.pdf

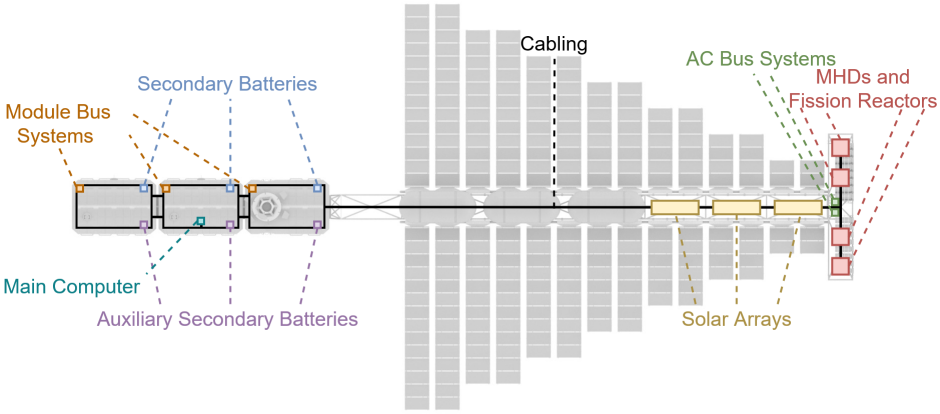

Figure 9.4: Electrical component locations on the Spacecraft

9.7. Electrical Power System

Having a primary power system and a backup power system is only as effective as the integration of both systems. This section will provide an overview of the combined Power Management and Distribution System (PMAD) and provide a preliminary, first iteration of the electronics.

Radiation Shielding

The radiation requirement for the full 20-year mission is 20 Gray assuming that it is shielded, as stated in Section 11.4.2. Juno's electronics vault was expected to have a radiation environment of 25 Mrad (250 kGray), with the electronics being designed to tolerate 50 Mrad[5] (500 kGray.) Juno's mission to Jupiter involved a much harsher radiation environment due to Jupiter's radiation belts[6]. As a result, it was decided to use Juno's design philosophy of ensuring that the electronics tolerate double the expected radiation environment. Meaning that the electronics will be designed to withstand 40 Gray of radiation throughout the 20 year mission. The Li-Ion battery radiation tolerance of 180 kGray is still met. Also the electronics on the outside the modules will have radiation shielding to maintain this standard.

Electrical Diagram

In Figure 9.4 is the generic power system to primarily showcase the locations of the major electrical systems. For simplicity and clarity the subsystems being powered were excluded. There are two Bus Systems for redundancy, however it is worth noting that their circuitry will also include redundancies to ensure no single point of failure is possible.
Each module will have its own Bus system to ensure that their power systems still work in case of disconnection. The solar arrays and MHDs both connect to two Bus systems located in their close vicinity. The Figure 9.5 below is the first iteration on the electronics design for the spacecraft. As stated before, a DET power control system was chosen due to its lower mass and higher efficiency. A DET system utilises shunt regulators to dissipate the excess power from the power generators such that the electronics have a controlled input. These shunt regulators will be placed externally of the system to dissipate the power out of the system. Electromagnetic interference was accounted for by use of a filter. All buses were chosen to operate under AC distribution rather than DC because AC buses can be more economical for a spacecraft with power requirements higher than 20 kW[5]. The mission is working with an 11 MW power supply from the MHDs. A drawback is that the heritage for space-qualified devices is lacking when compared to DC distribution systems. There would also need to be point-of-load AC-DC converters, which are taken to exist for this report. Since bus voltages have been increasing as missions become more power demanding[5], a high AC Bus voltage design is proposed. Due to the sheer importance and limitations that arise from

[5] http://spaceflight101./juno/spacecraft-information/
[6] https://www.nasa.gov/mission_pages/juno/news/juno20100712.html

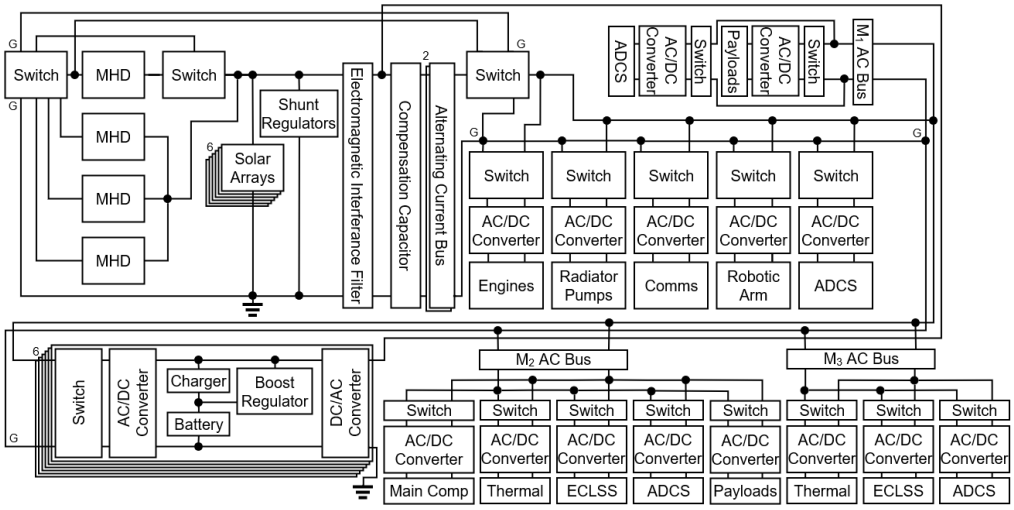

Figure 9.5: Electrical Block Diagram for the Spacecraft

the voltage at which the bus operates[99], this design constraint is left open to be chosen on a later date when more data and information is available. There are six solar arrays and six batteries in total, three batteries being auxiliary. Every system being powered has a switch and an AC-DC converter, except the module buses. The module buses regulate their respective subsystems, which also have switches and AC-DC Converters. For this report, it was assumed that all subsystems operate on DC since that is the more popular case for space missions. In actuality there would be a mix between subsystems that operate on AC and DC. All controlled loads are in parallel to the main bus structures. A concern were the cable losses due to how far the power generators and the modules themselves are, there are three techniques to minimise cable loss. The first is a power-factor correction, done by inserting a compensation capacitor after the AC generator output in order to compensate the reactive power consumed at the inductive elements of the load. This is already implemented in the electrical block diagram. The second is to use a higher AC voltage. The third is to use cables with larger diameter, however these cables are more expensive and heavier.

9.8. Sensitivity Analysis

The Sensitivity Analysis for power is divided into the MHDs, backup systems, and PMAD systems.

Fission reactors and MHDs

A reactor-MHD assembly is fixed at an electrical power output of 2.76 MW_e. In the current configuration, a total of 11 MW_e can be generated. The engines use 9.6, and other subsystems are expected to use up to 350 kW, which leaves an excess power of 1,050 kW. The most likely increase in power consumption would be due to an increase in dry mass and thus an increase in engines. The current excess power allows for the addition of one engine. As the power generated by each reactor assembly cannot be increased, a further increase in the number of engines would have to be facilitated by adding a fifth reactor assembly. This would increase the available power by 2.76 MW_e (enough for 13 engines), while increasing the mass by 6 tons.

Backup Systems

As everything related to the backup system calculations have already been elaborated on before in Section 9.6 and the sensitivity of the backup system can be deduced by going through the relations, the major ones will primarily be covered. Power requirements for the solar arrays scale linearly with the solar array and secondary battery parameters for mass, area, and volume. Should there be a more stringent worst-case scenario, it would drive the battery sizing primarily. An orbit altitude increase would reduce the size of the solar panels and reduce the battery capacity requirement. If a closer orbit is desired, for instance 300 km

altitude, the area of the solar arrays would be 260 m^2 and the battery capacity needed would be 21.5 kWh.

Power Management and Distribution System

The PMAD is very preliminary, circuitry design is a very iterative process and the PMAD is bound to change several times before its final iteration. Possible causes for change include adding more modules or more systems to be powered. The PMAD system is very sensitive to changes in architecture such as these, but not very sensitive to actual power requirements due to how considerable they already are. Architecture changes would include adding more system ports, generators, solar arrays, batteries, module buses, module systems, or changing major design considerations. Use of DC buses would be less efficient and substantially increase the mass of the overall electrical system.

9.9. Verification & Validation

The Verification & Validation for power is divided into the main constituents of the power system: the fission reactors and MHD systems, the solar arrays, the secondary batteries, and the PMAD.

Reactor-MHD Assembly

Both the reactors and MHDs will have to be designed, manufactured and tested for this mission specifically. The concept of a nuclear reactor is widely used, but the application to space propulsion generates additional safety concerns and importance of reliability. In order to prove the reliability of the reactor, it will be held under operation conditions for the duration of at least one mission cycle (i.e. 2.5 years). Finally, impact resistance of the reactor should be tested. This will ensure that a launcher failure cannot induce inadvertent criticality. The MHDs will undergo the same long term testing to prove the conversion efficiency of 55 %, After ground testing, both systems will be tested in flight in combination with the radiators for the same duration. This will validate the system functioning independent of ground systems, and the long term thermodynamic stability.

Solar Arrays

The software used to design the solar arrays was verified with Solar cells were already tested from the manufacturers. These results need to be validated with some test cells. Primarily efficiency, radiation degradation, and the EOL efficiency for the 20-year mission. Solar array electronics also need to be tested but that relates more to circuitry, which is discussed in the Power Management and Distribution System section. The complete solar array when finished needs to also be comprehensively tested to ensure all components are operating as designed.

Batteries

The batteries have already undergone testing from the manufacturers, however the results can be validated by purchasing test cells and further testing them. Test would orient around the depth of discharge, how many cycles they can tolerate, safety mechanism tests, and radiation tolerance tests.

Power Management and Distribution System

Circuitry must be constantly tested and ensured throughout every iteration to prevent any single point of failure and prevent concentrations of failures in regions. Special attention is paid during the iterative process to ensure that the subsystems actually work with the provided power configuration. The module and power circuitry will be tested individually and disconnected to the combined system, and then a comprehensive full system-integrated circuitry test will be made. Software simulation testing will be used to verify the results while live testing will serve to validate them. The final iteration being built and comprehensively tested to ensure operability for the full 20 year mission. Testing will include a test on the radiation tolerance, multiple failure mode scenarios, and a check to ensure that there is minimal electromagnetic interference throughout the mission.

10
Thermal Control

The thermal control subsystem is responsible for regulating the temperatures in the spacecraft for certain components and removing excess heat that is generated by the reactor. Regulating the temperature on the spacecraft is important for a variety of reasons. Most importantly is the survival and comfort of the passengers and the thermal relief that is necessary to keep the reactors and engines running. To design such a system it is important to recognise the total excess heat and the temperature requirements for other subsystems and parts.

10.1. Key requirements and constraints

- THERMAL-04 - The thermal control system shall not exceed a mass of 25,000 kg.
- THERMAL-05 - The thermal control system shall have an average power usage of lower than 300 kWe.
- THERMAL-06 - The thermal control system shall have a peak power usage of 250 kWe.
- THERMAL-DIST-07 - Thermal control system shall ensure the internal atmosphere will have a temperature of 20°C.

10.2. Thermal Analysis

Before a certain thermal loop and its required radiators can be decided upon it is important to determine the temperature ranges that are allowed. Furthermore it is necessary to analyse the contribution to the thermal power that the spacecraft experiences from the different heat sources. The thermal control subsystem should provide certain temperature ranges for different systems. The general operating temperatures for certain components in space systems are given below in Table 10.1.

Components	Operating Temperatures (Celsius)
Digital Electronics	0 to 50
Analog Electronics	0 to 40
Batteries	10 to 20
IR detectors	-269 to -173
Solar Panels	-100 to 125
CMG's	0 to 50
Cabin temperature	15 to 25

Table 10.1: Operating Temperatures for certain components in the spacecraft [63]

The control of operating temperature environments is also important to mitigate the thermal cycling damage that can deteriorate the structure over time. Additionally, the propellant can become unstable or can even become unusable if thermal control is not performed well.

Generally a spacecraft is experiencing thermal power input from the sun in both a direct and indirect manner. Also the planet that is being orbited is providing a certain amount of thermal input on the spacecraft. The main contribution of thermal power on the spacecraft can be dissected into [63]:

- Direct Solar Irradiance
- Albedo from nearby Planets
- Infrared radiation from nearby planets
- Emitted Radiation [1]

These individual contributions from the sun and the planets can be calculated for different distances from the sun [63] [130]. The resulting fluxes for this mission at different distances from the sun are given in Table 10.2.
It is important to note that the values found in Table 10.2 for the MHD Heat Generation are significantly large due to the large amount of excess heat the generator creates. therefore,

[1] This is heat in the form of radiation that comes from the engines and reactors

Type of Radiation	1 AU / Earth	1.5 AU / Mars
Direct Solar Irradiance [Watt/m^2]	1,369.7	608.8
Albedo from planets [Watt/m^2]	238.0	69.3
Earth/Mars Infrared [Watt/m^2]	239.7	110.5
MHD Heat Generation [Watt]	8,000,000	8,000,000

Table 10.2: Type of radiation fluxes at different positions of the mission.

dissipating the excess heat will be the primary objective for the thermal control subsystem. In space however getting rid of excess heat is only possible by means of thermal radiation. Thermal relief in the form of convection and conduction is not possible because of the lack of a medium in space. In order to get rid of heat the thermal control subsystem shall include radiators that will actively or passively radiate thermal power outboard.

10.3. Radiator Types

Since radiation is the only way to dissipate thermal heat, the thermal control system is required to facilitate for a radiator to dissipate this excess heat. Literature study showed various radiator designs and concepts that are feasible now or in the future. After some research [4] [52] it was found that there are three radiator designs/concepts that showed relevance towards the design constraints of this mission. These three will be further elaborated upon.

For a radiating thermal heat the following static thermal formula holds:

$$Q = \sigma \epsilon_{eff} A_{rad} (T_i^4 - T_o^4) \tag{10.1}$$

From this equation, which shows the heat radiated in Watts, it is clear that the effective emissivity coefficient (ϵ_{eff}), the radiator surface area (A_{rad}) and the initial equilibrium temperature (T_i) can be increased to increase the amount of heat to be radiated out of the radiator. The output equilibrium temperature (T_o) can also be lowered but since the heat is radiated out into space this temperature is typically fixed at 2.7 Kelvin. The Stefan Boltzmann constant is equal to 5.67×10^{-8} $\mathrm{Wm^{-2}K^{-4}}$. All three concepts follow, within their designs, the above mentioned formula [130].

High-Temperature Hybrid Radiator

Figure 10.1: Radiator system on the International Space station [15]

The solid radiator consists out of panels from aluminium that contain a coating that has a certain emissivity coefficient. Throughout the panels there are heat pipes that will introduce the working fluid into the radiator. It's typical areal density is between 6 and 10 kg/m^2, this is without pumps, coolant and piping [54]. The radiators used in previous space applications are not sufficiently efficient and do not sustain high enough conductivity to get rid of excess heat in the ranges of nuclear reactors. This is mainly because of its generally low equilibrium temperature (100 Kelvin on the ISS [108]). This is high enough to get rid of the heat produced by direct and indirect sunlight. The hybrid radiator, however, can still be used to get rid of higher thermal excess powers. This does make the design a bit more complicated. The emissivity of the radiator is often already between 0.85 and 0.91, thus changes in the emissivity

will not result in the significant improvements needed. Raising the equilibrium temperature of the radiator will on the other hand result in significant improvements. However, the aluminium radiator/fins and heat pipes start to become structurally weak at around 700 Kelvin. To raise the equilibrium temperature of the radiator some major design changes have to be made. According to the Glenn Research Center (NASA) and the University of Massachusetts (Amherst) [108][54],the radiator surface and radiator fins can be designed to be made out of a carbon-carbon high thermal conductivity composite. Together with lining the heat-pipes with a similar high thermal conductive composite [62] the equilibrium temperature of the radiators can be scaled up to around 900 Kelvin, resulting in a significant decrease in necessary surface area. Together with this advantageous temperature increase the areal density will decrease to between 1.0 and 3.0 kg/m^2 For durability the heat pipe radiator scores reasonably well having no single point of failure. Hence, a puncture of a radiator panel will not affect the performance of the whole system. The specific power that the radiator typically can dissipate will lie between 0.85 kW/m^2 (Solid aluminium radiator) and 7.5 kW/m^2 (Hybrid radiator) [4] [54].

Curie Point Radiator

The curie point radiator is a concept radiator currently under development for space and non-space applications. Due to the fact that higher power consumption will be required for future space missions, including the possibility of having space habitats on the moon or other planets, high power generation is necessary resulting in the production of significantly more excess heat. To efficiently deal with this amount of excess heat, without having to employ enormous radiators, two important factors have to be taken into account; the equilibrium temperature has to be scaled up and the effective surface area/volume ratio has to be increased. New radiators having a liquid metal working fluid can pose a solution to both of these factors. One of such designs is the Curie Point radiator. The radiator has a working fluid of liquid cobalt which is naturally black, resulting in a high emissivity and can attain very high temperatures before it starts to boil [1]. The Curie Point radiator, as the name suggest, relies on the Curie Point of the working fluid. When Cobalt is heated up to about 1,388 Kelvin the material loses its ferromagnetic capabilities and can be ejected out of the spacecraft in a very dense mist of liquid Cobalt. During the phase outside the spacecraft the liquid Cobalt will radiate its internal heat to space and as a result its temperature will drop down the Curie Point. This makes the liquid Cobalt retain its magnetic capabilities again and the working fluid is drawn back into the radiator for the cycle to repeat again [88]. The graphical illustration of the working radiator is shown in Figure 10.2.

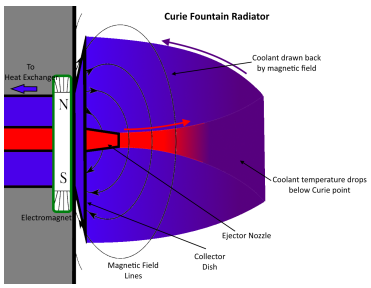

Figure 10.2: Graphical depiction of the Curie Point Radiator [13]

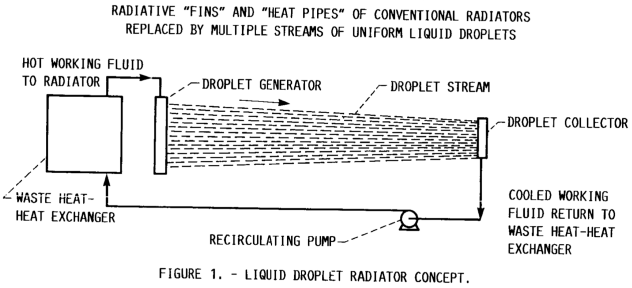

Figure 10.3: Graphical depiction of the Liquid Droplet Radiator [128]

The equivalent temperature of the radiator is able to operate under is between 800 and 1,600 K. Which makes it very efficient in dissipating large amounts of excess heat, especially from concentrated areas such as the engines including its core. The specific power, theoretically, is very large and is estimated to be around 300 kW/m^2 [1] and the specific density, estimated at around 35 kg/m^2, is quite high due to the bulky electromagnet and capturing shield.

Liquid Droplet Radiator

The last concept radiator is the Liquid Droplet radiator. This radiator is based on the same two principles as the Curie point radiator of having a high relative temperature of the working fluid and ejecting it in a dense mist to optimise the surface area. This radiator however has scored a higher TRL than that of the Curie Point radiator. The radiator has been tested in the Japan Microgravity Center (JAMIC) and a prototype was also brought to space to be tested during the STS77 mission [52]. The liquid droplet radiator, however, does not depend on the ferromagnetic behaviour of the working fluid. The hot liquid working fluid will be ejected at temperatures between 900 and 1,600 K, depending on the system requirement, and will travel in the vacuum of space to be collected a few meters later by the means of a (slightly) magnetic collector. The colder working fluid will be collected and fed back to the heat exchanger via designated heat-pipe for the process to be repeated [4]. Because the mist is containing a large amount of droplets the total surface area is incredibly large compared to their mass. This ensures rapid cooling while having a low areal density. The combination of high equilibrium temperatures and a large surface area will yield theoretical values for its specific power dissipation in the order of tens of megawatts [13] [128]. In practical experiments reaching values for specific power of about 35 kW/m^2 [100]. For issues that are the result of droplets travelling through open space like solar stripping of the droplets by solar wind and the merging and colliding of droplets together due to the different velocities of the droplets in the droplet sheet, solutions have already been devised [124]. The working fluid does not necessarily have to be liquid metal. It can also be a high thermal heat capacity oil with a low vapour pressure (as in the vacuum of space liquids quickly tend to evaporate) that will be coloured black, if necessary, to increase its thermal emissivity [53] [13]. The TRL is around 6 at the time of writing as the concept was proven in a space environment. In Figure 10.3 a graphical representation is given of the Liquid Droplet radiator.

Before a final radiator system will be chosen, some aspects of radiator and mission design has to be investigated in a bit more detail for the liquid droplet radiator (LDR) since it is not proven in flight yet.

Single point of Failure

The LDR primarily consist of two very important devices; the generator and the collector, for clarification look at Figure 10.3. One of the advantages of this radiator design is the low weight. The generator and collector make up 80 % of the total weight of the radiator [100]. The liquid metal coolant is directed directly through the generator using the designated piping. The generator and collector, while being protected from the heat, are pretty vulnerable. They are small in size so therefore the probability of being hit by a meteorite is relatively slim, however, the impact will be enormous. It can be argued that this risk can be mitigated using multiple (smaller) radiators that operate in unison or thicker protection. This is indeed a way to mitigate the risk of failure of the radiator but this will also weigh down the weight advantage of the LDR. For instance, to mitigate the risk, more surface area is needed and therefore significant more pumping power is required. The weight advantage of having limiting piping in the LDR design is also taken down when considering the protection against micro-meteorites that the piping must contain. To conclude, the LDR is inherently protected against micro-meteorites by not having a solid radiator panel but trillions of droplets, such that the micro-meteorite can pass through. While less probable, the generator and collector failure will have a disastrous, if not, catastrophic impact on the mission. To mitigate the risk the LDR will lose out on a fraction of the weight and size advantages [128].

Radiator usability during manoeuvres

During the burn and retro-burn towards Mars (and back to Earth) the spacecraft has to yaw 180 degrees about its z-axis. During this manoeuvre the radiator, while being less active due to the throttling down of the reactors, is still required to be operational. This manoeuvre, however, takes a significant amount of time, in the order of days. The droplets that are ejected out of the radiator travel with a speed between 20 to 30 m/s over a distance of roughly 8 to 15 m. Together with the fact that experiments showed generator ejection accuracy's of down to 1 miliradian for the liquid droplets, it can be concluded that during such manoeuvres the

radiator can remain fully functional and is on this criteria fully compatible with the mission [100].

Long term thermodynamic stability

The thermodynamic stability greatly depends on the temperature difference between the coolant and the heat source, in this case the engine and reactors. The temperature difference between these should be significant large enough for heat transfer to happen. While this thermodynamic principle has been proven in a multiple experiments, [100], the stability over longer duration is not proven yet. With stability the remaining temperature difference over longer period is meant to remain stable and significant enough for heat transfer to occur. This thermodynamic stability has not been modelled yet and therefore it is unsure if this radiator will be able to provide the heat relief (in the order of megawatts) over the time span of a mission to Mars and back to Earth [53].

Inter-reflective droplet efficiency

The radiation principle relies on the fact of infrared radiation radiating from the liquid droplets into the coldness of space. Since droplets in space are (almost) perfectly spherical the radiation therefore radiates in 360° . The efficiency of heat rejection depends on the density of the liquid mist. The closer the droplets are to each other the more heat is radiated towards their neighbouring droplet. A way to mitigate this lose of inter-reflective efficiency is to separate the droplet streams by making the generator and collector wider. During simulation in space during the STS-77 mission and the more elaborate experiments on the ground ([100]) this efficiency was already taken into account and the amount of heat rejection was still more efficient compared to the normal radiator.

R&D Schedule and Costs

One of the main requirements for this mission is to bring astronauts to Mars before 2040. The current technology readiness level of the liquid droplet radiator is at 6, meaning that the LDR concept has been demonstrated in a relevant environment. To bring the concept LDR to a TRL of 9 it should, in order, firstly perform a full system demonstration in a space environment. Until now only certain subsystems of the concept has been demonstrated during the STS-77 mission as the Liquid Metal Thermal Experiment (LMTE) experiment in 1996 [89]. Secondly, a complete thermal system including the thermal loop should be tested in space to bring the TRL to 8. Lastly, the LDR should be incorporated in an actual mission, preferably in human space flight to make the thermal system ”flight proven” and bring the TRL to 9.

Behind these three TRL levels there is a lot of research and development necessary. This *R&D* will, above high development cost, require a lot of time. The development of the LDR in estimated time and cost is dependent on a lot of factors. One of the most important of which is the Advancement Degree of Difficulty (AD), which will anticipate the difficulty over the course of a technology maturation project. AD is determined through consideration of cost, schedule, and risk across several dimensions, including, among others, design and analysis, manufacturing, test and evaluations and operations [6]. Assuming the average development rate in space flight the development time to bring the LDR from TRL 6 to 9 will take something between 15 and 25 years, including a safety factor for required reliability necessary human space flight obtained at the level 9 [6]. Given the requirement mentioned earlier it can be concluded that the mission will be significantly delayed if the LDR will be the chosen radiator design. The development costs for the LDR are estimated to be between 20 and 50 million US dollars. Although these ”millions” will be a fraction of the total cost of the mission it will still be millions that can be used for something else if the hybrid solid radiator is chosen.

10.4. Radiator Trade-off

For the radiator trade-off specific power, specific density, Technology Readiness Level, Reliability and durability were deemed the most important criteria for the radiator trade-off. The specific power, specific density and TRL were discussed earlier and in the trade-off their relative score towards each other is depicted. For reliability the stability of the excess heat output is the driving parameter. For the flight proven classic radiator with heat-pipes this is

obviously very high as it is optimised already for space applications. The reliability for the Curie Point radiator is low. This is because the collection of the hot metal working fluid is not constant and stable for longer duration where a high equilibrium temperature is maintained [88], but this is probably the result of the low TRL of the system. The reliability of the droplet radiator is proven to remain stable during longer operation. However the current design shows a decrease in efficiency over time [100]. Durability of the radiator system is really important to consider as the radiator will have a significant surface area at generally vulnerable less protected part of the spacecraft. The radiators are optimised for thermal heat dissipation and therefore generally not really protected for micro/macro meteorite impacts. The solid (hybrid) radiator scores low on this criterion as the surface area is much higher than for the other designs and the panel/heat pipe array generally affects a larger portion of the radiator when punctured. The Curie Point radiator is really durable as the mist generator is well protected and the there are no single points of failure. The durability of the liquid droplet radiator is also pretty good as the effective surface area of the radiator is made up out of liquid metal droplets. If a meteorite passes through this area of mist only a certain amount of coolant will be lost. In Figure 10.4 the scores for the criteria are shown.
The liquid droplet radiator is surely a very promising technique for the future of nuclear space propulsion. However, combining the reliability/ durability with the *R&D* schedule and costs this concept is not mature enough to be used, at this point, for interplanetary human travel. Therefore it is decided that the high-temperature hybrid radiator will be used for the Primary Thermal Control Subsystem.

				Risk		
Excellent	Concept \ Criterion	Cost				
Good/Baseline		Specific power	specific density	TRL	Reliability	Durability
Correctable	Classic Radiator with Heatpipes	0.85 kW/m2 to 7.5 kW/m2 1425 m2 first estimate	8 kg/m2 11400 kg first estimate	9	high	Low
Very challenging	Curie Point Radiator	300 kW/m2 33 m2 first estimate	35 kg/m2 1155 kg first estimate	5	Low	High
Unacceptable	Liquid Droplet Radiator	35 kW/m2 285 m2 first estimate	0.5 kg/m2 142 kg first estimate	6	Average	medium

Figure 10.4: The trade-off table for the radiator trade-off

10.5. Detailed Radiator Sizing

The radiator panel can now be designed for the excess heat that shall be dissipated according to Table 10.2. Besides the radiators also the spacecraft with its habitat will radiate some of the heat out. To calculate the total heat balance of the spacecraft first the radiator panel will have to be designed. The layout will be discussed later.

Radiator Panel Sizing

The radiator panel to be used is, as discussed earlier, a hybrid panel consisting of an aluminium-carbon hybrid combination heat-pipe with carbon-carbon fins. The outer-shell of the radiator panel is made out of aluminium with a matt-Carbon black paint known as NS-7 Carbon [130]. This paint will make the radiators attain an emissivity of 0.88. The heatpipes considered will be the elaborately tested Inconel 718 pipe made out of a TiCuSil braze with a lining of Mitsubishi KI3C2U (pitch) carbon fiber. The combination of carbon lining in the heat-pipes and the use of carbon fins will make it possible to reach temperatures between 800 and 900 degrees Celsius [108] [62]. The equilibrium temperature of the radiator, being the average temperature at which the complete cluster of radiators will radiate, is set to be 350°C. The panels accommodate for the attachment of other panels by the use of hinges. The coolant that flows through the radiator will be led to the other panels by the use of flexible hoses between the panels. Furthermore there will be a folding mechanism that will also provide structural strength in the radiators. The individual radiator panels will be positioned in an 25° angle. This will have reduction of radiator width of about 10 % which yields a significant reduction in moment of inertia. On the other hand some inter-reflective radiation occurs between the panels due to this 25 degrees angle but this will only result in a loss of efficiency of about 3.5 % [108]. The main heat-pipes coming from the main heat-exchanger will carry

the coolant through the adaptor into the (smaller) radiator heat-pipes. The technical drawing of the radiator panel is depicted in Figure 10.5.

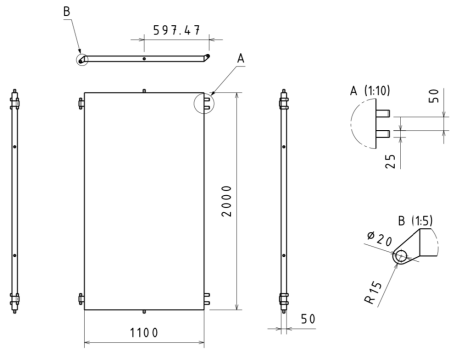

Figure 10.5: Technical Drawing of the individual radiator panel

The required surface area to get rid of the described excess heat in Table 10.2 depend on the surface area of the spacecraft subjected to the sun and in the shade, the distance from the sun and the emissivity of the spacecraft and radiators. This is summarised in Figure 10.6.

Planetary Specification		
	Earth	**Mars**
Albedo [-]	0.3	0.15
Planet Radius [m]	6371000	3389500
Orbiting Height [m]	8371000	3889500
Effective Radiation Temperature [Kelvin]	255	210.1

Spacecraft Specification	
Total Spacecraft Surface Area [m^2]	400
Surface Area pointed at the Sun [m^2]	120
Habitat Surface Area [m^2]	300
Emmissitivity of Spacecraft [-]	0.8
Emmissitivity of Radiator [-]	0.88
Equilibrium Temperature Radiator [Celsius]	350
Equilibrium Temperature Spacecraft [Celsius	4.5

Figure 10.6: Driving Parameters for Radiator Sizing

Input	1 AU/ Earth	1.5 AU/ Mars
Direct solar irradiance [Watts/m^2]	1369.7	608.8
Albedo from planets [Watts/m^2]	238.0	69.3
Earth/Mars Infrared [Watts/m^2]	239.7	110.5
Total Heat absorbed [Watts]	221695.1	94629.9
MHD Heat generation [Watts]	8000000	8000000
Total Heat to be radiated [Watts]	8221695.1	8094629.9
Total heat radiated by spacecraft [Watts]	32681.4	32681.4
Surface area radiator needed [m^2]	1089.47	1072.56
One side area radiator needed [m^2]	544.73	536.28
Including Safety Factor [m^2]	626.442942	616.7227108

Figure 10.7: Detailed Sizing of the Radiators

Using Equation 10.1 a detailed radiator size design can be made. This is depicted in Figure 10.7. Since the radiators of the spacecraft are in plane, in the travel direction, with the solar rays the flux on the radiators is minimised. Second to that, the radiators are designed to pivot around their longitudinal axis and can fold. This makes sure that the flux on this significant radiator surface area is minimised throughout phases in the mission where the nominal radiator position can not be guaranteed to remain in plane with the solar rays. Even though taking these assumptions the the radiator is designed for the worst case, close to earth, having to deal with the largest solar fluxes during the mission. The 25° angle underwhich the radiators are placed result in extra, be it a tiny portion, flux on the radiators. Hence the sizing of the radiators is an iterative process. To accommodate for the solar flux on the radiators and other uncertainties a safety factor of 1.15 was added to the required radiator surface area, this is estimate made by the preliminary sizing of the JIMO mission done by NASA [73]. The final surface area was found to be around 630 m^2 that is able to radiate on both sides.

Layout of radiators

The position and relative location of the radiators is important for the functionality of the thermal control system as a whole and for the integration of the spacecraft. First the layout of the radiator panels influence the efficiency of thermal radiation significantly. Secondly, the

radiators have a significant surface area compared to the engines and the habitat. therefore the location and integration of the radiators into spacecraft is important as it drastically influences the moment of inertia and the center of gravity location. This on its turn will also influences the propulsion and ADCS and even the communication subsystem. The layout of the individual radiator panels with respect to each-other influences the total efficiency. The hot coolant coming from the engine and reactors is introduced into the radiator to cool down. The speed and therefore areal efficiency at which this coolant is cooled is dependent on the thermal transfer coefficient of the radiator. The thermal transfer coefficient is dependent on the conductivity of the material and describes the rate of cooling that is directly proportional to the temperature difference and the heat transfer area following the relation described in Equation 10.2.

$$\frac{dQ}{dt} \propto hA\Delta T \tag{10.2}$$

Where h is the heat transfer coefficient (Watt/m$^2\cdot$ Kelvin) and, amongst others, depends on the characteristic length of the heat transfer area and the mean film temperature of the fluid. According to multiple studies in radiator designs it was proven that this relation describes the most efficient thermal transfer for radiators in a trapezoidal layout [7] [73]. Meaning that the hottest part of the coolant loop will be introduced in radiator panels having the smallest length/area. The smaller length of this particular radiator panel makes the thermal transfer more efficient as it can radiate out larger amounts of thermal power (at a very hot temperature) over a smaller length only. This trapezoidal design will therefore make more efficient use of the available radiator surface area, hence making the overall surface area smaller. Starting from the engine (where the temperature is highest) the radiator panels will increase step-wise in length as the coolant decreases in temperature towards the habitation module.
This trapezoidal layout makes the overall surface area for radiators smaller but the length of the required truss will increase. The trapezoidal layout can be worked out in multiple ways. The team decided upon analyse the two following concepts; the split up trapezoidal ”butterfly” design and the trapezoidal ”Delta wing” design. Both layouts are depicted in Figure 10.8 and Figure 10.9.

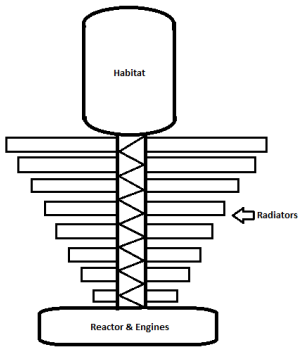

Figure 10.8: The trapezoidal ”butterfly” design schematic. Not to scale

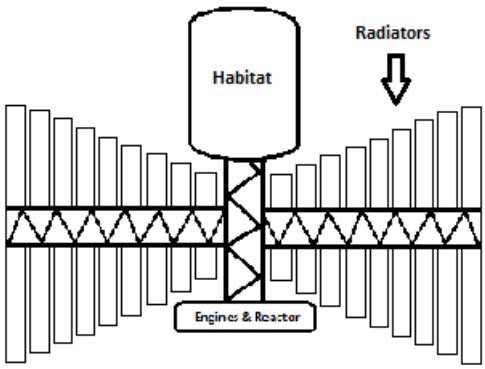

Figure 10.9: The trapezoidal ”Delta wing” design schematic. Not to scale

To find out what the best type of layout is for the spacecraft, taking into account the integration of all subsystems and the modularity of the concept, both concepts were analysed for the following points;

- **Changes in Moment of Inertia**
  The main difference between the two layouts is the difference in moment of inertia on its lateral axis. For the ”Butterfly” layout the two largest weight contributions of the habitat and the engines/reactors are lumped close to each other. Where in the ”Deltawing” layout the truss is required to be larger, separating the habitat and engines/reactors

further from each other. After analysis, Section 11.8, of the mass moment of inertia (MMOI) the ”Butterfly” concept showed a significant reduction in MMOI of about 75 % compared to the ”Deltawing” concept. However, the large MMOI for the ”Deltawing” concept is shown (Chapter 8) to not have a dramatic effect on the required ADCS capabilities, as the manoeuvres the spacecraft is expected to perform are generally with low accelerations and therefore over longer time duration’s.

- **Heat-pipe Flow Optimisation**
  The hot coolant coming from the heat source (the engines plus reactors) should be introduced into the radiators as efficient as possible, reducing the heat-pipe thermal adjustments necessary for the heat-pipe to carry the hot coolant over a longer duration. In the ”Deltawing” the coolant coming from the heat source is introduced very efficient (red. small amount of high thermal resistant pipes) into the radiators. Using the ”Butterfly” concept the coolant has to travel through longer thermal resistant heat-pipes located in the truss before it is introduced into the radiators. Also a more advanced valve infrastructure is needed to split the coolant in two separate radiator clusters.
- **Fuel Tank Placement**
  The propellant tanks have to be placed on the truss of the spacecraft. The ”Deltawing” concept provides a long enough truss to cope with the required propellant tank storage space. Furthermore they can be easily cryo-cooled as all the pumps, coolers and necessary piping and valves are located in-line of the truss, increasing the modularity potential. For the ”Butterfly” concept the truss is cut into smaller individual truss sections, limiting the size of the propellant tanks to be mounted. Furthermore the fluid infrastructure to cryo-cool the tanks and to direct the propellant towards the engines is more involved.
- **Required Heat Protection for Habitat**
  The radiators will radiate heat at high temperatures throughout the trapezoid. The short radiator panels radiate at the highest temperatures. The ”Deltawing” concept therefore provides enough spacing between the habitat and the hottest radiators plus that the temperature (going towards the habitat) of the radiator gradually decreases. This makes the heat protection that is necessary on the face of the habitat that ”looks” towards the radiators minimal. The width of the heat-shield at this side of the habitat is also minimised. On the contrary, the ”Butterfly” concept will have the hottest radiator panels significantly close to the habitat and the width of the radiator in lateral direction is significant larger. Resulting in more heat protection on the habitat and a wider heat-shield in lateral direction.

After analysis it was concluded that based on the points discussed above the ”Deltawing” concept is the optimal layout for the radiator, minimising the required heat protection for the habitat, making the piping and tank placement less complex and heat dissipation more efficient. The layout of the integrated radiator cluster within the spacecraft can be found in Figure 10.10. Figure 10.11 provides an isometric view of the radiator subsystem.

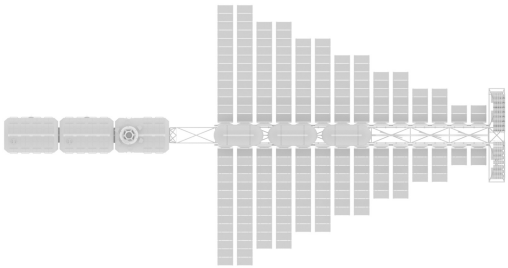

Figure 10.10: Topdown view of the integrated thermal control subsystem

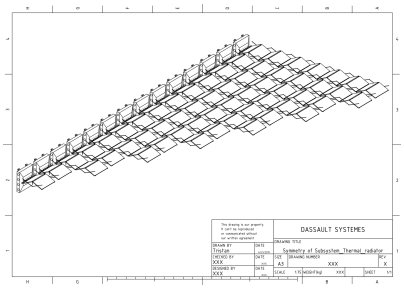

Figure 10.11: Isometric view of the cluster of radiator panels

Thermal Loop Design

To distribute the heat throughout the spacecraft the thermal control system is relying on the working fluid that will be main player in the thermal loop. The loop begins with at the MHD Generator which is the main heat source for the spacecraft. The thermal loop is therefore primarily designed to cool down the MHD and transferring the heat towards the radiators. The MHD units have a total heat output of 8 mega-watts. The working fluid throughout the reactors and engine is a combination of Xenon/Helium low temperature plasma. The excess heat of 8 mega-watts, carried by this plasma/working fluid, will be transferred into the primary thermal working fluid by means of a heat-exchanger. The plasma will enter the heat-exchanger with a temperature of 420 K [104]. The radiators are designed and optimise to radiate with a equilibrium temperature of about 350°C or 622 K. So the primary thermal working fluid that will flow through the radiators should be able to attain a temperature range between approximately 200 and 800 K. The working fluid chosen is the High Temperature Molten Salt Heat Transfer Fluid (MS-2) [2], that is a combination of molten salt dissolved in a combination of water and oils, having a low toxicity. The temperature range of MS-2 is between 130 and 500°C, or between 403 – 773 K. So the heat-exchanger will need to use a combination of compressors to heat up the working fluid from 420 K to around 800 K. After leaving the heat-exchanger the MS-2 working fluid is transported towards the radiators to cool it down, working at a equilibrium temperature of 620 K. After the working fluid leaves the radiator, considering a thermal transfer coefficient for aluminium of about 237 $Watt/m^2 \cdot$ Kelvin and a preliminary analysis that describes the conductivity between the working fluid and the radiator panels, the temperature will be somewhere between 180 and 220°C [2]. The (MS-2) working fluid now enters a second heat-exchanger that will transfer the heat into a thermal loop using a glycol/water combination as the working fluid. This working fluid has a great heat-capacity and is non toxic. The working fluid is used to heat up the habitat since the temperatures of the working fluid are still higher than the required equilibrium temperatures. To maintain equilibrium the working fluid can be redirected using valves to lower the amount of heat input in the habitat from this glycol/water loop. Coolers are used to cool down the habitat if required and the heat coming from the coolers will be added to the working fluid. After passing by the habitat the working fluid will have a temperature between 60 and 100°C approximately [2]. The thermal loop can be split into 4 groups; heat acquisition subsystem, heat rejection subsystem, external active thermal control subsystem (EATCS) and the internal active thermal control subsystem (IATCS). A schematic of the thermal loop is shown in Figure 10.12.

Thermal Design for Habitat

The habitat will be thermally insulated using a combination of different layers known as Multi-Layered Insulation (MLI). This material will passively control the thermal flux coming from the sun and radiators radiating into the habitat. However, MLI doesn't protect the spacecraft from internal heat conduction or convection but this is not unfavourable in space and will yield a distribution of the temperature over the spacecraft. MLI consists of multiple layers of lightweight reflective films. These films are typically made from a combination of polyimide, polyester and thin layers of aluminium. It also protects the habitat against dust impact and shield external delicate instruments. The side of the habitat that is directly oppose the radiators is receiving significantly more infrared radiation than the other parts of the habitat, the layer thickness of MLI will be increased. The MLI will be located underneath the radiation shielding of the habitat.
Internally, the habitat will be heated by the coolant loop described in Figure 10.12. To maintain an internal equilibrium temperature range of 15 to 25°C, coolers are located (using electrical power).

Mass and Power Estimation

Now that all the required systems are known and have been sized the mass and power budgets can be constructed. The mass is estimated based on the size and working fluid loop architecture of the thermal control system. The power required to power the thermal control

[2] https://www.dynalene.com/product-category/heat-transfer-fluids/dynalene-molten-salts/

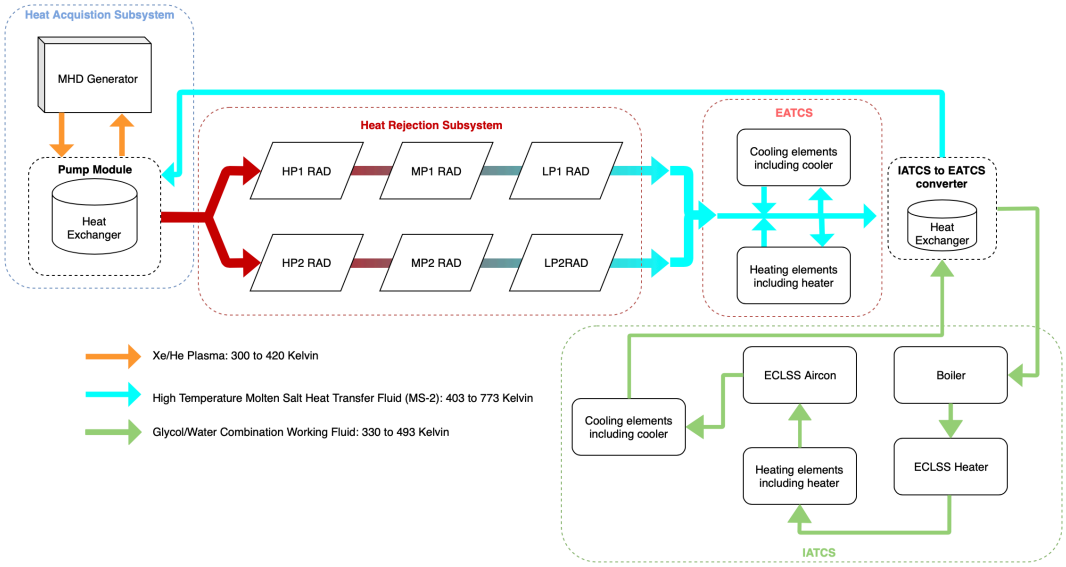

Figure 10.12: Thermal control loop graphical illustration

system is based on the amount of working fluid that have to be pumped around and the power the heatexchangers require. Both mass and power budgets are based on mass and power analysis of the ISS and scaled linearly, using multiple data points, accordingly [4].

Weight category	***Mass [kg]***	***Weight category***	***Mass [kg]***
Radiator Infrastructure:	**7971.1**	**Thermal Infrastructure:**	**9,909.2**
Radiator, Heatpipes and Connector	3,268.4	Large Heat Exchangers	377.4
Fluids [MS-2]	900.9	Small Heat Exchangers	250.0
Pumps	928.9	Piping and Plumbing	7,229.7
Instruments and Sensors	985.3	Fluid per EATCS Loop [MS-2]	656.1
Valves	291.5	Fluid per IATCS Loop [Glycol/Water]	1,396.0
Electrical Flow Control	1,596.1		

Weight category	***Mass [kg]***	***Weight Category***	***Mass [kg]***
Passive Thermal Insulation:	**696.2**	**Thermal Power system:**	869.2
Multi-Layered Insulation	696.2	Pumps and Valves	869.2

GRAND TOTAL: **19,445.5 kg**

Table 10.3: The Mass Budget of the Thermal Control Subsystem [4]

Thermal Control Component	***Power Required [Watt]***
Pumps and Compressors	148,633.2
Valve systems	10,617.4
Heat Exchangers	785,543.6
Radiator deployment mechanism	8,425.1
GRAND TOTAL:	**246,219.3**

Table 10.4: The Power Budget of the Thermal Control Subsystem [4]

Both the mass and power budgets are depicted in Table 10.3 and Table 10.4 respectively.

10.6. Special Thermal Load Cases

During different phases in the mission the thermal control requirement changes. For example, during the transfer to Mars with engines operative the thermal control requirement is different from the phase where the spacecraft orbits around Mars with the engines inoperative. The thermal control system should be flexible in the regards that it can provide the necessary thermal budgets throughout all the phases that might occur in the mission. Below a small explanation is given how the thermal control system will be operated throughout the different phases.

Engine Down in Pre-retro-burn Manoeuvre

During the yaw manoeuvre of the spacecraft to position itself for the retro-burn when entering the Mars or Earth parking orbit the engines are inoperative. The reactors still provide the necessary power to power the ECLSS and other crucial subsystems on the spacecraft. Since the reactors are less active the total excess heat is smaller, hence a portion of the radiators can be retracted. If a power outage occurs the back-up solar panels can power the thermal heaters in the habitat. If more thermal heat is required to heat up subsystems or modules the radiators can be used to generate extra heat. The spacecraft has to rotate 90° over its longitudinal axis to point the radiators perpendicular to the solar-rays. This will reverse the cooling effect of the radiator by heating up the working fluid by the use of the black radiator panels. This working fluid will then be pumped towards the systems that require thermal heating.

Orbiting

During the orbiting phase around Earth or Mars the engines will be inoperative. The reactors provide for the necessary power for the spacecraft. The heat that is the result of this power generation can be radiated out by the use of (a portion) of the radiators. In this case a significant portion of the radiators will be retracted. This decrease the chances of deterioration and collisions with micro meteorites. The same reversed heating principle can be used in case of a power outage as described above.

Working Fluid Leakage Mitigation

In case of a puncture by a micro-meteorite or an unexpected leakage of some kind, the working fluid has to be protected from leaking out. The radiators have sensors in the piping and panels to detect pressure lose in the heat pipes. Upon detection of a pressure loss as the result of a leak a involved valve system will close down the branch in which the leak was detected. This will temporarily make the designated radiator panel in-operative such that the panel and leak can be repaired by the crew and the robot-arm. The piping architecture minimises the effect of the loss of surface area during this temporarily period. The safety factor included in the sizing of the radiators also makes up for this temporarily smaller effective surface area.

10.7. Sensitivity Analysis

The thermal control system design is dependent on a lot of factors. The system is primarily connected to the reactors and the engines that deliver the largest portion of the excess heat. To take this connection and the consequence on the design into consideration for further design iterations a sensitivity analysis has to be performed. The sensitivity analysis will be performed on the top level design requirements for the thermal control system that primarily drive the sizing of the radiators. The sensitivity analysis will additionally give a lot of insight in how the subsystem will behave in the required modularity of the spacecraft.

System Response to Additional Reactor

Since the spacecraft is being designed for different mission characteristics the electrical power or thrust required for each individual mission can vary. This means that the reactor/engine subsystem has to scale accordingly, consequently varying the thermal excess heat per mission. The thermal control subsystem is driving the overall lay-out of the spacecraft significantly so the response of the required surface area of the radiators, after adding an extra radiator, is especially interesting. The nominal design surface area is, as discussed earlier, 620 m^2. Adding an extra reactor will scale up the excess thermal power with 25 %. By analysing the radiator surface area behaviour to this extra reactor it was found that the surface-area increased to 779 m^2 still including the safety factor. This is an approximate increase of 24.4 % and therefore it scales linearly with a gradient smaller than 1. The mass and power estimates went up from 19.4 t and 246 kW to 23.8 t and 306 kW respectively. That equates to a mass increase of about 22.8 % and a power increase of about 24.4 %. It can be concluded that the surface-area, mass and power scale up approximately linearly with larger excess heat power levels.

System Response to a Lower Equilibrium Temperature

The high temperature hybrid radiator panel that was designed to operate at an equilibrium temperature of 623 K has not been tested in space over a long duration. Exposure to the harsh space environment over the duration of multiple missions can negatively affect the radiator panel operating temperature. As described in Equation 10.1 the equilibrium temperature is the biggest contributor to the required surface area for the radiators. It scales with the power of four. To analyse the affect of this degradation of equilibrium temperature on the surface area, mass and power of the thermal control system the temperature will be scaled down to 523 K, a 16 % reduction. The analysis showed that the surface area increased from 620 m^2 to around $1,261$ m^2, a significant 200 % change. The power scaled up with the same factor to 496 kW. The mass increased to roughly 36 or with 183 %. Thus changing the equilibrium temperature, as expected, will greatly affect the thermal control subsystem.

Increasing Thermal Excess Power (25%)	*Old Value*	*New Value*	*Percentage Change*
Surface Area Sensitivity	620 m^2	779 m^2	24.4 %
Mass Sensitivity	19,445 kg	23,859 kg	22.8 %
Power Sensitivity	246 kW	306 kW	24.4 %

Table 10.5: Increasing Thermal Excess Power Sensitivity Analysis

Equilibrium Temperature Degradation (40%)	*Old Value*	*New Value*	*Percentage Change*
Surface Area Sensitivity	620 m^2	$1,261$ m^2	200 %
Mass Sensitivity	1,9445 kg	35,731 kg	183 %
Power Sensitivity	246 kW	496 kW	200 %

Table 10.6: Equilibrium Temperature Degradation Sensitivity Analysis

The results are summarised in Table 10.5 and Table 10.6.

10.8. Verification & Validation

Before the actual manufacturing and assembly phase the thermal control subsystem has to be verified and validated. The thermal analysis of the radiator design and the consecutive sizing should be analysed in more detail to check and iterate for further design stages. This verification can be done using a combination of a computational fluid dynamics tool and a thermal transfer program. This will give more insight in the actual heat transfer throughout the radiators and piping structure. The result from this verification can help estimate the temperature at each independent radiator position. Also the heat flux from the radiators on the habitat will tell a lot about the efficiency of the thermal control system as a whole. The structural strength of the carbon-fibre/aluminium integration and the durability of the radiators, when experiencing a small meteorite hit, can be modelled extensively with the use of Finite Element Analysis.

After the radiators and control loop have been manufactured the entire system can be tested extensively on the ground and in a space environment. The radiators should be tested by a simulated excess heat source and an analysis on the thermal conductivity and irradiance coming from the radiators, including their efficiency's, can be performed. This system can be tested as an integrated whole together with the MHD's and reactors since the reactors have to be tested for 2.5 years. During this demonstration the equilibrium temperature of specific components within the thermal control subsystem will give the possibility to tweak the design and to get rid of unforeseen anomalies.

11

Spacecraft Structures

The structures subsystem is comprised of all elements that allow the integration of other subsystems in the spacecraft (by providing attachment points, structures, modules and other), and allow the spacecraft to withstand all load cases throughout the mission. Additionally, the general external layout of the spacecraft is largely defined by the structures subsystems. This chapter outlines the general considerations made in the definition of the external layout of the spacecraft, as well as the detailed design of the module radiation shielding, module structure, docking ports and Remote Manipulator System (RMS).

11.1. Key requirements and constraints

The Structures subsystem is to comply with the following set of requirements:

- SYS-04 The system shall consist of interchangeable modules.
- SYS-05 The system shall be expandable with further modules.
- SYS-06 Each module of the system shall be able to autonomously rendezvous and dock in orbit.
- SYS-08 Each module of the spacecraft shall have a service life of at least 20 years.
- SYS-12 The system shall have a window.

11.2. External Layout

The external layout is mainly driven by a set of subsystems that are critical to the spacecraft functioning, and have a significant size. These are the following systems:

1. Pressurized modules
2. Radiators
3. Nuclear reactors, MHD assemblies
4. Propulsion systems
5. Fuel tanks
6. External payload

Several aspects of this mission drove the external layout to how it is depicted in Figure 11.1. Firstly, in order to keep the center of gravity of the spacecraft in line with the centre of thrust, all subsystem were mounted in line with the central axis, or placed symmetrically about that axis. The nuclear reactors are placed far away from the habitat modules, as they generate a large amount of heat that needs to be dissipated. The radiators are therefore also placed in between the modules and the reactors. As the engines require power from the nuclear reactors, it was considered most convenient to place the engines next to the reactors. The engines and reactor assemblies are clustered in the back of the spacecraft. Launcher payload mass constraints mean there will be a total of 6 Argon fuel tanks on the spacecraft.These are symmetrically mounted to the truss supporting the radiators and the engines. Finally, in order to satisfy NASA's recommended minimum volume per astronaut of 25 m^3, a total of three pressurized modules are included. The other subsystems that need to be place externally are the following:

1. Control moment gyro's
2. Attitude control thrusters
3. Attitude control fuel tanks
4. Communication antenna
5. Pressurisation tanks
6. Argon cryo-coolers

With the exception of the communication antenna and the attitude control thrusters, all these subsystems can be embedded inside the main truss structure. The thrusters are placed along the length of the spacecraft (as discussed in Chapter 8), and the antennas are placed on the truss structure to allow for the necessary field of view. Figure 11.1 shows the overall

external layout of the spacecraft, and as can be seen a truss structure was necessitated by the distance requirement of the habitat modules to the reactor as well as the radiators. The truss is primarily there to provide mounting points to the spacecrafts power, thermal, and propulsion subsystems. As the low thrust engines produce a trust in the 100 s of newtons the structure can be extremely light, and the current material of aluminium could possibly be replaced with a more lightweight material. The following sections will discuss the design of Structural elements of the spacecraft in more detail, and an overview of the full spacecraft dimensions can be found in Appendix B.

11.3. Attitude Considerations

During the trajectories, there are several requirements on certain subsystems regarding their attitude towards the Sun, Mars or Earth. These include:

- The heat radiators are preferably tangential to the Sun, in order to limit thermal power absorption from it
- As can be seen from Figure 6.8, the engines are required to point in many different directions with respect to the Sun, Earth and Mars
- The communication antenna should point towards Earth
- The solar panels (if deployed in case of a reactor shutdown) should point towards the Sun

The exact designs of these subsystems will be discussed in subsequent chapters, especially in Chapter 11 regarding the structure and layout of the spacecraft, but some preliminary conclusions can already be drawn from these requirements:

- The spacecraft will have to make a 180° flip around its vertical or transverse axis in the middle of the transfer to and from Mars
- The attitude of the spacecraft will be such that the radiators are in the orbital plane, so they will be tangential to the Sun. During Earth or Mars orbit this will be impossible, however, at these moments the engines are not burning, so there will be little heat to dissipate from the throttled down reactors
- The solar panels are ideally placed perpendicular to the radiators, and will likely need to be gimballed due to the aforementioned flip.
- The antennas will have to be placed in such a way that the line of sight is not blocked while the orientation with respect to Earth is changing

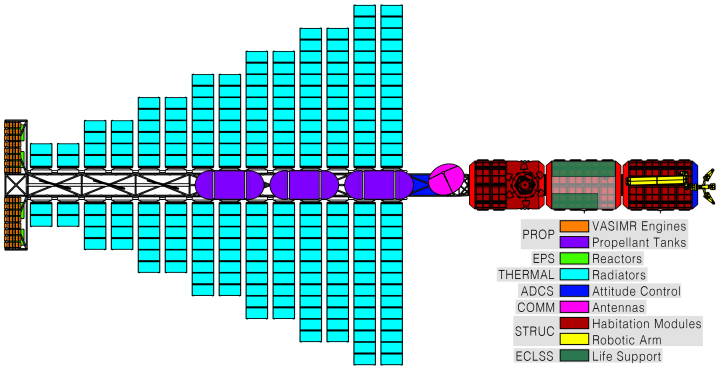

Figure 11.1: Mars Transfer Vehicle layout and subsystem overview

11.4. Module and spacecraft shielding

11.4.1. Micrometeorite and Orbital debris shielding

Micrometeorite and orbital debris (MMOD) is an omnipresent risk for space travel that must be adequately protected from to allow for safe operations. Even small particles can cause sever or catastrophic damage to unprotected systems, as an aluminium sphere at 7 km/s can penetrate up to 4 times its diameter of a solid plate. However this can be solved by using ”Whipple” shields which are up to 84 % lighter compared to a solid shield providing the same protection [19]. These shields employ multiple thin plates with a stand off area between

them, this allows for the incident particles to be broken up after penetrating the outer shell. Thereby greatly reducing the penetration power of the particle as after travelling through the standoff area, as the ”cloud” of material impacts on a larger surface.

The shielding of all mission critical surfaces of the spacecraft will be protected by stuffed Whipple shielding that is similar to the one used on the ISS [19]. With the back-plate or the wall of the pressure vessel is approximately twice as thick, the exact make up of the shield can be seen in Figure 11.2. This improves the performance of the shield however the main reason for the thicker aluminium layer was due to the radiation requirements. Furthermore additional removable outer panels are added that allow for ease of maintenance, with an average of 0.8 cm additional thickness.

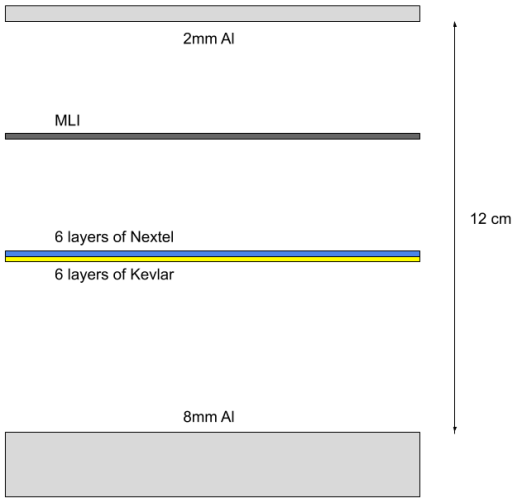

Figure 11.2: Whipple shielding used on the spacecraft

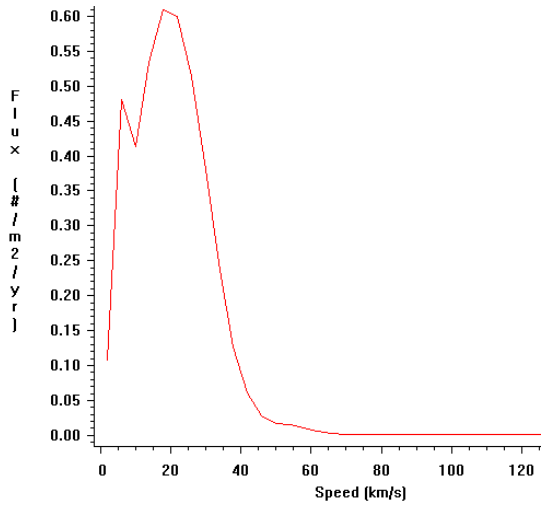

Figure 11.3: Flux distribution of velocities for the mission

In order to correctly size the required shielding thickness, the MMOD environment along the orbit must be analysed. This was achieved by using the MEMR2 program available from NASA, which uses the interplanetary trajectory of the spacecraft to find the average MMOD environment [82]. This provides the expected number of collisions on each face per square meter per year for different velocities, the aggregate on all surfaces can be seen in Figure 11.3.

Additionally the relationship between the micrometeorites mass and average flux can be seen in Figure 11.4 and is used in association with simulations of hyper velocity impacts on Whipple shields in Figure 11.5. The latter gives a relationship between the diameter of a particle, the velocity and whether the combination of which resulted in the penetration of the shield [24]. The simulated shield has significantly less protection than the one being used on the spacecraft as it does not include a nextel Kevlar layer, and the thicknesses of the two plates are 1.6 and 3.2 mm as opposed to 2 and 8 mm. This means that the penetrating power of particles will be overestimated. Interpolating and extrapolating both of these results to simplified mathematical equations allows for the chance of a MMOD particle penetrating the shielding to be calculated.
Using all of the above mentioned data and functions, the resulting number of penetrations are shown in Table 11.1. Therefore during the 3 year mission there will be 6×10^{-3} impacts that will cause penetration of the habitable modules.

	X Ram	-X Wake	+Z North	-Z South	+Y Port	-Y Starboard
Number of particle penetrations [10^{-6}/year$*m^2$]	5.058	0.609	3.316	3.314	3.973	7.096
Surface area of habitat module	16.619	16.619	115	115	115	115
Number of particle penetrations [10^{-3}/mission]	0.252	0.03	1.144	1.143	1.371	2.448

Table 11.1: Number of particle penetrations on the habitat module

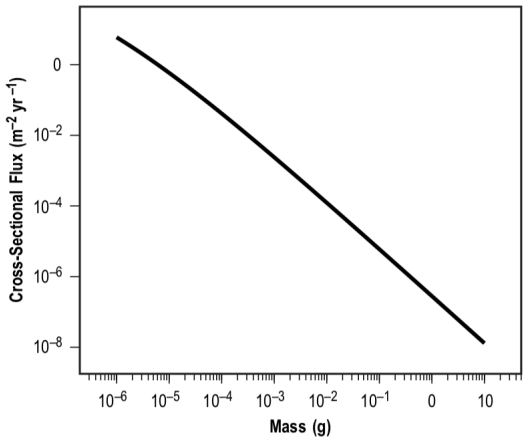

Figure 11.4: Average flux density for particles of different masses in interplanetary space

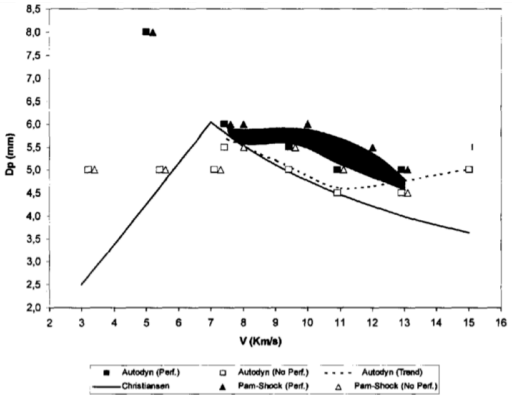

Figure 11.5: Perforation of a Whipple shield by spheres of aluminium of given diameter and velocity (solid shapes indicates penetration while empty shapes no penetration)

However it is important to reiterate that the equation used to estimate if a particle with a certain mass and velocity can penetrate underestimates the shielding used on the spacecraft. Furthermore the simulations for the shielding used aluminium particles which have a density of 2.7 g/cm^3, whereas micrometeorites have an average density of 1 g/cm^3 or less for particles heavier than 10^{-6} g [10]. As the penetration depends on the force and the area over which is applied, a less dense material provides less penetration. Therefore this also causes the underestimation of the shield performance. The combination of the above mentioned assumptions means that the real number of particles penetrating the habitable modules during a 3 year mission is well below 6×10^{-3}. This gives the spacecraft a failure risk of less than 0.6 % over 900 days which is in line with failure risk for other deep space mission such as Lunar outpost (NASA) with a risk of 0.2 % during a 210 day mission [28].

11.4.2. Radiation shielding

The radiation environment in interplanetary space is over two orders of magnitude higher than on earth, which has a significant effect on both the human occupants and electronics on board. Radiation has negative or even fatal heath consequences for both short and long term exposure, additionally it also degrades electronics. This means that necessary shielding must be implemented into all habitat modules as well as for electronics aboard.

The radiation environment outside of earths atmosphere is harsh and volatile, radiation sources include galactic cosmic rays (GCR), solar radiation, and solar flares additionally specific to earth orbit there are the Van Allen belts [69]. These contain both trapped electrons and protons that originate form the sun and are captured in the outer layers of earths magnetic field. Furthermore there is an 11 year solar cycle that describes the activity of the sun and is measured in the number of solar events or flare. Solar minima, a low number of solar events, means that the electromagnetic field of the sun is weak, this in turn allows for more GCR radiation into the solar system [36]. This periodic fluctuation can be see in Figure 11.6, in turn solar maxima means that GCR radiation decreases but there are more solar events. For both electronics and humans GCR radiation is more detrimental than solar flares, partly because GCR is omnidirectional while solar activity is not. Therefore solar minima will be used to calculate the worst case doses. In addition to the environmental radiation received by the astronauts the spacecraft also has 4 low enriched nuclear reactors, which add additional radiation mentioned in Section 9.4.1. These contribute relatively little to the total dose as, according to a research paper on a NASA thermal nuclear engine mission which has high enriched fuel only contributes approximately 3 % to the total equivalent dose. Fundamentally in order to stop radiation material must be placed in front of the incident rays, the total amount of mass determines the shielding amount with the type and density of material having less of an effect. The shielding amount is measured in g/cm^2 which corresponds to the thickness of the material in cm times its density in g/cm^3.

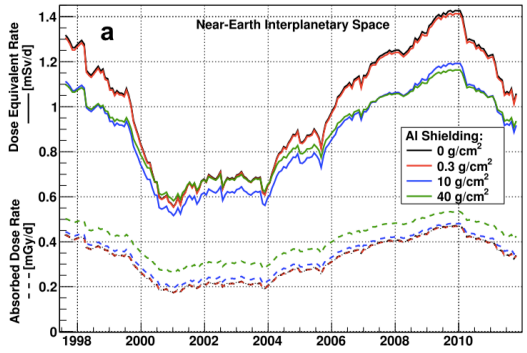

Figure 11.6: Change in interplanetary radiation with the 11 year solar cycle [36]

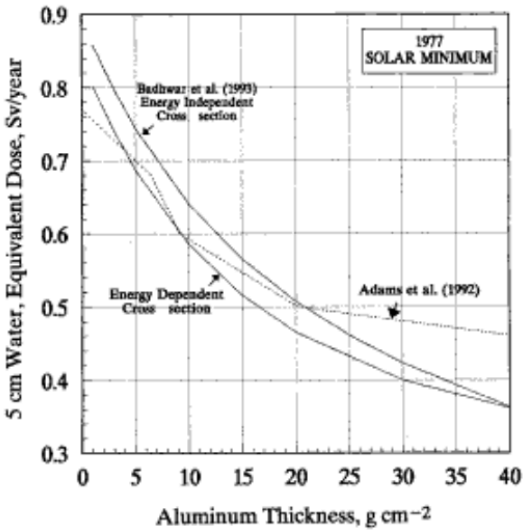

Figure 11.7: Equivalent dose per year for different shielding depths [48]

Once the radiation is reduced by the shielding the incident rays of particles will cause damage to the content of the spacecraft. The damage that is caused by radiation is determined by the amount of energy that is deposited in the target material, as energy is lost by causing damage. Hence the radiation effect is measured in Gray (GY) J/kg which is the energy deposited per mass, the change of which can be seen in Figure 11.6 with the dashed line. While this is sufficient for the estimation of the impact on the electronics it is not representative of the damage caused to humans. As tissue damage is not only dependent on the amount of energy deposition, but on the type of ionising particles as well. In order to estimate the impact of it on humans, the radiation has to be analysed and all of its components LET (Linear energy transfer) must be found. This value describes the amount of energy that an ionising particle deposits per unit length, this also depends on the target material and its thickness. After taking this value, the energy distribution, the flux, with a quality factor, that describes the impact of the previously mentioned factors on tissue, the amount of Sieverts (Sv) can be calculated. This value describes the effective radiation that humans experience. Figure 11.7 shows how the yearly equivalent dose at solar minima changes with different shielding depths which gives around 500 mSv per year at 20 g/cm^2. This is in agreement with Figure 11.6 which gives a 1.2 mSv per day for solar minima, approximately 440 mSv. However the 500 mSv value is from 1977 which is the lowest ever solar activity recorded and is commonly used as worst case scenario, while the 440 mSv value is from 2010.

As the astronaut must spend approximately 950 days in interplanetary space, and the maximum mission dose is set at 1500 mSv, this becomes equivalent to 1.58 mSv/day or 570 mSv/year. This amount corresponds to approximately 5 % chance of premature death due to exposure related medical issues. However the programs used to generate the data for the above graphs have an uncertainty of 10 %. By taking an additional 3 % to account for the reactors, the yearly dose requirement becomes 500 mSv to account for inaccuracies [69]. Hence the required shielding thickness is 20 g/cm^2 of aluminium. Some materials have slightly higher radiation performance than aluminium such as polyethylene and Kevlar which are 15 % more efficient [12][40]. This means that all materials can be converted to an equivalent aluminium thickness, the final radiation shielding is shown in Figure 11.2 without the additional 12 cm of polyethylene backing. This shielding configuration was confirmed by using NASA interplanetary radiation estimation tool oltaris. For a solar minimum with 20 g/cm^2, a total mission dose of 1350 mSv was estimated. Including the additional radiation form the reactors, this gives approximately 1400 mSv which means 20 g/cm^2 provides sufficient protection. Finally it is worth noting the the final radiation shielding is most likely larger as all the equipment and supplies are not accounted for which will line the spacecraft

walls, this could be an additional 5 g/cm^2 of shielding.

	Thickness [cm]	Density [g/cm^3]	Equivalent Aluminium shielding
Aluminium	1.8	2.7	4.9
MLI	0.1	1.38	0.14
Kevlar	0.5	1.45	0.84
Nextel	0.5	1.45	0.84
Polyethelene	12	0.96	13.2
Total			20

Table 11.2: Radiation shielding of the pressurised modules

11.5. Module Sizing and Structural Analysis

The design of the module structure is constrained by several functional requirements and mission characteristics. Modules will have to maintain atmospheric pressure inside of them, provide protection against radiation and micro-meteorite impacts, and provide enough strength to sustain all manoeuvres and launch loads. The outer diameter of the module is constrained by the fairing inner diameter of 4.6 m. A margin of 52 mm with the inner fairing wall was taken as an initial estimate. The module is cylindrical to optimise fairing volume usage. This shape is also ideal for pressure containment, but as the modules will only undergo a pressure differential of 1 bar this was not the driving constraint. Similarly round end-caps would provide more strength against pressure, but as this is not a high pressure vessel it was chosen to use a more easily manufacturable angled face. An overview of the general dimensions of the module can be found in Figure 11.8.

As the micro-meteorite shielding requires multiple layers with empty space in between them, the module was designed as an assembly of three co-centric shells with panels mounted on the outside. The panels provide attachment points for external hardware (such as the robot arm), and handles for EVA during assembly. The outer diameter of the last shell is sized to payload fairing constraints, and the layering is designed according to the micro-meteorite and radiation shielding discussed in Section 11.4.2. This results in a total of 4 structural layers in the module wall: Poly-ethylene liner, inner structural shell, outer structural shell and the shell panels. With additional thermal insulation and Kevlar lining between the inner and outer aluminium shell. Longitudinal stiffeners were added to the inner shell to provide additional compressive strength and attachment points for the outer shell. Figure 11.9 shows a cross section detail of the resulting structure, and an isometric view of the inner shell.

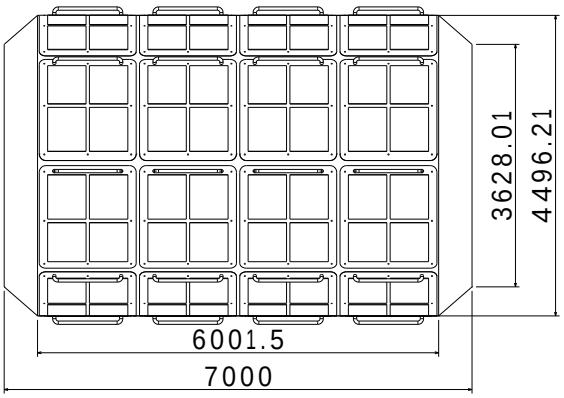

Figure 11.8: Module Dimensions

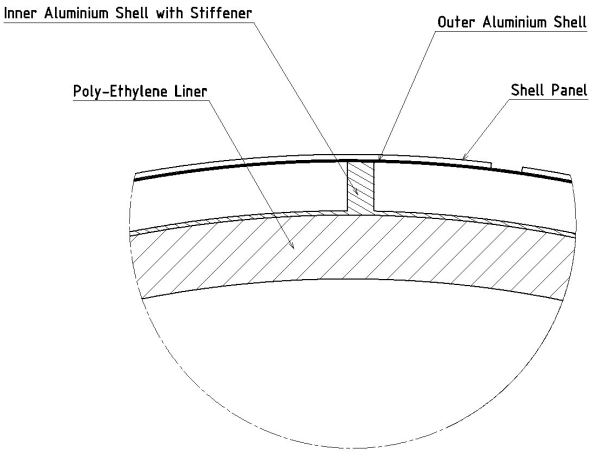

Figure 11.9: Cross section of structural layering

The shells were primarily designed to fulfil radiation and micro-meteorite shielding requirements. The resulting structure was then analysed in the most extreme load case: launch loading. During these calculations it is assumed that the launch loads are fully transferred to the inner and outer structural shell (i.e. poly-ethylene and shell panels do not contribute.) If additional strength was required, the design of the shell would then be iterated upon. Four scenarios for the structural shell were investigated:

1. Buckling of the shell under compressive launch loads
2. Frequency Analysis
3. Lateral deflection limit exceeded
4. Shear failure at payload adapter load introduction

Docking Module

In order to provide docking ports for external payloads and re-supply missions, one of the three modules is dedicated to storage and docking. This was chosen to be the module closest to the structural truss, as it allowed the habitation module to be located as far away as possible from the propulsion and power system (both due to safety concerns and noise reduction.) A more detailed overview is provided in Section 11.7, there are two types of docking ports. One allows for easier docking, and is the international standard used on crew capsules such as the Orion capsule and the Dragon capsule [14]. The other is used primarily for permanent structural connection between modules on the ISS, it has a much larger inner diameter, and could allow the transfer of larger systems into the spacecraft. The docking module will contain 2 of each of these docking ports, placed radially as shown in Figure 11.10. Furthermore one of the larger docking ports are going to house a cupola that is similar in design to the ISS, which will enable visual inspection of both the spacecraft and Mars once in orbit. As these docking ports are able to transfer loads, the structural analysis assumes that the addition of docking ports does not affect the design.

11.5.1. Material selection

Before any structural analysis is performed, a material must be selected. Due to their ease of manufacturing, relatively low cost and high strength, 2000 and 7000 series Aluminium alloys are commonly used in the aerospace industry. The material selection of the structural shells was done qualitatively, as an in depth analysis of all suitable alloys was considered out of scope. Two common alloys, Aluminium 2219 T62 and 7075 T6, were considered for the shell. Relevant properties of these alloys are listed in the table below:

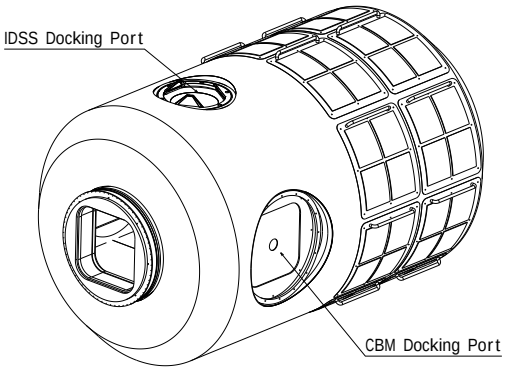

Figure 11.10: Docking module

Alloy	E [GPa]	G [GPa]	τ [MPa]	ρ [g/cm3]	E/ρ [GPa/g/cm3]
2219-T62	73.1	27	255	2.84	25.74
7075-T6	71.7	26.9	331	2.81	25.52

Table 11.3: Al2219-T62 and Al7075-T6 Material Properties

It can be seen that there is no major difference in material properties apart for the shear strength. It is expected that the radiation and impact shielding requirements are the driving factor in the shell design. The material with the highest specific stiffness E/ρ was chosen. All further calculations are therefore done with Al2219-T62.

11.5.2. Buckling Analysis

The goal of the buckling analysis is to identify the acceleration required to make the structural shell buckle. if the shell buckles at 6 g or less (longitudinal acceleration of the Falcon Heavy), it would need structural reinforcements. In order to simplify the calculation, the shell will be discretized to one cylindrical shell with a thickness of 10 mm, the combined thickness of the inner and outer shell, and a length of 7 m. This discretization is considered to be conservative, as the poly-ethylene and the shell panels are assumed to be non-load bearing. The critical buckling stress for a cylindrical shell under uniform compression is given by [18]:

$$\sigma_{critic} = \frac{E}{\sqrt{3(1-\nu^2)}} \times \frac{t}{R} \tag{11.1}$$

Applying a safety factor on the bucking stress of 1.5, and converting the force to an acceleration, the critical buckling acceleration is then:

$$a_{crit} = \frac{E}{1.5 \times \sqrt{3(1-\nu^2)}} \times \frac{t}{R} \times \frac{A_{cross-sec.}}{m_{shell}} \tag{11.2}$$

Aluminium 7075 T6 has an E-modulus of 71.7 GPa. For Al-7075T6, $\nu = 0.33$. The discretized shell has a cross-sectional area of $A_{cross-sec.} = 0.123$ m^2. The mass of the inner and outer shells combined is 3987.4 kg. In addition to this, the Poly-ethylene liner has a mass of 11,810.4 kg. During a launch, equipment and supplies will also be attached to the walls of the module. It will therefore be assumed that the shell is supporting a total of 25,000 kg, the maximum payload weight for the required orbit. Using Equation 11.2, a critical acceleration of 775 m/s^2 was found, this is equivalent to 79 g. Hence, the wall thickness requirements for radiation and impact protection are sufficient to prevent buckling during launch.

It is worth noting that these calculations were performed without the addition of the longitudinal stiffeners. They are thus not necessary for structural reinforcement, but still fulfill their function of providing attachment points for the outer shell and panels.

11.5.3. Vibration and Natural Frequency Analysis

All launch units have to be designed to maintain a minimum resonant frequency above 35 Hz to avoid interaction with the launch vehicle dynamics [113]. In an analytical approach the habitat modules' natural frequency is determined to verify that the launcher requirement is fulfilled. For this analysis the modules are represented as a thin walled cantilevered cylinder with a free end. The maximum lateral acceleration during launch is stated to be 2 g.

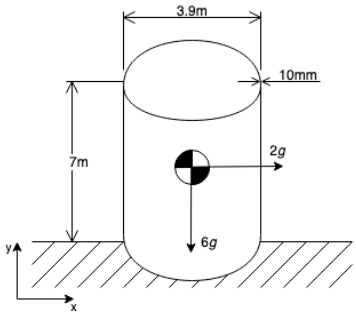

Figure 11.11: FBD of the thin walled cylinder representing the habitat modules.

The approach taken follows Rayleigh's method as it is described in chapter 10 of Megson (2013) [74] to approximate the beams natural frequency. Using Equation 11.3 the natural frequency of a structure can be determined if the particular function. Given in Equation 11.4, the amplitude of the vibration at any section z is known. The second part of the sum in the denominator is set to zero as no point masses are applied.

$$\omega^2 = \frac{\int_L EI\left(\frac{d^2V}{dz^2}\right)^2 dz}{\int_L \rho A\,(z)\,V^2 dz + \sum_{r=1}^{n} m_r \{V\,(z_r)\}^2} \tag{11.3}$$

As an assumed mode shape $V\,(z)$ describes the static deflection curve for a cantilevered thin-walled circular tube of radius r with thickness t supporting a tip load P and E-modulus E. The axial flexural rigidity EI is determined based on the moment of inertia for a thin-walled hollow cylinder I given in Equation 11.5 and the material's E.

$$V\,(z) = \frac{Pz^2}{\pi E r^3 t} \tag{11.4}$$

$$I = m * r^2 \tag{11.5}$$

Based on the geometrical specifications given in the section on Buckling Analysis, including a safety factor of 1.5, the natural frequency estimation calculated is 1,670 Hz. According to this analysis the natural frequency of the modules fulfill the launcher requirement.

11.5.4. Lateral deflection

The lateral deflection during launch can be determined by discretizing the module as a beam with the same flexural rigidity $E \times I$. I is the second moment of inertia, which for an empty shell can be found using[1]:

$$I = \frac{\pi}{4}(r_o^4 - r_i^4) \tag{11.6}$$

The flexural rigidity is then found to be 1.68×10^{10} Nm^2. The deflection for a uniformly loaded beam is then found using:

$$\delta = \frac{qL^4}{3EI} \tag{11.7}$$

Assuming the mass is uniformly distributed along the length of the module, the distributed load can be translated to lateral acceleration with $q = F/L = m \times a_{lateral}/L$. The formula for deflection can then be re-written as:

[1] https://www.engineeringtoolbox.com/area-moment-inertia-d_1328.html

$$\delta = \frac{m a_{lateral} L^3}{3EI} \tag{11.8}$$

This yields a maximum lateral deflection at the tip of the module of 3.328 mm, which is within the lateral clearance of 50 mm with the fairing. Note that this calculation assumes the payload adapter interface is a rigid connection. In reality, this connection will cause a larger deflection than what was calculated here. A more in depth analysis would be required to determine the effects of this connection.

11.5.5. Payload adapter load introduction

The final area of concern is the introduction of the launch loads into the structure. The payload adapter will be attached to a docking port, so the area of load introduction is known. Of specific concern is the the shear failure of the module wall, and a vertical (downward) deflection beyond acceptable limits. The shear stress can be calculated using the applied acceleration and the cross sectional area perpendicular to the force with:

$$\tau = \frac{F_s}{A} = \frac{m_{module} 6 g SF}{2rt} \tag{11.9}$$

This results in a shear stress of 110.36 MPa. Aluminium 7075 T6 has a shear strength of 330 MPa, so the module will not fail under shear during launch. In addition, a rough estimation of the vertical displacement of the outer walls was done using FEM analysis. The module was constrained at the docking port in both lateral axes directions. A force equivalent to the acceleration of 6 g with maximum payload weight was then applied to that face. Figure 11.12 shows a visualisation of the downward displacement along the longitudinal axis. For simplicity, this simulation was done with the actual shell weight, as the majority of payload mass will be directly loading the payload adapter:

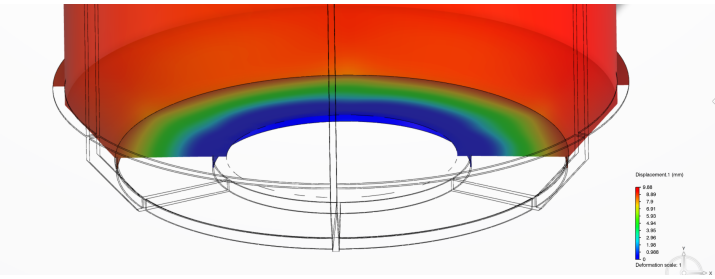

Figure 11.12: Vertical displacement under 6 g acceleration, supported at payload adapter

The maximum displacement is then 9 mm over a distance of 2248 mm (radius of the module). The recommendations section of the chapter addresses the relevance of this FEM model and potential improvements for future design.

11.6. Remote Manipulator System

The implementation of a RMS is based on the decision to berth spacecraft and modules instead of docking and undocking them. In berthing a manipulator arm, which can either be mounted on the target or the chaser vehicle, captures the opposite vehicles, attenuates the residual relative motion between the vehicles, and brings the interfaces of the structural latches into operational range. It was decided to use a berthing mechanism as it poses less constraints on approach velocity, spacial alignment, residual linear, and angular rates on the vehicles to be docked. It requires every vehicle or module to be docked to be equipped with a capture interface, called grapple fixture and it requires the chaser vehicle to be able to approach and keep its station inside the berthing box. Berthing box describes the volume in which the grapple fixture on the chaser vehicle can be captured by the arm [44]. The berthing procedure is described in detail in Section 13.4.3.

The RMS is based on the Space Station Remote Manipulator System (SSRMS) on the ISS, also known as Canadarm2, as it has been successfully used on the station since 2001 and as it has a maximum handling capacity of 116,000 kg. Furthermore, it has a span of 16.9 m, a weight of 1,336 kg, 7 offset joints, and a Latching End Effector (LEE) on each end which provides a mechanical and electrical connection to a payload or the ISS when connecting to a grapple fixture. This allows it to use each of these fixtures as bases of the arm [92]. In this way, the RMS can ”walk” over the ISS, and be used in multiple locations. It is designed to resemble the human arm, fixed to the station with the LEE at the shoulder, which is comprised of three revoluting mechanical joints followed by a boom segment and an elbow joint. As the SSRMS is symmetric about the elbow the wrist, which is attached to the second boom, is identical to the shoulder. To reduce the system’s complexity all joints are functionally identical with an angular range of ±270°.

11.6.1. RMS Sizing

The sizing of the system concerns its span and the maximum handling capacity. As a handling capacity similar to the SSRMS is desired all dimensions except the span are kept similar. The span is to be sized in a way that allows for visual inspection of the whole spacecraft with the cameras on the LEEs. Based on the external layout of the habitation modules the span is then sized to allow for full RMS coverage of each module’s surface with a minimum amount of grappling fixtures while also keeping the berthing box at a reasonable size. Based on these requirements the dimensions given in Figure 11.13 are determined.

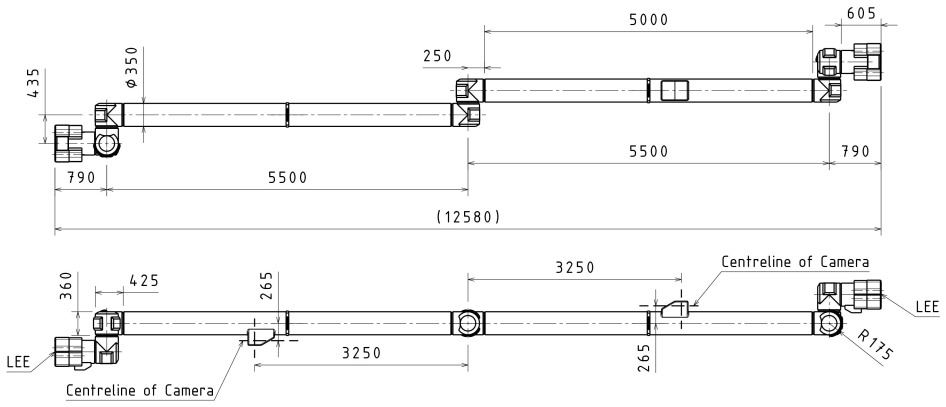

Figure 11.13: Technical drawing of the RMS including dimensions in mm.

The boom span of 5 m allows the arm to reach every point on the surface of the habitation modules with only three grappling fixtures per module. These fixtures are positioned at equal distance at the front, in the middle and at the end of each module with an offset of 120° each. The fixtures are also attached to the truss structure at equal distance allowing the RMS to ”walk” over the whole length of the vehicle. The camera on each boom allows to track the movement and to determine the position of shoulder/wrist and each LEE.

11.6.2. LEE Design

The main parameters which determine the end-effector design’s efficiency are misalignment tolerance and soft capture capabilities. The soft capture capability allows low-impact contact between the end-effector and the mechanical interface of the grappling fixture which is especially important for the capture of floating targets with low mass. A steel cable-snared end-effector is chosen to be implemented as this design has been implemented on the SSRMS and the Space Shuttle Remote Manipulator System already and its use in space application is well understood. Furthermore, this type offers a high misalignment tolerance while being able to soft capture. Experimental data shows that a steel cable-snared end-effector with the required dimensions can tolerate translation misalignment from 0 to 115 mm in axial and ±124 mm in radial direction. The angular misalignment tolerances are ±16° in roll and ±18°

in pitch and yaw [42]. Based on this the LEE pictured in Figure 11.14 is designed to be implemented on the RMS. The matching Power and Data Grapple Fixture (PDGF) in Figure 11.15 allows the RMS to be controlled when it is attached and connected to it.

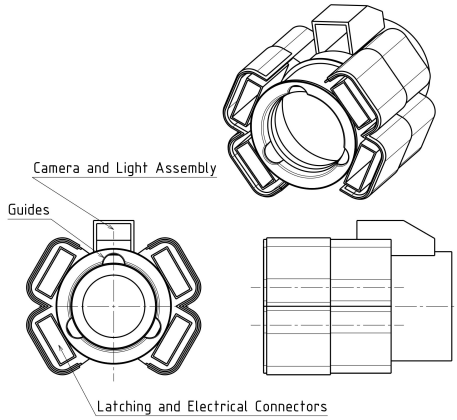

Figure 11.14: The LEE which is used on the RMS.

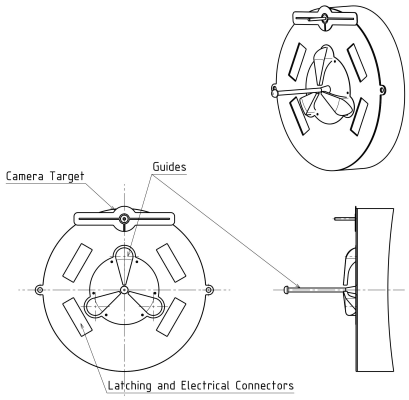

Figure 11.15: The PDGF which is installed on the spacecraft.

The capturing process uses three steel cables attached to a rotating ring which can be tightened around the capturing probe as detailed in Figure 11.16 and Figure 11.17. The ring in the LEE is then pulled in and the LEE is guided to hard capture by the three guide ramps.

Figure 11.16: The contacting situation between the cables and the capturing probe [42].

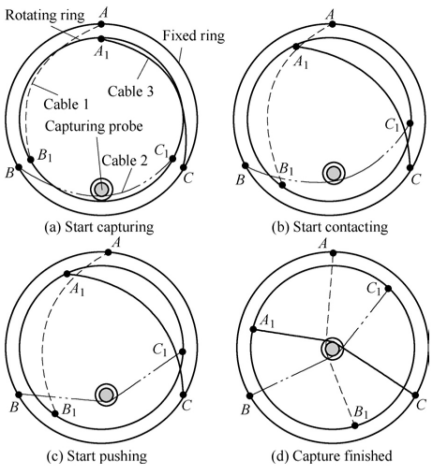

Figure 11.17: The capturing process of the steel cable-snared end-effector [42].

Each motorised joint is equipped with its own brakes, motor speed control and a device measuring joint angles. The joint housings are made from titanium and the booms are constructed out of CFRP with a protective Kevlar outer layer. The whole RMS is covered with a multi-layer insulating thermal blanket providing passive thermal control and electric heaters are implemented to ensure stable operating temperature of critical hardware components. Electric wiring consists of two redundant strings and it can be controlled from two redundant on-board control terminals to prevent single points of failure. Cameras on each boom and each LEE aid in manual control of the RMS. Based on the specifications of the SSRMS and the newer European Arm it is determined that the mass is 1,000 kg, the average power consumption is 1,000 W and the position accuracy is 40 mm and 1°. It is possible to control the RMS from ground and orbit while in Earth orbit. While in transfer and Martian orbit, only on-orbit operation will be possible due to the latency from Earth.

11.6.3. Small Manipulator

To add further inspection and repair capabilities to the RMS a smaller robot with two manipulator arms is added to the spacecraft. This robot and its operations are not designed in detail at this stage of the mission but it is equipped with a mechanism that allows to attach different tools to it. In further iterations tools will be designed to allow it to execute different maintenance and repair tasks on the spacecraft. Preliminary sizing results in a torso that can rotate around its axis with two smaller RMS attached to its sides, a LEE and a grapple fixture on its two ends. This smaller robot shown in Figure 11.18 can be attached to the LEE of the spacecraft's RMS.

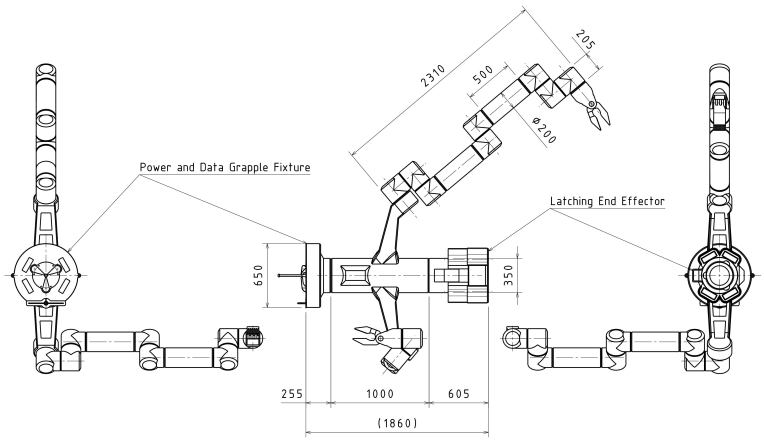

Figure 11.18: The Small Manipulator.

11.7. Docking

The docking system has to comply with SYS-06. This section only treats the two interfaces which are used for docking on the spacecraft and their connection. The berthing procedure is described in Section 13.4.3.

11.7.1. International Docking System Standard Interface

The IDSS provides common design parameters to allow developers to independently design compatible docking systems [123]. Two docking interfaces complying with it will be used to dock crewed or autonomous space vehicles for crew transfers, resupply missions or payload transportation. This interface also allows for docking of the space transportation systems currently developed under NASA's Commercial Crew Program [14].

The docking interface is based on the NASA Docking System and has an androgynous docking mechanism which allows for low impact docking when the soft capture system is active. In active mode axial, radial, and angular rates of 0.06 m/s, 0.04 m/s and 0.15 °/s, respectively, can be compensated for by the capturing mechanism. Lateral misalignment of 110 mm and angular misalignment of 5 deg can also be compensated for [81]. The system allows docking and berthing and once mated the present version of the interface can transfer power, data, commands, air, and communication with possible future revisions adding water source and return, fuel, tank pressurisation, and oxidiser transfer capabilities. In case of emergency pyrotechnics are integrated into the docking interface for contingency undocking.

11.7.2. Common Berthing Mechanism

The CBM is a autonomous system that aligns, captures, and secures two elements together, providing an atmospheric seal as well as throughput for a number of utilities. This system is used to connect all habitat modules and serves as the main resupply point due to its large internal passable area. The main differentiating function compared to the IDDS Section 11.7 is the requirement of assisted attachment, which will be provided by the RMS Section 11.6.

The CBM was developed for the ISS, and is a standard for connecting habitable modules of

all Western space agencies and JAXA. It provides the supply of the following items between modules; power, data, air, nitrogen, oxygen, water, waste water, and coolant [33]. Furthermore propellant for the ADCS thrusters will also be supplied through the interface, which is not part of the standard design. However this does not require a structural alteration to the main structure, therefore it will stay compatible with all standard CBM's.

The CBM has two parts, each connected to an opposing module, an active and passive half. The active half houses all of the electronics and actuators required for the mating of the ports, while the passive half houses all the necessary accepting mechanisms. Once berthed the only major physical difference is a slight difference in length, as most of the mechanisms and electronics are removed to make the internal area of the port larger. The outer and inner diameter are 2 m and 1.8 m respectively with throughput area of a rounded square with 127 cm sides. The remaining area is used for transpiration of utilities [55] [106].

The berthing procedure of the CBM is initiated by moving the modules to be connected together with the use of the RMS, once the CBM's of the two parts are withing approximately 11.4 cm the arm is disengaged and the autonomous mechanism of the port takes over. First the capture latches pull the two half's together initiating contact between the pressure seals, then the 16 powered bolts pull the system together and are pre-loaded in tension by 6.6 kN for each bolt. Once pre-loaded the bolting operations is halted for 12 hours allowing for the thermal equalization between the two halves, this is necessary in order to ensure that the atmospheric seal is not damaged due to thermal strain. Once thermally equalized, the bolts are incrementally tightened in in pairs to a tensions load of 46.7 kN [105].

11.8. CG location and MMOI

In order to determine the Center of Gravity and the Mass Moment of Inertia, a simplified model of the spacecraft is set up, consisting out of point masses and simple geometries [103]. The masses of the subsystems m_i are taken from the most recent mass budgets (Section 4.4), and the longitudinal distances from a reference point x_i (taken to be the end of the engine section) from the most recent CATIA model, as shown in Figure 11.1. From these, the Center of Gravity is calculated using

$$x_{cg} = \frac{\sum m_i x_i}{\sum m_i} \tag{11.10}$$

The y and z location of the CG are taken to be at the central axis of the spacecraft, as the mass distribution is approximately symmetric around this axis. After the CG location is determined, the Mass Moments of Inertia around the CG in the x-, y- and z-direction are calculated. This is done by summing the MMOI of the individual components around there principal axes and their Steiner terms

$$I_{Steiner,i} = d_i^2 m_i \tag{11.11}$$

The MMOI around the y- and z-axis are assumed to be the same due to the large contribution of the Steiner term of the modules and reactors far away from the CG. These calculations give the following results:

Property	Value	Reference
x_{cg}	$34m$	From the back of the engines
y_{cg}	$0m$	The center of the trusses and modules
z_{cg}	$0m$	The center of the trusses and modules
$MMOI_{y/z}$	$105 \times 10^6 kgm^2$	
$MMOI_x$	$4 \times 10^6 kgm^2$	

Table 11.4: Center of Gravity and Mass Moments of Inertia of the spacecraft

11.9. Recommendations

The structural analysis performed in this chapter contains a number of simplifying assumptions that less accurately represent both the load case and the loaded structure. These simplifications are in line with the level of detail that the structure was designed to. Bolts and bolt holes are not included in the shell design, and so the load introduction through bolts was simplified to a force applied to a surface. Thus the first part of recommendations on the structure apply to the design of the shell. The second part concerns the analysis of said shell.

Shell design

The shell is composed of 5 layers: inner shell, Kevlar, Nextel, MLI, outer shell, and shell panels. In the structural analysis, only the inner and outer shell were considered. In addition, they were assumed to be made of the same material. In reality, the shell panels will have a significant effect on the structural rigidity, and different materials should be considered for each for layer. The assembly of these layers will also add a number of nuts, bolts and rivets. Their weight was not taken into account specifically in the analysis, although the over-estimation of launched mass most likely compensates for it.

Structural analysis

The structural analysis considered four cases: buckling, frequency analysis, lateral deflection, and load introduction. Each of these was applied to a level of detail equal to that of the design of the structural shell itself. This means that load introduction and stress concentrations in bolts should still be considered. In addition, the type of fastening should be analysed under the specified vibrations environment. It is worth noting that the FEM analysis of the payload adaptors load introduction provides only a rough idea of the stresses and deflections the shell will undergo. An accurate FEM model would require more time to prepare: a more detailed CAD model, and the load introduction and meshing should be revised to be more representative. Finally, because the shell is composed of several different materials, the effect of thermal expansion should be investigated.

11.10. Sensitivity Analysis

To reduce uncertainties inputs which might require significant changes to the spacecraft structure are investigated.

The first scenario concerns the unavailability of the Falcon launcher. Depending on the reasons and the duration of this scenario some of the modules might have to be launched with a different launcher. For the analysis the Delta Heavy IV launcher is chosen as replacement and the consequences of the different launcher requirements on the structural elements is described. The fairing size of the new launcher increases in all dimension compared to the Falcon fairing [8] hence all modules can still be fitted. The payload adapter will possibly need a redesign. The decreased payload capacity to LEO and the possible consequences are treated in Chapter 13. The design load factors of the Delta Heavy IV are the same as for the Falcon launcher and the both minimum axial and lateral frequency are lower than the ones of the Falcon. Therefore, the structural analysis yields the same results and the launcher requirements are fulfilled.

Secondly, a scenario where the radiation budget according to SYS-15 decreases to 1000 mSv per mission is considered. To lower the radiation dose of the astronauts an increase in radiation shielding is considered or a decrease in mission time resulting in an increase in the amount of engines. Additional engines can increase the number of reactors needed on board the spacecraft. Due to the modularity of the spacecraft structure these additional systems can be accommodated by the addition of new truss elements. However if the shielding must be increased in order to reduce the radiation amount, from Figure 11.7 it can be extrapolated that a yearly radiation limit of 0.35 Sv can be achieved with approximately 40-50 g/cm^2 of shielding. This would mean that an additional 45-60 t of shielding would be needed in order to comply with the new requirements. Due to the modular nature of the spacecraft this additional weight could be accommodated but only by increasing the number of engines and

reactors as well as reducing payload capability.

11.11. Verification & Validation

RMS V&V

The testing of robotic manipulator for space applications requires special facilities as these robots are not designed to operate under gravity. While it is possible to perform and test 2D operations with a special support system general 3D tasks cannot be performed on ground. Therefore, computer simulations will be used to enhance the design and to verify if the requirements are met. To verify the accuracy of these simulations the underlying mathematical models need to be verified. For their verification process a space-manipulator simulation facility will have to be set up which allows for hardware-in-the-loop simulations. In this hybrid simulation the mathematical model of the RMS is used to drive a hydraulic manipulator to mimic on-orbit operations. Validation of the simulation facility will consist of multiple validation tests with growing complexity. In addition to verifying the manipulator's dynamics the facility will also be used for development and verification of operation procedures, ground and crew training, and mission planning. Preferably the verification and validation procedure of the RMS will be carried out in collaboration with the Canadian Space Agency which has extensive experience in the field of design and simulation validation of space-manipulators.

MMOD and Radiation Shielding V&V

In order to verify the currently assumed MMOD environment future interplanetary mission should include micrometeorite detectors that can detect the velocity and size of the particles. These new findings then should be used to update the current models, and if enough data can be collected then the model could be changed form an omnidirectional model to a directional one. Furthermore special hyper velocity impact simulation codes should be ran on the shielding used on the spacecraft, as the expected average velocity is around 20 km/s. While current light gas guns have had speeds of up to only 7 km/s.

While the effects of short term high levels of radiation are relatively well understood while the long term effects of medium high radiation on living organisms have very little research done on them. The current issue with verifying the design is quality factor, which describes how different ionising radiation damages organic cells, used to calculate the equivalent dose in sieverts. Once the medical effects of long term exposure and the correct quality factor for the radiation is found, the radiation environment must be validated by equipping interplanetary mission to Mars with radiation detectors to collect and refine the current models being used.

Structure V&V

The verification and validation of the structural shell will have several steps. Firstly, the design will be iteratively refined with the use of FEM simulations, which will be tested with FEM V&V tools to ensure they accurately represent the analysed load case. After simulating, manufactured shells will undergo a series of destructive and non-destructive tests:

- Compression test (to failure i.e. buckling)
- Vibration testing (to launcher specification)
- Lateral load (to launcher specification)
- Adapter shear load test (to launcher specification)
- Pressurisation/leak test (1 bar pressure differential)

12

Communications & Data Handling

To provide the ability to the spacecraft, ground control and humans on-board to function according to predefined performance requirements, it is key that they are all able to communicate with each other. This function will be performed by the communications and command and data handling subsystem (C&CDH). While in previous missions, this subsystem accounted for 21 % of all critical mission failures [130], an in-depth design and analysis will be performed. After the driving requirements are discusses, all the design options and decisions faced during this detailed design phase are presented in Section 12.2. Second, the final detailed subsystem design is presented in Section 12.3 and finally the systems engineering and effects on the system for C&CDH is summarised in Section 12.4.

12.1. Key requirements and constraints

The driving requirements and constraints for the C&CDH system are:

- Limit the power required during reactor failure to prevent larger solar panels (COMS-09).
- The data rate that shall be sent to Earth is a major constraint.
- The mass shall be limited to 1,000 kg in total (COMS-08).
- At the furthest distance to Earth during mission life, the spacecraft shall still be capable of transmitting data to Earth (COMS-03).

12.2. Design Options and Decisions

To end up with a detailed C&CDH system, a lot of design decisions are made by small trade-offs and thorough analysis to check if a certain feature is feasible for this specific mission.

12.2.1. Communication Method

With current technology two methods to communicate are possible: *using optics or using radiowaves*. For Free-space Optical Communication principle, no solid medium is required to transmit a infrared laser beam where the photon density of the beam can be changed to contain information on bits [51]. Radiowave communication is based on sending high frequency carrier radiowaves with a certain phase, amplitude, frequency or noise pattern that corresponds to a bit pattern. The main advantage of using an optical communication link is the fact that data rates of 3 up to 5 times higher can be achieved than with current radiowave technologies in the Ka-band, which is the highest frequency band that is deep space proven [39]. A Lunar mission has been performed using this technique, however, the TRL for deep space missions is still 3 and expected to be developed to 6 within twenty years as completely new deep space ground stations should be build [51]. Furthermore, the pointing accuracies that are required for using optical links are in the range of several microradians, for the recently developed BOEING LADAR it is 10 microradians (0.00057°)[51]. State-of-the-art ADCS systems can only give a 0.001° pointing accuracy. Also, optical communication is very sensitive for interference with background solar radiation[51]. Due to the very low TRL for both the system itself as for the required ADCS system and the fact that solar interference will degrade the optical signal severely when travelling to Mars, it is decided to use radiowave communication.

The choice between using *a relay-satellite network or a direct communication link from the spacecraft to Earth* should also be made. In a relay-network, the spacecraft itself has a smaller communication system as it only has to send the data to the closest relay-satellite instead of sending it all the way to Earth. This can have the advantage that also during conjunction (Mars and Earth cannot see each other due to the Sun that is blocking the signal) data can be sent to Earth. Only ESA considered in 2009 the development of a relay-satellite in deep space, in a Mars-cycler orbit, but this idea has been cancelled due to money constraints [25]. Because the dependency of such a network would be to large if it is not there in 2040, a relay-network is not chosen. Also, relay to an Earth orbit communication satellite is not used due to the fact that the losses due to the atmospheric attenuation (discussed in Section 12.3)

is lower than the increased data rate that is required due to lower communication times for a satellite that is not always in sight while the deep space ground stations are [47].

12.2.2. Beam and Access

According to the business plan in Chapter 15, multiple space agencies are involved. To provide access for all involved parties to the data generated and to give commands to the spacecraft, a structured approach shall be decided on to prevent an over-demand of the spacecraft capabilities and conflicting commands by different instances. This can be done by *using multiple spot beams on different regions or set up an accessibility structure for the parties*. Multiple beams can be formed by using multiple feed horns and has the advantage that frequencies can be reused, which means that one can use the same bandwidth more than once, increasing the data rate capacity. However, interference between the adjacent beams can distort the signal in a drastic way that information gets lost when the required pointing accuracy cannot be achieved [47]. Note that the pointing accuracy that is required at the furthest distance between Mars and Earth for communication (396×10^6 km, [58]) already requires a pointing accuracy of 0.00184°. Splitting the beam in several smaller beams will require an even higher accuracy by a factor equal to the amount of beams used. As the ADCS system only has an accuracy of 0.001°, the required pointing accuracy for a satisfactory link budget cannot be achieved. Therefore, the multiple access methods will be considered. The different ground segments can access the spacecraft by three methods in a structured way.

- The bandwidth can be split in several smaller sub-bands where every ground segment gets its own sub-band. This is called *Frequency Division Multiple Access (FDMA)*. Result is constant transmission power, however, interference and low power efficiency are a serious concern for deep space communications [130].
- *Code Division Multiple Access (CDMA)* is based on modulating the signals from the different ground segments on different phases of the carrier wave. This has the advantage that it is almost immune to interference, however, a larger bandwidth is required than with the other methods, increasing the costs a lot [130].
- *Time Division Multiple Access (TDMA)* is a method where every ground segment gets a certain time slot to communicate, all using the same bandwidth. Main advantage is no inference and small bandwidth. Disadvantage is that the ground segments and spacecraft requires a precise time synchronisation, but this can be coped with before launch [130].This disadvantage is the smallest for our specific mission and therefore TDMA will be used. Specification of the exact time slots can only be performed when the investing agencies are determined.

12.2.3. Communication Strategies

First thing to consider is the frequency band will be used. The International Telecommunication Union, responsible of the band allocations, has defined the *S- (2-4 GHz), X-(8-12 GHz) and Ka-bands (27-40 GHz)* as deep space communications bands for space research service, according to the ITU 1.55 article and 201, Revised B Frequency and Channel Assignments released on December 15, 2009. The S and X band are however already pretty occupied by a lot of other missions, also ones that do not go into deep space. The Ka-band is not that occupied yet because it was only deep space proven from the MRO mission of in 2005 [58] while X and S were used way more before and also have a smaller range of frequencies. The Ka-band has the advantage that the data rate can be 2 to three times as high, as it has a smaller wavelength and therefore smaller beam-width which increases the gain. The Ka-band has the disadvantage that it is more sensitive for atmospheric attenuation due to rain or fog. This property is thoroughly analysed in the link budget that can be find in Section 12.3. Choosing the Ka-band over the X-band with the worst case atmospheric attenuation still gives a saving of 1.1 m in reflector diameter and mass saving of 42 %. This will be elaborated on in Section 12.3. From SFCG7-1R5, published by the Space Frequency Coordination Group, Channel 40 in the Ka-band was chosen to operate in. Downlink: 32269.814816 MHz and Uplink: 34559.841822 MHz. This gives a turnaround ratio ($f_{downlink}/f_{uplink}$)of 0.93.

The spacecraft will communicate over this Ka-band to ground stations that are visible. For this deep space mission where different agencies cooperate, use will be made of their Deep

Space Stations. The Deep Space Network (DSN) from *NASA* has three ground stations at Canberra (Australia), Madrid (Spain) and Goldstone (USA) with an antenna diameter of 70 m. These are separated from each other by an angle of 120°, which results in a 100 % coverage, one of the three is always visible. *ESA* has an own ESTRACK network, with deep space ground antenna diameters of 35 m. However, they have a contract with NASA that they can also use the DSN. *Roscosmos* has a deep space network of a 70 m antenna at Yevpatoria, a 64 m antenna near Moscow and a 70 m antenna at Ussuriisk. *The Chinese agency* has a 64 m antenna at Jiamusi. *JAXA* has a 64 m antenna at Usuda Deep Space Complex. The smallest ground station antenna diameter that will be used will be 64 m. Those stations together have a enviable service availability rate above 95 %[1]. Other agencies that wants to participate have to make arrangements with the current deep space ground stations to communicate. All these antennas are equipped for different polarised Ka-band radiowaves [47].

Thing that should be noted is that there can be a severe delay in time of sent of data and time of receive. The maximum and minimum distance between Mars and Earth were they can communicate are 396×10^9 m and 59×10^9 m respectively. These values are determined by a simple Python script where the distance between Mars and Earth is determined by modelling their trajectory around the Sun. The waves travel with the speed of sound (2.998×10^8 m/s) which results in delays of 1,325 and 202 s delay for maximum and minimum distance respectively. This includes 3 s margin for terrestrial (from antenna to ground control centre), propagation through equipment and processing on both transmission ends [47].

The spacecraft cannot communicate with the ground stations during two periods, when it is in *Mars eclipse with respect to Earth* due to the spacecrafts orbital altitude (Mars blocks the signal) and when there is a *Mars-Earth conjunction* (Mars and Earth cannot see each other due to the Sun that is blocking and particles are distorting the signal). Commands could be partly lost and the spacecraft can interpret it wrong. Data generated during these periods determine the memory size required and data throughput rate. First the eclipse time will be discussed. When the spacecraft is in its circular 400 km orbit above the surface of Mars, the time that it cannot communicate to Earth can be calculated by Equation 12.1. The radius of Mars is 3,389.5 km. μ_{Mars} has a value of 4.28×10^{13} $m^3 s^{-2}$.

$$a_{Mars} = R_{Mars} + Height \tag{12.1}$$

$$t_{orbit} = 2\pi\sqrt{a_{orbit}/\mu_{Mars}} = 7,085s \tag{12.2}$$

$$t_{eclipse} = (2 \cdot sin^{-1} R_{Mars}/a_{Mars})/2\pi) \cdot t_{orbit} = 2,024s \tag{12.3}$$

The conjunction time is determined by analysing the relative positions of Mars and Sun, seen from Earth. The angular distance (the angular separation between two objects as perceived by an observer from Earth) between the Sun and Mars are plotted in Figure 12.1 and when this is angle is lower than 1.0°, there is a severe conjunction and inference and blockage that prevents communication [23].The line in crossing the Sun in the right picture of Figure 12.1, is the line of view between Earth and Mars at this date.
One can see that on average this conjunction takes 10 days before communication from Mars is possible to Earth (dotted line). This will happen once every synodic period (780 Earth days) so it should definitely be included in the design considerations.

Regarding *the tracking of the spacecraft*, the Doppler effect and spacecraft pointing data will be used. The Doppler law states that the frequency of a sent signal changes for the observer when there is an observer who is moving relative to the wave. This frequency change can be determined by Equation 12.4[47].

$$\Delta f = \frac{\Delta v}{c} f_0 \tag{12.4}$$

[1] https://deepspace.jpl.nasa.gov/files/820-100-F1.pdf

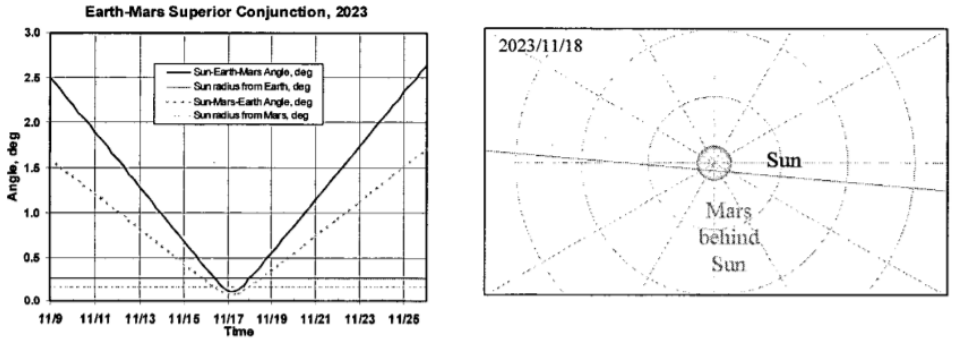

Figure 12.1: Angular distance between Mars and Sun during conjunction in November 2023 [23]

Δf is the observed frequency change which can be determined by comparing with the observed frequency with the predetermined frequency, Δv is the relative difference in velocity between the Earth and the spacecraft and f_0 is the transmission frequency. From this, it can first be determined if the tracked satellite is moving towards or away from Earth, a positive Δf means blue-shift, which means moving towards Earth, while a negative Δf means red-shift and moving away from Earth. Furthermore, by determining the delay between the receive and transmitting time (put as a tack on the data sent), the precise distance can be determined. Lastly, also the pointing data can give information of the orientation with respect to the ground segment. Also, comparing the received signal for two deep space ground station used can give a relative positioning of the spacecraft in between those two stations. Using these methods, an accurate 3D positioning can be done compared to predefined simulated trajectories [47]. Note that attenuation effects can also cause a distorted signal and therefore extra research should be performed in the future to filter this.

The modules have to communicate to each other when docking, with a very low data rate (only positional information and commands). This will be done by a *very small antenna system on every module* which is something that is not designed by now due to time constraints, but is definitely something that needs to be considered in a later iteration after DSE.

Furthermore, the main C&CDH system that communicates to Earth will be *completely redundant* as it still is the cause of 21 % of critical mission failures. This is elaborated on in Figure 16.2. Another reason for full redundancy is to prevent communication blockage by the spacecraft due to other parts, like the tanks in the neighbourhood. Therefore, the redundant system will be located exactly opposite of the other to assure communication at every instance.

12.2.4. Main Antenna Configuration

The antenna that will be used was selected from the criteria that it needs to be able to cope with the Ka-band chosen and with this band, limit the mass and size as much as possible to fit in the launcher and reduce the wet mass. A wired helix antenna was therefore not chosen as due to its lower gain above 2 GHz, the (structural) mass and size would grow to enormous amounts of tenth's of meters [130]. The horn antenna was also not selected as above 4 GHz the beam width becomes very large, increasing the gain would increase the length, mass and installation effort in a killer requirement way. Same reasoning goes with lens and phased array antennas, above 0.5 meter the mass advantage for the same gain that they have below 0.5 m is not valid anymore with respect to a *parabolic reflector* with a horn as feed system. A preliminary estimation showed that the antenna would be in the order of meters. Due to the respectively very low mass, low complexity, low cost and design maturity for antennas above 0.5 m diameter the reflector will be used with a horn feeder.

Further research into parabolic reflectors showed that the already large antenna efficiency (55-60 %) could be even increased to 65-70 % by using an extra sub-reflector, also called a *Cassegrain configuration*, displayed in Figure 12.2. It has several advantages over a standard

reflector configuration, listed below.

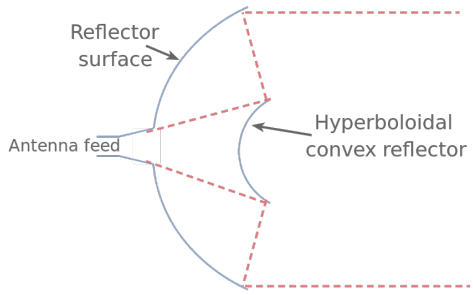

Figure 12.2: Cassegrain reflector configuration [122]

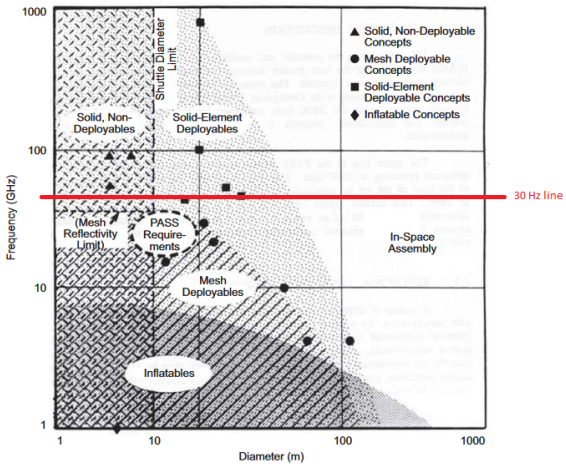

Figure 12.3: NASA's antenna configuration decision chart [50]

- An increase in antenna efficiency of around 10 % due to the effect that the illumination pattern is more uniform in terms of magnitude over the main reflector. Increasing the antenna gain by 0.9 dB.[47]
- The antenna configuration is geometrically more compact, which is better for launch. The feeder is very close to the main reflector, the sub-reflector is less far away from the main reflector as when the feeder would be positioned in front of the reflector looking towards it, when no sub-reflector is used (for no-Cassegrain configuration). [47]
- The noise temperature at the feeder is lower. It looks now into space, which however gives it extra background noise, however it is looking away from the spacecraft and not directly into for example the radiators. This saves an enormous amount of noise temperature, as a lot of radiated heatwaves would otherwise also go into the feeder. [47]

Disadvantage is that the design phase is more complex and a feeder system with a small beam width (around 30 degrees) is required. However, current feeder technologies exist to cope with this[2]. Also, the sub-reflector blockage will give an estimated 0.47 dB loss (see Section 12.3), however due to the 0.9 dB gain it is still better.

It was found that the antenna should be *solid* and not have a foldable configuration, a diameter of 3.45 m at 32.26 GHz downlink was found which will be elaborated on in Section 12.3. From Figure 12.3, it can be seen that a solid antenna is still favourable (mind the logarithmic scale) as it fits in the launcher and the disadvantage of extra increase in risk of failure of deployment is for these numbers worse than the advantage of mass reduction.
The solid main reflector and sub-reflector will be made of *Carbon Fibre Reinforced bisphenol-A epoxy Polymer matrix skin and 8 mm aluminium honeycomb core* (to provide sufficient strength and stiffness). This was chosen from ESA's Materials handbook 3A 2011 [34] from the antenna section. Other materials currently used for the reflectors are also given in Table 12.1, however, they showed worse combined performance with respect to surface quality and mass which are determined as main drivers for material selection together with space environment readiness, for antennas by ESA[34]. More research into the chosen material showed that a lot of tests have been conducted already to their behaviour under high radiation doses for doses that will not even be achieved and temperature changes (123-423 K).The surface quality and mechanical behaviour showed no apparent change and it can therefore be considered as a suited reflector material [32]. The surface quality is of course also dependent on the manufacturing method that the reflector manufacturer will use, this is not included yet. The main antennas will be positioned in between where the radiators end (coldest side) and the habitats to prevent enormous disturbing noise temperatures from the reactors or radiators. They will be positioned on a truss that makes sure that view is not blocked by the

[2] https://www.sagemillimeter.com/content/datasheets/SAF-2434231535-328-S1-280-DP.pdf

Reflector material used	Surface quality (RMSE mm)	Density per squared meter antenna (kg/m^2)
CFRP skin + 8mm aluminium honeycomb core	0.4	2.8
Conductive wire band on Kevlar skin + 6.2 mm Nomexcore	2	3.7
Conductive crosses bonded on Kevlar skin + 20 mm Nomexcore	0.3	4.5
Sandwich panels with CFRP skin + 40 mm Kevlarcore	0.8	6

Table 12.1: Material selection for antenna reflector

propellant tanks, solar panels and radiators. Realise that still a safety factor of 300 K is added to the noise budget to account for eventually noise from the radiators. The redundant system will be on the opposite side of the truss and both will have an antenna pointing mechanism (selected in Section 12.3) to achieve the required orientation.

12.2.5. Data Management

To analyse the data rates, 3 different scenarios are considered to select the most critical to design for.

- Data transmission and storage under *nominal conditions*, 2024 s eclipse.
- Data transmission and storage *during and directly after conjunction*, where all the data generated during the conjunction should be sent to Earth spread over 300 days.
- Data transmission and storage *during a reactor failure*, where the power consumption should be minimised to reduce the solar panels but communication and information should still be possible with Earth by voice and images.

All data rates that are sampled are first multiplied by the Nyquist factor (2.2) to ensure a reconstruction from the analogue signal. The components, compression rates, data rates and required storage included in the data rate analysis for the three scenarios can be found in Section 12.3.

12.3. Detailed Design

An overview of the detailed design phase for the C&CDH system will be given in this section.

12.3.1. Data Rate Analysis

The overall data analysis per scenario can be found in Table 12.2.

Downlink					**Uplink**		
Component	*When used?*	*Datarate I [bit/s]*	*Datarate II [bit/s]*	*Datarate III [bit/s]*	*Component*	*When used?*	*Datarate I,II,III [bit/s]*
Humans: Audio	I, II, III	48,416	48,417	48,416	Command: ADCS (M)	I, II, III	8,000
Humans: Video	I, II	907,799	907,821	0	Command: Power (M)	I, II, III	8,000
Humans: Images	I ,II, III	127	135	2,352	Command: Propulsion (H)	I, II, III	16,000
Humans: Text	I, II, III	316	316	0	Command: Communication (S)	I, II, III	4,000
Camera	I, II	195,109	201,613	0	Command: CDH (M)	I, II, III	8,000
Spectrometers	I, II	128,326	131,382	0	Command: ECLSS (H)	I, II, III	16,000
Magnetometers	I, II	128,326	131,382	0	Command: Thermal (M)	I, II, III	8,000
Radiation instruments	I, II	128,326	131,382	0	Command: Structures (S)	I, II, III	4,000
Other payload	I, II	128,326	131,382	0	Command: Payload (S)	I, II, III	4,000
HK: ADCS (M)	I, II, III	821	420	1,600	Humans: Audio	I, II, III	46,933
HK: Power (M)	I, II, III	821	841	1,600	Humans: Video	I, II, III	1,268
HK: Propulsion (H)	I, II, III	821	841	3,200	Humans: Images	I, II, III	880,000
HK: Communication (S)	I, II, III	205	210	800	Humans: Text	I, II, III	316
HK: CDH (M)	I, II, III	411	420	1,600			
HK: ECLSS (H)	I, II, III	821	841	3,200			
HK: Thermal (M)	I, II, III	411	420	1,600			
HK: Structures (S)	I, II, III	205	210	800			
HK: Payload (S)	I, II, III	205	215	800			
Total storage eclipse [GB][8E9 bits]		0.4		0.4			
Total storage conjunction [GB][8E9 bits]			**61.1**				
I:Total data rate nominal [Mb/s]		1.6698					1.0045
II:Total data rate after conjunction [Mb/s]			**1.6882**				1.0045
III:Total data rate reactor failure [Mb/s]				0.066			1.0045

Table 12.2: Data Budget. I stands for nominal conditions. II stands for after data gathering and transmitting of this data after conjunction. III stands for during reactor failure. S-M-H stands for the complexity of the system, telemetry- and command-wise (Simple-Medium complex-Highly complex). HK stands for Housekeeping data.

For the images, a high colour (16 bits per pixel) image (20,048 pixels) is considered with a compression ratio of 10, the astronauts have the possibility of making maximum 200 images per orbit which is based on reporting failures to the ground segment[111]. The video link is based on a 360p YouTube video that will be used for making the vlogs, documentary and ground/homefront contact (63 seconds limit per Mars orbit, required for all these contacts together) in combination with audio and text messages (200,000 characters) with

8 bits per character [3]. All other components have a lossless compression ratio of 3. The complexity of the subsystem determines the amount of telemetry points (500-1,000-2,000, rough estimate[130]) which will be gathered once a minute in normal conditions and ones per 5 seconds during reactor failure. Commands per subsystem that it needs per orbit also has a complexity scale (25-50-100, rough estimate[130]) with an average character length of 20 (8 bits per character). Payload data rate consists of scientific payload and for example housekeeping data from satellites that are transported, approximated at 1 Mb/s [4]. The camera will only generate data when not in eclipse, data rate can be calculated by Equation 12.5 where a scenery length of 1,000 m is taken as reference [130]. The data after an eclipse will be sent before the start of the new eclipse, after conjunction within 300 days, this fitted the budgets. The data rate that has to be sent can therefore be calculated by Equation 12.6 and the storage by Equation 12.7. It can be concluded that the design requirement will be for a *memory storage of 61.1 GB and a downlink data rate of 1.7 Mb/s after conjunction and 0.066 Mb/s when there is a reactor failure.* The limiting signal-to-noise ratio (SNR) that is required will be 21, which is the acceptable level of noise set by the ITU for audio communication, which is a more stringent constraint than the required signal-to-noise level required for video, which is 17.2. [5].

$$Datarate_{camera}[bit/s] = \#Images \cdot \frac{pixel}{image} \cdot \frac{bits}{pixel} \cdot length_{scene} \cdot v_{orbit} \cdot \frac{R_{Mars}}{R_{Mars} + height} \tag{12.5}$$

$$Datarate_{general}[bit/s] = Datarate_{live}[bit/s] + \frac{Storage[bits]}{Time_{orbit}[s] - Time_{eclipse}}[s] \tag{12.6}$$

$$Storage[bits] = Datarate_{eclipse} \cdot Time_{eclipse}[s] \tag{12.7}$$

12.3.2. Link Budget

In Table 12.3, the link budget is given to achieve a SNR of 21. This is the link budget with the final design parameters, which will be explained below. All the formulas come from [47]. The SNR in decibels is determined by adding up all components of the link budget. The main formulas and design parameters will be discussed below to give the reader the possibility to re-analyse the budget. ”L” stands for loss. The Stefan Boltzmann constant and noise temperature are also added as those two compute the white noise at the receiver.

		Downlink I	Uplink I	Downlink II	Uplink II
Component	***Limiting design factor***	***Value***	***Value***	***Value***	***Value***
$G_{Spacecraft}$	Antenna geometry and frequency	59.31 dB	59.91 dB	59.31 dB	59.91 dB
G_{Ground}	Antenna geometry and frequency	84.33 dB	84.93 dB	84.33 dB	84.93 dB
$P_{Transmitter}$	Amplifier technology	53.01 dBm	50.00 dBm	42.04 dBm	50.00 dBm
$Datarate$	Frequency reuse	-59.29 dB	-56.98 dB	-48.19 dB	-56.98 dB
$L_{Cassegrain}$	Sub-reflector diameter	-0.46 dB	-0.46 dB	-0.46 dB	-0.46 dB
$L_{Spacecraft}$	Communication architecture	-0.85 dB	-0.85 dB	-0.85 dB	-0.85 dB
L_{Ground}	Communication architecture	-0.89 dB	-0.89 dB	-0.89 dB	-0.89 dB
L_{Path}	Distance to Earth	-294.58 dB	-294.58 dB	-294.58 dB	-294.58 dB
$L_{Attenuation}$	Weather condition ground station	-12.28 dB	-12.28 dB	-12.28 dB	-12.28 dB
$L_{Pointing}$	Pointing accuracy and 3 dB angle	-0.02 dB	1.13 dB	-0.02 dB	1.13 dB
$L_{Polarisation}$	Farraday effect	- 0.13 dB	-0.13 dB	- 0.13 dB	-0.13 dB
T_{Noise}	Antenna configuration and pointing	-34.57 dBK	-34.66 dBK	-34.57 dBK	-34.66 dBK
$Boltzmann_{Constant}$	Nothing	228.60 dBJ/K	228.60 dBJ/K	228.60 dBJ/K	228.60 dBJ/K
SNR		**21.04 dB**	**21.53 dB**	**21.17 dB**	**21.53 dB**

Table 12.3: Link budget for case I (after conjunction, downlink 1.7 Mb/s data rate and 200 W transmitting power) and case II (when reactor failure, downlink data rate 0.066 Mb/s and 16 W transmitting power)

$$Gain_{max}, G(dB) = 10 \cdot log(\eta_{Illumination} \cdot \eta_{Spillover} \cdot \eta_{Surface} \cdot \frac{Diameter_{antenna}[m] \cdot f[Hz]}{c[m/s]}) \tag{12.8}$$

$$\eta_{Surface} = exp(-0.9(4\pi \cdot RMSE_{Material}/\lambda)^2) \tag{12.9}$$

$$Power, P(dBm) = 10 \cdot log(Power[W]) + 30 \tag{12.10}$$

[3] https://en.wikipedia.org/wiki/Bit_rate
[4] https://public.ccsds.org/Pubs/120x0g3.pdf
[5] https://www.itu.int/dms_pub/itu-r/opb/rep/R-REP-BS.1058-1986-PDF-E.pdf

$$L_{system} = L_{Connectors}(dB) + L_{Splices}(dB) + Length_{Cable}(m) \cdot L_{Fibreattenuation}(dB/m) \tag{12.11}$$

$$L_{Path}, Friisloss(dB) = 10 \cdot log((4\pi \cdot Distance_{S/C-Earth}[m]/\lambda[m])^2) \tag{12.12}$$

$$L_{Atmosphere}(dB) = L_{Rain_{Attenuation}}(dB) + L_{Rain_{Depolarisation}}(dB) + L_{Gasses}(dB) + L_{Clouds}(dB) + L_{Scintillation}(dB) \tag{12.13}$$

$$Halfgainbeamwidth, \theta_{3dB}(degrees) = 70(c[m/s]/f[Hz] \cdot Diameter_{Antenna}[m]) \tag{12.14}$$

$$L_{Pointing}(dB) = 12 \cdot (Accuracy_{transmitter}/\theta_{3dB}) + 12 \cdot (Accuracy_{Receiver}/\theta_{3dB}) \tag{12.15}$$

$$L_{Polarisation}(dB) = 20 \cdot log(cos(\beta)) \tag{12.16}$$

$$T_{Noise}(dBK)atreceiver = 10 \cdot log(T_{LNA} + T_{lines+filters} + T_{feeder} \cdot (1 - L_{feeder}) + (\frac{T_{sky}}{L_{Rain_{Attenuation}}} + T_{Antenna} + T_{Earth/Mars} \cdot \frac{ApparentAngle}{\theta_{3dB}} + T_{Sun})/L_{feeder}) \tag{12.17}$$

Parameter	Value	Reasoning
$\eta_{Illumination}$	0.91	Standard value for Cassegrain [47]
$\eta_{Spillover}$	0.8	Compromised industry standard reflectors [47]
RMSE Material	0.4 mm	Selected CFRP skin [34]
Power case I	200 W	Current maximum power for travelling wave tube amplifiers (TWTA) for Ka-band [118]
Data rate I	0.85 Mb/s	Data rate is halved because use will be made of orthogonal polarisation
$L_{Connectors}$	0.75 dB	Standard value from industry resource [9]
$L_{Splices}$	0.1 dB	Standard value from industry resource [9]
L_{Fibres}	0.3 dB / km	Standard value from industry resource [9]
Length cables	20 m and 200 m	20 m at the spacecraft and 200 m at the ground station, rough estimate
Distance Earth-SC	396×10^6 km	Maximum distance is taken to design for the worst case scenario
$L_{Rain_{Attenuation}}$	9.357 dB	Analysis made from ground station Canberra (largest latitude), based on rain rates and location[47]
$L_{Rain_{Depolarisation}}$	1 dB	Worst case scenario estimate from the University of Porto [87]
L_{Gasses}	0.7 dB	Frequency specific value from SMAD [130]
L_{Clouds}	0.22 dB	Estimate with thick fog (0.5 g/m^2) with a cloud height of 0.5 km [47]
$L_{Scintillation}$	1 dB	0.01% of the time caused by variations of refractive index of the tropo- and ionosphere [47]
$L_{Polarisation}$	-0.13 dB	Rotation of the polarised wave of 10 degrees is assumed by interference with the ionosphere [47]
Accuracy spacecraft pointing	0,0024°	The most accurate current existing antenna pointing mechanism was selected [30]
Accuracy ground station pointing	0,008°	Pointing accuracy from the Deep Space Network [47]
T_{LNA}	200 K	Average low noise amplifier noise temperature for frequencies above 30GHz [47]
T_{feeder}	35 K	Feeder noise temperature from SMAD [130]
L_{feeder}	2 dB	Worst case feeder losses due to connection to transponders [47]
T_{sky}	15 K	Average background noise in the milky way [47]
$T_{Antenna}$	290 K	Margin for radiowaves from the radiators, based on an estimate for the antenna location
Apparent Angle	0.012°	Defined as under which angle the antenna sees the planet. 2*arctan(diameter planet / distance to planet)
$T_{Earth-Mars}$	290 K and 210 K	Defined noise temperatures of both planets by [47]
T_{Sun}	4432 K	$120,000 * (f[Hz]^{-0,75}) * 0,5$[47], was used to determine the noise from the sun
Diameter main reflector	3.45 m	Sized to close the link budget for a SNR of 21
Diameter sub-reflector	0.264 m	Sized by an optimised sub-reflector method, discussed below [127]
Power case II	40 W	To close the link budget for a SNR of 21 and based on commercially available TWTA's [118]

Table 12.4: Used parameters for the link budget and justification. "I" stands for the nominal operation case (1.7 Mb/s data rate). The order in which the values were determined is from top to bottom.

12.3.3. Communication and command and data-handling Architecture

The major components for the communication sub-system that are used in the link budget will now briefly be discussed. First off all, the choice of using *orthogonal polarised waves* (proved by Voyager II [96]) is something that poses a constraint on the feeder. Orthogonal polarisation is the principle that a polarised wave for which the electric field strength vector at a given point in space rotates in the same plane and in an opposite sense to that of a reference polarised wave of the same direction of propagation, they make an angle of 90° with each other and do not interfere. This enables frequency reuse, the same bandwidth can be used twice at the same time. The data rate is divided over the two waves, therefore decreasing the required power and diameter of the reflector. However, these two waves should come from two different transponders and amplifiers and should be modelled together to one wave by an *orthomode transducer* (OMT). This makes sure that the cross-polarisation level (measure for interference) is high enough and is also able to split one wave with two polarisation to two waves with one polarisation. This OMT is therefore a diplexer for polarisation and is connected to a *corrugated horn* that feeds the reflectors. Corrugated means that there are small notches in the feeder which makes sure that the cross-polarisation level is above

35 dB, which is proven to be enough to prevent interference of the two polarisation's[47]. Such a feeder is capable for doing both transmission and receiving at the same time due to this principle. The dual-polarised corrugated horn feeder with OMT selected can be found in Table 12.5. Furthermore, realise that the ground stations defined can all cope with a right- or left-handed-circularised orthogonal polarisation [47].

As stated in Table 12.4, the available *Travelling Wave Tube Amplifiers (TWTA)* for the Ka-band frequencies is limited to 200 W. The working principle is that a radiowave is transported through a vacuum tube with an electron gun that emits electrons that exchange electric energy for kinetic energy due to a cathode and anode. A beam is formed by a magnetic field around it. The speed of the electrons is set to the same speed as the incoming radiowave by changing the voltage over the cathode and anode. The radiowave that is in the tube now passes a helix, which creates induction. The induction pattern is used to form the electron beam with high energy to an analogue of the radiowave that was entered, but now amplified [47]. Two 200 W TWTA's and one 40 W (for low data rate, does not have to be orthogonalised) TWTA's are required per antenna system for amplification of the two orthogonal polarised waves for the nominal and reactor failure conditions and the selected ones can be found in Table 12.5. The TWTA's should be fed by a *Electronic Power Conditioner (EPC)* that is able to give the required (adaptable) power to achieve the amplification. The ones that are chosen can also be found in Table 12.5.

The carrier waves are created by a *transponder module* were the data is modulated on. A transponder is also capable of demodulating a receiving signal. To distinct the incoming and outgoing wave, the transponder should have a *diplexer* that functions with a turnaround ratio that is the same as the turnaround ratio used for up- and downlink communication (0.93, Section 12.2). Furthermore, because transponders are very sensitive for radiation (damage and interference), a deep space proven one should be used. Two transponders are required to be able to module two polarised transmitting waves that are brought together by the OMT and to demodulate the two receiving channels. One that fulfils all demands can be found in Table 12.5. This transponder is deep space proven on the MRO mission [58], BepiColombo and JUNO missions [39]. It has a turnaround ratio of 0.93 that suits the requirement and it makes use of Pseudo-Random-Noise Modulating (PRN) to put data on the carrier wave. PRN has a deterministic sequence of pulses that is recognised by the transponders but, which stands for a certain bit pattern. Each sequence has its corresponding bit pattern. It has the advantage that due to an almost zero correlation of the random noise and that it is already an encrypting modulation method as the pattern is not recognisable by external systems.

The pointing mechanism used is a gimbal that is able to point with a 0.0024°precision and can provide full rotations in azimuth and elevation with respect to Earth. The detailed sizing of the reflectors is done by using [127]. Current research to Cassegrain optimisation by the University "Tunku Abdul Rahman" showed that the largest aperture and spillover efficiency is achieved when a ratio of focal-length over main reflector diameter ($\frac{f_{main}}{D_{main}}$) of 0.5 is used [64] and for the corrugated horn feeder focal-length over diameter of the sub-reflector ($\frac{f_{feeder}}{D_{sub}}$) 0.75 [127] and a taper illumination ($taper_{ill}$, feed illumination reduced at the edges of the reflector) of 11.76 dB is optimal for a 3.45 m diameter[127]. The design is based on parabolic and hyperbolic geometry and optimisation by Kildal to prevent sub-reflector and feeder blockage as much as possible [127] and can be summarised by Table 12.6 and Figure 12.4.The feeder will be located on the focal point of the sub-reflector (f_{sub}).

12.3.4. Command and Data Handling Architecture

The CDH unit has to be spaceflight proven for radiation environments and thermal fluctuations, although it is allocated in the pressurised module. Furthermore, it shall have a very accurate and synchronised time manager to ensure the Time Divided Multiple Access communication strategy from Section 12.2. The processor shall have the capability of dealing with the 1.7 Mb/s downlink data rate and can decode the commands from uplink on a rate of at least the uplink rate of 1 Mb/s. The system also needs a solid memory capacity of at

Component	Selected equipment	Mass per unit[kg]	Power peak per unit[W]	Additional constraining information
Feeder	WR-28 Dual Polarised Scalar Feed Horn Antenna + 1 for redundancy [109]	0.16	15	233-358 K Temp-range. Needs active thermal control.
TWTA nominal	2 x L3 EDD 99xH + 2 for redundancy [118]	1.5	400 (50 % efficiency)	Functional for Ka-band.
TWTA reactor failure	1 x MEC 5496 Continuous Wave TWT + 1 for redundancy [119]	3.4	73 (55 % efficiency)	Functional for Ka-band.
EPC	4x Thales Electronic Power Conditioner + 4 for redundancy [120]	1.3	250 (95 % efficiency)	Fully ESA Qualified.
Transponder	2x Thales KaT transponder + 2 for redundancy [39]	3	40	215x140x175 mm. Modulation speed 25 Mcps.
Pointing mechanism	2x NEA interactive G35 Gimbal Model [30]	1.8	27.4	0.0024° accuracy. 173-423K Temp-range.

Table 12.5: Selected communication equipment

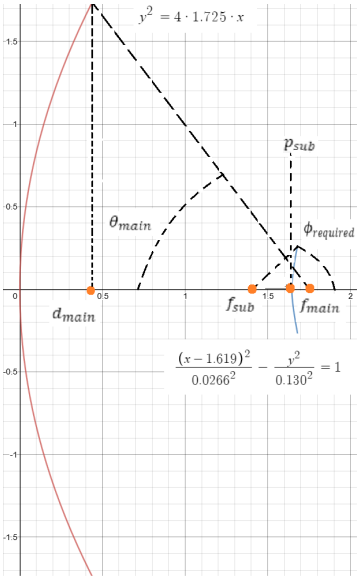

Table 12.6: Antenna design components

Part	Formula	Result
Main reflector, focal length, f_{main}	$\frac{f_{main}}{D_{main}} \cdot D_{main}$	1.725 m
Main reflector, depth, d_{main}	$\frac{D^2_{main}}{16 f_{main}}$	0.43125 m
Main reflector, equation	$y^2 = 4 \cdot f_{main} \cdot x$	See sketch
Taper illumination factor, E	$10^{\frac{taper_{ill}}{10}}$	15
θ_{main}	$tan^{-1}(\frac{D_{main}}{f_{main}-d_{main}})$	69.4 deg
$\phi_{required}$	$2 \cdot tan^{-1}(\frac{1}{4\frac{f_{feeder}}{D_{sub}}})$	36.97 deg
Sub reflector, optimum diameter, D_{sub}	$D_{main} \cdot [\frac{cos^4(\phi_{required}/2)}{4\pi \cdot sin(\theta_{main}) \cdot E \cdot \frac{1}{D_{main}}}]^{1/5}$	0.264 m
Sub reflector, loss	$10 \cdot [1 - \frac{-10ln(E)}{1-\sqrt{E}}(1 + 4\sqrt{1 - \frac{D_{sub}}{D_{main}}})(\frac{D_{sub}}{D_{main}})^2]^2$	-0.46 dB
Magnification factor, M	$\frac{\frac{f_{feeder}}{D_{sub}}}{\frac{f_{main}}{D_{main}}}$	1.5
Sub reflector, focal length, f_{sub}	$0.5 \cdot D_{sub} \cdot (cot(\phi_{required}) + cot(\theta_{main}))$	0.265 m
Sub reflector, eccentricity, e	$\frac{M+1}{M-1}$	5
Sub reflector, c	$\frac{f_{sub}}{2}$	0.1325
Sub reflector, a	$\frac{c}{e}$	0.0266
Sub reflector, b	$\sqrt{c^2 - a^2}$	0.130
Sub reflector, off-set p_{sub}	$f_{main} - (c - a)$	1.619 m
Sub reflector, equation	$\frac{(x-p_{sub})^2}{a^2} - \frac{y^2}{b^2} = 1$	See sketch

Figure 12.4: Reflectors Geometry

least 61.1 GB for conjunction data storage, see Table 12.2, and another 100 GB for software (rough estimate for manned missions [130]). It has to have a watchdog unit, which is an electronic timer that is used to detect and recover from computer malfunctions. The working principle of such a watchdog can be seen in Figure 12.5, it measures how long the CPU does over a task and cancels the task if it takes longer than pre-programmed. Last, the configuration should comply with the MIL-STD-1553 regulations (the mechanical, electrical, and functional characteristics of a data bus, see Figure 12.5), as a lot of interfaces used are designed by this [47]. Two units are required for redundancy. The bus controller unit controls is transmitting commands to the remote terminals (all sub-system connected pins) at predetermined time intervals. The commands may include data or requests for data (including status) from the remote terminals. The selected CDH bus with the specifications that adhere to the requirements can be found in Figure 12.5, together with the additional external flash memory Solid-State Recorder, which is oversized but still lighter and using less power than no-flash memory with less capacity (realise that the watchdog and bus controller and monitor are already included in the chosen CDH unit).

Component	Equipment selected	Mass per unit [kg]	Power Peak per unit [W]	Additional information
CDH Bus	2x Magellan CDH [72]	10	34	Processor: Power PCTM 750FX Memory: 2.0 GB of mass memory 2.0 MB of essential bus memory and status log Data: Command decoding rates up to 5 Mbps Downlink data rates up to 8 Mbps Reliability:0.98 for 2 years
Solid memory	2x NEMO SSR Airbus [112]	6.5	10	Qualified by NASA GSFC Parts Document EEE- INST-002. Memory size: 0.5 TB

Table 12.6: CDH equipment and characteristics

The *overall C&CDH architecture* of the spacecraft can be found in Figure 12.5. This in-

cludes actually three diagrams in one. The data handling block diagram, the communication architecture and the communication flow diagram.

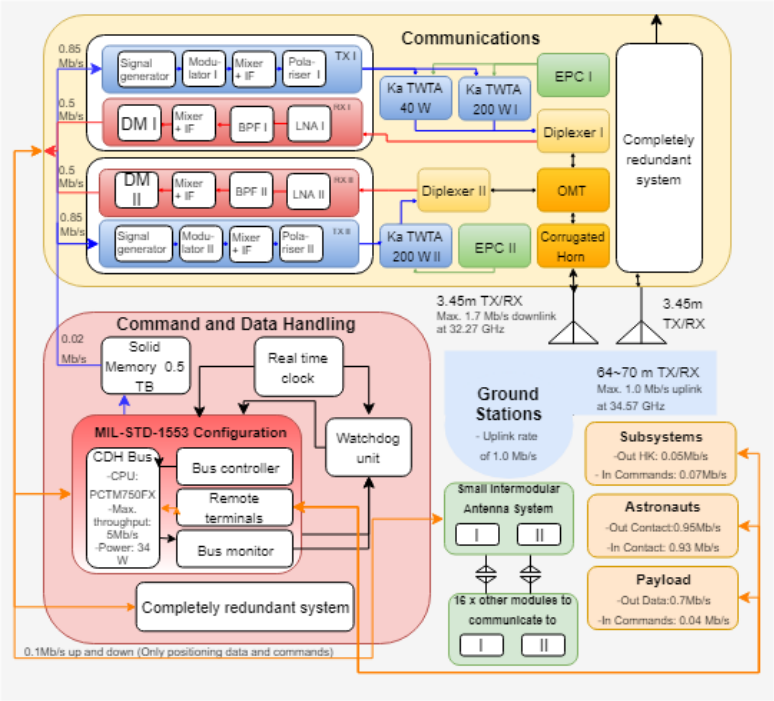

Figure 12.5: C&CDH Architecture. Black arrows stand for data flow that does not go to Earth. Orange arrows stand for both transmitting and receiving data. Blue arrows for transmitting data. Red arrows receiving data. BPF means Band Pass filter. IF stands for an intermediate frequency used for modulation or demodulation. LNA stands for Low-noise-amplifier for the receiving signal. DM stands for demodulator. The data rates per component are also given. A grey background means that the component is in the spacecraft system while a blue background means part of the external ground system

12.4. Systems Engineering for C&CDH

12.4.1. Design development and system effects

Note that when the final equipment was selected it was found that the feeder needs active thermal control which changes the system piping configuration a bit. From a structural and operational perspective, the truss that is required to attach the gimbals influenced the launch configuration and plan by changing the order of launch as communication should be possible from the start. Also, after the first iteration the ADCS design was heavily influenced by the large antenna size, however this effect is diminished at the end due to the smaller dishes and larger solar panels. Another system effect is that all the subsystem interfaces to the CDH bus, shall have a MIL-STD 1553 configuration adaptability. In Table 12.7 one can see the development of the design parameters. Mass and power can be computed by adding the values from the selected equipment for the different scenarios. The initial sizing was done after a data rate of 1.7 Mb/s was found for the downlink, where a preliminary link budget was used. Then, for the first iteration it was already found that the power was constraint to the 200 W that could be delivered by the TWTA for Ka-bands. This reduced the power consumption, however, to achieve the 1.7 Mb/s data rate the reflectors and therefore the mass increased enormously, foldable antenna's were considered here, which is an idea that is not used anymore, see argumentation in Section 12.2. This increased the Mass Moment of Inertia drastically as the main reflector has an off-set from the centerline and heavier CMG's were required. For the second iteration it was found that by using orthogonal polarised carrier waves, the data rate downlink could be reduced to 0.85 Mb/s for one channel. This reduced the required reflector sizes and therefore the masses. The difference in power between the second iteration and the final, is due to the fact that the efficiency of the TWTA's was not included in the second one and also the power of the CDH system was not included. The

mass increased, as the most accurate values for the selected equipment could be used and the redundant system was also added now.

Parameter	Initial sizing	First iteration	Second Iteration	Normal Peak (396×10^6 km) Final	Reactor Failure Peak (396×10^6 km) Final	Normal Nominal (227×10^6 km) Final
Total Mass [kg]	470	1,200	235	457	457	457
Peak Power [W]	2,300	967	967	1411	277	594
Main diameter[m]	4.4	6.9	3.1	3.45	3.45	3.45

Table 12.7: Design parameters development for the C&CDH system

12.5. Sensitivity Analysis

The main constraints and driving criteria for the C&CDH system were the data rate downlink, the frequency band used and the power available by the TWTA's. A brief sensitivity analysis will be performed on them now.

- **Downlink data rate**
  If this is increased by 0.65 Mb/s, for example for payload that produces a larger data rate or astronauts that need longer contact to ground, the diameter of the main reflector should be 4.6 m to still achieve a SNR of 21. This would lead to a reflector that does not fit in the launcher fairing. This would mean that a deployable antenna should be used, which changes the design procedure drastically as other materials, structures and packing design constraints will determine the design than.
- **Frequency band allocation**
  If no permission is given by the ITU for the Ka-band, the X-band would probably be the other option. This would change the downlink frequency to 12 GHz, decreasing the link budget by $\sim$ 2.5 dB, and to still achieve the SNR of 21, a main reflector of 4.5 m is necessary. This would still fit in the fairing of 4.6 m , however the clearance is very small and due to vibrations damage could easily occur.
- **Amplifier power development**
  If in the upcoming 20 years, the maximum power that TWTA's can use to amplify Ka-band waves increases, the antenna sizes will reduce, but not as much as the change in power. An example, imagine that the power gets doubled to 400 W, the link budget will increase by $\sim$ 1.6 dB. However, the main reflector can only be reduced to 3.2 m (-6 %). Changing the mass by ~ -14 %.

12.6. Verification & Validation

Some verification and validation can still be performed on the already deep space proven equipment and materials, but more important is to verify and validate the used link budget, which determined the sizing. The budget code itself can be *verified* by several unit tests on the losses and gains. For example, the Friss Transmission loss can be checked by a hand-calculation and the overall link budget system integration test can be performed by checking the feasibility of the outcome of the link budget by changing the parameters to unreasonable extent, for example a antenna gain of 1,000 dB now gives a SNR of 971 dB, which seems like a correct implementation of such a large input. This can be done on system level by changing more components easily.

Regarding *validation*, especially the RMSE of the material should be analysed by an electron-microscope. Also, the performance over such a long distance should be tested to validate the transmission losses in all different harsh environments, by using the antenna configuration in a experiment in vacuum, radiated by the dose that it experiences, where the waves are reflected millions of times until the distance is covered. The energy of the transmitted and received waves should be compared and the transmission loss in the link budget can be validated. As the Ka-band is so sensitive for both depolarisation and atmospheric attenuation's, a geostationary satellite positioned in a region where there is a lot of rain and fog (like the Amazones) enables to analyse the loss in energy that the waves experience and validate this with the computed loss in the link budget. Noise temperature of the entire spacecraft and at the antenna can be validated by a test where the radiators are connected to an external thermal source, start radiating and measuring the power flux density around the antenna feeder by sensors.

13
Technical Operations

This chapter details elements of the technical operations considered during the detailed design phase. This includes the payload, maintenance and resupply elements of the mission, as well as ground - spacecraft interactions and launch scheduling.

13.1. Key requirements and constraints

The main challenge regarding the technical operations of the Delta Mars mission concerns the requirement of having to launch such a large spacecraft using an existing rocket family (SYS-09). This immediately implied the spacecraft having to assemble in Earth orbit (SYS-06). Although there is no hard requirement on the amount of launches used to bring the spacecraft in orbit, the goal is to reduce it to a minimum, to reduce launch costs.

13.2. Midterm Trade-off Results

In the Midterm Report[126], it was decided to use the Falcon launch family, mainly due to its low cost and added flexibility to choose between a (more reliable) Falcon 9 and a (high capability) Falcon Heavy. Next to this, it was considered beneficial to include an Earth-orbiting station to the mission, to ease and speed up resupply missions and to assist in assembling the Mars Transfer Vehicle. The latter is done by leaving supplies and materials required to assemble the spacecraft in Earth-Orbit, and not having to take it to Mars. This chapter will go into more detail on how the Falcon family and Earth-Orbit station are used during In-Orbit Assembly.

13.3. Launcher specifications

As discussed in the Midterm report, the Falcon family will be used[126]. This section will describe several characteristics of the Falcon family which impact the design of the spacecraft.

13.3.1. Fairing dimensions

The size of the modules sent into orbit will be constrained by the fairing size of the Falcon. As shown in Figure 13.1, the maximum diameter is 4.6 m, and the maximum length 11 m with a taper at the end.[113]

13.3.2. Launch environment

An overview of important launch characteristics is given in Table 13.1[113].

13.4. In-Orbit assembly

In order to keep the fissile material away from Earth, the spacecraft will assemble in a relatively high orbit compared to space stations so far, around 950 km altitude. The Falcon Heavy can bring about 35 t in this orbit, which means the spacecraft will have to be brought into space in sections smaller than this. As described in Section 11.7, berthing will happen autonomously using a berthing arm. As the Falcon launchers only have an apogee accuracy of 10 km[113], each module either needs to have its own propulsion system and ADCS to steer it to the correct orbit, or an external system is used.

13.4.1. Space tug

As described in the Midterm report[126], it was decided to use an Earth orbiting station to facilitate resupplying the spacecraft and assist during assembly. However, as from the detailed trajectory planning in Chapter 6 it became clear that the spacecraft will be orbiting Earth for 1.1 years between missions, there is plenty of time to resupply the spacecraft, and the Earth station will not have to provide this functionality. The ”Earth station” will thus primarily be used as external system to rendez-vous with the individual modules, and guide it towards the partially assembled spacecraft. This reduces the size of the Earth station strongly, and makes it more similar to a ”Space tug” as researched by NASA in earlier decades [21].

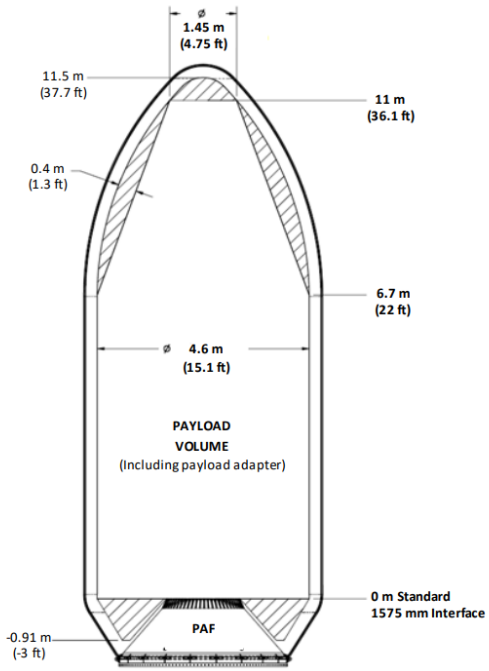

Figure 13.1: Fairing dimensions of the Falcon family

Capability to 950 km	35 t
Apogee error	10 km 3σ
Lateral acceleration	± 2 g
Axial acceleration	-2 to 6 g
GRMS	7.63
Temperature	$50 - 85\ ^oC$
Minimum required resonant frequency	35 Hz

Table 13.1: Important launch characteristics on board of the Falcon Heavy

The space tug will consist primarily of a propulsion and ADCS module, used to provide the required ΔV to each module and propel it towards the other modules. Basic orbit calculations showed that for a worst case apogee error of 10 km for each module, a ΔV of 6 m/s is required. For a specific impulse of 260 s, this results in a propellant mass required of 19 t to manoeuvre all modules for initial assembly. Additionally, the space tug will have its own short-range communication system, a small solar array for its own power and the robotic arm, and the same docking port as the other modules have.

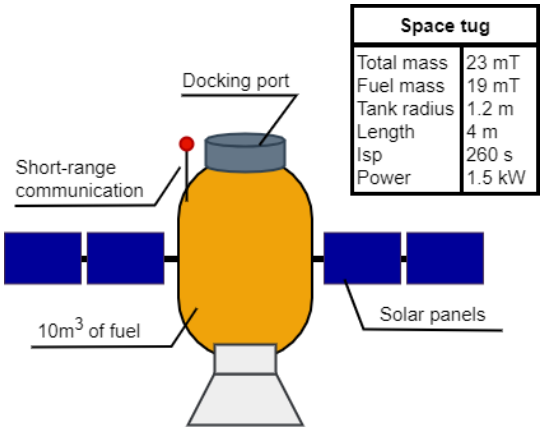

Figure 13.2: Concept of the space tug

Each module will still need it own attitude and location determination system (such as GPS), and a short-range radio communication system to send its location to the space tug.

13.4.2. Order of modules launched

To launch the entire spacecraft, 17 launches are required, as shown in Figure 13.3. The launches are roughly broken down in the trusses including radiators, the habitat modules, the tanks including fuel, the propulsion modules, the supplies and the crew. Additionally, the space tug and external payloads need to be launched and berthed with the spacecraft.

First of all, the truss section closest to the habitat modules is launched as first module. This includes a section of the radiators, the CMGs, the antennas (folded) and the berthing arm (RMS). It will also have a rudimentary board computer and small batteries to perform the initial berthing operations. Once it has reached its orbit, it will unfold its antennas and establish contact with the ground stations. Right after, the space tug is launched and will rendez-vous with the first truss, to move it to the correct orbit. They will communicate through short-range communication antennas, and if required, the space tug can communicate with the ground stations using the initial truss as relay. Following this, the other four truss sections including the solar panels and power distribution system are launched in pairs of two, will rendez-vous with the space tug, and are brought towards the initial truss. From this moment, the partially assembled spacecraft can be powered from the solar panels.

Now that the central truss is assembled, the habitat modules including all internal systems (the ECLSS, the instruments, additional batteries, et cetera) are launched and berthed with the truss. The cupola, airlock and RCS module are docked to the top of the habitat modules during launch to fit in the fairing, even though the first two will not be used here during operation of the spacecraft. The RMS will move them to the correct location before the next habitat module is berthed, as discussed in Chapter 11.

Six tanks filled with Argon are launched next. They are already connected to small trusses into which feedsystem components,cryocoolers and possibly pressurant tanks are integrated,

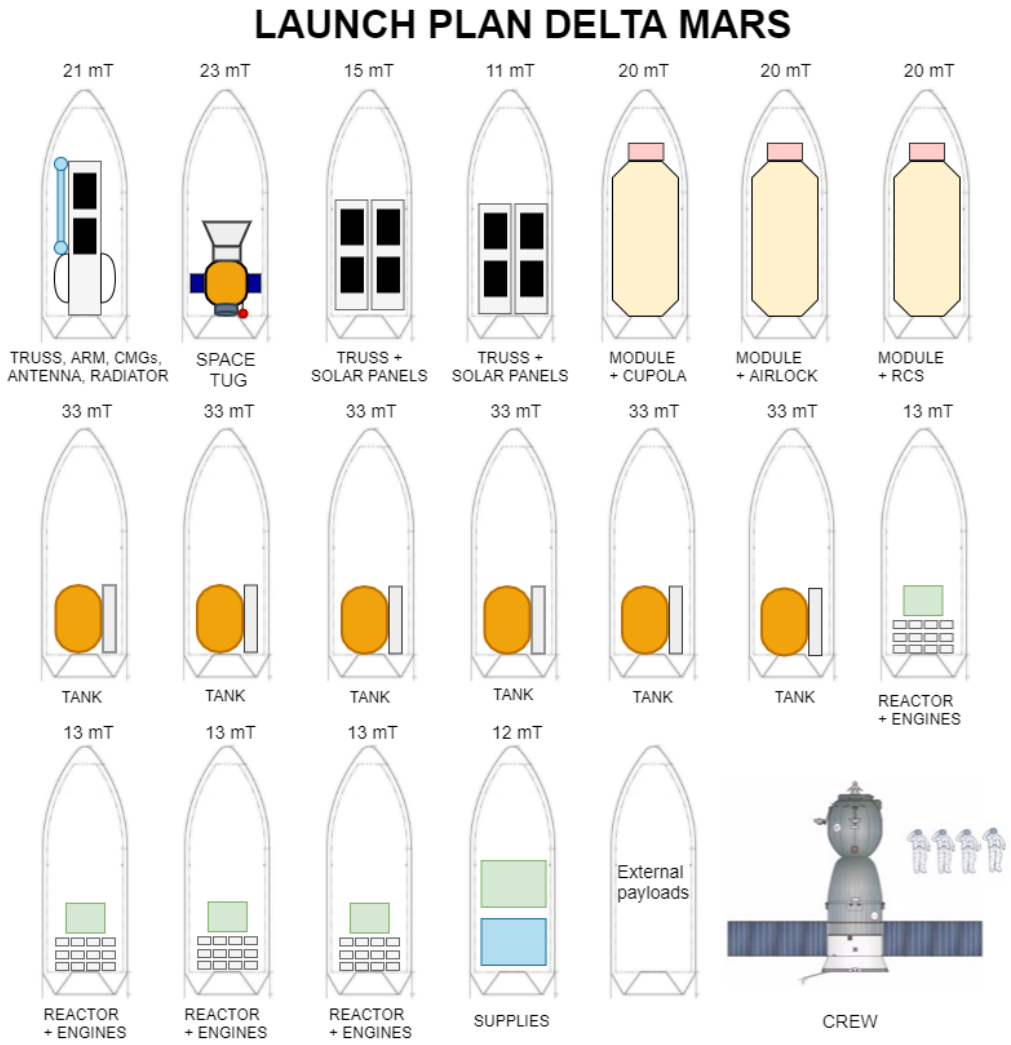

Figure 13.3: The Launch Plan for Delta Mars

to limit the amount of hydraulic connections that need to be berthed autonomously. As final sections of the spacecraft, four launches are required with each one reactor and 13 VASIMR engines on-board. The reactors are not connected electronically to the engines yet, but will both connect to the Electrical Distribution System in the end of the central truss first. It should be noted that the reactors and 12 engines together are relatively light, and it could be considered to launch these modules with a Falcon 9 instead of Heavy, to increase the reliability of the launches of nuclear material.

At this stage, the spacecraft is completely assembled. Final launches are required to bring supplies such as food, water and compressed air to the spacecraft, and to send up external payloads to the spacecraft. When this is done, the space tug will be de-orbited, and a new one will be launched to assist with resupplying the spacecraft. Operations to make the spacecraft ready for its mission include deploying the radiators, openings valves to close the heat exchange and feedsystem loops, and starting up the Life Support systems. These operations are explained in more detail in the Functional Flow Diagram in Figure 16.3. Due to the fact that many berthing interfaces include hydraulic and electrical connections, it is currently deemed likely that human system checks are required before the spacecraft can start its mission. This would mean astronauts are sent up while the spacecraft is still in LEO, rendez-vous with it, and perform EVAs from the spacecraft to check the functionality of the system. After this, the crew leaves the spacecraft again and flies back to Earth, as they cannot stay on board of the spacecraft while it is slowly spiralling through the Van Allen Belt. The final berthing operation will occur once the spacecraft is in High-Earth Orbit, when the crew is launched to the spacecraft.

13.4.3. Berthing operations

This section only covers the operations required to berth two modules together, for the specifications of the RMS and the docking interfaces refer to Section 11.6 and Section 11.7. The RMS can be mounted on either of the both vehicles to be berthed and correspondingly the grapple fixture has to be mounted on the opposite vehicle as shown in Figure 13.4. The chaser has to approach the berthing box on a trajectory taking into account safety considerations to prevent a collision between the two vehicles if capture fails. When acquiring the berthing box the residual velocity between the two vehicles shall not be larger than 0.02 mm/s to allow for a window of at least 2 minutes in which the chaser is inside the berthing box to be captured by the RMS [44]. Once inside the berthing box the chaser's thrusters are switched off and capture is initiated. The RMS positions itself automatically dependent on the attitude data it receives from the chaser until the LEE can position itself by using the camera target on the grapple fixture. The soft capture mechanism is activated when the grapple fixture is in reach of the LEE and once hard capture is achieved the docking interfaces are brought together for docking.

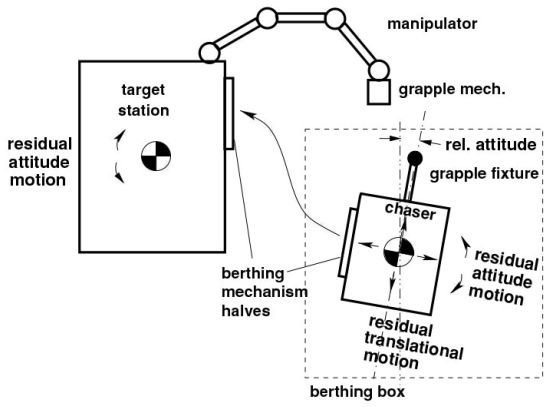

Figure 13.4: Berthing conditions at capture [44].

13.4.4. Resupply

To resupply the spacecraft between missions, a reduced version of the process described above is required. First of all, waste (primarily from the ECLSS) is removed from the spacecraft and de-orbited. Afterwards, a new space tug is launched, to assist in berthing the resupply modules to the spacecraft. Following the same procedures described above, new Argon tanks, ADCS fuel, supplies and external payloads are brought to the spacecraft, requiring a minimum of 8 launches. Additionally, extra habitat or propulsion modules could be launched, in order to expand or reconfigure the system.

13.5. Payload

Requirement SYS-16 states that ”half of the system volume shall be reserved for payload”. After discussion with the stakeholders, this is taken to refer to the pressurised volume, which is $260 m^3$ as discussed in Chapter 11. Currently, 80 m^3 is available inside the habitat modules for scientific equipment, as shown in Figure 13.5. The other 50 m^3 comes from payload (primarily satellites and landers) docked to the outside of the spacecraft, for which 15 t is reserved in the mass budgets. This implies a payload density of 300 kg/m^3, lower than for example the 440 kg/m^3 of the Mars Global Surveyor[1]. Taking into account that the satellite payloads do not have to bring their own propellant for the transfer to Mars, which is usually a high-density part of the satellite[130], this however is not an unreasonable assumption.

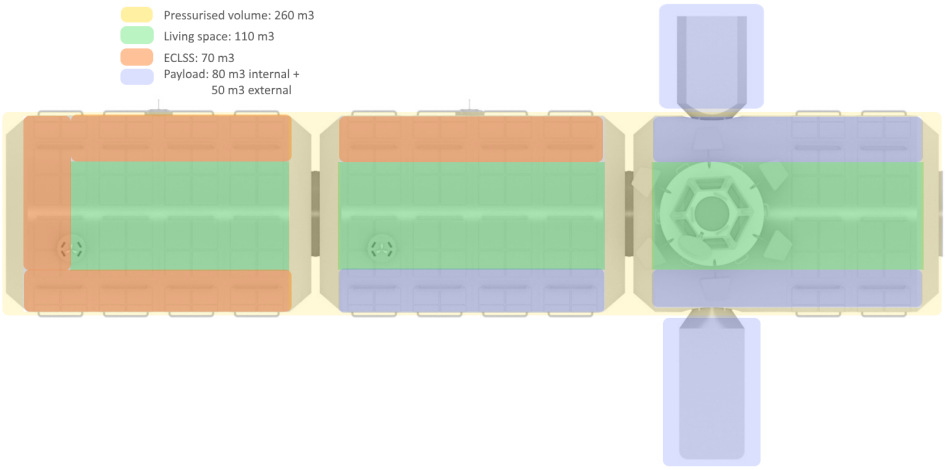

Figure 13.5: An overview of the volume reserved for payload

13.6. End-Of-Life

According to the United Nations Office for Outer Space Affairs guidelines [85] all vehicles in LEO that have terminated their operational phase have to be removed from orbit in a controlled way. Due to the size of the individual modules deorbiting them poses several risk and therefore it was decided to bring them to a graveyard orbit instead. In the decommissioning phase after the last mission has been finished the possibility of retrieval of resources from the vehicle will be evaluated before the decommissioned modules will be brought into their final orbit. The reactors will either stay connected to the propulsion system or will be connected to a new propulsion system in order to bring them to a safe heliocentric orbit.

13.7. Logistics

Due to the size of the mission, many facilities and external partners will be required. Figure 13.6 gives an overview of the various facilities and parties required before, during and between missions. Important components to note already are the manufacturing and integration halls (potentially the same building), the test facilities (internal and external), various forms of transport, the launch providers, the crew training centres and the ground segment.

[1] https://mars.nasa.gov/mgs/mission/spacecraft.html

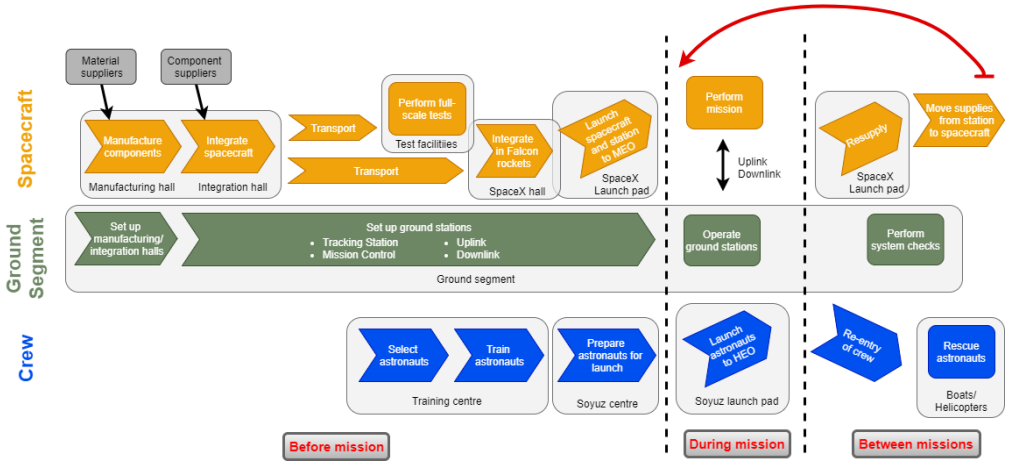

Figure 13.6: Operational and Logistical flow diagram

13.8. Sensitivity Analysis

An important parameter that would change the technical operations is the amount of launches, either because the spacecraft becomes heavier or because the launcher capabilities are reduced, for instance due to a higher assembly orbit. The first has a relatively low impact on the system, as the spacecraft is modular and simply more modules are berthed to the system. The main change would be that the space tug has to be resized, to ensure it has enough fuel to move the additional modules to the correct orbit. The latter, a reduction of mass per launch, has large implications on the whole system. Especially the tanks have been sized to the maximum mass capabilities of the Falcon Heavy, meaning the number of tanks would have to be increased. An even further reduction of the launch capabilities would also require a redesign of the habitat modules, meaning large parts of the spacecraft need modifications. This means the system design is very sensitive to a reduction in launcher capabilities, which thus needs to be closely monitored.

The system is also sensitive to the assumption that the space tug will be a feasible option. As the concept has never been used in earlier missions, this is still a realistic scenario, for example due to the complicated logistics of the many docking operations. In this case, each launched module will require its own ADCS and propulsion system to make it rendez-vous with the spacecraft. This would increase the mass and size of each module, and in case the ADCS and propulsion sections cannot be fit into the Falcon fairing, the modules will have to be redesigned. Especially the habitat modules are very tight in the fairing at this moment, meaning they are most likely to change. It will be important to perform a feasibility study on the space tug, including a potential test program in LEO, before the design of the habitat modules is finalised.

13.9. Verification & Validation

V&V is required for both the In-Orbit assembly operations and the ground stations. Regarding launch, integration tests will have to be performed together with the launch provider, SpaceX, to ensure each module interfaces well with the fairing. This will also include vibration and electrical interference tests, as specified by the Falcon user guide. [113] Furthermore, the berthing operations will have to be tested, including the space tug. It is proposed to dock a representable module, using the space tug, with the ISS, as this uses the same (standard) docking ports.

The other large part of Operations V&V considers the ground stations. All ground stations will require dry runs to get the crew acquainted with the systems, check if all communication systems functions well, and improve the procedures. Furthermore, the crew will have to be trained, which requires mockups of the spacecraft (especially the habitat modules) inside the astronaut training centres.

14

Designing for Sustainability

Space missions have a large environmental impact due to their complexity and the required launches. Even though the vehicle's reusability and its modularity have a positive impact on the mission's sustainability material is still removed from Earth's ecosphere and evaluating the environmental impact after the end-of-life poses several difficulties. In this stage the identified elements concern the creation of additional orbital debris, inadvertent atmospheric entry and the use of harmful substances. Additionally a Life Cycle Assessment is conducted.

14.1. Debris Mitigation Plan

The common definition of space debris comprises all non-functional man-made objects, their fragments and elements in Earth orbit. Issues related to it concern the potential for pollution of the atmosphere and on Earth surface, the orbit resource used, the risk and effects related to collisions and explosion and the casualty risk on ground. Similar criteria can be applied for the creation of space debris in Martian orbit. Special concerns regarding these issues arise from the use of nuclear reactors for power generation as a breach of the core containment could result in the release of fission products.

The altitude of the assembly orbit in LEO is dependent on multiple factors concerning the mass which can be launched, radiation exposure, spatial density of orbital debris and safety concerns. To mitigate the risk of collision and resulting break up of the spacecraft the assembly orbit altitude defined in Section 13.4 is increased to 950 km as the spatial debris distribution is favourable at this altitude [60]. This lowers the risk of impact of space debris dependent on the orbit inclination also lowering the probability that the mission will generate an increase in space debris. Current ground based radars can detect debris larger than 1 cm in LEO[1] which can then be actively avoided. All critical components of the spacecraft have to be designed to withstand impact of debris below this threshold or need to be protected by the application of extra MMOD shielding as described in Section 11.4.1. As the reactors are one of the most critical elements of the spacecraft they are not only designed to withstand such impacts but also MMOD shielding is externally applied to each of them to further decrease the probability of fuel being released if an event occurs. The tracking capabilities for debris and asteroids in deep space and around Mars are limited and the mitigation strategy for this part of the mission relies on the application of MMOD shielding and the ADCS' avoidance manoeuvres as described in Section 8.4.

To mitigate the creation of debris after the spacecraft's end-of-life it has to be disposed in a way that removes its mass from densely populated orbits in a controlled way. In the decommissioning phase after the last mission has been finished the possibility of retrieval of resources from the vehicle will be evaluated and all decommissioned modules will be brought to a graveyard orbit. The reactors will either stay connected to the propulsion system or will be connected to a new propulsion system in order to bring them to a heliocentric orbit without the risk of future planetary impact.

14.2. Atmospheric Entry

Uncontrolled entry of an object into Earth or Martian atmosphere pose the risk of environmental pollution. Composition and reactivity of re-entry smoke particles created during atmospheric re-entry depends on the object's configuration and they could have significant effect on the atmospheric chemistry [76] comparable to the changes of the atmospheric composition caused by the emissions of launchers which are identified as a source of ozone depletion [71]. In a worst case scenario atmospheric entry can result in the release of fission products inside the atmosphere in a wide and unpredictable area. Due to the size of the spacecraft and its modules the probability of objects not fully demising during entry and

[1] http://www.esa.int/Our_Activities/Space_Safety/Space_Debris/Scanning_and_observing2

impacting the ground cannot be neglected. To prevent the contamination of the ground the nuclear components have to be designed to withstand the high temperatures, stresses and impact loads of an atmospheric entry or they have to be designed in a way that eliminates the possibility of atmospheric entry.

The highest environmental impacts are connected to the risk of inadvertent atmospheric entry. Three possible scenarios are investigated here and are included in the risk assessment. They are re-entry from an Earth orbit during a launcher failure, failure in assembly orbit and a failure placing the spacecraft on an Earth or Mars-impacting trajectory. As a first mitigation to lower the impact of a launch failure all four reactors are launched on separate launchers. As the reactors are launched inactive with not critical fuel elements the consequences of a launch failure are considered to be limited to a small area comparable to the 24 km radius contaminated by the NERVA Nuclear Thermal Rocket test[46]. When launched with a Falcon launcher from Kennedy Space Center, FL all failures up to 700 s will furthermore result in the reactors impacting on water, lowering the impact force. No release of fuel is expected if this scenario occurs. Failure in assembly orbit can result in the loss of control but as the assembly orbit is at an altitude above 900 km the orbital decay results in a orbit lifetime of 200 years[41]. The risk of atmospheric re-entry in this mission phase is negligible. Short-term inadvertent Earth or Mars atmospheric entry occurs when the spacecraft is placed on a Earth or Mars impacting trajectory during one of its missions. The long-term Earth or Mars-impact component concerns a failure during the interplanetary trajectory which places the spacecraft on a heliocentric orbit with the possibility of planetary impact. To lower the probability of short-term entry the spacecraft's deep space trajectory has to be such that it misses Earth and Mars without further manoeuvres, and only be placed on a trajectory passing the planets when necessary. Based on the determined probability of Earth impact for the Cassini mission which implemented an Earth flyby at an altitude of 1200 km the probability of impact is estimated to be smaller than 1.9×10^{-7}[121]. Similarly long-term impact probability is based on theory on Earth-crossing asteroids to determine the possibility of the spacecraft impacting Earth and estimated to be smaller than 4.0×10^{-7} over 100 years.[121]

14.3. Use of Harmful Substances

To lower environmental impact and to comply with present and future regulations the use of substances identified to pose harm to human health and biodiversity has to be controlled and limited. Substances are evaluated based on their classification in the EU Registration, Evaluation, Authorisation and Restriction of Chemicals (REACH) framework.

14.3.1. Spacecraft Propellants

The primary propulsion system's propellant, argon, is abundant in Earth's atmosphere and is classified as non-hazardous[29]. The secondary propulsion system, implemented in the ADCS, is a bipropellant system using monomethylhydrazine, which poses serious health hazards and is classified as acute toxic and hazardous to the environment[29], and dinitrogen tetroxide, which poses serious health hazards and is classified as acute toxic[29]. Alternative propellants with lower toxicity were investigated and a monopropellant currently under development under the name AF-M315E by Aerojet-Rocketdyne was considered as replacement [101]. Propulsion systems based on this propellant are anticipated to be available in the next decade with a limit thrust up to 25 N. As this thrust level would require the implementation of 200 thrusters to comply with the ADCS requirements it was discarded. The developments of lower toxicity propellant thrusters will be monitored and a change of secondary propulsion system will be proposed if an alternative is identified. The design strategy includes the implementation of measures protecting workers and assuring safe storage.

14.3.2. Batteries

The power backup system uses lithiated nickel cobalt aluminium oxide batteries. The batteries' elements pose various hazards, nickel is classified to pose serious health hazards[29], the rare Earth element cobalt poses serious health hazards, acute toxicity and is classified as hazardous to the environment[29] and aluminium oxide poses health hazards[29]. Currently no batteries composed of materials with lower toxicity and without rare Earth elements of-

fer similar performance. Design strategies include the inspection of the battery producer's supply chain and the implementation of safety measures protecting workers and users.

14.3.3. Nuclear Material

The implemented fission reactors' fuel is 20 % enriched Uranium ^{235}U poses several mainly radiological hazards and exposure should be avoided. As no alternative means of power production are deemed feasible the design strategy is limited to reducing the risk of radioactive contamination. The uranium enrichment facilities must comply with the safety standards set up by the International Atomic Energy Agency [3] and handling, processing and storage shall be closely monitored in alliance with the agency.

14.4. Life Cycle Assessment

The application of a Life Cycle Assessment (LCA) allows to evaluate the environmental impact of large projects over their whole life cycle. Sources from which the highest emissions are expected either due to their production process or their quantity are identified and further researched. The CO_2-equivalent, which has been determined for each occurrence, is a measure which combines the emissions of various greenhouse gases and converts them to the equivalent amount of CO_2 on the basis of their global-warming potential[29]. An overview over the LCA is given in Table 14.1. Operations includes all management, design and development tasks and ground control during missions.

Mission Phase	Source	10^3kg * CO_2-eq per occurence	Number of occurences	Total [10^3kg * CO_2-eq]
Production	Lithium-Ion Batteries	0.2[9]	50 kW-h	10.0
	Solar Arrays	0.89[10]	250.5 m^2	222.9
	Uranium Enrichment	197[11]	5.4×10^3 kg * U_{nat}	1,063.8
	Aluminium	8.2[12]	60×10^3 kg_{Al}	492.0
	Polyethylene	1.3[13]	34×10^3 kg_{PE}	44.2
	CFRP	5[14]	10×10^3 kg_{CFRP}	50.0
	Titanium	8.1[12]	1×10^3 kg_{Ti}	8.1
	Production	1,540[15]	1	1,540.0
Launch	Falcon Heavy Launch	1,010[16]	12 Launches	12,115.9
	Falcon 9 Launch	337[17]	5 Launches	1682.7
Resupplies	Falcon Heavy Launch	1,010[16]	35 Launches	35,337.9
	Falcon 9 Launch	337[17]	5 Launches	1,682.7
	Food Supplies	0.0045[18]	18.66 day * capita	83.9
	Argon	0.00008[19]	785 m^3_{Ar}	0.1
Operations	Operations for 50 years	12[20]	15,000 m^2	180,000.0
	Total Amount			**234,334,415.0**

Table 14.1: LCA conducted for the whole mission duration with sources ordered to mission phase. Additional launches might be required for decommissioning. Footnotes on the emissions per occurence refer to the sources of each number.

The resulting $234,334,425 \times 10^3$ kg * CO_2-eq are an approximation of the emissions until the decommissioning of the spacecraft in the 2060s. This is equal to roughly 1 % of the global emissions of CO_2 in 2018[21]. The predicted emissions of the project are expected to increase with an increasing level of detail in the LCA as more sources of emissions are to be identified. Possible reductions of emissions can be achieved by selecting producers and service providers based on their sustainability and by minimising transport routes.

[9] http://www.ivl.se/download/18.5922281715bdaebede9559/1496046218976/C243%20The%20life%20cycle%20energy%20consumption%20and%20CO2%20emissions%20from%20lithium%20ion%20batteries%20.pdf
[10] https://aip.scitation.org/doi/pdf/10.1063/1.4965731
[11] https://www.iaea.org/sites/default/files/publications/magazines/bulletin/bull39-2/39205693436.pdf
[12] https://www.ncbi.nlm.nih.gov/pmc/articles/PMC4085040/
[13] https://link.springer.com/article/10.1007/BF02978888
[14] http://citeseerx.ist.psu.edu/viewdoc/download?doi=10.1.1.893.5802&rep=rep1&type=pdf
[15] https://fenix.tecnico.ulisboa.pt/downloadFile/395142223995/Tese_JoaoVascoLopes.pdf
[16] http://spaceflight101.com/spacerockets/falcon-heavy/
[17] http://spaceflight101.com/spacerockets/falcon-9-ft
[18] https://ccafs.cgiar.org/bigfacts/#theme=food-emissions
[19] http://www.diva-portal.org/smash/get/diva2:532125/FULLTEXT01.pdf
[20] http://www.arcom.ac.uk/-docs/proceedings/ar2002-129-136_Aye_et_al.pdf
[21] https://www.iea.org/geco/emissions/

15 Business Elements and Planning

Delta Mars is with respect to other missions a special case, not only by its technical content but especially due to its requirements on the business aspect. The enormous costs should be gathered in a way such that the system can still give a return on investment of 20 % to a group before the end of 2050. First, the life cycle costs will be analysed in detail in Section 15.1. Second, the current and potential markets for revenue are analysed in Section 15.2 and finally an elaborated analysis of the return on investment before 2050 will be performed in Section 15.3.

15.1. Life-cycle Cost Analysis

In this section all the cost that will be made from 2019 until mission end in 2060 will be discussed.

15.1.1. AND-Tree

In Figure 15.1 all Delta Mars specific costs that can be expected over the upcoming 41 years are categorised under four major space-cost components.

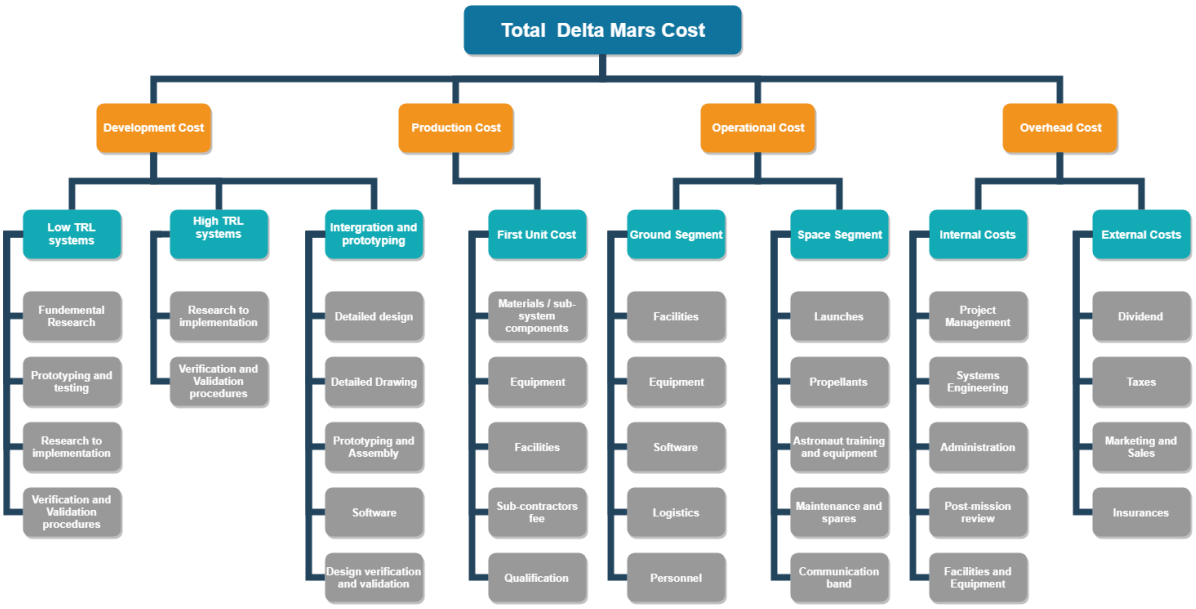

Figure 15.1: Cost Breakdown Structure for Delta Mars

15.1.2. Detailed cost estimation and planning

To get an accurate estimate of the return on investment, it is of importance that all the cost components that are given in Figure 15.1, get a (preliminary) cost estimate. Realise that due to inflation, the amount of money required for a investment now will be increased by a factor $(1 + 0.015)^X$ for the same investment in X years. An average inflation rate of 1.5 % is used in the calculations, this is based on a Moving Average Analysis from the European Commission [1] for the Netherlands. A lot of costs found were in dollars, but our company is located in Europe, a conversion factor of 1$=0.87 EU is used, based on last year market conditions [2]. Both factors can be a large risk. Significant changes in inflation rate or conversion rate due to a change in economic climate, can change the overall cost and income estimation. FY2019 stands for how much the investment would cost today, FY2040 for how much this

[1] https://ec.europa.eu/info/sites/info/files/economy-finance/ecfin_forecast_spring_070519_nl_en.pdf

[2] https://www.x-rates.com/graph/?from=USD&to=EUR&amount=1

investment would cost in FY2040. The development, production and overhead cost for the first 20 year are allocated under FY2040 as a worst case scenario of 20 years of inflation. In the periods FY2040-2050 and FY2050-2060 there are only operational and overhead costs and the inflation is accounted for every year individually. The cost estimate used is based on parametric and analogues methods from SMAD, as the design phase is not passed completely and a single large spacecraft is used, see Figure 15.2 and Figure 15.3.

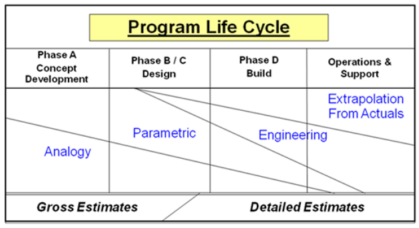

Figure 15.2: Cost method selection [3]

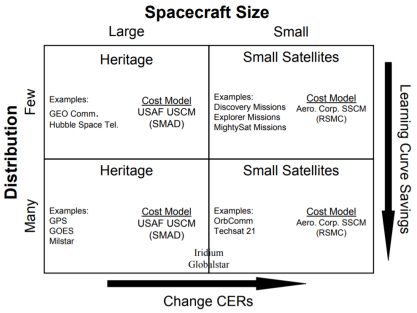

Figure 15.3: Cost relationships selection [4]

Development Costs

The cost estimation is based on a general model tool for the spacecraft systems excluding propulsion and power. The relationship used can be found in Equation 15.1.

$$Cost = a \cdot k \cdot M_{dry}^{b} \tag{15.1}$$

For the Design, Development, Test and Evaluation (DDT&E) cost, the $a \cdot k$ and b are 18.05 and 0.55 respectively [86], slide 7 of the University of Maryland slides for preliminary cost estimation for manned spacecraft. From this top level cost, the breakdown can be made to the Low and High TRL and the integration. The division can be made that 50 % will be approximately for the integration and that the Low TRL requires more money dependent on the system mass and TRL [86]. From [130] it is found that a TRL level 4, 5 and 6 require 17.5 %, 12.5 % and 10 % respectively more cost than the High TRL. While the dry mass of the spacecraft is 180.7 t, the Space Tug t (TRL 5-6), the 52 Vasimir engines 28.1 t (TRL 5), the 4 reactors (TRL 5) and MHD (TRL 4) together 24t this leads to a mass fraction of the low TRL systems of 56.1/184. When the required extra cost is included per low TRL system and one weights the mass fraction by this, one ends up with a development cost percentage for the low TRL systems of 34.57 % of total development cost. The calculated development cost with Equation 15.1 is excluding the cost of the engines and reactor. The VASIMR engine that will be used has not yet a fixed cost estimate, however, the statements are made that it will cost 10.5 million dollars to use for the ISS per year of mission extension. Therefore, for this mission, it is assumed that for 52 engines, operating over 20 years, this results in the 9.5 billion dollars of which 87.8 % is development cost [86]. The Nuclear Reactors cost for development, testing, and constructing the engines is taken as to be equal to the cost per reactor of the NERVA program, which was 1.4 billion dollars from 1955 to 1973. Accounting for inflation it becomes 1.87 billion Euros of which 87.8 % is development costs [86]. The division of the costs for the integration part is based on [130]. It is assumed that the costs are equal spread out from 2020 to 2040. As no information was found on the division of the low and high TRL cost parts and while the cost of the methods that will be used to develop are not defined yet, it is for now assumed to be equally divided over the parts, however, a more detailed analysis of these cost is required when the developments methods are defined.

Production Costs

For the flight unit cost (production costs for 1 spacecraft), Equation 15.1 can be used with $a \cdot k$ and b are 0.5686 and 0.662 respectively with a dry mass of 180.7 t + 4 t for the space tug,

[4] NASA Cost Estimation Handbook Version 4.0

[4] https://ocw.mit.edu/courses/aeronautics-and-astronautics/16-851-satellite-engineering-fall-2003/lecture-notes/l15_costmodellec.pdf

from the same source as the development costs. The division of percentages over the parts is based on preliminary estimates from [130].The 12.2 % (of the total costs mention before) for production of the VASIMR engines and Nuclear reactors is added to this. The division of costs is based on [130]. Those costs are made in the period 2035-2045.

Operational Costs

The operational costs is based on the current yearly operational costs for the ISS, which is 2.9 billion euro per year of which approximately 46 % is related to ground and space segments and the other 54 % is related to overhead costs [5]. However, realise that this 2.9 billion also includes the redundant inventory for the ISS and EVA costs (1.1 billion Euro) that are not relevant for Delta Mars. Together with around 300 million Euro of extra launch costs for the ISS with respect to Delta Mars, Delta Mars operational costs are estimated at 1.5 billion Euro per year. By this substraction of the redundant costs with respect to the ISS, the annual cost estimate is more specified to this project. The costs are broken down to percentages where for the ground segment those are based on [130], Table 20.11. The launch costs are based on two missions in the period 2040-2050 where 18 Falcon Heavy launches (FY 2019 95 million Euro) are required for the first mission and 9 Falcon Heavy launches for every extra mission. Also, per mission 4 Soyuz launches are required (FY 81 million Euro per launch). Propellant costs for 5 missions include 635 kg Uranium (44,200 Euro) [6], 203.5 t liquid Argon (1.87 euro per liter) and 2,421 kg per mission for fuel for ADCS thrusters (1,000 Euro per kg) [7]. From those costs per mission, the percentage of total operational cost was determined for the periods 2040-2050 (two missions) and 2050-2060 (three missions). The other space segment costs are equally divided as no information was found on that and those are heavily dependent on the required maintenance equipment, spares and astronaut training, which were not defined yet. However, the cost for the frequency spectrum auctions are not unfeasible as those are often sold to parties in terms of billions of Euros[8].

Overhead Costs

The overhead costs are the other 54 % of the yearly estimate of 1.5 billion Euro operational costs for Delta Mars. The cost is broken down to the 20 % ROI dividend that is paid out to the private investors once in 2050, and other project related cost from which the percentage division is based on [130], Table 20.5. A 25 % Corporation tax over the overhead costs is expected when the company remains located in the Netherlands.[9] All these costs are made during the whole 40 year duration as they are all related to daily company components. Regarding the insurance, International Space Brokers (ISB), part of Aon Risk Solutions, is the worlds only insurance broker for high risk space missions. The insure high risk spacecrafts when in orbit and when in laucher by a rate of 0.85 1 % and 5 % respectively of the overhead costs [10]. An insurance of 6 % will be taken (both the in orbit constellation and in launcher), to prevent large losses during failure. Also, by research from Deloitte in 2017, the percentage of marketing and sales in energy and transportation (most suited category) is 4 % of the overhead costs[11].

Learning curve

When a product is produced more often two things can be noted. First, the fixed investment costs are more spread out over the products, and second the effort and therefore cost to produce one object is reduced due to the fact that the workers are more familiar with the task and therefore the process is more and more efficient. However, as this spacecraft is only build once, Delta Mars cannot take advantage on this. The accumulated life cycle costs per category, including the total accumulated costs over 40 years can be found in Figure 15.5. In 2050, the total accumulated costs are 98.5 billion Euro (FY 2050) and in 2060 130.5 billion

[5] https://oig.nasa.gov/docs/IG-14-031.pdf
[6] https://www.wise-uranium.org/nfcch.html
[7] https://ntrs.nasa.gov/archive/nasa/casi.ntrs.nasa.gov/20160005781.pdf
[8] https://en.wikipedia.org/wiki/Spectrum_auction
[9] https://www.belastingdienst.nl/wps/wcm/connect/bldcontentnl/belastingdienst/zakelijk/winst/vennootschapsbelasting/veranderingen-vennootschapsbelasting-2019/tarief
[10] https://www.aon.com/industry-expertise/space.jsp
[11] https://deloitte.wsj.com/cmo/2017/01/24/who-has-the-biggest-marketing-budgets/

Euro (FY 2060), both including 25 % margin.

COST ESTIMATE FOR DELTA MARS OVER 10 YEARS AND 20 YEARS MISSION							
			June 2019	1$ = 0.87 Euro	Inflation per year = 1.5%		
				Period 2019	*Period 2020-2040*	*Period 2040-2050*	*Period 2050-2060*
Category	**Component**	**Part**	**% of category**	**Unit: FY2019 EU**	**Unit: FY2019 EU**	**Unit: FY2019 EU**	**Unit: FY2019 EU**
Development Cost				€ 22.359.910.172,79	€ 30.567.290.316,66	€ 0,00	€ 0,00
	Low TRL systems		34,57%	€ 7.730.288.144,94	€ 10.567.723.608,28	€ 0,00	€ 0,00
		Fundemental Research	8,64%	€ 1.932.567.036,23	€ 2.641.930.902,07	€ 0,00	€ 0,00
		Prototyping and testing	8,64%	€ 1.932.567.036,23	€ 2.641.930.902,07	€ 0,00	€ 0,00
		Research to implement	8,64%	€ 1.932.567.036,23	€ 2.641.930.902,07	€ 0,00	€ 0,00
		V&V procedures	8,64%	€ 1.932.567.036,23	€ 2.641.930.902,07	€ 0,00	€ 0,00
	High TRL systems		15,43%	€ 3.449.686.941,46	€ 4.715.921.550,05	€ 0,00	€ 0,00
		Research to implement	7,71%	€ 1.724.843.470,73	€ 2.357.960.775,03	€ 0,00	€ 0,00
		V&V procedures	7,71%	€ 1.724.843.470,73	€ 2.357.960.775,03	€ 0,00	€ 0,00
	Intergration		50,00%	€ 11.179.955.086,39	€ 15.283.645.158,33	€ 0,00	€ 0,00
		Detailed design	15,00%	€ 3.353.986.525,92	€ 4.585.093.547,50	€ 0,00	€ 0,00
		Detailed drawing	5,00%	€ 1.117.995.508,64	€ 1.528.364.515,83	€ 0,00	€ 0,00
		Prototyping and assembly	5,00%	€ 1.117.995.508,64	€ 1.528.364.515,83	€ 0,00	€ 0,00
		Software	15,00%	€ 3.353.986.525,92	€ 4.585.093.547,50	€ 0,00	€ 0,00
		Design V&V	10,00%	€ 2.235.991.017,28	€ 3.056.729.031,67	€ 0,00	€ 0,00
Production Cost						€ 0,00	€ 0,00
	First unit cost		100,00%	€ 2.908.272.827,93	€ 3.975.777.145,99	€ 0,00	€ 0,00
		Materials / sub-systems	10,00%	€ 290.827.282,79	€ 397.577.714,60	€ 0,00	€ 0,00
		Equipment	30,00%	€ 872.481.848,38	€ 1.192.733.143,80	€ 0,00	€ 0,00
		Facilities	10,00%	€ 290.827.282,79	€ 397.577.714,60	€ 0,00	€ 0,00
		Sub-contractors fee	40,00%	€ 1.163.309.131,17	€ 1.590.310.858,40	€ 0,00	€ 0,00
		Qualification	10,00%	€ 290.827.282,79	€ 397.577.714,60	€ 0,00	€ 0,00
Operational Cost				€ 0,00	€ 0,00	€ 10.161.695.787,50	€ 11.793.062.812,87
	Ground segment		50,00%	€ 0,00	€ 0,00	€ 5.080.847.893,75	€ 5.896.531.406,44
		Facilities	3,00%	€ 0,00	€ 0,00	€ 304.850.873,62	€ 353.791.884,39
		Equipment	13,50%	€ 0,00	€ 0,00	€ 1.371.828.931,31	€ 1.592.063.479,74
		Software	16,50%	€ 0,00	€ 0,00	€ 1.676.679.804,94	€ 1.945.855.364,12
		Logistics	2,50%	€ 0,00	€ 0,00	€ 254.042.394,69	€ 294.826.570,32
		Personnel	14,50%	€ 0,00	€ 0,00	€ 1.473.445.889,19	€ 1.709.994.107,87
	Space segment		50,00%	€ 0,00	€ 0,00	€ 5.080.847.893,75	€ 5.896.531.406,44
		Launches	58,96%	€ 0,00	€ 0,00	€ 5.990.982.386,02	€ 4.937.704.125,56
		Propellants	1,32%	€ 0,00	€ 0,00	€ 133.866.549,09	€ 233.036.392,98
		Astronauts training + equipment	-3,42%	€ 0,00	€ 0,00	-€ 348.000.347,12	-€ 403.868.609,96
		Maintenance and spares	-3,42%	€ 0,00	€ 0,00	-€ 348.000.347,12	-€ 403.868.609,96
		Communication band	-3,42%	€ 0,00	€ 0,00	-€ 348.000.347,12	-€ 403.868.609,96
Overhead Cost				€ 16.200.000.000,00	€ 22.146.336.872,70	€ 11.928.947.228,80	€ 13.844.030.258,59
	Internal costs		59,50%	€ 9.639.000.000,00	€ 13.177.070.439,26	€ 7.097.723.601,14	€ 8.237.198.003,88
		Project management	15,00%	€ 2.430.000.000,00	€ 3.321.950.530,91	€ 1.789.342.084,32	€ 2.076.604.538,79
		Systems engineering	18,00%	€ 2.916.000.000,00	€ 3.986.340.637,09	€ 2.147.210.501,18	€ 2.491.925.446,55
		Administration	5,50%	€ 891.000.000,00	€ 1.218.048.528,00	€ 656.092.097,58	€ 761.421.664,22
		(Post-mission) review	8,00%	€ 1.296.000.000,00	€ 1.771.706.949,82	€ 954.315.778,30	€ 1.107.522.420,69
		Facilities and equipment	13,00%	€ 2.106.000.000,00	€ 2.879.023.793,45	€ 1.550.763.139,74	€ 1.799.723.933,62
	External costs		40,50%	€ 6.561.000.000,00	€ 8.969.266.433,44	€ 4.831.223.627,66	€ 5.606.832.254,73
		Dividend	5,50%	€ 0,00	€ 0,00	€ 4.960.346.772,90	€ 0,00
		Taxes	25,00%	€ 4.050.000.000,00	€ 5.536.584.218,18	€ 2.982.236.807,20	€ 3.461.007.564,65
		Marketing and Sales	6,00%	€ 972.000.000,00	€ 21.526.239.440,266	€ 256.785.374.317,4	€ 3.554.944.492.014.15
		Insurances	4,00%	€ 648.000.000,00	€ 14.350.826.293,511	€ 171.190.249.544,9	€ 2.369.962.994.676.10
Total excl. margin				€ 41.468.183.000,72	€ 56.689.404.335,36	€ 78.780.047.351,65	€ 104.417.140.423,11
Total + 25% margin				€ 51.835.228.750,90	€ 70.861.755.419,19	€ 98.475.059.189,56	€ 130.521.425.528,89

Figure 15.4: Cost Estimation for Delta Mars

15.2. Market analysis

15.2.1. Prediction of current possible markets

Already existing market for creating revenue are the following:

Transport of non-human payload to Mars

The Mars Delta can be used to transport non-human payloads to Mars such as satellites, rovers and scientific instruments. This payload is divided in pressurised and non-pressurised payload. Some payloads need to be pressurised to be able to perform their functions during transit to Mars as computers, which introduces higher costs and thus higher prices for the costumer. In Section 15.3 it is elaborated why one should choose this option instead of an own satellite that travels to Mars.

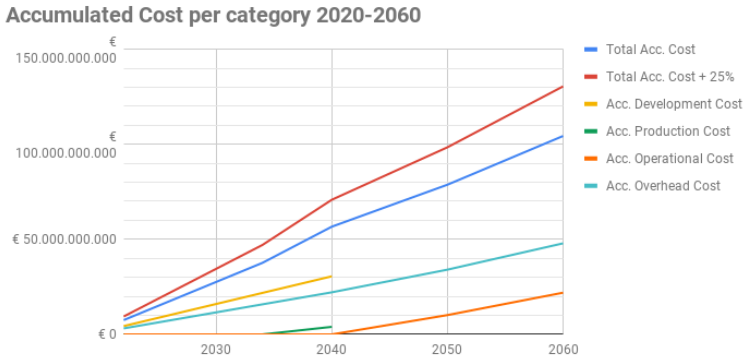

Figure 15.5: Life-cycle cost overview

Documentary

A documentary will be made prior, during and after the Mars mission, including all interesting parts of the mission such as development, launch, transit, orbit and a possible Mars landing.

Television Rights

The selling of television rights is expected to generate 4 billion, comparing this number to the Olympic games in London 2012 this is almost the same, but considering that this mission might include the first ever landing on the Mars surface, the team found this a valid estimation considering all large part the world will be watching (8.5 billions people expected in 2040) [12] .

Private investment funds

Billion dollar investment companies and private equity firms such as KKR, BAIN CAPTIAL, BERKSHIRE, PAI, LONE STAR have managed assets of hundreds of billions and invest in opportunities to make profit so they can become share holder of this mission, with the benefit of receiving a 20 % return of their investment in 10 years by the external cash flows that do not have a share, like the sponsorships. They are only there to give the start capital and do not expect anything other than 20 % ROI in 2050.

Agencies funding

A large part of the generated income comes from the agencies funding, since these agencies achieve a revenue of 9 dollars per every dollar they initially invest in terms of scientific and technological return to society, according to prof. W. Fowler from Cockrell School of Engineering[13]. This Mars mission is special in its way that it is the first manned Mars mission and can provide ground breaking findings about the possibilities of living in deep space and further research topics as the spacecraft also returns to Earth. The investment of these agencies is crucial for the mission.

15.2.2. Establishing of new possible markets

Non-existing markets which will be applicable for the Mars mission are the following:

Space Tourism to Mars

Space tourism was considered an option of generating revenue, however having passengers on board requires a lot of training and preparing. Also the demand for space travel is not that high when the price for a ticket is in the order of billions. This business plan is thus discarded and instead spots on the spacecraft are sold to space agencies.

Maintenance contract of in-orbit satellites

The spacecraft will orbit Mars for more than a year, beforehand contracts can be made in which the Delta Mars will perform maintenance that are close to Delta Mars in terms of orbit

[12] https://stillmed.olympic.org/media/Document%20Library/OlympicOrg/Games/Summer-Games/Games-Rio-2016-Olympic-Games/Media-Guide-for-Rio-2016/IOC-Marketing-Report-Rio-2016.pdf

[13] https://alcalde.texasexes.org/2014/07/exploring-space-is-still-worth-the-cost-says-ut-expert/

altitude. The spacecraft can manoeuvre itself close to a satellite and perform maintenance using the robot arm, which is discussed in Section 11.7.

Remote robot control base building

As payload a robot can be brought to Mars and with a lander vehicle as payload on the first mission, this can be brought down to the Martial surface, from the spacecraft this robot can be operated by one of the astronauts. The revenue that comes from this lies in the prospect of finding out new technological and scientific discoveries or building up a new base on the Martian surface, where Delta Mars offers the platform.

Returning objects

The Martian surface is full of not yet discovered rock types and not known compositions of the soil, from returning Martian objects research can be performed and pieces of rock can be sold to third parties, this is however discarded as this is not allowed by international space law.

Space Sponsorship Programme by Delta Mars

Income is generated from sponsorships of companies that are interested. As an example the brand Coca Cola is proposed which has an investment budget of 4 billion each year [20]. Since the spacecraft will be viewed worldwide this is the ideal way to advert your brand, for this reason it is estimated that half of Coca Cola's budget could be used to sponsor the spacecraft, hence realizing a budget of 20 billion. Coca Cola is a nice example since the modules look like Coca Cola cans, however this is just an example and multiple brands are considered to increase income. Short term (launch-focused) and long term contracts are considered

Scientific research (E.g. Medical)

The spacecraft orbits Mars for over a year, creating options for long term research, for example regarding radiation doses. This is of high value for medical research departments who would invest for the information about this radiation exposure data. As already low dose radiation research by the USA costs 100 million over 4 years, revenue can be made by this as the experiments are way more easy on board a spacecraft that is radiated already[14].

15.2.3. SWOT-analysis

SWOT analysis	
Strengths	Weaknesses
Intellectual capacity	Lack of experience
Networking	Resources
TU Delft specialists support	
Location	
Opportunities	Threats
Funding opportunities	Expensive/scarce materials and equipment
Returning of Martian objects	Limited time
Space tourism	SpaceX competitor
Media attention	Limited reference data
Sponsorships	

Table 15.1: SWOT analysis

The SWOT analysis shows where the teams opportunities and strengths lay and where the team has to be careful with regards to their weaknesses and threats. The internal strengths of the young team of bachelor students are its intellectual capacity, network, support of specialist and the location of where the project is held, however this team of young students has the weakness that they are lacking in experience and resources are limited.

The main opportunities regarding the Mars mission lie in the fact that it is the first manned mission to Mars. This fact generates immense attention for the mission which results in sponsoring, funding and the media attention. Making use of these opportunities results in revenue for television rights, broadcasting of a documentary, sponsorships and investments. External threats are that materials and equipment is scarce and expensive, limited time, SpaceX as a competitor and since this is the first manned mission there is very limited reference data.

[14] https://www.proclinical.com/blogs/2019-3/the-top-10-pharmaceutical-companies-in-the-world-2019

15.3. Return on investment analysis

Requirement

The requirement is that the system can create 20 % return on investment within 10 years of operation. It is not specified which investor is meant by this, so there is freedom to create a Delta Mars business philosophy regarding the division of the 20 % ROI.

15.3.1. Revenue analysis

As only one spacecraft will be build and used, all the earnings have to be made by using this single object and the market volume is therefore very limited. However, as there is currently not a similar concept in terms of mission architecture, Delta Mars still has a monopoly position. Some things still should be discussed regarding the money that can be earned by the external cash flows.

- 15 t of payload, like satellites, can be taken with Delta Mars per mission. It is only interesting for a satellite, rover, lander or other instrument to go with Delta Mars when enough savings are made by choosing for this. Travelling with Delta Mars would decrease the communication system size (Delta Mars used as relay satellite), propulsion system size and especially lower operational cost, which ends up in a 20.3 % savings in cost per kilogram [15]. A cost of 1 million Euro/kg is average for a deep space mission, so per kilogram of payload 203,000 Euro can be asked.
- The best paid documentary earned 120 million Euro [16]. A little bit less is expected for the Delta Mars documentary.
- For the contracts, no resources can be found yet as it is quite new. It is a rough estimate based on the cost related to mission failure (around hundreds of millions) and a 1 % insurance cost for that and for the robot control the money is mainly asked for providing the platform (facility and equipment costs).
- It is expected that 0.001 % (10 million people) of the world population watches the 20 vlogs made. Revenue per 1000 views on YouTube gives 5 Euro from advertisement [17].
- The percentages of the agencies and private investors is determined by making sure the investors can get their ROI of 20 % in 2050 that originates only from external cash flows that do not have a share, like sponsorships. It can therefore be said that the agencies money does not flow as ROI to the private investors.

The income that can be generated is visualised over the period 2020-2050 in Figure 15.6 and Figure 15.7.Note the difference in moment of investment for the different incomes, as those are heavily dependent on the mission starts.

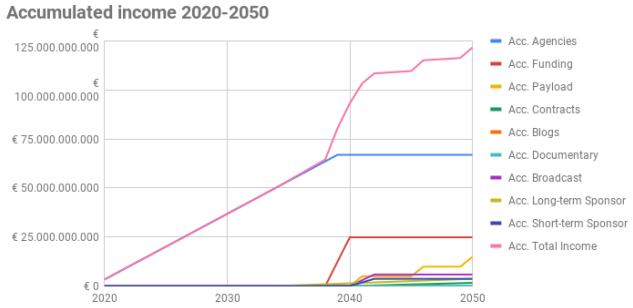

Figure 15.6

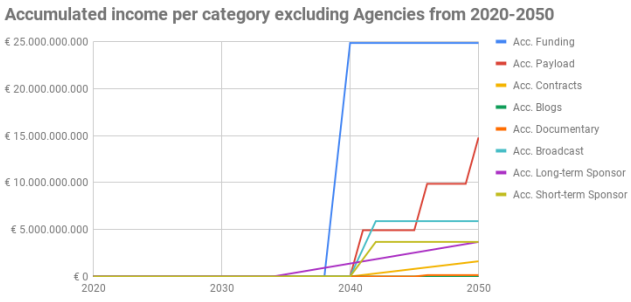

Figure 15.7

15.3.2. Business profile and construction

It can be concluded that only around 25-30 billion Euro can be gathered by external cash flows. A return on investment of 20 % can therefore not be realised over the total invested

[15] https://pdfs.semanticscholar.org/4d21/b8134099d456057af96539533861edfd5401.pdf?_ga=2.182751023.826990487.1560332475-1423830552.1558445443

[16] https://www.thewrap.com/top-grossing-documentaries-box-office/

[17] https://influencermarketinghub.com/how-much-do-youtubers-make/

money of all parties. Therefore, a collaboration is required between private investors and the public domain (agencies). When those to work together, the ROI of 20 % can be given to the private investors and the agencies already expect a return over decades in society that is 9 times higher. To generate a 20 % ROI for the investors, the division of incomes given in Figure 15.8 should be used. The division of the costs over this period is also given Figure 15.9.

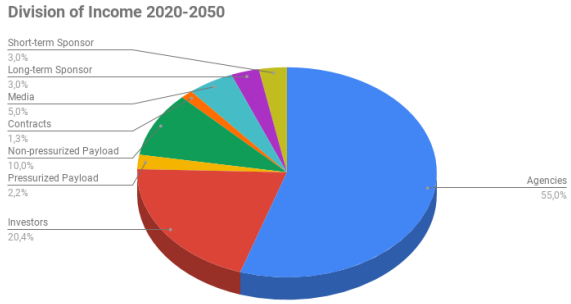

Figure 15.8

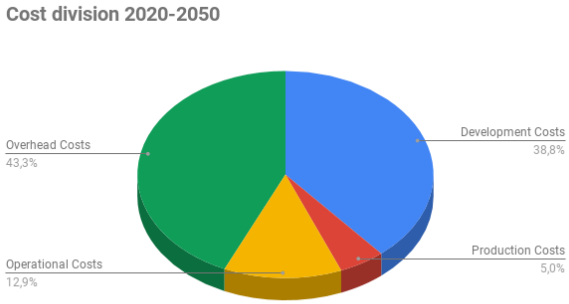

Figure 15.9

15.3.3. Balance

The overall income and expenses can be summarised for the period 2040-2050 in Figure 15.10. The accumulated total cost and total income for the period of 2040-2050 can be visualised by Figure 15.11. One can observe here that there is a constant surplus due to the fact that especially at the beginning, the agencies invest per year a little bit more than the costs. When the first mission occurs, the money of the private investors (FY2039-2040, funding period) other external cash flows make the surplus growing. The income will be lower after this first event, ending up with a decreasing surplus. However, at the end of 2050, the surplus is (after the dividend to the private investors) still 23.13 billion Euro, equal to the money that the investors invested and will be refunded.

INCOME STATEMENT DELTA MARS FOR 10 YEARS AFTER MISSION START

					June 2019	1$ = 0,87 Euro	Inflation per year = 1,5%			
REVENUES						EXPENSES				
			Period: 2019	Period: 2020-2050				Period: 2019	Period: 2020-2040	Period: 2040-2050
Category	Component	% of category	Unit: FY2019 EU	Unit: FY2019 EU		Category	Component	% of category	Unit: FY2019 EU	Unit: FY2019 EU	Unit: FY2019 EU
Funding		100,00%	€ 62.321.577.446,38	€ 91.781.581.305,35		*Development Cost*		100%	€ 22.359.910.172,79	€ 30.567.290.316,66	€ 0,00
	Agencies	72,92%	€ 45.446.941.846,38	€ 66.930.144.567,37			Low TRL systems	34,57%	€ 7.730.268.144,94	€ 10.567.723.608,28	€ 0,00
	Investors	27,08%	€ 16.874.635.600,00	€ 24.851.436.737,98			High TRL systems	15,43%	€ 3.449.686.941,46	€ 4.715.921.550,05	€ 0,00
Payload		100,00%	€ 10.045.062.720,00	€ 14.793.459.641,59			Intergration	50,00%	€ 11.179.955.086,39	€ 15.283.645.158,33	€ 0,00
	Pressurized	18,18%	€ 1.826.375.040,00	€ 2.689.719.934,83		*Production Cost*		100,00%	€ 2.908.272.827,93	€ 3.975.777.145,99	€ 0,00
	Non-pressurized	81,82%	€ 8.218.687.680,00	€ 12.103.739.706,75			First unit cost	100,00%	€ 2.908.272.827,93	€ 3.975.777.145,99	€ 0,00
Contracts		100,00%	€ 1.100.000.000,00	€ 1.619.980.487,86		*Operational Cost*		100,00%	€ 0,00	€ 0,00	€ 10.161.695.787,50
	Maintenance	9,09%	€ 100.000.000,00	€ 147.270.953,44			Ground segment	50,00%	€ 0,00	€ 0,00	€ 5.080.847.893,75
	Robot control	90,91%	€ 1.000.000.000,00	€ 1.472.709.534,42			Space segment	50,00%	€ 0,00	€ 0,00	€ 5.080.847.893,75
Media		100,00%	€ 4.104.500.000,00	€ 6.044.736.284,03		*Overhead Cost*		100,00%	€ 16.200.000.000,00	€ 22.146.336.872,70	€ 11.928.947.228,80
	Blogs	0,11%	€ 4.500.000,00	€ 6.627.192,90			Internal costs	60,00%	€ 9.639.000.000,00	€ 13.177.070.439,26	€ 7.097.723.601,14
	Documentary	2,44%	€ 100.000.000,00	€ 147.270.953,44			External costs (excl. dividend)	34,55%	€ 6.561.000.000,00	€ 8.969.266.433,44	-€ 129.123.145,24
	Broadcast rights	97,45%	€ 4.000.000.000,00	€ 5.890.838.137,68			Dividend investors	5,45%	€ 0,00	€ 0,00	€ 4.960.346.772,90
Sponsorships		100,00%	€ 5.000.000.000,00	€ 7.363.547.672,10		*Previous made cost*		100%			€ 56.689.404.335,36
	Long-term	50,00%	€ 2.500.000.000,00	€ 3.681.773.836,05			Before 2040	100%			€ 56.689.404.335,36
	Short-term	50,00%	€ 2.500.000.000,00	€ 3.681.773.836,05							
Total before Extra's			€ 82.571.140.166,38	€ 121.603.305.390,92						€ 56.689.404.335,36	€ 78.780.047.351,65
Total before Extra's + 25%											€ 98.475.059.189,56
Delta before Extra's				€ 23.128.246.201,36							
Extra						*Dividend DSE 14*					
							0,2% of profit				€ 59.643.448,17
						Refund					
							Investors				€ 23.068.602.753,19
Delta after Extra's				€ 0,00							€ 0,00

Figure 15.10: Income Statement Delta Mars

15.4. Business Risk

15.4.1. Risks

The main risks concerning the business plan are the following:

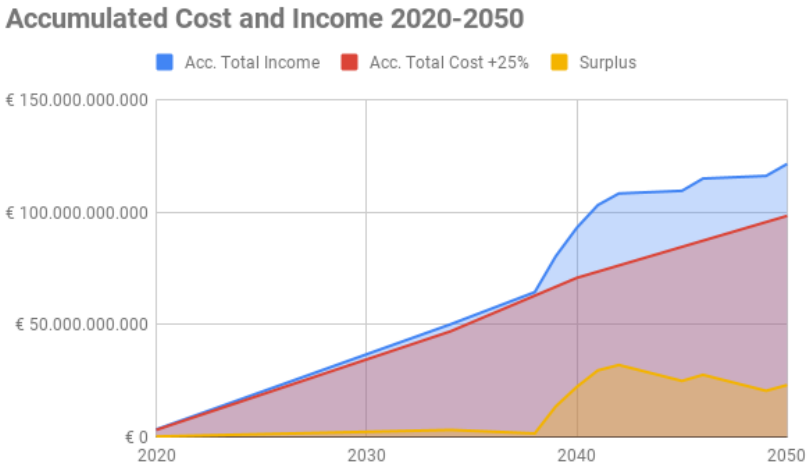

Figure 15.11

- Inflation and euro conversion changes.
- Loss of interest from politics, public, sponsors, agencies, investors and companies.
- Geopolitical or sponsor conflicts.
- Distrust of sponsors and investors
- Incapable crew for documentary.
- Watching TV becomes outdated.
- Insufficient demand for payload.
- Failure of data for research investors.
- Higher cost than expected.

15.4.2. Mitigation

The cost estimation includes a 25 % margin to cope with the inflation, conversion and the risk of higher costs than expected. Also, billions are spent on the marketing, with the main attention drawer of being the pioneers in a manned orbit around Mars, with a successful mission worldwide interest will be guaranteed. Since the manned crew will be orbiting Mars, bringing payload becomes much more interesting. The payload that is brought there can be controlled by the crew, creating more possibilities for scientific research.The crew should be trained in making a documentary to guarantee a quality documentary and multiple platforms of providing this media should be considered since TV might become outdated.

16

System Integration and Analysis

This chapter describes the integration of the subsystems and mission elements described up to this point, and the top-level system is analysed. To test the robustness of the design, a sensitivity analysis is performed, and the expandability of the system is discussed. The RAMS (Reliability, Availability, Maintenance & Safety) aspects of the system and it functions are analysed, and finally the compliance of the system to the requirements is tested.

16.1. Iterations

After the preliminary sizing of the system in the Midterm report[126], two iterations have been performed. In each iteration, the design became more detailed, and the budgets were revised. Next to this, the dry mass contingency was reduced due to increasingly accurate mass estimates, from 20 % in the preliminary design to 10 % in the current iteration.

During the first iteration, the design changed significantly compared to the preliminary design. It was found that the required radiator surface dominates the layout of the spacecraft, and that the habitat modules needed to be significantly larger due to the long mission duration following from using low-thrust propulsion. This and other subsystem research results were integrated into a new design, forming the first iteration of the system.

An important finding was that due to optimisation of the trajectory, the required Thrust-to-Weight ratio could be lowered. This meant that the amount of reactors could be reduced from 5 to 4, as long as the dry mass excluding propulsion modules was kept below 130 t. This lead to a direct reduction in the dry mass, in addition to an indirect reduction, as the radiators could be reduced in size now that there was less heat to dissipate. This redesign started the second iteration.

The dry mass (excluding propulsion modules) of 130 t became a new target in the mass budget of the second iteration. Furthermore, sizing and optimising of the radiators became a high priority to reduce the dry mass further. Analysing the trajectory and the functionality of other subsystems, it was found that it is possible to keep the radiators tangent to the Sun at all times, while they were initially sized taking solar influx into account. This reduced the radiator size further. Finally, as described in the design N2-chart of Section 4.2, the ADCS was sized now that an estimate could be made of the Mass Moment of Inertia. Integrating the results of all subsystem research again, resulted in the design presented in this chapter.

16.2. System characteristics

An overview of the system and mission characteristics, at the time of the last iteration performed, are shown in Table 16.1. Final technical drawings are shown in Appendix B.

16.3. Sensitivity Analysis

The sensitivity of all subsystems has already been discussed in the previous chapters; here, the most important ones that have impact on a system level, and several sensitive system requirements are discussed.

16.3.1. Critical subsystem assumptions and dependencies

First of all, an overview is given of sensitivity analysis of the subsystems which have a large impact on the system design:

- The whole system is most sensitive to the design and assumptions originating from the Propulsion and Power systems. The VASIMR engine has been assumed to be operational by 2040, from which flowed the large electrical power requirement and thus the choice for nuclear reactors. If this assumption turns out to be incorrect, the current design becomes unfeasible. The same holds for the Closed-Cycle Magneto-Hydrodynamic Generators: the design is largely based on their future existence. Thirdly, Zero-Boil Off cryocoolers are assumed to be fully developed, which for long-duration missions was

System characteristics		Mission characteristics	
Wet Mass	399.2 t		
Dry Mass	180.7 t	Astronauts (baseline)	4
Payload Mass	15 t	Mission duration	1148 days
Length	65 m	Mars stay	520 days
Width	41 m	First scheduled launch	2041
Height	6 m	Earth orbit altitude	950 km
$MMOI_x$	5 Mkgm^2	Earth orbit decay time	200 year
$MMOI_y/z$	110 Mkgm^2	Earth orbit period	1h 44m
Habitable volume	100 m^3	Mars orbit altitude	400 km
Pressurised volume	260 m^3	Mars orbit decay rate	Undefined
Engine	VASIMR	Mars orbit period	1h 58m
Propellant	Liquid Argon	Launcher	Falcon family
Thrust	278.4 N	No. of initial launches	17
ΔV	35.2 km/s	No. of resupply launches	9
Thermal Power	20 MW$_{th}$	Expected received radiation	1300 mSv
Electrical Power	11 MW$_e$		
Backup Power	10 kW$_e$		
Data rate	5 Mbit/s		
Transmitting power	800 W		
Memory size	500 GB		

Table 16.1: Overall spacecraft characteristics

found to be of critical importance. With current boil-off rates in cryogenic tanks, the wet mass of the spacecraft could as much as double, which impacts all subsystems.

- As Chapter 10 showed, the design will also strongly change if the equilibrium temperature of the radiators is lowered. A reduction from 350 to 250 ^oC requires a radiator area and mass increase of up to 100 % compared to the current design. This would result in a significant redesign, and would require more research to determine its feasibility.
- On the operational level, the feasibility of the Space Tug will impact the design of the other modules. If the space tug is infeasible, each module will require the incorporation its own ADCS and propulsion system in order to allow autonomous orbital assembly .
- A change of launch capabilities would also result in drastically altered assembly plan or even design, either due to a change in launcher or in assembly and parking orbit. The habitat modules are sized to fit exactly into the Falcon payload fairing, so a reduction in fairing diameter would mean a redesign of these modules. Furthermore, a reduction in mass capabilities would increase the number of tanks required, and thus change the layout of the feedsystem.

16.3.2. System level changes

While the system is currently designed for a dry mass contingency of 10 %, the sensitivity analysis of various subsystems (especially ECLSS and Electronics) showed that the dry mass could increase more than this. Calculations show that as long as the dry mass does not increase more than 20 %, the design changes relatively little. For a larger increase, a fifth reactor is required to provide power to the additional engines, which starts a snowball effect in the mass by also requiring more heat to be radiated. As will be explained in the next section, adding this reactor does not make the design infeasible, but does change it significantly.

An important system requirement that would change the overall mission is SYS-15: *The human occupants of the system shall have a maximum exposure of 1500 mSv per mission.* As at this stage, long-term low-dose radiation effects on humans are still not fully understood, this requirement could become more stringent. As discussed in Chapter 11, increasing the shielding slightly more will rapidly increase the habitat module mass. At the same time, much shorter mission durations are unfeasible as shown in Chapter 6, due to the long Mars stay required to wait for the next transfer window. This leads to the conclusion that, in order to fulfil more stringent radiation requirements, other options must be considered such as:

- A descent to Mars surface, where the astronauts are shielded by both the planet and the limited atmosphere
- Physiological solutions that can mitigate the damage caused by the radiation
- Active shielding using electromagnetic fields

All of these options require more research, meaning the mission concept is still very sensitive to a reduction in acceptable radiation levels.

16.4. Expandability

As specified in System Requirement 5, the system shall be expandable with further modules. While this report is focused on designing the baseline for four astronauts, preliminary sizing has been performed for extended configurations using the methods described in Section 4.3. Habitat modules can be added both in length direction as well as on the side. As first example, a fourth module of 25 t is added, which could accommodate two additional astronauts. This would increase the dry mass to beyond the point where 5 reactors are required, meaning 12 t of engines and reactors is added. Furthermore, 5.3 t of radiators has to be added, as well as 47 t of propellant and tanks. This means a total increase of 85 t in wet mass for adding one module. For comparison, adding yet another habitat module would increase the wet mass by only 60 t, half of which is propellant.

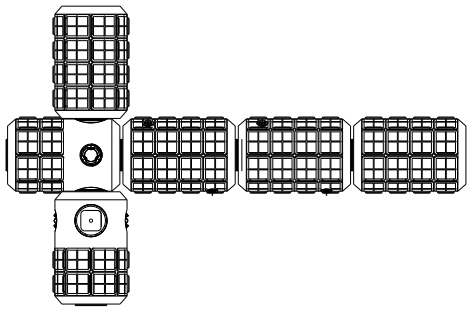

Figure 16.1: Example on the expandibility of habitat modules

In general, adding additional or different habitat modules is relatively simple, because of the standard docking ports. Adding additional reactors and tanks is more complicated, but still feasible. Adding additional radiators will be the most challenging part of expanding the spacecraft, as either trusses have to be added in between the existing trusses and the habitat modules, or the radiators need to be extended. The extended configurations will require more research in future design phases, and their own detailed mass and power breakdowns.

16.5. RAMS characteristics

In this subsection the RAMS characteristics of the design are evaluated. Realise that after the detailed design, this RAMS analysis can be updated and elaborated with more accurate values and conclusions as more is known about the characteristics of the mission.

The **Reliability** of the spacecraft and the whole mission architecture is analysed, and shown in Figure 16.2. The total launcher reliability is the multiplication of the Falcon and Soyuz reliability. Two references are used, one based on statistical analysis (S/C) [56] and one based on general ISS failures (General ISS) [77]. The reliability is for a certain period of time or amount of launches. This time indication is also given. For the series reliability, all the subsystems are multiplied which each other. The mission reliability is a result of the multiplication of the Total S/C or Total General ISS with the Total Launchers. For the full redundancy, every element is included twice, resulting in a reliability per part of $1-(1-SeriesReliability)$. This would actually result in an over-designed and significantly heavier spacecraft. For the partial redundancies, the three parts of the S/C with the largest percentage of origin for spacecraft failure are chosen to include redundancies. For the General ISS the electronics and electromechanical parts, as these are not that heavy and can be included easily. These are indicated by an orange box. For the others, the reliability of the series reliability is again used.

Availability outlines the percentage of time the spacecraft is operational in its 20 year life cycle. Availability can therefore give a clear insight in the turn-around time of the vehicle, but also the time needed to supply the vehicle before it can head back to Mars. Furthermore, availability will help to prospect potential earnings and will further specify possibilities in the business case and other financial manners. As the primary target of the mission is to bring astronauts in Mars orbit with the transfer vehicle, the vehicle is said to be operational

System	Part	% Of failure	Series Reliability	Full Redundancy	Partial Redundancy
Launcher					
	Falcon Family (2011-2019,#69)		0,97100	0,97100	0,97100
	Soyuz (1966-2019, #1700)		0,97400	0,97400	0,97400
Total Launchers			0,94575	0,94575	0,94575
S/C (15 years)					
	TTC	16	0,98200	0,99968	0,99968
	GNC	6	0,99370	0,99996	0,99370
	Battery	12	0,98500	0,99978	0,99978
	Electrical distribution	9	0,99150	0,99993	0,99150
	Power source	10	0,98850	0,99987	0,98850
	Propulsion	11	0,98900	0,99988	0,98900
	Structures + Thermal	7	0,99480	0,99997	0,99480
	ECLSS (ISS 1000 days mission)	5,5	0,98000	0,99960	0,98000
	Payload + Data Handling	3,5	0,99650	0,99999	0,99650
	ADCS	20	0,97900	0,99956	0,99956
Total S/C (15 years)			0,88612	0,99821	0,93482
Mission (15 years)			0,83805	0,94406	0,88411
General ISS (6 months)					
	Electronics		0,99400	0,99996	0,99996
	Electrical		0,99300	0,99995	0,99300
	Electro-Mechnical		0,97500	0,99938	0,99938
	Mechanical		0,97200	0,99922	0,97200
Total General ISS (6 months)			0,93542	0,99851	0,96456
Mission General ISS (6 months)			0,88468	0,94434	0,91223

Figure 16.2: Preliminary reliability analysis [56][77]

when astronauts are on board, so from the moment the astronauts board to the moment they undock and re-enter Earth atmosphere. To put that in numbers, the total mission duration, that is from LEO to Mars and back to LEO, will be 1,080 days. It can be found that the total time that astronauts will be on-board the passenger spacecraft will be roughly 980 days. After the mission to Mars the spacecraft has to be resupplied with food, breathables, water and propellant during which the spacecraft will remain in LEO. The resupply of the spacecraft approximately takes 150 days. This can easily fit in the time that the spacecraft spends in LEO according to the launchdates described in Chapter 6, resulting in a total turnaround time of approximately 1,250 days. Out of which the spacecraft will be operational around 980 days, approximately 78.4 % of the time.

Maintainability outlines the vehicle's maintenance capacity. First of all the level of detail in which the ship can be maintained is important to note. During the transfer to and stay at Mars, minor flaws and repairs can be taken care of by either the system or the astronauts. Major repairs, such as replacing an entire module or repairing a significant component, shall be taken care of in LEO as the spacecraft can receive the necessary parts and equipment from the Earth. Because the spacecraft will spiral out of LEO when departing and spiral in upon arrival without the astronauts on-board, the maintainability of this mission phase concerning smaller repairs and other failures is limited. The larger repairs and replacements necessary can only be done during its resupply time in LEO. In percentages, minor repairs and failures can be taken care of 90.7 % of the time during the mission whereas the major repairs and possible replacements can be made approximately 12 % of the time.

Regarding **Safety**: As always during the design phase of aerospace structures, safety margins are included to cope with uncertainties. For safety, and also to some extent reliability of the overall spacecraft redundancies are included. During production, modules, other structural components, and important life sustaining devices will be elaborately tested to check if they comply with the predetermined safety margins. The safety margins for aerospace engineering are used by space agencies such as NASA and ESA. For example the same safety protocols that hold for NASA will be used. These are the NPD 8700.1E "Crew, Health and Safety" protocol and the NPR 8715.3 "General Safety Program Requirements" protocol that will focus on the successful mission continuation [38]. The safety will be built in by the use of risk mitigation and the resulting necessary redundancies. Safety is guaranteed, to some extent, for either the mission duration (fail safe) or the entire lifetime of the spacecraft (safe life).

16.6. Functional Analysis

The Functional Flow Diagram is shown in Figure 16.3, depicting the different functions the system has to fulfil during the entire mission. The upper row shows the top-level functions, while the middle and bottom row show a more detailed breakdown of these functions, in chronological order. The Functional Breakdown Structure, shown in Figure 16.5, shows the same functions, but ordered by function instead of in time.

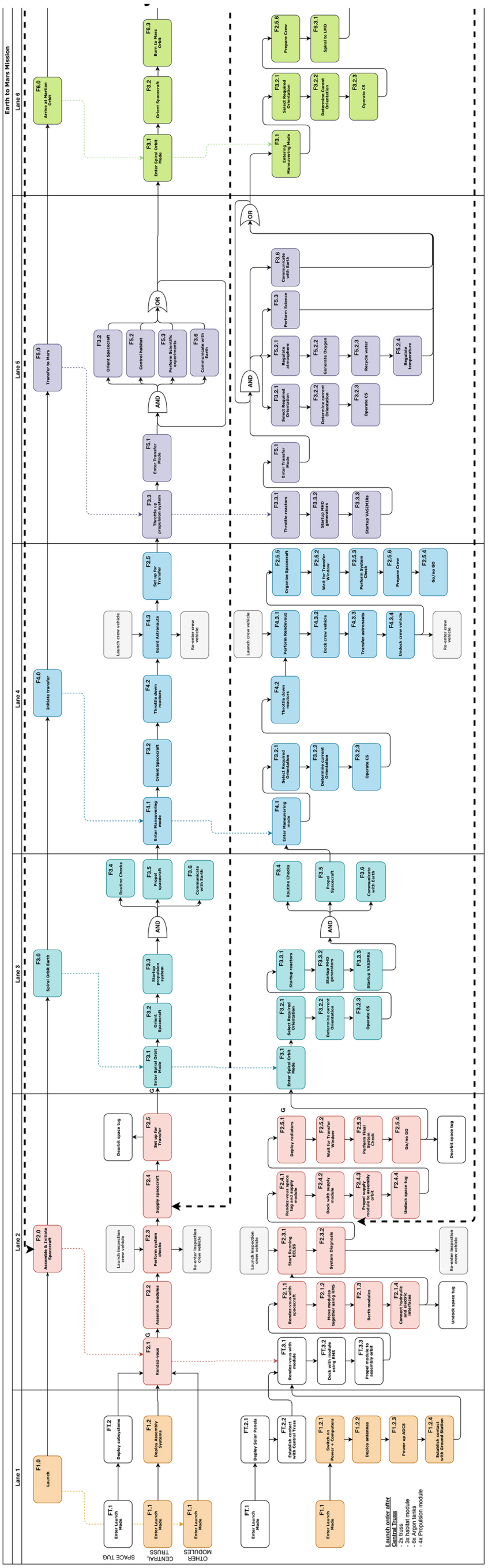

Figure 16.3: The Functional Flow Diagram for the Delta Mars mission

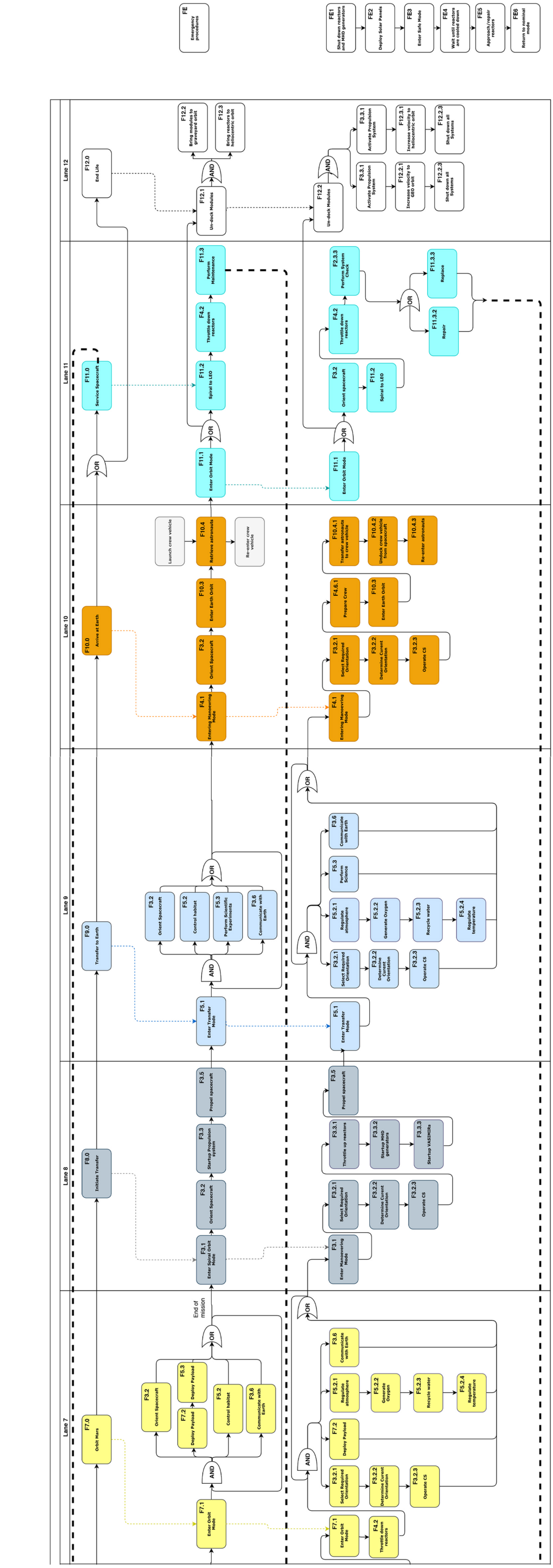

Figure 16.4: The Functional Flow Diagram for the Delta Mars mission (Continued)

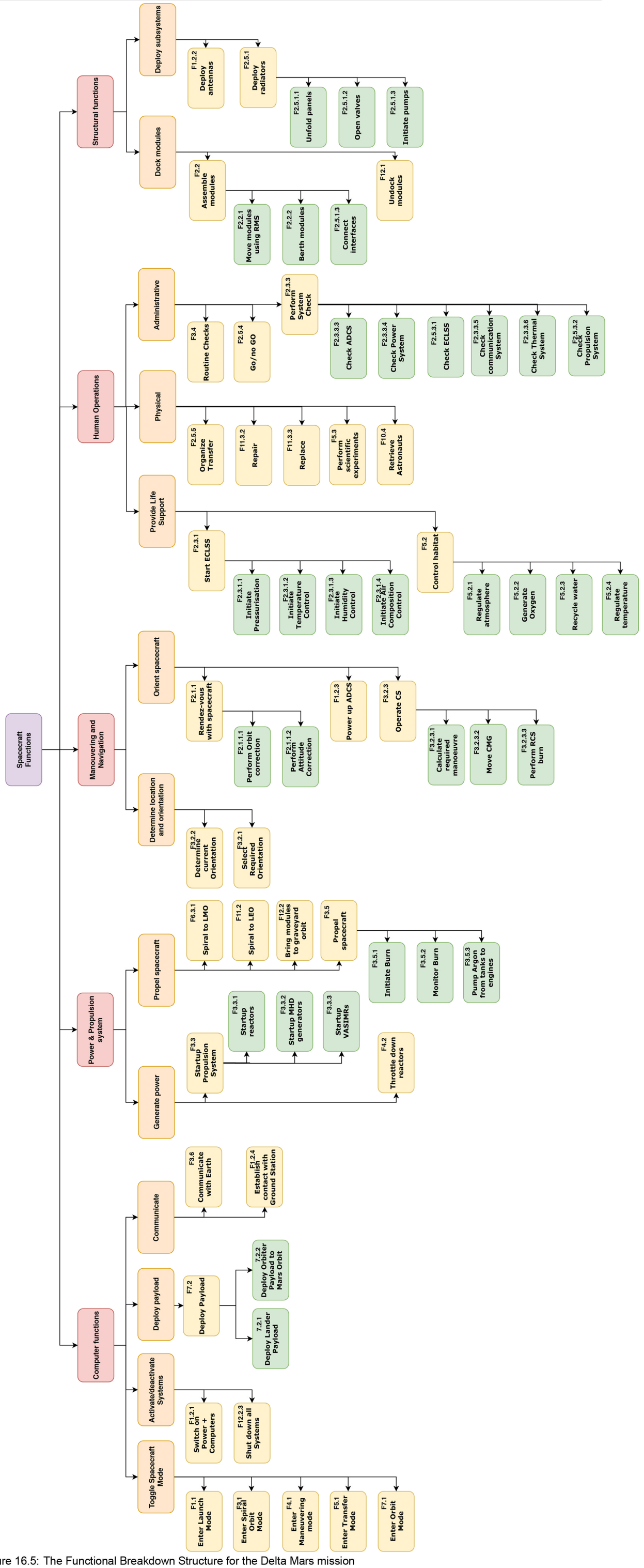

Figure 16.5: The Functional Breakdown Structure for the Delta Mars mission

16.7. N2 chart

To identify the most important interfaces between subsystems, a technical N2 chart has been set up. Unlike the design N2 chart presented earlier, the order of systems on the diagonal do not have a specific order, and the interfaces mentioned below the diagonal to not represent feedback.

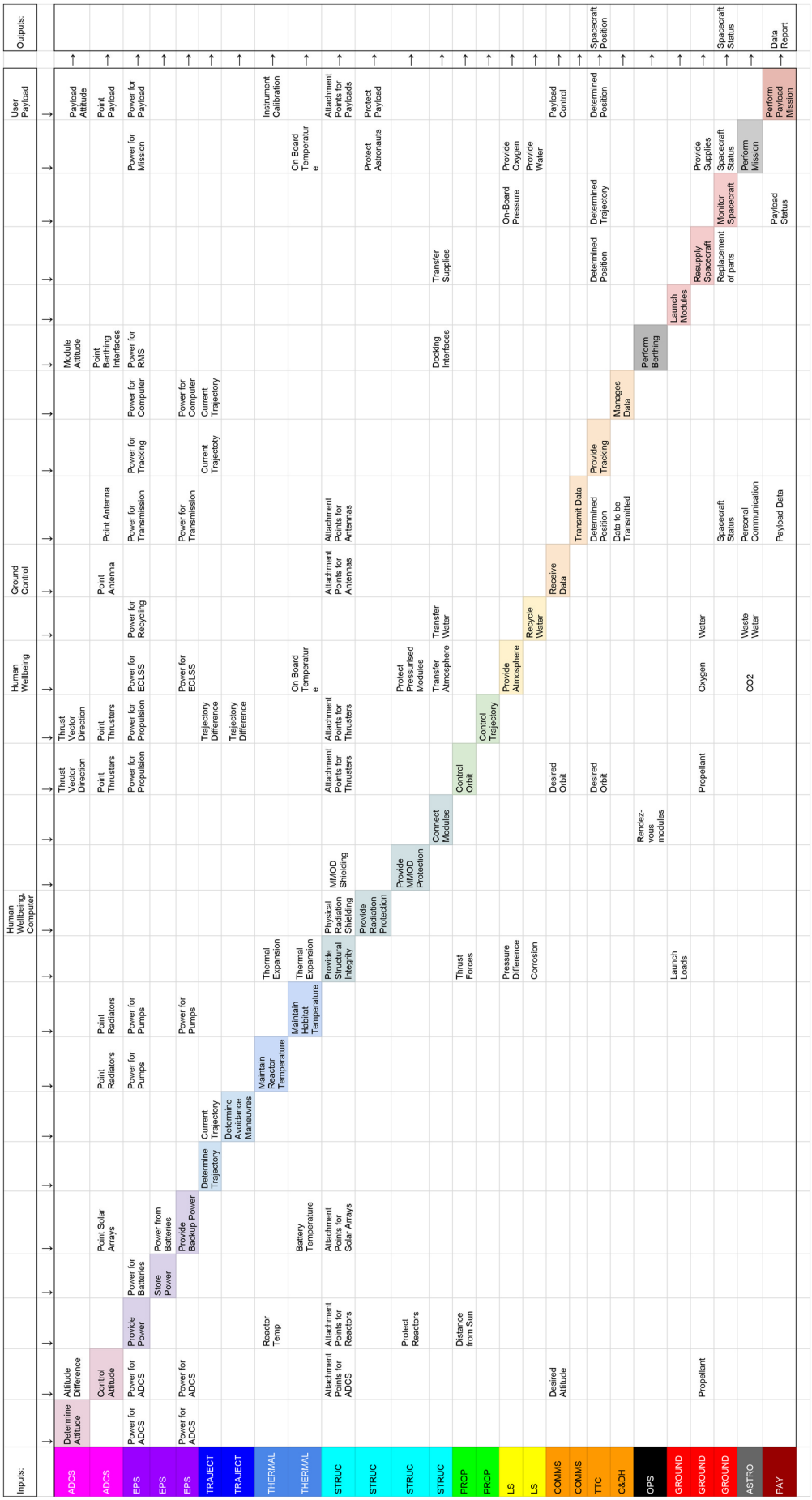

Figure 16.6: The technical N2 chart, describing interfaces between the subsystems

16.8. Compliance Matrix

In the matrix below, compliance to all requirements identified in the Baseline Report[90] is discussed. Green means that for this stage of the design, the requirement is being met, while red means it is already certain is will not be met. Yellow means it is either uncertain or the requirement needs modification due to new insights since the Baseline Reports. Furthermore, verification methods are mentioned for the system requirements. I, A, D and T stand for Inspection, Analysis, Demonstration and Test respectively.

It also needs to be noted that many more requirements can be conceived now that the subsystems have been researched and designed in more detail. The list of requirements in the compliance matrix has not been extended with these new requirements, but focus has been put on analysing the system and top-level subsystem requirements.

16.8.1. System requirements

Identifier	Requirement	Comment	Verification method
SYS-01	The system shall have the capability of transferring at least 4 astronauts to Mars orbit and back.		I of layout
SYS-02	The system shall put humans in Mars orbit before 2040	Moved to 2041 due to launch windows	
SYS-03	The system shall have the capability to stay in Mars orbits for at least 2 Earth weeks.	Designed for a 1.5 year Mars stay	A of mission profile
SYS-04	The system shall consist of interchangeable modules.	Modules contain standard docking ports	D of multiple configurations
SYS-05	The system shall be expandable with further modules.		D of multiple configurations
SYS-06	Each module of the system shall be able to autonomously rendezvous and dock in orbit.	1	T in practice mission
SYS-07	The system shall have the capability of transferring 12 astronauts to Mars and back using additional modules.	No detailed design yet	A of mission profile
SYS-08	Each module of the spacecraft shall have a service life of at least 20 years		A of design
SYS-09	The system shall be launched using one existing launcher family.	Design to launch on the Falcon	I of design
SYS-10	The system shall have the capability of being resupplied for a new mission to Mars		A of mission profile
SYS-11	The system shall maintain environmental conditions to within the same bounds as the International Space Station.	ECLSS based on ISS	A of design, T on ground
SYS-12	The system shall have a window.	Dockable cupola	I of design
SYS-15	The human occupants of the system shall have a maximum exposure of 1500 mSv per mission	Worst case of 1300 mSv with current shielding	A of mission profile
SYS-16	At least half of the system volume shall be reserved for payload.	2	I of design
SYS-17	The system shall generate at least 20% return on investment over a 10 year window after start of operations	For private investors	A of business model
SYS-18	The cost to launch payload to Mars orbit using the system shall be less than 2 m Euro/kg	Business model uses 2 m Euro/kg	A of business model
SYS-19	Each subsystem shall be dual modular redundant.		I of design
SYS-20	All materials onboard of the systems shall comply with REACH regulations.		I of design
SYS-21	All electronic components shall comply with RoHS regulations		I of design
SYS-22	The system shall create no orbital debris at nominal end-of-mission	3	A of mission profile
SYS-23	The system design process shall be documented for continuation missions		-

1. Autonomous rendez-vous and docking is debatable in the current design. The spacecraft still assembles autonomously, however, each module requires the space tug to berth with the spacecraft. Next to this, while the arm is able to perform simple repairs, it is deemed infeasible to not perform any human checks once the spacecraft has been assembled, due to the many electric and hydraulic connections between all modules.
2. The ”volume” is taken as the pressurised volume of the habitat modules, 260 m^3. Inside the modules, there is still 80 m^3 available for scientific instruments, which can be extended to $130 m^2$ with the 15 t reserved for external payloads docked to the outside of the spacecraft, as explained in Chapter 13.
3. Designed to de-orbit valuable modules, bring the others in a graveyard orbit, and send the reactors on a heliocentric trajectory.

16.8.2. Attitude Determination & Control System

Identifier	Requirement	Comment
ADCS-01	The ADCS of each module shall be capable of detumbling from <tbd> deg/s to <tbd> deg/s in <tbd> time	
ADCS-02	The ADCS of the assembled spacecraft shall be capable of detumbling from <tbd> deg/s to <tbd> deg/s in <tbd> time	
ADCS-03	The ADCS shall perform nominally for <tbd> years with <tbd> % reliability	Currently unquantifiable
ADCS-04	The ADCS shall not exceed a mass of 2800 kg	Updated for new budget
ADCS-05	The ADCS shall have an average power usage of 500 W	Updated for new budget
ADCS-06	The ADCS shall have a peak power usage of 1000 W	Updated for new budget
ADCS-POINT-01	The ADCS of each module shall provide a pointing accuracy of 0.01 deg per axis	No AC in each module anymore
ADCS-POINT-02	The ADCS of the assembled spacecraft shall provide a pointing accuracy of 0.01 deg per axis	
ADCS-STAB-01	The ADCS of each module shall limit jitter to less than 1 deg/s per axis	Unclear
ADCS-STAB-02	The ADCS of the assembled spacecraft shall limit jitter to less than 1 deg/s per axis	Unclear
ADCS-SLEW-01	The ADCS of each module shall provide a slew rate of 0.5 deg/s per axis	Required slew rate decreased
ADCS-SLEW-02	The ADCS of the assembled spacecraft shall provide a slew rate of 0.5 deg/s per axis	Required slew rate decreased
ADCS-DETR-01	The ADCS of each module shall be capable of coarse attitude determination to an accuracy of <tbd> deg while rotating at a rate less than <tbd> deg/s	
ADCS-DETR-02	The ADCS of the assembled spacecraft shall be capable of coarse attitude determination to an accuracy of <tbd> deg while rotating at a rate less than <tbd> deg/s	
ADCS-DETR-03	The ADCS of each module shall be capable of fine attitude determination to an accuracy of <tbd> deg while rotating at a rate less than <tbd> deg/s	
ADCS-DETR-04	The ADCS of the assembled spacecraft shall be capable of fine attitude determination to an accuracy of <tbd> deg while rotating at a rate less than <tbd> deg/s	
ADCS-SAFE-01	The ADCS shall maintain a pointing accuracy of TBD degrees per axis in Safe Mode	Not yet designed for
ADCS-DOCK	The ADCS of each module shall be able to perform autonomous docking operations	Together with space tug
ADCS-REL-01	External parts of the ADCS shall withstand an average radiation of 10 mGy/day	Not yet designed for
ADCS-REL-02	External parts of the ADCS shall withstand a total irradiation of 20 Gy over 20 years	Not yet designed for
ADCS-REL-03	The ADCS shall have no single points of failure	Redundant CGM and thrusters
ADCS-REL-04	The ADCS shall remain nominally operational within a temperature range of <tbd> K	Unspecified at this stage

16.8.3. Electrical Power System

Identifier	Requirement	Comment
EPS-01	The main power system shall be capable of providing 10 MWe for 5 months at any given moment	Updated for current budget
EPS-02	The main power system dry mass shall be at most 25000 kg including redundancies.	Updated for current budget
EPS-03	The EPS shall provide an average power of 10 MWe	Updated for current budget
EPS-04	The EPS shall provide a peak power of 10.5 MWe	Updated for current budget
EPS-05	The backup power system shall be at most 3000 kg including redundancies.	Updated for current budget
EPS-06	The backup power system shall provide an average power of 9 kWe	Updated for current budget
EPS-07	The backup power system shall provide a peak power of 10 kWe	Updated for current budget
EPS-DIST-01	The EPS shall be capable of supporting all subsystems that need to be turned on at the same time	Specified by power budgets
EPS-DIST-02	The EPS shall be able to turn on and off all subsystems.	
EPS-DIST-03	The EPS shall have a back-up generator for life critical systems	
EPS-STORE-01	The main EPS shall have a min capacity of 21 kWh.	Updated from new calculations
EPS-STORE-02	Each module shall have 1 kW power available for autonomous docking	No, space tug will have its own power supply
EPS-STORE-03	Each module shall be rechargeable at a rate of <tbd>.	Not specified yet
EPS-STORE-04	EPS Storage shall be accessible and replaceable	Not specified yet
EPS-STORE-05	EPS Storage shall have a safety factor of 10%	
EPS-STORE-06	EPS Storage shall have a life of at least 20 years	No, radiation degrades the batteries
EPS-GEN-01	The EPS Generators shall have an efficiency of 20%	More efficient solar panels are available
EPS-GEN-02	EPS Generator shall have a safety factor of 10%	
EPS-GEN-03	EPS Generator shall have a life of at least 20 years.	Both reactors and solar panels
EPS-REL-01	The EPS shall withstand a radiation of 10 mGy/day	Designed for degradation
EPS-REL-02	The EPS shall withstand a total irradiation of 20 Gy over 20 years	Designed for degradation
EPS-REL-03	The EPS shall have no single points of failure	Multiple reactors and PMADs
EPS-REL-04	The EPS batteries shall remain nominally operational within a temperature range of -20-40 K	

16.8.4. Tracking, Telemetry & Command

Identifier	Requirement	Comment
TTC-01	The system shall provide for a live feed of performance data from the system	
TTC-02	The system shall be able to provide telemetry during all mission phases	Except for conjuntions
TTC-03	The system shall be able to provide location data during all mission phases	
TTC-04	The system shall relay all commands to the relevant subsystems	
TTC-05	All electronic components of the telemetry subsystem shall comply with RoHS regulations	
TTC-06	The system data shall store backup data	Enough memory available
TTC-07	The TTC shall not exceed a mass of 200 kg	Only C&DH on-board
TTC-08	The TTC shall have an average power usage of <tbd> W	Irrelevant for TTC on ground, scrapped
TTC-09	The TTC shall have a peak power usage of <tbd> W	Irrelevant for TTC on ground, scrapped
TTC-DL-01	The system shall be able to handle command, telemetry and tracking data simultaneously	
TTC-DL-02	The system shall use pseudo-random noise modulation	Changed from encryption
TTC-TRACK-01	Tracking of the spacecraft shall be provided during the entire lifetime of the system starting with launch	Not designed for yet
TTC-TRACK-02	The system shall determine the spacecraft location with an accuracy of 0.1 m in Earth orbit	Not designed for yet
TTC-TRACK-03	The system shall determine the spacecraft location with an accuracy of 1.0 m in Mars orbit	Not designed for yet
TTC-TRACK-04	The system shall provide measurements of vibrations within the spacecraft with a reliability of <tbd> %	Not designed for yet

16.8.5. Thermal Control

During the baseline report, the decision to use Nuclear-Electric Propulsion was not made yet, which strongly impacted the scope of the thermal control system. This means the requirements are outdated and incomplete, and need to be extended upon in next design phases.

Identifier	Requirement	Comment
THERMAL-01	Thermal control system shall sustain proper temperature for equipment fuction	Requires specifications
THERMAL-02	Thermal control system shall function for at least 3 years before maintenance	Áccording to current redundancy measures
THERMAL-03	Thermal control system shall have a backup for reactor-off scenarios	Updated
THERMAL-04	The thermal control system shall not exceed a mass of 20000 kg	Updated for current budgets
THERMAL-05	The thermal control system shall have an average power usage of 250 kWe	Updated for current budgets
THERMAL-06	The thermal control system shall have a peak power usage of 240 kWe	Updated for current budgets
THERMAL-DIST-01	Thermal control system shall make sure electrical systems are kept cool	Requires specifications, but met so far
THERMAL-DIST-02	Thermal control system shall ensure the EPS system has no malfunctions	Requires specifications, but met so far
THERMAL-DIST-03	Thermal control system shall ensure the life support system has no malfunctions	Requires specifications, but met so far
THERMAL-DIST-04	Thermal control system shall ensure the modules function properly	Requires specifications, but met so far
THERMAL-DIST-05	Thermal control system shall ensure the computer systems do not overheat	Requires specifications, but met so far
THERMAL-DIST-06	Thermal control system shall ensure the structures do not overheat or get too cold	Requires specifications, but met so far
THERMAL-DIST-07	Thermal control system shall ensure the internal atmosphere has a temperature of 20 ^oC	
THERMAL-DIST-08	Thermal control system shall ensure that the temperature-sensitive payload is protected	Requires specifications, but met so far
THERMAL-REL-01	The thermal control system shall not experience corrosion over 3 years	Not designed for yet
THERMAL-REL-02	The thermal control system shall have no single points of failure	
THERMAL-REL-03	The thermal control system shall remain nominally operational within a temperature range of 2.7 and 400 K	Updated for current estimates

16.8.6. Structures

Identifier	Requirement	Comment
STRUC-01	Each module shall be able to withstand the launch loads.	But requires more detailed analysis
STRUC-02	Each module shall have a a first lateral frequency greater than or equal to 35 Hz.	Only hab module analysed so far
STRUC-03	Each module shall have a a first axial frequency greater than or equal to 35 Hz.	Only hab module analysed so far
STRUC-04	Each module shall fit into the Falcon payload bay.	
STRUC-05	Each module's structure configuration shall comply with the launcher interface.	Standard docking interface
STRUC-06	The assembled system shall have a combined window area of at least 1 m^2 with a maximum of 10cm between adjoined windows.	
STRUC-07	Each module's structure shall be able to withstand the space environment for at least 20 years without losing its integrity.	Needs more analysis
STRUC-08	Each module shall not exceed a mass of 35000 kg	Updated to launcher capabilities
STRUC-CONFIG-01	The system shall consist of modules which can be reconfigured	
STRUC-CONFIG-02	The system's configuration shall be expandable by the addition of more modules.	
STRUC-CONFIG-03	The assembled system shall have a combined window area of at least 1 m^2 with a maximum of 10cm between adjoined windows.	Duplicate for subsubsystem
STRUC-CONFIG-04	The assembled system shall have at least a volume of 25 m^3 per astronaut.	
STRUC-CONFIG-05	The manned areas of the assembled system shall have a physical radiation shield reducing the radiation to an average of 1.2 mSv/day during transfer	Updated with new insights
STRUC-CONFIG-06	The assembled system shall be able to maintain a pressure difference of 120000 Pa.	Shielding became key requirement
STRUC-CONFIG-07	The assembled system shall have a air leak rate lower than 0.06 kg/day for the whole mission duration.	Not designed for yet
STRUC-DOCK-01	The docking interfaces shall be androgynous.	
STRUC-DOCK-02	Each module shall have at least 2 docking ports.	Only the habitat modules require 2 docking ports for reconfiguration
STRUC-DOCK-03	The docking interface shall comply with autonomous rendezvous and docking systems	

STRUC-DOCK-04	The docking interface shall allow for docking of a fully functional module with a non-cooperative module.	Arm can be used, according to IDSS
STRUC-DOCK-05	The docking interfaces shall be closable manually in case of emergencies.	Complying with IDSS
STRUC-PAY-01	The structure shall provide a mounting location for an external payload	
STRUC-PAY-02	Half of the system structure volume shall be reserved for the payload	

16.8.7. Propulsion

Identifier	Requirement	Comment
PROP-01	The propulsion system shall be able to deliver a Delta-V of at least 35.2 km/s.	
PROP-02	The propulsion system shall have an operational lifetime of at least 20 years.	Needs demonstration
PROP-03	The propulsion system shall be able to still perform as required when one engine fails.	4 redundant engines included
PROP-04	The propulsion system shall not limit the functionality of other modules sytems.	Unclear requirement
PROP-05	The propulsion system shall be operational in vacuum and deep-space temperatures	Needs demonstration
PROP-06	The propulsion system shall be able to provide three-axis control.	ADCS will provide this, req scrapped
PROP-07	The propulsion system shall be technical ready before 2040.	Needs demonstration
PROP-08	The propulsion system shall be refulable	
PROP-09	The propulsion system shall not exceed a dry mass of 36000 kg	Updated for current budgets
PROP-10	The propulsion system shall have an average power usage of less than 10 Mwe	
PROP-11	The propulsion system shall have a peak power usage of less than 10.5 Mwe	
PROP-THR-01	The specific impulse that can be delivered by the thruster system used shall be 5000 s.	VASIMR specifications
PROP-THR-02	The amount of thrusters used shall be able to provide three axis control.	ADCS will provide this, req scrapped
PROP-THR-03	The thrusters shall fulfil their functionality after failure of one component.	Not designed for yet
PROP-THR-04	The thrusters shall fulfil their functionality for a radiation dose of 20 Gy over 20 years.	Updated, needs demonstration
PROP-THR-05	The reliability of the thruster system used shall be larger than <tbd> over a period of 20 years.	Not specified yet
PROP-ENS-01	The energy sources used for propulsion shall not influence the health of the astronauts.	Radiation risk is increased
PROP-ENS-02	The energy sources used for propulsion shall not influence the performance of other sub-systems.	Other systems designed for radiation
PROP-ENS-03	The energy sources used for propulsion shall be available during the whole mission duration.	
PROP-REL-01	The propulsion system shall withstand radiation of 10 mGy/day	Not designed for yet
PROP-REL-02	The propulsion system shall withstand a total irradiation of 20 Gy over 20 years	Not designed for yet
PROP-REL-03	The propulsion system shall have no single points of failure	Redundant engines
PROP-REL-04	The propulsion system shall remain nominally operational within a temperature range of <tbd> K	Not specified yet
PROP-REL-05	The propulsion system shall maintain performance with one fission reactor inoperational	With lower thrust or less engines

16.8.8. ECLSS

Identifier	Requirement	Comment
LS-01	There shall be a water recovery system.	
LS-02	There shall be equipment for physical exercises.	
LS-03	There shall be equipment to facilitate psychological help.	
LS-04	There shall be equipment to facilitate medical help.	
LS-05	There shall be sleeping spaces for all astronauts.	
LS-06	There shall be food on the spacecraft to feed the astronauts for the whole mission duration.	
LS-07	The atmosphere in the living module shall be pressurised.	
LS-08	The atmspheric composition in the living module shall be similar to that of the International Space Station within ranges of 5%.	
LS-09	There shall be the possibility for the astronauts to communicate with home.	
LS-10	There shall be equipment to facilitate personal hygiene.	
LS-11	There shall be group activities on board.	
LS-12	The living module shall not induce physical injuries.	
LS-13	The living module shall not induce psychological injuries.	
LS-14	There shall be the possibility to store non-recyclable waste.	
LS-15	There shall be the possibility to dispose non-recyclable waste.	
LS-16	The life support system shall not exceed a mass of 8000 kg	Updated for current budgets
LS-17	The life support system shall have an average power usage of 5 kWe	Updated for current budgets
LS-18	The life support system shall have a peak power usage of 6 kWe	Updated for current budgets
LS-WR-01	The water recovery system shall have a recycling efficiency of at least 80%.	
LS-WR-02	The urine of the astronauts shall be recycled to drinking water.	
LS-WR-03	The non-recyclable waste shall be stored up and till the next disposal.	
LS-WR-04	The waste recycling system shall be operational during the whole mission lifetime.	
LS-ATM-01	The humidity in the living module shall be between <tbd> %.	Not designed for yet
LS-ATM-02	The temperature in the living module shall be between 288-298 K	
LS-ATM-03	Oxygen partial pressure shall be maintained at 19.4 - 23.7 kPa	Updated from O2 percentage
LS-ATM-04	The percentage of carbon-dioxide in the living module shall be between <tbd> %	Not specified yet
LS-ATM-05	The percentage of all other gasses than mentioned in LS-ATM-03 and LS-ATM-04 shall be together be between <tbd>%	Not specified yet
LS-ATM-06	The light intensity in the spacecraft shall be between <tbd> W/m^2 in the living and working spaces.	Not specified yet
LS-ATM-07	The light intensity in the spacecraft shall be between <tbd> W/m^2 in the sleeping spaces.	Not specified yet
LS-ATM-08	There shall be no toxic substances in the living module.	
LS-ATM-09	There shall be no pathogenic substances in the living module.	Not designed for yet
LS-ATM-10	The atmospheric pressure inside the living module shall be between 96.5 - 102.7 kPa	

LS-ATM-11	There shall be no cold spots in the living module.	Needs to be demonstrated
LS-PHY-01	The astronauts shall be fed with at least 3 meals per day.	
LS-PHY-02	The amount of calories that the astronaut gets per day shall be determined by the Mifflin-St Jeor Equation.	
LS-PHY-03	The astronauts shall get a medical examination once a week.	
LS-PHY-04	The astronauts shall do exercises 1 hour a day.	
LS-PHY-05	There shall be at least 4 different types of exercise equipment in the living module.	
LS-PHY-06	There shall be space to store medicines and food from radiation.	
LS-PHY-07	There shall be one toilet per living module.	Reduced to one toilet in the spacecraft
LS-PHY-08	There shall be one bathroom per living module.	Reduced to one bathroom in the spacecraft
LS-PHY-09	There shall be equipment to perform first aid.	
LS-PHY-10	There shall be a volume of at least $25\ m^3$ per astronaut in the living module.	
LS-PHY-11	There shall be no physical changes that prevent successful mission operation.	Experience from ISS
LS-PSY-01	The astronauts shall get a psychological examination once a week.	
LS-PSY-02	The astronauts shall sleep at least 8 hours a day.	
LS-PSY-03	The astronauts shall be able to communicate with home once a month by sound.	
LS-PSY-04	The astronauts shall have the possibility to use 1 hour of spare time a day.	
LS-PSY-05	The astronauts shall perform group activities 1 hour per week.	
LS-PSY-06	The astronauts shall have the possibility to get privacy once a day.	
LS-PSY-07	The astronauts shall communicate in English.	
LS-PSY-08	There shall be no psychological changes that prevent successful mission operation.	Experience from ISS
LS-PSY-09	The astronauts shall be selected using NASA's astronaut selection program	
LS-PSY-10	The day and night schedules of the astronauts should remain constant over time.	
LS-REL-01	The Life Support System shall keep the human occupants safe with a reliability of 99.9% in nominal case	
LS-REL-02	The Life Support System shall withstand radiation of 10 mGy/day	Needs demonstrated
LS-REL-03	The Life Support System shall withstand a total irradiation of 20 Gy over 20 years	Needs demonstrated
LS-REL-04	The Life Support System shall have no single points of failure	
LS-REL-05	The Life Support System shall remain nominally operational within a temperature range of 288-298 K	

16.8.9. Communications

Identifier	Requirement	Comment
COMS-01	The system shall provide the ability to contact earth	
COMS-02	All electronic components within the communication system shall comply with RoHS	
COMS-03	The system shall be able to function during all segments of the mission	Except for contact during conjunction
COMS-04	Communication from and towards earth shall be encrypted	Through modulation
COMS-05	Autonomous communication between modules shall be possible	Short-range radio waves
COMS-06	Receiving and transmitting data shall be able to happen simultaneously	
COMS-07	All materials onboard of the systems shall comply with REACH regulations.	
COMS-08	The C&CDH system shall not exceed a mass of 600 kg	Updated for current budget
COMS-09	The C&CDH system shall have an average power usage of less than 600 W	Updated for current budget
COMS-10	The C&CDH system shall have a peak power usage of less than 1400 W	Updated for current budget
COMS-RX-01	After receiving the data shall be decoded onboard	
COMS-RX-02	Receiving data shall not cost more than 150 Watts in nominal operations	
COMS-RX-03	The reception speed on board of the spacecraft shall be a minimum of 125000 kbps	Reduced to 100 Mbps
COMS-RX-04	The antenna shall always be pointed towards the target	
COMS-RX-05	The receiver shall have a reliability of at least <tbd> %	Not specified yet
COMS-RX-06	The system shall work coherently together with the transmitter when active	
COMS-RX-07	The system shall be able to receive data from earth at its largest mission distance	Sized for Mars opposition
COMS-TX-01	Before transmitting the data it shall be coded onboard	Through modulation
COMS-TX-02	Transmitting the data shall not cost more than 450 Watts in nominal operations	
COMS-TX-03	The transmission speed on board of the spacecraft shall be a minimum of 25000 kbps	
COMS-TX-04	The transmitter shall always be pointed towards the target	
COMS-TX-05	The transmitter shall have a reliability of at least <tbd> %	Not specified yet
COMS-TX-06	The system shall work coherently together with the receiver when active	
COMS-TX-07	The system shall be able to transmit data from earth at its largest mission distance	Sized for Mars opposition
COMS-TX-08	The transmitter shall have a sufficient gain in order to attain a SNR of 21	
COMS-REL-01	The communication system shall withstand radiation of 10 mGy/day	Needs to be demonstrated
COMS-REL-02	The communication system shall withstand a total irradiation of 20 Gy over 20 years	Needs to be demonstrated
COMS-REL-03	The communication system shall have no single points of failure	
COMS-REL-04	The communication system shall remain nominally operational within a temperature range of 123-423 K	

16.8.10. Ground Systems

Identifier	Requirement	Comment
GS-01	The ground segment shall provide the launcher for the mission	
GS-02	The ground segment shall take care of the resupply of the mission	
GS-03	The ground segment shall provide for adequate ground control	
GS-04	The system shall adhere to the mission in an clear and efficient way	Unclear requirement
GS-05	The system shall have the capability of being resupplied for a new mission to Mars	
GS-LAUNCH-01	The launcher system shall be able to mount all types of modules	Modules adapted to launcher reqs
GS-LAUNCH-02	The system shall be able to reach LEO	

GS-LAUNCH-03	The cost to launch the payload to LEO shall be less than 10 000 euro/kg	
GS-LAUNCH-04	The launcher shall have a reliability of at least 95%	
GS-LAUNCH-05	The launchers used during the mission shall all fit within one family	
GS-LAUNCH-06	The launcher shall be launched from a compatible location	
GS-LAUNCH-07	The launcher fairing shall have sufficient volume to fit the module	Modules adapter to fairing
GS-RESUP-01	The system shall provide for the resupply of food	
GS-RESUP-02	The system shall provide for the resupply of fuel	
GS-RESUP-03	The system shall provide for the resupply of water	
GS-RESUP-04	The system shall provide for the resupply of breathables	
GS-RESUP-05	The system shall provide for the resupply of payload	
GS-RESUP-06	The resupply phase shall happen in LEO	
GS-RESUP-07	The resupply mission shall happen at specific moments in time	
GS-RESUP-08	The resupply mission shall be able to accomodate for maintenance equipment	
GS-GC-01	Ground control shall be able to perform long distance diagnostics on crew and machine	
GS-GC-02	Ground control shall be able to contact the spacecraft at all times	Except during conjunctions
GS-GC-03	During launch, Ground Control shall be able to perform diagnostics on the launcher	
GS-GC-04	Ground control communication shall be secured using end-to-end protocol algorithms	
GS-GC-05	The system shall acommodate for a emergency stop authorisation during launch	

16.8.11. Manufacturing, Assembly & Integration

Identifier	Requirement	Comment
MAI-01	The manufacturing process shall not pose any harm to the workforce.	
MAI-02	The manufacturing process shall be continuously evaluated by the quality control.	
MAI-03	The manufacturing timeline shall be consistent with the mission timeline.	
MAI-PROD-01	The whole material supply chain shall be monitored.	
MAI-ASSEM-01	The assembled systems shall adhere to the defined tolerances.	
MAI-ASSEM-02	The distance the assembled systems have to be transported shall be limited.	

16.8.12. Business

Identifier	Requirement	Comment
BUSI-01	The system shall generate at least 20% return on investment over a 10 year window after start of operations	
BUSI-02	The cost to launch payload to Mars orbit using the system shall be less than 2 m Euro/kg	
BUSI-03	The spacecraft shall bring payload to Mars cheaper than existing competitors	
BUSI-04	The spacecraft shall be able to transport untrained human passengers to Mars	Deemed too unsafe as revenue model
BUSI-05	The spacecraft shall be able to transport a satellite to Mars orbit	
BUSI-06	The spacecraft shall be able to transport a Lander to Mars orbit	
BUSI-MED-01	The spacecraft shall be able to transmit video footage to Earth from space	
BUSI-MED-02	There shall be space inside the habitat modules for commercial computer systems	

16.8.13. Payload

Identifier	Requirement	Comment
PAY-01	The payloads shall not interfere with the mission goal	External payload not found yet
PAY-02	Payload shall only be stored in the designated spaces	External payload not found yet
PAY-03	The External Payload shall have its own power source	External payload not found yet
PAY-04	Payload shall be checked to be functional before departure	External payload not found yet
PAY-DIM-01	The payload shall have a maximum size of TBD x TBD x TBD m when packed	Not specified yet
PAY-DIM-02	The payload shall have a maximum mass of 15000 kg	
PAY-DIM-03	The payload shall have a CG at TBD m from the spacecraft	Not specified yet
PAY-MOD-01	Payloads shall be modular attachable on the outside of the spacecraft	
PAY-COMM-01	The Payload shall have its own communication system	External payload not found yet
PAY-COMM-02	The Payload shall not use frequencies in the range 31-35 GHz	

16.8.14. Sustainability

Identifier	Requirement	Comment
SUST-01	The system shall comply with the REACH regulatory framework	
SUST-02	The system shall comply with the RoHS regulatory framework	
SUST-03	The system shall not increase the amount of orbital elements around Earth except the operational system itself	
SUST-REACH-01	The system shall not contain any Substances of Very High Concern (SVHC)	Use of hydrazine
SUST-REACH-02	The production of the system shall not use any SVHCs	Use of hydrazine
SUST-REACH-03	All procurement sourced from outside the European Union shall be screened for SVHCs	
SUST-RoHS-01	The system shall not contain larger than allowable concentrations than defined by RoHS	
SUST-RoHS-02	All products sourced from outside the EU shall be screened for compliance with RoHS	
SUST-DEBRIS-01	All system elements in Earth orbit shall be deorbited at end of life within 6 months	
SUST-DEBRIS-02	All expendable system elements shall be deorbited following ejection within 3 months	
SUST-DEBRIS-03	In the event of system failure, all Earth orbiting elements shall deorbit within 12 months	Will require an active system to deorbit

17

Technical Risk Assessment

Technical risk assessment allows the risks associated with specific system and mission design choices to be monitored closely, and is thus an essential part of the detailed design phase for any engineering project. The three major steps in risk management are their identification, assessment and handling. During the assessment, the likelihood of an event occurring and the impact of said event are evaluated. The handling refers to the application of mitigation and contingency strategies to reduce likelihood and impact respectively. Risk assessment is then repeated to evaluate the effectiveness of the mitigation and contingency strategies.

This chapter presents the complete technical risk assessment for the design project. Mission risks are associated with the development and organisation of the whole mission and operational risks with the spacecraft itself. Operational risks are described on both system and subsystem levels. Where possible, mission level risks are traced to specific technical failures which would lead to risk occurrence. Mitigation strategies are discussed, and the post mitigation risk map is presented. The chapter concludes with a discussion of further mitigation efforts which should be made following the Design Synthesis Exercise.

Risk exposure is dependent on the likelihood of the event happening and its resulting impact. Likelihood is measured in 5 levels ranging from unlikely (1) to frequent (5) and the impact is measured in 4 levels ranging from negligible (1) to catastrophic (4). Risk likelihood and impact are judged using engineering intuition by engineers working in the specific area. Risk exposure is calculated by multiplying the likelihood level by the impact level. Exposure levels below 5 are deemed low, from 5 to 9 medium and 10 and above is deemed high. The three exposure levels are assigned the colours green, orange and red respectively and are used in risk maps throughout this chapter. In order to reduce likelihood and impact, mitigation and contingency strategies are applied where possible. Mitigation strategies aim at reducing the likelihood of an event occurring, while contingency is aimed at reducing the impact after an occurrence.

17.1. Mission Risk

17.1.1. Risk Identification

Mission risks were identified and assigned to the following categories: General mission risks are top level risks that can lead to a severe or complete mission failure. Development risks are associated with the technical development of subsystems required for the operation of the spacecraft. Production risks are associated to the production of components and assembly on ground. Maintenance risks are associated to the maintenance of the spacecraft over its lifetime and sustainability risks are associated to the possible impact of the mission on the environment.

- **MI - General Mission Risk**
  - Mission failure due to bankruptcy: The company goes bankrupt due to failure of the business plan (MI1).
  - Mission failure due to spacecraft failure: Catastrophic failure of the spacecraft leads to mission failure (MI2).
  - Mission failure due to development failure: The mission is cancelled due to major development complications (MI3).
  - Catastrophic launcher failure: Module or payload destroyed during launch (MI4).
- **DEV - Development Risk:**
  - Delays due to technical complications: Any delays caused by unforeseen technical issues that need to be addressed (DEV1).
  - Failure of component development: Assumed component not possible to be developed (DEV2).
- **PR - Production Risk:**
  - Manufactured parts do not fit: Parts are not possible to assemble due to errors in their design (PR1).

  - Part tolerances are not met: Parts are manufactured with lower accuracy than needed (PR2).
  - Parts cannot be manufactured: The parts designed cannot be manufactured with the available manufacturing techniques (PR3).
  - Parts damaged during assembly: Improper assembly leads to parts being damaged (PR4).
  - Low quality material is used: Supplier delivers material of lower quality than requested (PR5).
- **MA - Maintenance Risk:**
  - Damaged part cannot be replaced: Accessibility or binding method makes it impossible to replace damaged part (MA1).
  - Spacecraft damaged during maintenance: Improper maintenance procedures lead to damage (MA2).
  - Damaged parts not detected: Damaged parts are not detected during during maintenance checks (MA3).
- **SU - Sustainability Risk:**
  - Release of radioactive material due to launcher failure: Nuclear reactor does not withstand a failure of the launcher and radioactive material is released into the environment (SU1).
  - Production of debris in Earth orbit: Orbital debris is produced upon a collision (SU2).
  - Extra-terrestrial contamination: Celestial bodies are contaminated by living organisms from Earth (SU3).
  - Contamination of Earth with extra-terrestrial life: Extra-terrestrial life is brought to Earth upon return (SU4).

17.1.2. Pre-mitigation Risk assessment

The likelihood and impact of the identified risks was assessed and the results are presented in Table 17.1.

	Unlikely	Seldom	Occasional	Likely	Frequent
Catastrophic	SU4	SU3	MI1, MI2, MI3, MI4 SU1		
Critical		PR5, MA2, MA3	MA1, SU2	DEV1, DEV2	
Moderate		PR3	PR1, PR2, PR4		
Negligible					

Table 17.1: Risk map of the most important identified mission risks.

17.1.3. Mitigation and Contingency strategies

Mitigation and contingency strategies were applied in order to reduce the likelihood and impact of the mission risks discussed above. The general mission risks MI1 to MI3 did not receive a contingency strategy as they lead to a complete mission failure by definition. The strategies are presented in Table 17.2.

17.1.4. Post-mitigation risk assessment

The risks were analysed once more, after the mitigation and contingency strategies were applied. The results are presented in Table 17.3. As can be seen the likelihood of most risks and the impact of some was reduced. All risks have been eliminated from the most severe, red zone, however a significant amount of risks still lies in the orange zone. These risks of this mission are high because of multiple reasons. Space mission are risky by nature and many new technologies need to be developed. Special care should therefore taken in planning and monitoring the progress, in order to maximise the possibility of success. As discussed in Chapter 15, a high risk insurance should be used.

Desig.	Mitigation	Contingency
MI1	In depth business plan	-
MI2	In depth operational risk analysis	-
MI3	In depth development plan	-
MI4	Use of reliable launcher	Launch insurance
DEV1	In depth development plan	Incorporate contingency time into schedule
DEV2	Use of high TRL components	Plan back up options
PR1	Use of CAD, perform checks	Use of CAD for ease of change of design
PR2	Adequate training of personnel	Quality checks, non-destructive testing
PR3	Manufacturing is kept in mind throughout designing	Use of CAD for ease of change of design
PR4	Adequate training of personnel	Spare parts in stock
PR5	Use trusted suppliers, test material before use	Non-Destructive component testing
MA1	Maintenance is kept in mind throughout designing	Use fail-safe design strategies
MA2	Extensive astronaut training	Have spare parts on hand
MA3	Use of sensors on critical parts	Use fail-safe design strategies
SU1	Reactor designed to withstand launcher failure	Launch over inhabited areas
SU2	Use of active collision avoidance systems	Design spacecraft to produce minimal debris
SU3	Avoid unnecessary contact with celestial bodies	Sterilise objects that shall contact celestial bodies
SU4	Avoid unnecessary contact with celestial bodies	Sterilise, quarantine astronauts upon return

Table 17.2: Mitigation and Contingency strategies applied to mission risks.

	Unlikely	Seldom	Occasional	Likely	Frequent
Catastrophic	SU1, SU3, SU4	MI1, MI2, MI3			
Critical	MA3	MA1, SU2, MI4	DEV1		
Moderate	PR3, PR5, MA2	PR1, PR2	DEV2, PR4		
Negligible					

Table 17.3: Post mitigation risk map.

17.2. Operational Risk

17.2.1. Risk identification

For the operational risk map the technical risk/failures are identified per specific subsystem. The risk that were found for the subsystems can be closely related to the risk involved for other subsystems. Therefor the identification of the risk has to be set up with a subsystem specific identifier. Below a small overview will be given for the assigned identifier per subsystem and a small explanation is provided for the highest risk identified per subsystem.

- **GEN - General Mission Risk**:
  - Collision risk: Collisions with either with other space vehicles, orbital space debris, (micro-)meteorites (GEN1).
  - Interface failure: Issues associated with the connections between modules, either during assembly or during the mission (GEN2).
  - General human error: Issues caused by human negligence or incompetence (GEN3).
  - Incapacitated crew: The reduction in crew capacity due to a physical, physiological or medical issue (GEN4).
  - System diagnostics incorrect (NO GO): A false system signal that a (sub)system is nonfunctional (GEN5).
- **LA - Launch Risk**
  - Spacecraft gets damaged during Launch (LA2)
  - Failure during Uranium provisioning launch (LA4)
  - Module trajectory anomaly after separation (LA5
- **DO - Docking Risk**
  - Seal Malfunction (DO1)
  - Micro-meteorite and orbital debris impact (DO3)
  - Misalignment of the docking ports (DO5)
  - Failure of transfer connection (DO6)
- **PR - Propulsion Risk**
  - Magnetic field containment failure (PR2)
- **TR - Trajectory Risk**

  - Interrupted burn due to engine failure (TR2)
  - Deviation due to planning error (TR4)
- **PO - Power Risk**
  - Unstable power generation/transfer (PO5)
- **TH - Thermal Risk**
  - Degradation of the radiator panel over time (TH1)
  - Impacts from micro-meteorites (TH3)
  - Thermodynamic instability over time (TH4)
  - Failure of working fluid pumps (TH6)
- **TC - Telecommunication Risk**
  - Disrupted communication view spacecraft (TC5)
  - Disrupted communication view ground station (TC6)
  - Overheated Feeder (TC7)
- **AS - ADCS Risk**
  - CMG failure
  - IMU error
- **LS - Lifesupport Risk**
  - Running out of spare components (LS1)
  - Fire aboard spacecraft (LS5)
  - Food Spoilage (LS7)
  - Oxygen Generation Failure (LS9)
- **AM - Assembly Risk**
  - In-proper feed-system assembly (AM2)
  - Robot arm failure (AM4)
- **NC - Nuclear Risk**
  - Inadvertent criticality during launch (NC1)
  - Inadvertent criticality during manned phase of mission, orbiting earth (NC2)
  - Inadvertent criticality during manned phase of mission, deep space (NC3)

17.2.2. Pre-mitigation Risk assessment

The above identified risks were first assessed pre-mitigation. More risk were identified per subsystem but the mentioned risk above were deemed the most important risk to discuss. The mentioned risks will now be graded according to their likelihood and its impact. This is schematically depicted in Table 17.4.

	Unlikely	Seldom	Occasional	Likely	Frequent
Catastrophic	LA4, PR2	DO1, TC6, LS5, LS7, LS9	DO3, TH4, TH6, TC5, TC7, AS1, AS3, AM4, NC1, NC2, NC3	GEN4, LS1, AM2	
Critical		GEN1,GEN2, LA2, PO5	LA5, DO5, DO6, TR4, TH1	GEN3, TR2, TH3	
Moderate		GEN5			
Negligible					

Table 17.4: Risk map of the most important technical risks involved

17.2.3. Mitigation and Contingency strategies

Mitigation and contingency strategies were applied in order to reduce the likelyhood and impact of the risks. Similarly to the risk assessment, contingency strategies are highly dependent on the time and location of occurrence. In case of emergency, earth orbiting spacecraft may have access to fast rescue missions and resupply missions compared to deep space situations. The following 2 tables give an overview of the applied strategies.
The risk score is calculated by multiplying the likelihood with impact, where likelihood ranges from 1 to 5 and impact form 1 to 4. Risks with a score of 10 or higher are considered to be most severe. The mitigation and contingency strategy for these risks will thus be explained in more detail below table Table 17.5 and Table 17.6 .

Designation	Mitigation
GEN1	collision evasion, use of prediction models
GEN2	re-enforced interfaces
GEN3	warning lights, simple user interfaces, extensive training
GEN4	manage working hours, monitor psychological state and tiredness, use medicine, no critical crew members,
GEN5	develop good diagnostics tool, test extensively
LA2	adequate adapter interface
LA4	Multiple mitigation's. Reliable falcon 9, abort system
LA5	Use a Space Tug
DO1	Select space-grade sealing material and check over time/ replace
DO3	Smaller docking ports, recess docking ports
DO5	Add camera targets, Increase attitude determination accuracy
DO6	Monitor Flows through connectors
PR2	Install capacitors that sustain magnetic field while engine shuts down
TR2	Design propulsion with redundant engines
TR4	Verify and validate calculations / use reliable software
PO5	Use specialised electrical engines
TH1	Use space-grade coatings and check every mission cycle
TH3	Fold radiator panels when not operative, point radiators in plane with probability of meteorites
TH4	Perform heat transfer analysis during validation phase, perform CFD on entire system
TH6	Perform regular visual and softwar ematic inspection on pump system
TC5	Extra antenna on spacecraft
TC6	Design for worst case scenario (heavy rain and fog)
TC7	Cooling the feeder
AS1	Have sensors on board and re calibrate them regularly
AS3	Re-calibrate the IMU's regularly and use space-grade equipment with high reliability
LS1	Care full analysis of component failure rates
LS5	Use of inflammable materials
LS7	Conduct research on food preservation
LS9	Extensive testing of oxygen generation system
AM2	Perform EVA checks in LEO before initiation of the mission
AM4	Brush less motors, space bearings, all joints can be replaced, spare parts.
NC1	Low-enriched (i.e. negative reactivity curve) + control rods + safety rods
NC2	Control rods and Safety rods to control the reaction and use sensors to determine
NC3	Control rods and Safety rods to control the reaction and use sensors to determine

Table 17.5: Mitigation strategies for the risks associated with the mission

Designation	Contingency
GEN1	Shielding
GEN2	Module autonomy, spread resources, airlocks
GEN3	Routine checks
GEN4	Rest more, swap members
GEN5	Run software again, have investigation procedures
LA2	in orbit repairs, replacements available, insurance, budgeting contingency
LA4	Multiple launches, Launching non-critical Uranium
LA5	Have back-up modules
DO1	Sensors to detect and automatic sealing of docking ports
DO3	Add MMOD shields to the outside
DO5	Increase miss-alignment tolerance
DO6	Use valves and multiple connector pipes
PR2	Ensure proper shielding between engines
TR2	Take additional propellant for a less favourable trajectory
TR4	Take additional propellant for a less favourable trajectory
PO5	Have redundant electrical engine's
TH1	Include a safety-factor to cope with loss of efficiency
TH3	Have spare radiator panels, use valve system to only close specific panel
TH4	Throttle down the reactors, use electric heaters/coolers to reduce instability
TH6	Have redundant pumps for every separate loop
TC5	Point antenna + data storage
TC6	Communicate to other ground station
TC7	Use other satellite dish
AS1	Have redundant CMG's on-board to take over tasks
AS3	Have redundant IMU's to take over tasks
LS1	Take backup/emergency supplies
LS5	Implement sensors and extinguishers
LS7	Take extra and diverse food
LS9	Use oxygen candles
AM2	Include a interrupt fluid flow option
AM4	Simulate tasks, crash abort option
NC1	Contain reactor in crash box and shielding, cool down the reactor remotely
NC2	In-space shutdown en switch to backup power + provide enough cooling and increase shielding
NC3	In-space shutdown en switch to backup power + provide enough cooling and increase shielding

Table 17.6: Contingency strategies for the risks associated with the mission

The human element of any mission is a great source of risk due to their unpredictabil-

ity and reliability. Thus risks **GEN3** and **GEN4** are considered to be mission critical, these risks are general human error and incapacitated crew respectively. For **GEN3** the mitigation strategy is mostly composed of eliminating the chance of incompetent use of a system or reducing the chance of a mistake by training, and optimising the human machine interface, respectively. As for the contingency factors if the error was catastrophic such as rapid depressurisation, no contingency plan can be made. However if the error has no immediate effect, or is slow acting rigorous and frequent checks are proposed to reduce the effect of it. Risks **GEN4**, are the physiological, physical and medical issue of the crew, the main mitigation strategy is reduction of the workload and monitoring of the well being of the crew by ground control, furthermore no one member will be mission critical. In case of an issue with one of the crew members the contingency plan is to make the crew member rest and provide medical help for the issue, if needed through consultation with ground controls experts. Finally if a crew member is permanent or temporarily incapacitated reorganising of responsibilities will be executed.

17.2.4. Post-mitigation risk assessment

The effectiveness of mitigation and contingency strategies can be evaluated by re-assessing risks after their application. The following table shows the risk assessment post-mitigation.

	Unlikely	Seldom	Occasional	Likely	Frequent
Catastrophic					
Critical	DO1, PR2, TC7, LS1, LS5, LS9, AM4, NC3				
Moderate	GEN1,GEN2,GEN5, LA2, LA4, TR4, PO5, TH1, TH4, TC5, AS3, LS7, NC2	GEN3,LA5, DO6, GEN4 TH3, TC6, NC1			
Neglegible	DO3, DO5, TH6	TR2, AS1, AM2			

Table 17.7: Risk map of the mission after mitigation strategies

17.2.5. Recommendations for Future Risk Analysis

From Table 17.7 it can be deducted that most of the risk both decreased in likelihood and the impact was reduced by the mitigation and contingency strategies. These mitigation and contingencies have been implemented in the detailed design a long the way of designing it. However, still some risks have a moderate risk factor post mitigation/contingency. These risks are **LA5,DO6,TH3,TC6,NC1** respectively. They all score approximately moderate impact under a seldom likelihood after risk mitigation. For risk **LA5** this is because assembly in space using autonomous modules at a certain fixed trajectory is hard and the concept of a space tug is required. To minimise this specific risk, the concept of the space tug has to tested in space before the initiation of the mission. For risk **DO6** the connection between the modules is still really vulnerable. The connection should be tested in the validation period to possibly reduce the risk by looking into new connecting techniques. For **TH3**, working fluid systems that have a certain substrate in it that can tight a hole/leak, this will drastically reduce the impact of a meteorite impact. This will lower the TRL but can be tested elaborately before launch into space. For risk **TC6** earth orbiting or other planetary orbiting satellites can be used to increase the view period for communication. Lastly, risk **NC1** can be mitigated by using smaller portions of Uranium in better confined spaces to counteract the factors that cause increased reaction.

18
Project Planning

This chapter concludes the technical and operational discussion of this report by laying the framework for future design and development to be conducted post Design Synthesis Exercise. The project design and development logic as well as the project Gantt chart are described. System level verification and validation procedures to be performed are discussed.

18.1. Project Design & Development Logic

Development of the post DSE mission phases concerns the future company profile, the partners required for a successful mission and the logical ordering of activities to be executed in this phase.

18.1.1. Company Characteristics after DSE

To make a useful analysis of all the steps that have to be taken after finishing the DSE, it is of great importance to determine what the company that grows out of this DSE actually does and more important what it not does. After a group discussion the following company profile was set up.

- The detailed design will be worked out further by the company, with all required tasks that flows down from that.
- The company will not manufacture the spacecraft (modules) itself but will outsource this.
- The selection and training of astronauts will be done by the company itself, however, existing equipment will be used for this.
- Existing ground segments are going to be used.
- The launch will be done by an external party.
- The mission control and operations will be done by the company itself.
- The marketing department of the company will attract external investors and is responsible for the marketing plan and commercial use of the spacecraft.

18.1.2. Partners

From the previous company description, it flows down that some partners should be involved to achieve the required mission objectives. All contracts will be given by open tendering. These can be summarised as:

- Part manufacturing partners shall be selected.
- Assembly partners shall be selected.
- Material suppliers shall be selected. This will still be done by the company itself to ensure the quality of the half-fabricates, prevent extra costs and the use of sustainable options.
- An external launch party shall be selected.
- Existing ground segments shall be selected.
- External investors and clients shall be attracted.
- Logistic partners shall be selected.
- Existing astronaut selection and training facilities shall be selected.
- Verification and validation resources shall be selected from external parties.
- Verification and validation shall be performed by external parties to achieve objectiveness and prevents the company of building new equipment for this.

18.1.3. Timeline

The company plan for after the DSE with regards to the development logic can be summarised in Figure 18.1

18.2. Project Gantt Chart

On basis of the activities layed out in the previous section a Gantt cart is set up to schedule future activities in a time order adding start and end dates to them. The schedule is divided into seven big phases: The detail design phase will continue after the end of the DSE further

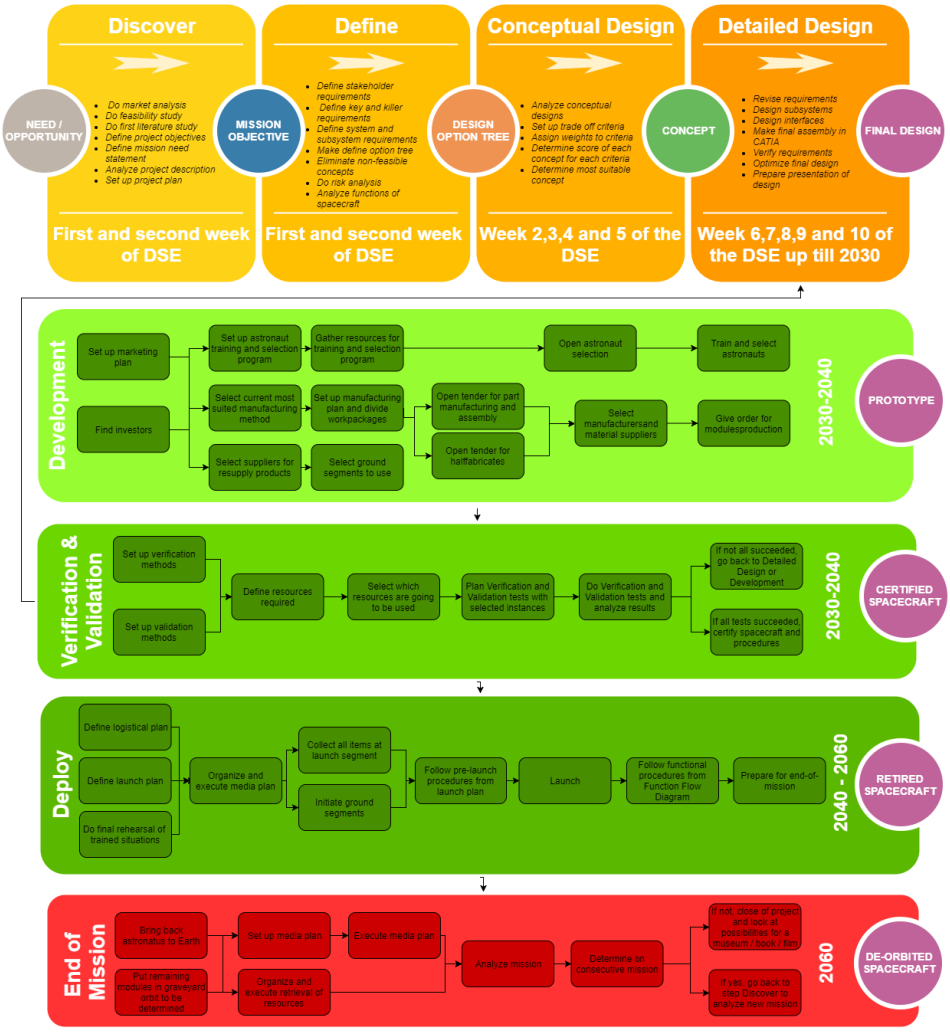

Figure 18.1: Design and Development Logic

refining the subsystems and setting up operations. Midway in this phase the development phase is initiated in which the subsystems and their components are verified and validated and tests are conducted based on the specific procedures per subsystem. Shortly after this phase has started production and certification will start and all elements will be produced and certified if required before they will be integrated. In the mission preparation phase ground operations and crew will be prepared for the in-orbit assembly phase and the mission execution phase. After the final mission has been executed the decommissioning phase follows in which the vehicle will be prepared to be brought to its end-of-life orbit.

ID	Task Name	Duration	Start	Finish
1	**Detailed Design**	**3950 days**	**Mon 8-7-19**	**Wed 1-5-30**
2	**Subsystem Design**	**941 days**	**Mon 8-7-19**	**Wed 1-5-30**
3	**Propulsion**	**941 days**	**Mon 8-7-19**	**Wed 1-5-30**
4	Cryocooler	941 days	Mon 8-7-19	Tue 30-4-30
5	Feedsystem	941 days	Mon 8-7-19	Tue 30-4-30
6	Docking Interfaces	941 days	Mon 8-7-19	Tue 30-4-30
7	**Trajectory**	**941 days**	**Mon 8-7-19**	**Wed 1-5-30**
8	Low-Thrust Interplanetary Trajectory Simulation	941 days	Mon 8-7-19	Tue 30-4-30
9	Required Thrust	941 days	Mon 8-7-19	Tue 30-4-30
10	Required Fuel Mass	941 days	Mon 8-7-19	Tue 30-4-30
11	Transfer Time	941 days	Mon 8-7-19	Tue 30-4-30
12	Trajectory Optimisation	941 days	Mon 8-7-19	Tue 30-4-30
13	**ECLSS**	**941 days**	**Mon 8-7-19**	**Wed 1-5-30**
14	Carbon Dioxide Removal Assembly	941 days	Mon 8-7-19	Tue 30-4-30
15	Carbon Dioxide Reduction System	941 days	Mon 8-7-19	Tue 30-4-30
16	Urine Processor Assembly	941 days	Mon 8-7-19	Tue 30-4-30
17	Water Processor Assembly	941 days	Mon 8-7-19	Tue 30-4-30
18	Oxygen Generator Assembly	941 days	Mon 8-7-19	Tue 30-4-30
19	Spare Sizing	941 days	Mon 8-7-19	Tue 30-4-30
20	Supply Sizing	941 days	Mon 8-7-19	Tue 30-4-30
21	Volumetric Sizing	941 days	Mon 8-7-19	Tue 30-4-30
22	**ADCS**	**941 days**	**Mon 8-7-19**	**Wed 1-5-30**
23	Sensors	941 days	Mon 8-7-19	Tue 30-4-30
24	Actuators	941 days	Mon 8-7-19	Tue 30-4-30
25	Layouts	941 days	Mon 8-7-19	Tue 30-4-30
26	Positioning	941 days	Mon 8-7-19	Tue 30-4-30
27	Sizing	941 days	Mon 8-7-19	Tue 30-4-30
28	**Power**	**941 days**	**Mon 8-7-19**	**Wed 1-5-30**
29	Multi-MW Fission Reactor	941 days	Mon 8-7-19	Tue 30-4-30
30	Closed-Cycle Magneto-Hydrodynamic Generator	941 days	Mon 8-7-19	Tue 30-4-30
31	Solar Arrays	941 days	Mon 8-7-19	Tue 30-4-30
32	Batteries	941 days	Mon 8-7-19	Tue 30-4-30
33	**Thermal**	**941 days**	**Mon 8-7-19**	**Wed 1-5-30**
34	Radiators	941 days	Mon 8-7-19	Tue 30-4-30
35	Fluid	941 days	Mon 8-7-19	Tue 30-4-30
36	Thermal Loop	941 days	Mon 8-7-19	Tue 30-4-30
37	**Structures**	**941 days**	**Mon 8-7-19**	**Wed 1-5-30**
38	Modules	941 days	Mon 8-7-19	Tue 30-4-30
39	Layout	941 days	Mon 8-7-19	Tue 30-4-30
40	MMOD Shielding	941 days	Mon 8-7-19	Tue 30-4-30
41	Radiation Shielding	941 days	Mon 8-7-19	Tue 30-4-30
42	Materials	941 days	Mon 8-7-19	Tue 30-4-30
43	Remote Manipulator System	941 days	Mon 8-7-19	Tue 30-4-30
44	Docking Interfaces	941 days	Mon 8-7-19	Tue 30-4-30
45	Production	941 days	Mon 8-7-19	Tue 30-4-30
46	**Communications**	**941 days**	**Mon 8-7-19**	**Wed 1-5-30**
47	Communication Strategy	941 days	Mon 8-7-19	Tue 30-4-30
48	Frequency Band	941 days	Mon 8-7-19	Tue 30-4-30
49	Tracking	941 days	Mon 8-7-19	Tue 30-4-30
50	Intermodul Communication	941 days	Mon 8-7-19	Tue 30-4-30
51	Main Antenna	941 days	Mon 8-7-19	Tue 30-4-30
52	Data Management	941 days	Mon 8-7-19	Tue 30-4-30
53	Data Rate	941 days	Mon 8-7-19	Tue 30-4-30
54	Link Budget	941 days	Mon 8-7-19	Tue 30-4-30
55	**Operations**	**941 days**	**Mon 8-7-19**	**Wed 1-5-30**
56	Launcher Packing	941 days	Mon 8-7-19	Tue 30-4-30
57	In-Orbit Assembly	941 days	Mon 8-7-19	Tue 30-4-30
58	Space Tug	941 days	Mon 8-7-19	Tue 30-4-30
59	Resupply	941 days	Mon 8-7-19	Tue 30-4-30
60	Logistics	941 days	Mon 8-7-19	Tue 30-4-30
61	Ground Control	941 days	Mon 8-7-19	Tue 30-4-30
62	**Sustainability**	**941 days**	**Mon 8-7-19**	**Wed 1-5-30**
63	Debris Mitigation Planning	941 days	Mon 8-7-19	Tue 30-4-30
64	Atmospheric Entry Avoidance	941 days	Mon 8-7-19	Tue 30-4-30
65	Life Cycle Assessment	941 days	Mon 8-7-19	Tue 30-4-30
66	Use of Harmful Substances	941 days	Mon 8-7-19	Tue 30-4-30
67	**Business**	**941 days**	**Mon 8-7-19**	**Wed 1-5-30**
68	Cost-Breakdown	941 days	Mon 8-7-19	Tue 30-4-30
69	Market Analysis	941 days	Mon 8-7-19	Tue 30-4-30
70	Return on Investment Analysis	941 days	Mon 8-7-19	Tue 30-4-30
71	Business Profile	941 days	Mon 8-7-19	Tue 30-4-30
72	**Development**	**3811 days**	**Wed 28-5-25**	**Sat 3-11-35**
73	**Subsystem Verification and Validation**	**908 days**	**Wed 28-5-25**	**Sat 3-11-35**
74	**Propulsion**	**908 days**	**Wed 28-5-25**	**Sat 3-11-35**
75	VASIMR Engine Testing	908 days	Wed 28-5-25	Sat 3-11-35
76	Cooler System Testing	908 days	Wed 28-5-25	Sat 3-11-35
77	Feedsystem Testing	908 days	Wed 28-5-25	Sat 3-11-35
78	**Trajectory**	**908 days**	**Wed 28-5-25**	**Sat 3-11-35**
79	Simulation Verification	472 days	Wed 28-5-25	Tue 29-10-30
80	Optimised Trajectory Validation	435,33 day	Fri 1-11-30	Sat 3-11-35
81	**ECLSS**	**908 days**	**Wed 28-5-25**	**Sat 3-11-35**
82	Ground Testing	472 days	Wed 28-5-25	Tue 29-10-30
83	Testing On Board ISS	435,33 day	Fri 1-11-30	Sat 3-11-35
84	**ADCS**	**908 days**	**Wed 28-5-25**	**Sat 3-11-35**
85	CMG Ground Testing	908 days	Wed 28-5-25	Sat 3-11-35
86	Thruster Ground Testing	908 days	Wed 28-5-25	Sat 3-11-35
87	Sensor Space Simulator Testing	908 days	Wed 28-5-25	Sat 3-11-35
88	**Power**	**908 days**	**Wed 28-5-25**	**Sat 3-11-35**
89	Reactor Ground Testing	472 days	Wed 28-5-25	Tue 29-10-30
90	MHD Ground Testing	472 days	Wed 28-5-25	Tue 29-10-30
91	Reactor and MHD In-Flight Testing	436 days	Wed 30-10-30	Sat 3-11-35
92	Solar Array Ground Space Simulator Testing	908 days	Wed 28-5-25	Sat 3-11-35
93	Battery Testing	908 days	Wed 28-5-25	Sat 3-11-35
94	**Thermal**	**908 days**	**Wed 28-5-25**	**Sat 3-11-35**
95	Verification through CFD Simulations	300 days	Wed 28-5-25	Mon 6-11-28
96	Structural Analysis of Radiators	300 days	Wed 28-5-25	Mon 6-11-28
97	System Ground Testing	300 days	Tue 7-11-28	Mon 19-4-32
98	System In-Flight Testing	308 days	Tue 20-4-32	Sat 3-11-35
99	**Structures**	**908 days**	**Wed 28-5-25**	**Sat 3-11-35**
100	Thermal Expansion	300 days	Wed 28-5-25	Mon 6-11-28
101	Structural Analysis	300 days	Wed 28-5-25	Mon 6-11-28
102	MMOD Shield Testing	300 days	Tue 7-11-28	Mon 19-4-32
103	Radiation Shield Testing	300 days	Tue 7-11-28	Mon 19-4-32
104	RMS Simulations	300 days	Tue 7-11-28	Mon 19-4-32
105	Structural Testing	247,33 day	Sat 1-1-33	Sat 3-11-35
106	**Communications**	**908 days**	**Wed 28-5-25**	**Sat 3-11-35**
107	Link Budget Unit testing	300 days	Wed 28-5-25	Mon 6-11-28
108	Antenna Space Simulator Testing	608 days	Tue 7-11-28	Sat 3-11-35
109	Antenna Radiation Testing	608 days	Tue 7-11-28	Sat 3-11-35
110	Atmospheric Attenuation Testing	608 days	Tue 7-11-28	Sat 3-11-35
111	Noise Temperature Testing	608 days	Tue 7-11-28	Sat 3-11-35
112	Travelling Wave Tube Amplifier Space Simulator Testing	608 days	Tue 7-11-28	Sat 3-11-35
113	**Operations**	**647,33 day**	**Sun 28-5-28**	**Sat 3-11-35**
114	Integration Test	473,33 day	Tue 28-5-30	Sat 3-11-35
115	Berthing Operation Testing	473,33 day	Tue 28-5-30	Sat 3-11-35
116	Space Tug Ground Testing	472 days	Sun 28-5-28	Thu 27-10-33
117	Space Tug In Flight Testing	175,33 day	Fri 28-10-33	Sat 3-11-35
118	Ground Station Test Runs	175,33 day	Fri 28-10-33	Sat 3-11-35
119	Crew Simulator Training	175,33 day	Fri 28-10-33	Sat 3-11-35
120	**Sustainability**	**908 days**	**Wed 28-5-25**	**Sat 3-11-35**
121	Compliance with REACH	908 days	Wed 28-5-25	Sat 3-11-35
122	Compliance with RoHS	908 days	Wed 28-5-25	Sat 3-11-35
123	Compliance with European Battery Directive	908 days	Wed 28-5-25	Sat 3-11-35
124	**Business**	**908 days**	**Wed 28-5-25**	**Sat 3-11-35**
125	Monitor Investments	908 days	Wed 28-5-25	Sat 3-11-35
126	Set up Contracts with Agencies	908 days	Wed 28-5-25	Sat 3-11-35
127	Secure Sponsors	908 days	Wed 28-5-25	Sat 3-11-35
128	Set up Cooperations	908 days	Wed 28-5-25	Sat 3-11-35
129	**Production and Certification**	**3393 days**	**Wed 4-10-28**	**Mon 18-1-38**
130	**Subsystem Certification**	**808 days**	**Wed 4-10-28**	**Mon 18-1-38**
131	**Propulsion**	**808 days**	**Wed 4-10-28**	**Mon 18-1-38**
132	Feedsystem	808 days	Wed 4-10-28	Mon 18-1-38
133	Tanks	808 days	Wed 4-10-28	Mon 18-1-38
134	**ECLSS**	**808 days**	**Wed 4-10-28**	**Mon 18-1-38**
135	ECLSS Assemblies	808 days	Wed 4-10-28	Mon 18-1-38
136	Tanks	808 days	Wed 4-10-28	Mon 18-1-38
137	Piping	808 days	Wed 4-10-28	Mon 18-1-38
138	**ADCS**	**808 days**	**Wed 4-10-28**	**Mon 18-1-38**
139	Feedsystem	808 days	Wed 4-10-28	Mon 18-1-38

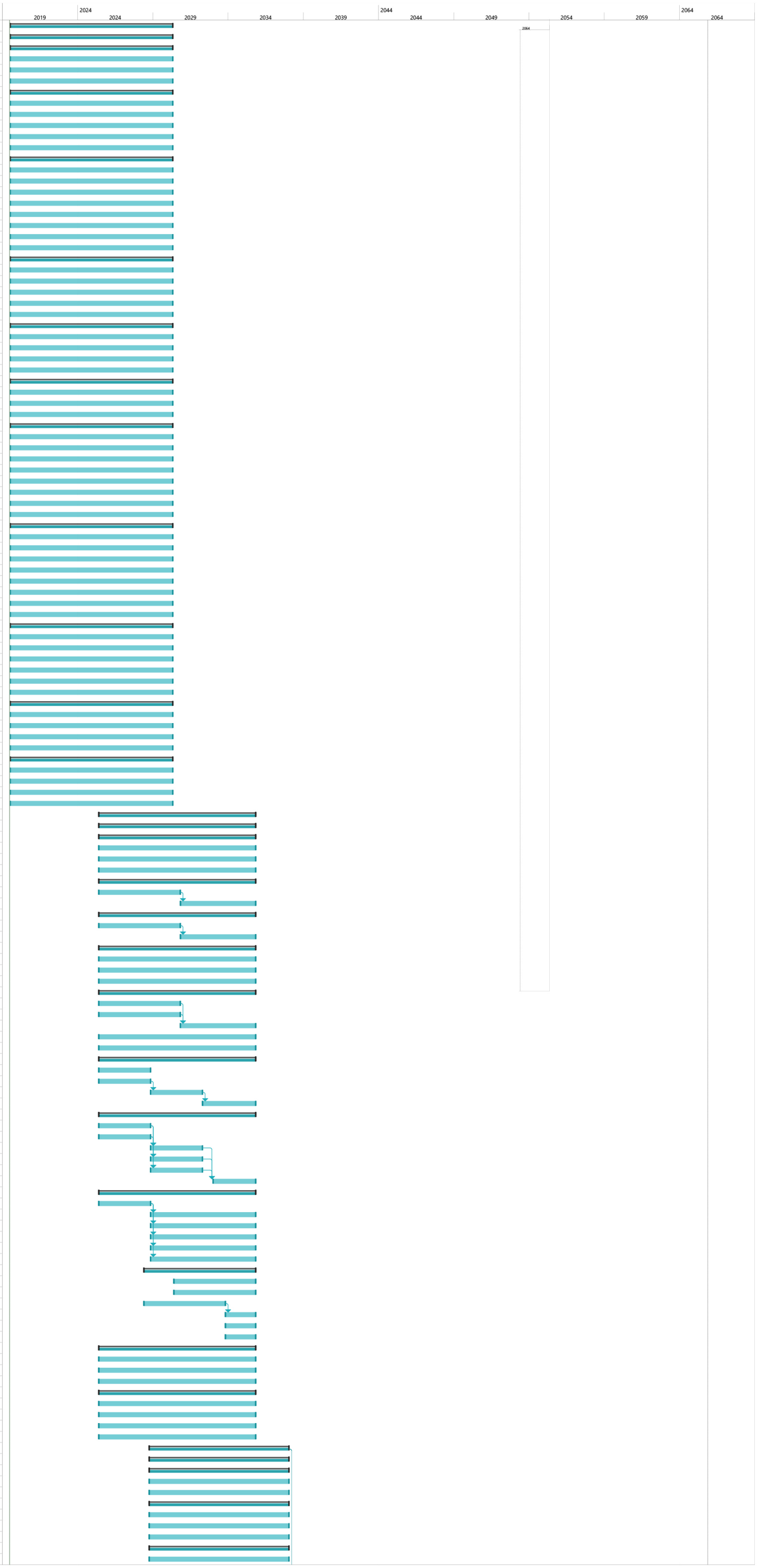

Figure 18.2: Part 1 of the project Gantt chart including phases 1 to 3.

ID	Task Name	Duration	Start	Finish
140	Tanks	808 days	Wed 4-10-28	Mon 18-1-38
141	**Power**	**808 days**	**Wed 4-10-28**	**Mon 18-1-38**
142	Reactor	808 days	Wed 4-10-28	Mon 18-1-38
143	Solar Arrays	808 days	Wed 4-10-28	Mon 18-1-38
144	Batteries	808 days	Wed 4-10-28	Mon 18-1-38
145	**Thermal**	**808 days**	**Wed 4-10-28**	**Mon 18-1-38**
146	Fluid	808 days	Wed 4-10-28	Mon 18-1-38
147	Piping	808 days	Wed 4-10-28	Mon 18-1-38
148	**Structures**	**808 days**	**Wed 4-10-28**	**Mon 18-1-38**
149	Materials	808 days	Wed 4-10-28	Mon 18-1-38
150	Components	808 days	Wed 4-10-28	Mon 18-1-38
151	Assemblies	808 days	Wed 4-10-28	Mon 18-1-38
152	Launch Assemblies	808 days	Wed 4-10-28	Mon 18-1-38
153	**Communications**	**808 days**	**Wed 4-10-28**	**Mon 18-1-38**
154	Frequency Band	808 days	Wed 4-10-28	Mon 18-1-38
155	Antenna	808 days	Wed 4-10-28	Mon 18-1-38
156	Tracking	808 days	Wed 4-10-28	Mon 18-1-38
157	**Operations**	**808 days**	**Wed 4-10-28**	**Mon 18-1-38**
158	Launcher Packing	808 days	Wed 4-10-28	Mon 18-1-38
159	Space Tug	808 days	Wed 4-10-28	Mon 18-1-38
160	Ground Station	808 days	Wed 4-10-28	Mon 18-1-38
161	Simulator	808 days	Wed 4-10-28	Mon 18-1-38
162	In-Orbit Assembly Procedure	808 days	Wed 4-10-28	Mon 18-1-38
163	Supply Launches	808 days	Wed 4-10-28	Mon 18-1-38
164	**Sustainability**	**808 days**	**Wed 4-10-28**	**Mon 18-1-38**
165	Certify Compliance with Regulations	808 days	Wed 4-10-28	Mon 18-1-38
166	**Business**	**808 days**	**Wed 4-10-28**	**Mon 18-1-38**
167	Budgeting	808 days	Wed 4-10-28	Mon 18-1-38
168	Collect Funds	808 days	Wed 4-10-28	Mon 18-1-38
169	**Subsystem Production**	**808 days**	**Wed 4-10-28**	**Mon 18-1-38**
170	Propulsion	808 days	Wed 4-10-28	Mon 18-1-38
171	Trajectory Planning	808 days	Wed 4-10-28	Mon 18-1-38
172	ECLSS	808 days	Wed 4-10-28	Mon 18-1-38
173	ADCS	808 days	Wed 4-10-28	Mon 18-1-38
174	Power	808 days	Wed 4-10-28	Mon 18-1-38
175	Thermal	808 days	Wed 4-10-28	Mon 18-1-38
176	Structures	808 days	Wed 4-10-28	Mon 18-1-38
177	Communications	808 days	Wed 4-10-28	Mon 18-1-38
178	**Mission Preparations**	**713 days**	**Wed 19-1-33**	**Sat 30-3-41**
179	Setup Ground Operations	435 days	Wed 19-1-33	Mon 18-1-38
180	Crew Training	279 days	Sat 16-1-38	Sat 30-3-41
181	**In-Orbit Assembly**	**261 days**	**Tue 19-1-38**	**Wed 16-1-41**
182	**Launches**	**236 days**	**Tue 19-1-38**	**Wed 3-10-40**
183	Truss 1	0 days	Tue 19-1-38	Tue 19-1-38
184	Space Tug	0 days	Tue 19-1-38	Tue 19-1-38
185	Truss 2	0 days	Thu 1-4-38	Thu 1-4-38
186	Truss 3	0 days	Thu 1-4-38	Thu 1-4-38
187	Module 1	0 days	Thu 1-7-38	Thu 1-7-38
188	Module 2	0 days	Thu 1-7-38	Thu 1-7-38
189	Module 3	0 days	Wed 1-9-38	Wed 1-9-38
190	Tank 1	0 days	Wed 1-12-38	Wed 1-12-38
191	Tank 2	0 days	Wed 1-12-38	Wed 1-12-38
192	Tank 3	0 days	Tue 1-2-39	Tue 1-2-39
193	Tank 4	0 days	Tue 1-2-39	Tue 1-2-39
194	Tank 5	0 days	Fri 1-4-39	Fri 1-4-39
195	Tank 6	0 days	Fri 1-4-39	Fri 1-4-39
196	Reactor 1	0 days	Mon 1-8-39	Mon 1-8-39
197	Reactor 2	0 days	Tue 1-11-39	Tue 1-11-39
198	Reactor 3	0 days	Wed 1-2-40	Wed 1-2-40
199	Reactor 4	0 days	Tue 1-5-40	Tue 1-5-40
200	Supplies	0 days	Mon 1-10-40	Mon 1-10-40
201	External Payloads	0 days	Mon 1-10-40	Mon 1-10-40
202	Assembly	242 days	Tue 19-1-38	Mon 29-10-40
203	System Checks	185 days	Wed 1-12-38	Mon 14-1-41
204	**Mission Execution**	**7608 days**	**Wed 16-1-41**	**Tue 15-11-61**
205	**Mission I**	**1192 days**	**Wed 16-1-41**	**Fri 22-4-44**
206	Earth Spiral Out	103 days	Wed 16-1-41	Mon 29-4-41
207	Launch Crew	0 days	Sat 30-3-41	Sat 30-3-41
208	Transfer	200 days	Mon 29-4-41	Fri 15-11-41
209	Mars Spiral In	33 days	Fri 15-11-41	Wed 18-12-41
210	Martian Orbit Stay	520 days	Wed 18-12-41	Fri 22-5-43
211	Mars Spiral Out	33 days	Fri 22-5-43	Wed 24-6-43
212	Transfer	200 days	Wed 24-6-43	Sun 10-1-44
213	Earth Spiral In	103 days	Sun 10-1-44	Fri 22-4-44
214	**Intermission Operations**	**412 days**	**Fri 22-4-44**	**Thu 8-6-45**
215	Re-Enter Crew	0 days	Fri 22-4-44	Fri 22-4-44
216	Resupply Launches	0 days	Fri 22-4-44	Fri 22-4-44
217	Resupply	412 days	Fri 22-4-44	Thu 8-6-45
218	Maintenance	412 days	Fri 22-4-44	Thu 8-6-45
219	**Mission II**	**1192 days**	**Thu 8-6-45**	**Sat 12-9-48**
220	Earth Spiral Out	103 days	Thu 8-6-45	Tue 19-9-45
221	Launch Crew	0 days	Wed 23-8-45	Wed 23-8-45
222	Transfer	200 days	Tue 19-9-45	Sat 7-4-46
223	Mars Spiral In	33 days	Sat 7-4-46	Thu 10-5-46
224	Martian Orbit Stay	520 days	Thu 10-5-46	Sat 12-10-47
225	Mars Spiral Out	33 days	Sat 12-10-47	Thu 14-11-47
226	Transfer	200 days	Thu 14-11-47	Mon 1-6-48
227	Earth Spiral In	103 days	Mon 1-6-48	Sat 12-9-48
228	**Intermission Operations**	**412 days**	**Sat 12-9-48**	**Fri 29-10-49**
229	Re-Enter Crew	0 days	Sat 12-9-48	Sat 12-9-48
230	Resupply Launches	0 days	Sat 12-9-48	Sat 12-9-48
231	Resupply	412 days	Sat 12-9-48	Fri 29-10-49
232	Maintenance	412 days	Sat 12-9-48	Fri 29-10-49
233	**Mission III**	**1192 days**	**Fri 29-10-49**	**Sun 2-2-53**
234	Earth Spiral Out	103 days	Fri 29-10-49	Wed 9-2-50
235	Launch Crew	0 days	Fri 14-1-50	Fri 14-1-50
236	Transfer	200 days	Wed 9-2-50	Sun 28-8-50
237	Mars Spiral In	33 days	Sun 28-8-50	Fri 30-9-50
238	Martian Orbit Stay	520 days	Fri 30-9-50	Sun 3-3-52
239	Mars Spiral Out	33 days	Sun 3-3-52	Fri 5-4-52
240	Transfer	200 days	Fri 5-4-52	Tue 22-10-52
241	Earth Spiral In	103 days	Tue 22-10-52	Sun 2-2-53
242	**Intermission Operations**	**412 days**	**Sun 2-2-53**	**Sat 21-3-54**
243	Re-Enter Crew	0 days	Sun 2-2-53	Sun 2-2-53
244	Resupply Launches	0 days	Sun 2-2-53	Sun 2-2-53
245	Resupply	412 days	Sun 2-2-53	Sat 21-3-54
246	Maintenance	412 days	Sun 2-2-53	Sat 21-3-54
247	**Mission IV**	**1192 days**	**Sat 21-3-54**	**Mon 25-6-57**
248	Earth Spiral Out	103 days	Sat 21-3-54	Thu 2-7-54
249	Launch Crew	0 days	Thu 4-6-54	Thu 4-6-54
250	Transfer	200 days	Thu 2-7-54	Mon 18-1-55
251	Mars Spiral In	33 days	Mon 18-1-55	Sat 20-2-55
252	Martian Orbit Stay	520 days	Sat 20-2-55	Mon 24-7-56
253	Mars Spiral Out	33 days	Mon 24-7-56	Sat 26-8-56
254	Transfer	200 days	Sat 26-8-56	Wed 14-3-57
255	Earth Spiral In	103 days	Wed 14-3-57	Mon 25-6-57
256	**Intermission Operations**	**412 days**	**Mon 25-6-57**	**Sun 11-8-58**
257	Re-Enter Crew	0 days	Mon 25-6-57	Mon 25-6-57
258	Resupply Launches	0 days	Mon 25-6-57	Mon 25-6-57
259	Resupply	412 days	Mon 25-6-57	Sun 11-8-58
260	Maintenance	412 days	Mon 25-6-57	Sun 11-8-58
261	**Mission V**	**1192 days**	**Sun 11-8-58**	**Tue 15-11-61**
262	Earth Spiral Out	103 days	Sun 11-8-58	Fri 22-11-58
263	Launch Crew	0 days	Sat 26-10-58	Sat 26-10-58
264	Transfer	200 days	Fri 22-11-58	Tue 10-6-59
265	Mars Spiral In	33 days	Tue 10-6-59	Sun 13-7-59
266	Martian Orbit Stay	520 days	Sun 13-7-59	Tue 14-12-60
267	Mars Spiral Out	33 days	Tue 14-12-60	Sun 16-1-61
268	Transfer	200 days	Sun 16-1-61	Thu 4-8-61
269	Earth Spiral In	103 days	Thu 4-8-61	Tue 15-11-61
270	**Intermission Operations**	**0 days**	**Tue 15-11-61**	**Tue 15-11-61**
271	Re-Enter Crew	0 days	Tue 15-11-61	Tue 15-11-61
272	**Decomissioning**	**1464 days**	**Tue 15-11-61**	**Wed 18-11-65**
273	Retrieval of Resources	1099 days	Tue 15-11-61	Tue 18-11-64
274	Graveyard Orbit	365 days	Tue 18-11-64	Wed 18-11-65
275	Put Reactors on Heliocentric Orbit	365 days	Tue 18-11-64	Wed 18-11-65
276	End of Mission	0 days	Wed 18-11-65	Wed 18-11-65

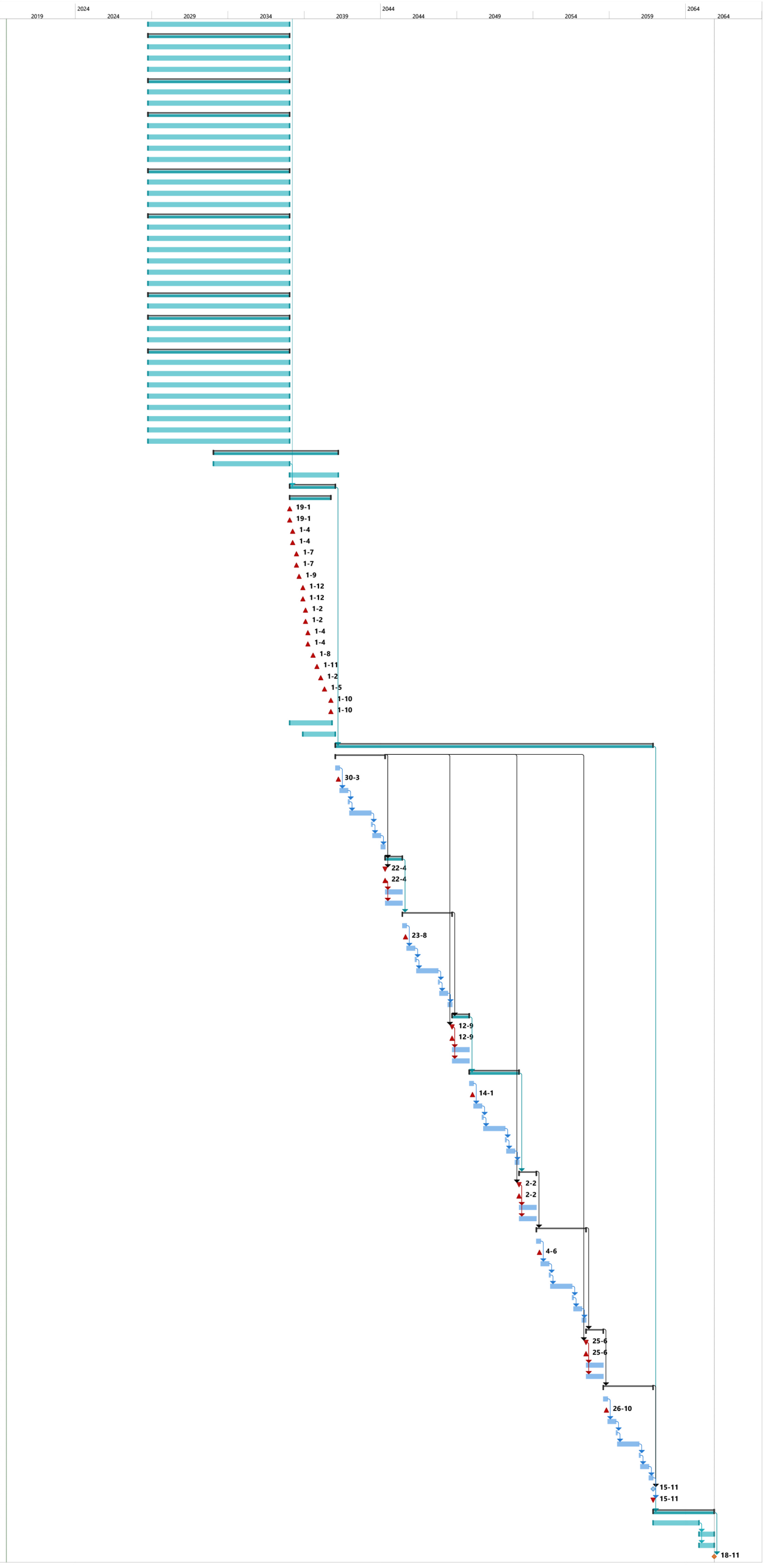

Figure 18.3: Part 2 of the project Gantt chart including phases 3 to 7.

18.3. Manufacturing, Assembly, Integration Plan

The production phase can be further detailed by outlining the processes and activities required in the construction of the system. In Figure 18.4 an outline is given in form of a manufacturing, assembly, integration plan which orders these elements in a timely manner from top to bottom. Starting from raw materials to sub-assemblies the source and components for the different subsystems are given, then they are assembled to their specific launch assembly, integrated in the launcher, launched and assembled in-orbit.

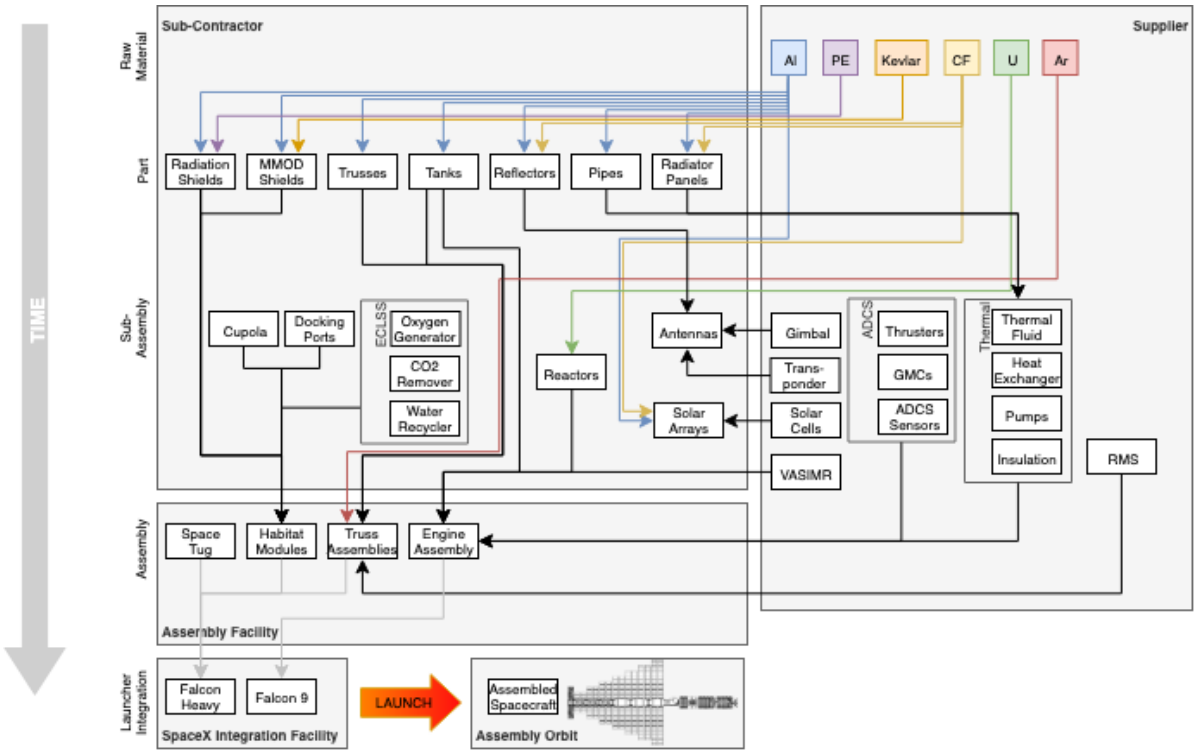

Figure 18.4: The Manufacturing, Assembly, Integration Plan for the production plan of the production phase. Time progresses from top to bottom and the grey boxes specify where a step is carried out.

The production processes for some of the more complex and larger parts have been investigated and manufacturing options have been determined. The propellant tanks will be friction stir welded out of Al2219-T62 as this process creates high strength bonds with only little defects and is currently used in the production of NASA's SLS tanks [17]. The same manufacturing process will be used to produce the habitation modules. It is also considered to use Directed Energy Deposition, an additive manufacturing process for the production of the modules but it was finally dismissed as aluminium is difficult to process [49]. The internal panels of the radiation shielding which are made out of the thermoplastic polyethylene will be additive manufactured and the external MMOD shields will be manufactured by using automatic tape-laying for the composite elements.

Every subsystem is elaborately verified and validated as outlined in their respective sections. The majority incorporate some form of live testing on ground before complete assembly as well as a fully assembled live test both on ground and in orbit where applicable.

19
Conclusion

Having conducted the first phase detail design of the Mars Transfer Vehicle, all subsystems have gone through at least two iterations and are integrated in a coherent vehicle design. With an planned vehicle lifetime of at least 20 years, the system's durability, along with many additional challenges have been addressed in order to qualify the design for flight. The large required ΔV to return to Earth orbit forced all propulsive system options, other than low thrust ion engines, to become obsolete due to their comparatively low ISP. This in turn constrained the mission length, which made the already stringent radiation requirements for the astronauts a key requirement. Furthermore, rendering such a pioneering mission profitable was another challenge that was made possible by incorporating funding from and cooperation with the major space agencies. One aspect of the mission that will become increasingly important is sustainability. In the upcoming years it is uncertain whether any change in legislation could make the current design unfeasible. However, potential novel options and technologies could allow the current mission to lower its total emissions. Finally, sustaining life in the hostile environment of interplanetary space leads to many functions that the life support system must fulfil while being extremely reliable.

Throughout this design project, a number of discoveries were made that had a large effect on the design. Following the simulation of low thrust trajectories form Earth to Mars, it was found that a direct return trajectory would be very inefficient for anything other than a return after 520 days stay. This made large variations in mission length unfeasible, and an early return necessitated by a unexpected event near impossible. Additionally, after iterating through several engine options and arriving at the VASIMR, it became clear that especially around Mars solar panels would be insufficient at providing the required power. This meant that the Delta Mars mission will become the first manned spacecraft with operating nuclear reactors on board that provide electrical power. While an interesting proposition, this leaves the project in a grey area with regard to a number of key technologies such as Magneto-Hydrodynamic nuclear reactors, Zero Boil-Off cryogenic coolers, and the VASIMR engines all being relatively experimental. This means that the current design must rely on the development and maturation of such technologies, before it can be designed, let alone built.

With this in mind, after conducting a number of iterations on all the subsystems, there are further items that need more immediate attention in order to allow for the project to thrive. One of the key driving factors of this interplanetary mission is the required ΔV, and with the use of more efficient optimisation methods and more computational power, a more efficient trajectory could be found. This would have a snowballing effect that could affect all subsystems and therefore it should be a priority in the upcoming iterations. Moreover, a further understanding of long-term radiation impact on humans could impact the overall mission strongly, as additional shielding will render the modules too heavy and faster trajectories cannot be obtained using low-thrust propulsion.

Overall, it became clear that the requirement for a modular platform capable of bringing humans to Mars orbit before 2040 and returning them to Earth orbit is very challenging. In the current design, all technical requirements are met, but due to its reliance on experimental technology, several mission requirements come into danger. These include the necessity to launch before 2040, the aim for low-cost options, and the full modularity of the spacecraft. From this conceptual design, as well as the context it fits in of the many conceptual mission architectures developed by space agencies, it can be seen that many challenges are still to be overcome and much research to be performed to enable humanity becoming an interplanetary species.

A

ECLSS Spares Sizing

Assembly	Component	MTBF (hours)	Failure rate (10^-4/hr)	Probability of failure	Required parts (1 means no spares)	Mass per spare (kg)	Total spare mass (kg)	Probability of all spares failing
Oxygen Generation System	Hydrogen ORU	29551	0,338	0,795	6	125,2	751,2	0,000158
	Controller	75677	0,132	0,310	4	37,1	148,4	0,000284
	Oxygen ORU	99252	0,101	0,237	4	32,7	130,8	0,000103
	Pump ORU	189433	0,053	0,124	3	10,5	31,5	0,000281
	Inlet DI Bed ORU	442487	0,023	0,053	3	20	60	0,000024
	Nitrogen Purge ORU	140195	0,071	0,168	3	23,2	69,6	0,000664
	Power Supply Module	49202	0,203	0,478	5	46,6	233	0,000128
	Water ORU	37885	0,264	0,620	5	34,6	173	0,000411
	Rack				1	277	277	
	Total						**1874,5**	**0,000664**
Urine Processing Assembly	Wastewater storage tank	82200	0,122	0,286	4	47,9	191,6	0,000209
	Firmware controller assembly	13453	0,743	1,747	8	24,1	192,8	0,000374
	Separator plumbing assembly	88993	0,112	0,264	4	16,3	65,2	0,000155
	Pressure control and pump assembly	59221	0,169	0,397	4	44,9	179,6	0,000694
	Distillation assembly	41376	0,242	0,568	5	75,7	378,5	0,000279
	Fluids control and pump assembly	22759	0,439	1,032	6	45,7	274,2	0,000599
	Rack				1	376	376	
	Total						**1657,9**	**0,000694**
Water Processor Assembly	Catalytic reactor	27077	0,369	0,868	6	57,5	345	0,000249
	Gas separator	61182	0,163	0,384	4	39,4	157,6	0,000617
	Ion exchange bed	442478	0,023	0,053	3	12	36	0,000024
	Microbial check valve	178447	0,056	0,132	3	3,7	11,1	0,000334
	MFB 1	349650	0,029	0,067	3	50,5	151,5	0,000047
	MFB 2	349650	0,029	0,067	3	50,5	151,5	0,000047
	Particulate filter	560695	0,018	0,042	2	26,8	53,6	0,000842
	pH adjuster	-	-	-	0	-	-	-
	Process controller	70745	0,141	0,332	4	36,9	147,6	0,000364
	Pump separator	39429	0,254	0,596	5	27,6	138	0,000345

Figure A.1

	Reactor health sensor	134077	0,075	0,175	3	8,6	25,8	0,000753		
	Sensor	184618	0,054	0,127	3	3,6	10,8	0,000303		
	Separator filter	642342	0,016	0,037	2	7,3	14,6	0,000645		
	Start up filter	226850	0,044	0,104	3	9,5	28,5	0,000167		
	Water delivery	81797	0,122	0,287	4	39,2	156,8	0,000213		
	Waste water	43669	0,229	0,538	5	87,5	437,5	0,000219		
	Water storage	40463	0,247	0,581	5	49,3	246,5	0,000308		
	Oxygen filter	342548	0,029	0,069	3	1,1	3,3	0,000050		
	Rack				1	288	288			
	Total						**2403,7**	**0,000842**		
Carbon Dioxide Removal Assembly	Air pump two-stage ORU	156200	0,064	0,150	3	10,9	32,7	0,000488		
	Blower	129700	0,077	0,181	3	5,6	16,8	0,000827		
	Check valves	-			1	39,9	39,9	-		
	Desiccant beds	77100	0,130	0,305	4	42,6	170,4	0,000265		
	Heat controller	242700	0,041	0,097	3	3,3	9,9	0,000137		
	Precooler	129700	0,077	0,181	3	5,6	16,8	0,000827		
	Pump fan motor controller	2272000	0,004	0,010	2	2,7	5,4	0,000053		
	Selector valves	117000	0,085	0,201	4	3	12	0,000055		
	Sorbent beds	77100	0,130	0,305	4	42,6	170,4	0,000265		
	Rack				1	39	39			
	Total						**513,3**	**0,000827**		
Carbon Dioxide Reduction System	Sabatier reactor				5	120	600	No Data		
	Condensing heat exchanger				5	49,71	248,55	No Data		
	Phase separator				5	11,93	59,65	No Data		
	Valves				5	3,04	15,2	No Data		
	Sensors				5	4,81	24,05	No Data		
	Controller				5	3	15	No Data		
	Compressor				5	27	135	No Data		
	Rack				1	329	329			
	Total						**1426,45**	No Data	**Total mass**	**7875,85**

Figure A.2

Spacecraft sizing

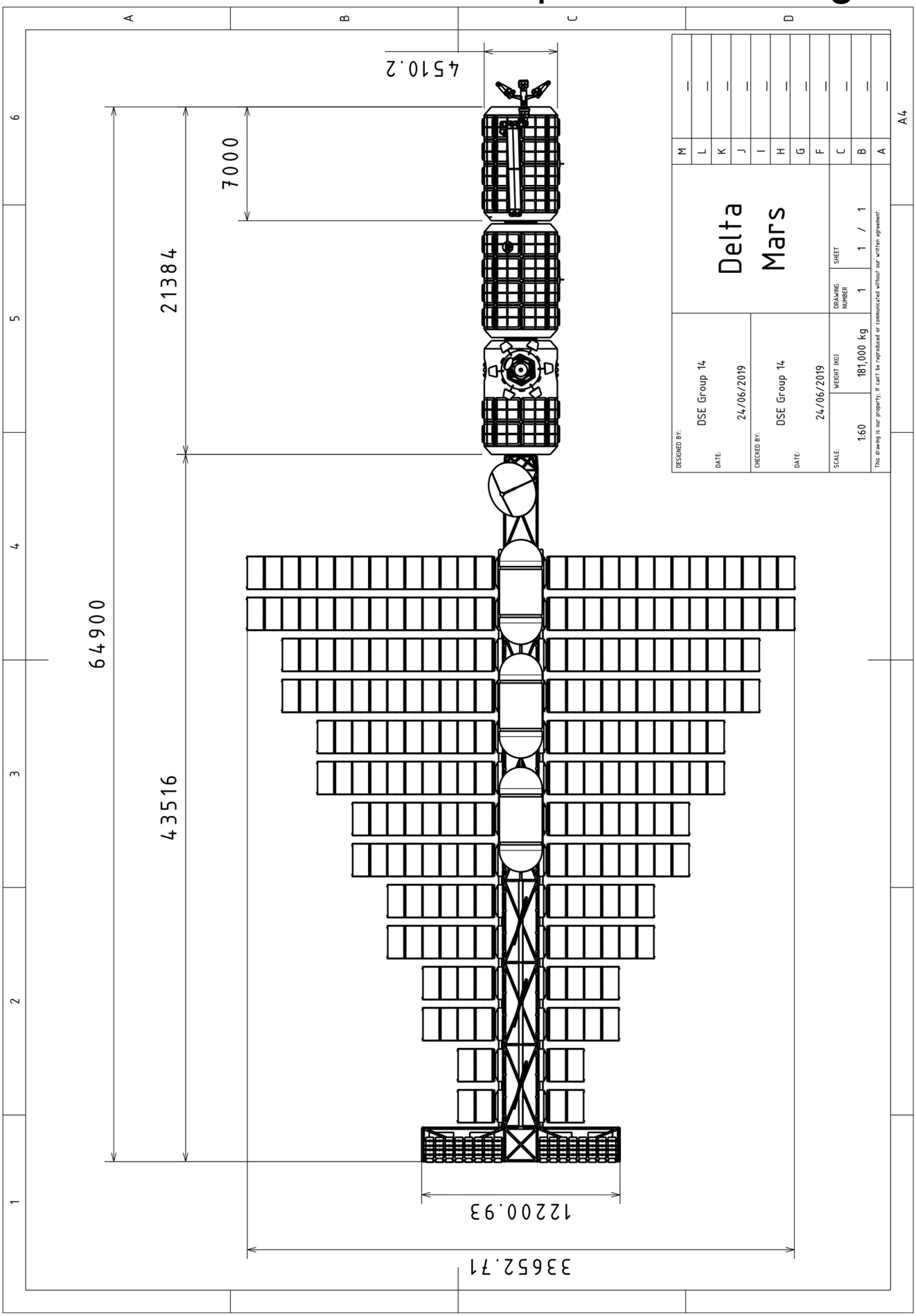

Bibliography

[1] G. P.Peterson A. J. Juhasz. Review of advanced radiator technologies for spacecraft power systems and space thermal control. Technical report, Lewis Research Center (NASA), 1994. URL https://ntrs.nasa.gov/archive/nasa/casi.ntrs.nasa.gov/19940032314.pdf.

[2] G.C. Birur A.D. Paris, P. Bhandari. High temperature mechanically pumped fluid loop for space applications – working fluid selection, 2004. URL https://www.pd-tech.com/wp-content/uploads/2014/08/pdt-paris.pdf.

[3] INTERNATIONAL ATOMIC ENERGY AGENCY. *Safety of Conversion Facilities and Uranium Enrichment Facilities*. Number SSG-5 in Specific Safety Guides. Elsevier, Vienna, 2010. ISBN 978-92-0-104809-7. URL https://www.iaea.org/publications/8104/safety-of-conversion-facilities-and-uranium-enrichment-facilities.

[4] M.K. Ewert A.J. Hanford. Advanced active thermal control systems architecture study. Technical report, National Aeronautics and Space Administration, 1996. URL https://ston.jsc.nasa.gov/collections/TRS/_techrep/TM104822.pdf.

[5] G. Halpert D.J. Flood S. Sabripour A.K. Hyder, R.L. Wiley. *Spacecraft Power Technologies*. World Scientific, 2000. ISBN 978-1-86094-117-7. URL https://app.knovel.com/hotlink/toc/id:kpSPT00001/spacecraft-power-technologies/spacecraft-power-technologies.

[6] S. K. Cole Et Al. Technology estimating: A process to determine the cost and schedule of space technology research and development. Technical report, NASA, 2013. URL https://ntrs.nasa.gov/archive/nasa/casi.ntrs.nasa.gov/20140005476.pdf.

[7] S.M.J. Al-Azawi. Effect orientation on performance of longitudinal (trapezoidal) fins heat sink subjected to natural convection. Technical report, Anbar Journal of Engineering Sciences, 2009. URL https://www.iasj.net/iasj?func=fulltext&aId=14224.

[8] United Launch Alliances. Delta iv launch services user's guide, June 2013.

[9] Arcselect. Losses due to fibres and connectors, 2019. URL https://arcelect.com/Calculating_fiber_loss_and_distance.pdf.

[10] W.J. Cooke Marshall A.V. Moorhead, H.M. Koehler. *NASA Meteoroid Engineering Model Release 2.0*, 2015.

[11] D.W. Beaty B. Drake, S.J. Hoffman. Human exploration of mars, design reference architecture 5.0. *2010 IEEE Aerospace Conference*, pages 1–24, 2010.

[12] P.L. Barry. Plastic spaceship, 2015.

[13] Matter Beam. Radiators explained. Technical report, Tough SF Blogspot, 2017. URL http://toughsf.blogspot.com/2017/07/all-radiators.html.

[14] Boeing. Boeing commercial crew transportation capability contract (cctcap). Technical report, NASA, 2013.

[15] S. Borenstein. Iss radiator leakage. Technical report, The Associated Press, 2013. URL https://www.ctvnews.ca/sci-tech/hadfield-says-iss-radiator-leak-serious-but-not-life-threatening-1.1275224.

[16] I. Le Bars C. Galet. Nuclear criticality risks and their prevention in plants and laboratoria. Technical report, Institut de Radioprotection et de Sureté Nationale, 2011.

[17] Bob Carter. URL https://ntrs.nasa.gov/archive/nasa/casi.ntrs.nasa.gov/20150009520.pdf.

[18] M.A. Peletier C.G. Hunt, G.J. Lord. Cylindrical shell buckling: A characterization of localization and periodicity. *Discrete and Continuous Dynamical Systems-Series B*, 3, 2003.

[19] E. Christiansen. Mmod protection and degradation effects for thermal control systems. Technical report, NASA, 2014.

[20] Coca. Coca cola sponsorship, August 2016. URL https://www.nrc.nl/nieuws/2012/10/20/adrenaline-in-het-energiedrankje-en-in-de-marketing-1164242-a1234593.

[21] C.J. Corso. Technical study for the use of the saturn 5, int-21 and other saturn 5 derivatives to determine an optimum fourth stage. Technical report, NASA, February 1971.

[22] J. C. Knox D. El Sherif. International space station carbon dioxide removal assembly (iss cdra) concepts and advancements. Technical report, NASA STI, January 2005.

[23] R. Hastrup D. Morabito. Communicating with mars during periods of solar conjunction. Technical report, NASA, April 2002.

[24] R. Destefanis M. Marchetti D. Palmieri, M. Faraud. Whipple shield ballistic limit at impact velocities higher than 7 km/s. Technical report, University of Rome, 2001.

[25] F. Bosquillon de Frescheville. New earth-mars communication concept. Technical report, ESA, 2009. URL https://www.esa.int/Our_Activities/Operations/New_concept_may_enhance_Earth-Mars_communication.

[26] B. Dick. Current status of the nitrogen oxygen recharge system. *41st International Conference on Environmental Systems*, 2011.

[27] M.C. Guzik D.W. Plachta. Cryogenic boil-off reduction system. *Cryogenics*, 60:62 – 67, 2014. ISSN 0011-2275. doi: https://doi.org/10.1016/j.cryogenics.2013.12.006. URL http://www.sciencedirect.com/science/article/pii/S0011227513001239.

[28] D.M. Lear E. Christiansen. Micrometeoroid and orbital debris environment and hypervelocity shields. Technical report, NASA, 2012.

[29] ECHA. Substance information, 2019. URL https://echa.europa.eu/substance-information/-/substanceinfo/.

[30] NEA Electronics. Antenna pointing mechanism p3, 2019. URL https://www.neaelectronics.com/products/gimbals-and-pointing-mechanisms/.

[31] D.M. Bardot E.M. Mattox, J.C. Knox. Carbon dioxide removal system for closed loop atmosphere revitalization, candidate sorbents screening and testresults. *Acta Astronautica*, 86:39–46, 2013. doi: https://doi.org/10.1016/j.actaastro.2012.09.019. URL https://www.sciencedirect.com/science/article/pii/S0094576512003761?via%3Dihub.

[32] T.E.Skidmore E.N.Hoffman. Radiation effects on epoxy/carbon-fiber composite. *Journal of nuclear materials*, 392(2):371–378, 2009.
[33] ESA. International berthing docking mechanism (ibdm). Technical report, ESA ERASMUS center, 2001.
[34] ESA. Ecss-e-hb-32-20 part 3a. Technical report, ECSS, March 2011.
[35] A. V. Ilin et AL. Vasimr® human mission to mars, 2011.
[36] A.I. Mrigakshia et AL. Estimation of galactic cosmic ray exposure inside and outside the earth's magnetosphere during the recent solar minimum between solar cycles 23 and 24. *Individual Article*, 2013.
[37] B. W. Longmier et AL. Vasimr® vx-200 performance measurements and helicon throttle tables using argon and krypton. Technical report, Ad Astra Rocket Company, 2011.
[38] Dr. C. H.Shivers et AL. Nasa space safety standards and procedures for human rating requirements, 2004.
[39] F. De Tiberis et AL. The x/x/ka-band deep space transponder for the bepicolombo mission to mercury. *Acta Astronautica*, 68(1):591–598, 2009.
[40] L. Narici et AL. Performances of kevlar and polyethylene as radiation shielding on-board the international space station in high latitude radiation environment. Technical report, None, 2017.
[41] V. Braun et AL. Orbital lifetime estimation using esa's oscar tool, July 2013.
[42] H. Liu H. Cai F. Feng, Y. Liu. Design schemes and comparison research of the end-effector of large space manipulator. *Chinese Journal of Mechanical Engineering*, 25:674–687, 2012.
[43] R. Farley. Satellite design course spacecraft configuration structural design preliminary design methods. None, February 2003.
[44] W. Fehse. *Automated Rendezvous and Docking of Spacecraft*. Cambridge University Press, Cambridge, UK, 2003.
[45] M. Zandieh F.F. Saberi. Design and analysis of gimbal thruster configurations for 3-axis satellite attitude control. *International Journal of Computer Applications*, 112(6), 2015.
[46] R. V. Fultyn. Environmental effects of the kiwi-tnt effluent: A review and evaluation. Technical report, LOS ALAMOS SCIENTIFIC LABORATORY of the University of California, April 1968.
[47] M. Bousquet G. Maral. *Satellite Communication Systems*. John Wiley & Sons Ltd, Chichester, England, 2002.
[48] P.M. O'Neill G.D. Badhwar, F.A. Cucinotta. An analysis of interplanetary space radiation exposure for various solar cycles. *Radiation Research Society*, 138, 1989.
[49] Ian Gibson, David Rosen, and Brent Stucker. *Additive Manufacturing Technologies: 3D Printing, Rapid Prototyping, and Direct Digital Manufacturing*. Springer New York, New York, NY, 2015.
[50] R. L. Tanimoto G.L. Davis. Mechanical development of antenna systems, 2005. URL https://descanso.jpl.nasa.gov/monograph/series8/Descanso8_08.pdf.
[51] H. Hemmati. Deep space optical communications. *NASA*, 2005.
[52] A. Hertzberg. Thermal management in space. Technical report, NASA Ames Research Center, 2008. URL https://space.nss.org/settlement/nasa/spaceresvol2/thermalmanagement.html.
[53] A.T. Mattick; A. Hertzberg. The liquid droplet radiator—an ultralightweight heat rejection system for efficient energy conversion in space. *Acta Astronautica*, 9:165–172, 1982. doi: https://doi.org/10.1016/0094-5765(82)90084-4. URL https://www.sciencedirect.com/science/article/pii/0094576582900844.
[54] R.W. Hyers and B.N. Tomboulian. Lightweight, high-temperature radiator for in-space nuclear-electric power and propulsion propulsion. Technical report, University of Massachusetts Amherst, 2014. URL https://scholarworks.umass.edu/cgi/viewcontent.cgi?referer=&httpsredir=1&article=1217&context=dissertations_2. In collaboration with NASA MSFC.
[55] E. Illi. Space station freedom common berthing mechanism. Technical report, The Boeing company, 2003.
[56] J. Saleh J. Castet. Satellite and satellite subsystems reliability: Statistical data analysis and modeling. *Reliability Engineering and System Safety*, 94:1718–1728, 2009.
[57] G. Halpert J. Mondt. Energy storage technology for future space science missions, November 2004.
[58] S. Shambayati J. Taylor, D.K. Lee. Mars reconnaissance orbiter telecommunications. Technical report, NASA, September 2006.
[59] B. David J.A Reiter. An analytical solution to quick-response collision avoidance manoeuvres in low earth orbit. *26th AAS/AIAA Space Flight Mechanics Meeting, 2016*, 2016.
[60] A. Vavrin A. Manis J.C. Liou, M. Matney and D. Gate. Nasa odpo's large constellation study. *Orbital DebrisQuarterly News*, 22:4 – 5, September 2018.
[61] H. Jones. Would current international space station (iss) recycling life support systems save mass on a mars transit? Technical report, NASA STI, July 2017.
[62] A. J. Juhasz. High conductivity carbon-carbon heat pipes for light weight space power system radiators. Technical report, Glenn Research Center, Cleveland, Ohio, 2008. URL https://ntrs.nasa.gov/archive/nasa/casi.ntrs.nasa.gov/20080045532.pdf.
[63] C. E. Keesee. *Spacecraft Thermal Control System*. Massachusetts Institute of Technology, 2010.
[64] K.C. Ting P.C. Teh H. Nisar W.L. Yeo K.H. Yeap, K.C. Lai. Optimization of reflector antennas in radio telescopes, 2017. URL https://www.researchgate.net/publication/320408522_Optimization_of_reflector_antennas_in_radio_telescopes/download.
[65] N. Orozco L. Carter, C.Brown. Status of iss water management and recovery. Technical report, NASA STI, 2014.
[66] L. Salerno P Kittel L.J Hastings, D.W Plachta. An overview of nasa efforts on zero boiloff storage of cryogenic propellants. *Cryogenics*, 41(11):833 – 839, 2001. ISSN 0011-2275. doi: https://doi.org/10.1016/S0011-2275(01)00176-X. URL http://www.sciencedirect.com/science/article/pii/S001122750100176X. 2001 Space Cryogenics Workshop.

[67] P. Kittel L.J. Salerno. Cryogenics and the human exploration of mars1paper presented at the 1997 space cryogenics workshop, eugene, or, usa, 4–5 august 1997.1. *Cryogenics*, 39(4):381 – 388, 1999. ISSN 0011-2275. doi: https://doi.org/10.1016/S0011-2275(99)00043-0. URL http://www.sciencedirect.com/science/article/pii/S0011227599000430.
[68] M. Perchonok M. Cooper, G. Douglas. Developing the nasa food system for long-duration missions. *Journal of Food Science*, 76:R40–R48, 2011. doi: https://doi.org/10.1111/j.1750-3841.2010.01982.x. URL https://onlinelibrary.wiley.com/doi/full/10.1111/j.1750-3841.2010.01982.x.
[69] F.A. Cucinotta M. Durante. Physical basis of radiation protection in space travel. *Reviews of Modern Physics*, 83, 2011.
[70] B. Dick S.L. Phoenix M. Kezirian, A. Cook. Providing pressurized gasses to the international space station (iss): Developing a composite overwrapped pressure vessel (copv) for the safe transport of oxygen and nitrogen. Technical report, Boeing, August 2012.
[71] M. Peinemann P. Ross M. Ross, D. Toohey. Limits on the space launch market related to stratospheric ozone depletion. *Astropolitics*, 7(1):50–82, 2009.
[72] Magellan. Command and data handling unit, 2019. URL http://magellan.aero/wp-content/uploads/C&DH%20-%20Web%20Version.pdf.
[73] L.S. Mason. A power conversion concept for the jupiter icy moons orbiter. Technical report, NASA, 2003. URL https://ntrs.nasa.gov/archive/nasa/casi.ntrs.nasa.gov/20030105581.pdf.
[74] T. H. Megson. *Aircraft structures for engineering students*. Elsevier, Amsterdam, 2013.
[75] LA Morine and BJ Oconnor. A description of the cmg and its application to space vehicle control. *Journal of Spacecraft and Rockets*, 6(3):225–231, 1969.
[76] J. Vedda M.Ross. The policy and science of rocket emissions. *None*, April 2018.
[77] NASA. Derivation of failure rates and probability of failures for the international space station probabilistic risk assessment study, 2004.
[78] NASA. International standard payload rack, 2009. URL https://web.archive.org/web/20090613005742/https://mistprod.hosc.msfc.nasa.gov/E-basicaccomodations/E3.html#ispr.
[79] NASA. Interplanetary mission design handbook, 2010.
[80] NASA. Alternative strategies for exploring mars and the moons of mars, August 2012. URL https://ntrs.nasa.gov/archive/nasa/casi.ntrs.nasa.gov/20120009026.pdf.
[81] NASA. Nasa docking system (nds) interface definitions document (idd) revision h. Technical report, NASA, 2013.
[82] NASA. Nasa meteoroid engineering model v2.0. Technical report, NASA, 2015.
[83] NASA. Nasa sustainable acquisition, August 2016. URL https://alcalde.texasexes.org/2014/07/exploring-space-is-still-worth-the-cost-says-ut-expert/.
[84] NASAarch. Alternative strategies for exploring mars and the moons of mars, January 2016. URL https://ntrs.nasa.gov/archive/nasa/casi.ntrs.nasa.gov/20120009026.pdf.
[85] United Nations. Space debris mitigation guidelines of the committee on the peaceful uses of outer space, 2010. URL http://www.unoosa.org/pdf/publications/st_space_49E.pdf.
[86] University of Maryland. Cost estimation relationship, 2002. URL https://slideplayer.com/slide/10084871/.
[87] University of Porto. Protocol of communications for vorsat satellite - transmission losses -, 2012. URL https://paginas.fe.up.pt/~ee97054/Transmission%20Losses.pdf.
[88] Committee on Advanced Nuclear Systems. *Proceedings of a symposium - Advanced Compact Reactor System*. National Academy of Sciences, 1982.
[89] R. W. Orloff. Space shuttle mission sts-77. Technical report, NASA, 1996. URL https://historycollection.jsc.nasa.gov/JSCHistoryPortal/history/shuttle_pk/pk/Flight_077_STS-077_Press_Kit.pdf.
[90] N. van der Hijden M. Katona C. Klop P.L.M. de Kok T. Kukucka M. Osowski P. Papadopoulos A. Thiam P. Elferink, T. Faschinger. Baseline report dse: Transfer to mars and back in the next two decades. Technical report, TU Delft Faculty of Aerospace Engineering, 2019.
[91] Y. Kim P. F. Venneri. A feasibility on low enriched uranium fuel for nuclear thermal rockets - ii: Rocket and reactor performance. Technical report, Elsevier, 2015.
[92] O. Layi O. Marius K. Nara L. Aris T. Ed P. Laryssa, E. Lindsay. International space station robotics: A comparative study of era, jemrms and mss. Technical report, ESA ESTEC, November 2002.
[93] B. Mattfeld C. Stromgren K. Goodliff P. Lopez Jr, E. Schultz. Logistics needs for potential deep space mission scenarios post asteroid redirect crewed mission. Technical report, NASA STI, 2015.
[94] Arnauld E. Nicogossian; James F. Parker. *Space Psychology and Medicine*. National Aeronautics and Space Administration, 1982.
[95] Y. Kim P.F. Venneri. A feasibility study on low enriched uranium fuel for nuclear thermal rockets–ii: Rocket and reactor performance. *Progress in Nuclear Energy*, 87:156–167, 2016.
[96] J. Taylor R. Ludwig. Voyager telecommunications. Technical report, NASA, NASA 2002.
[97] G. Gentry M. Gault R. M. Bagdigian, J. Dake. International space station environmental control and life support system mass and crewtime utilization in comparison to a long duration human space exploration mission. Technical report, NASA, 2015.
[98] A.J. Cook R. N. Schaezler. Iss o2 production, gas supply and partial pressure management. Technical report, NASA STI, July 2015.
[99] J. Soeder R. Scheudeggerm. Advanced life support research and technology development metric, 2015. URL https://ntrs.nasa.gov/archive/nasa/casi.ntrs.nasa.gov/20150019744.pdf.
[100] A.T. Mattick R. T. Taussig. Droplet radiator systems for spacecraft thermal control. *J. Spacecraft*, 23:10 – 18, 1986. ISSN AIAA-25077-715. doi: https://doi.org/10.2514/3.25077. URL forum.nasaspaceflight.com/index.php.

[101] S. Kimbrel C. McLean R.A. Spores, R. Masse. Gpim af-m315e propulsion system. Technical report, Aerojet Rocketdyne, Ball Aerospace and Technologies Corporation, 2008.
[102] D. Rapp. Mars life support systems. *The International Journal of Mars Science and Exploration*, 2:72–82, 2006.
[103] S.C. Fan R.C. Hibbeler. *Statics and mechanics of materials*, volume 2. Prentice Hall Singapore, 2004.
[104] N. Harada R.J. Litchford. Multi-mw closed cycle mhd nuclear space power via nonequilibrium he/xe working plasma. Technical report, NASA, February 2011.
[105] W.H. Warr R.J. McLaughlin. The common berthing mechanism (cbm) for international space station. Technical report, Honeywell Engines & Systems, 2001.
[106] P.R. Smudde M.A. Henry R.M. Foster, J.G. Cook. Space station berthing mechanisms, attaching large structures on-orbit that were never mated on the ground. Technical report, The Boeing Company, 2004.
[107] D.J. Leonard R.N. Schaezler, A.J. Cook. Trending of overboard leakage of iss cabin atmosphere. Technical report, NASA STI, June 2011.
[108] B.N. Tomboulian R.W. Hyers. Lightweight, high-temperature radiator for space propulsion. Technical report, University of Massachusetts, 2019. URL https://ntrs.nasa.gov/archive/nasa/casi.ntrs.nasa.gov/20130001608.pdf. In collaboration with NASA MSFC.
[109] Sage. Dual-polarised corrugated feed horn technology, 2019. URL https://www.sagemillimeter.com/content/datasheets/SAF-2434231535-328-S1-280-DP.pdf.
[110] Ä.M. Schinder. Optimized low thrust trajectories compared to impulsive trajectories for interplanetary missions, 2016.
[111] E. Seedhouse. *SpaceX: making commercial spaceflight a reality*. Springer Science & Business Media, 2013.
[112] Airbus Space and Defense. Flash solid state memory, 2019. URL https://www.airbus.com/newsroom/press-releases/en/2014/05/fully-qualified-flash-memory-optimizes-satellite-data-storage.html.
[113] SpaceX. Falcon user's guide. Technical report, SpaceX, January 2019. URL https://www.spacex.com/sites/spacex/files/falcon_users_guide_0219.pdf.
[114] Spectrolab. Spectrolab xte data sheet, 2019. URL https://www.spectrolab.com/photovoltaics/XTE_32_Percent.pdf.
[115] P. Spores. Gpim af-m315e propulsion system. *51st AIAA/SAE/ASEE Joint Propulsion Conference*, page 3753, 2015.
[116] S. R. Starin. Attitude determination control systems. *NASA*, 2019. URL https://ntrs.nasa.gov/archive/nasa/casi.ntrs.nasa.gov/20110007876.pdf.
[117] Daan Stevenson and Hanspeter Schaub. Nonlinear control analysis of a double-gimbal variable-speed control moment gyroscope. *Journal of Guidance, Control, and Dynamics*, 35(3):787–793, 2012.
[118] L3 technologies. Twta ka-band equipment, 2019. URL https://www2.l3t.com/edd/products/twt_hp.htm.
[119] Teledynemicrowave. Twta 40 w, 2019. URL https://www.teledynemicrowave.com/images/2016_Catalogs/MEC_Product_Selection_Guide.pdf.
[120] Thales. Epc equipment, 2019. URL https://www.thalesgroup.com/sites/default/files/database/d7/asset/document/EPC_single-dual_TWTA102012.pdf.
[121] P. Ulrich. Final environmental impact statement for the cassini mission. Technical report, NASA, 1995.
[122] Unknown. Cassegrain configuration, 2009. URL https://www.electronics-notes.com/articles/antennas-propagation/parabolic-reflector-antenna/feeder-feed-systems.php.
[123] Unknown. International docking system standard (idss) interface definition document (idd) revision d. Technical report, International Space Station Multilateral Control Board, 2015.
[124] Unknown. Droplet cooling in nuclear-powered spacecraft engines. Technical report, Moscow Institute of physics and technology, 2015. URL https://mipt.ru/en/news/cooling_201508.
[125] J.M.J.F. van Campen. Project guide design synthesis exercise transfer to mars and back in the next two decades. None, April 2019.
[126] P. Elferink; T. Faschinger; N. van der Hijden; M. Katona; C. Klop; P.L.M. de Kok; T. Kukucka; M. Osowski; P. Papadopoulos; A. Thiam. Midterm report dse: Transfer to mars and back in the next two decades. Technical report, TU Delft Faculty of Aerospace Engineering, 2019.
[127] P. Wade. Multiple reflector design, 2004. URL http://www.w1ghz.org/antbook/conf/Multiple_reflector_antennas.pdf.
[128] K. A. White. Liquid droplet radiator development status. Technical report, Lewis Research Center (NASA), 1987. URL https://ntrs.nasa.gov/archive/nasa/casi.ntrs.nasa.gov/19870010920.pdf.
[129] D. R. Williams. Mars fact sheet, September 2018. URL https://nssdc.gsfc.nasa.gov/planetary/factsheet/marsfact.html.
[130] J. R. Wertz W.J. Larson. Space mission analysis and design. Technical report, Torrance, CA (United States); Microcosm, Inc., 1992.
[131] M. Sghedoni X. Roser. Control moment gyroscopes (cmg's) and their application in future scientific missions. *Spacecraft Guidance, Navigation and Control Systems*, 381:523, 1997.
[132] J.L. Perry Z. W. Greenwood, M. B. Abney. Increased oxygen recovery from sabatier systems using plasma pyrolysis technology and metal hydride separation. Technical report, NASA STI, July 2015.